Synthetic Modifications of Responsive MRI Contrast Agents-Development of Multifunctional Conjugates for Novel Class of fMRI

Synthetische Modifizierung von Intelligenten MRI Kontrastmitteln-Entwicklung von Multifunktionalen Verbindungen für eine neuartige Klasse von fMRI

Dissertation
der Mathematisch-Naturwissenschaftlichen Fakultät
der Eberhard Karls Universität Tübingen
zur Erlangung des Grades eines
Doktors der Naturwissenschaften
(Dr. rer. nat.)

vorgelegt von
Sandip M. Vibhute
aus Anfhale (Indien)

Tübingen
2013

Tag der mündlichen Qualifikation: 22.04.2013
Dekan: Prof. Dr. Wolfgang Rosenstiel
1. Berichterstatter: Prof. Dr. Martin E. Maier
2. Berichterstatter: Priv.–Doz. Dr. Goran Angelovski

This doctoral thesis was carried out at the Dept. of Physiology of Cognitive Processes of the Max Planck Institute for Biological Cybernetics, Tübingen under the supervision of Prof. Nikos K. Logothetis, Priv.–Doz. Dr. Goran Angelovski and in collaboration with the Institute for Organic Chemistry, Eberhard-Karls-University, Tübingen under the guidance of Prof. Dr. Martin E. Maier during the period from June 2009 to January 2013.

To

Shivamama

Acknowledgements

The work described in this thesis has not been possible without the help of many people and I believe, only acknowledging them here would not be sufficient. But still I would like to mention few names here.

Foremost, I would like to thank my supervisors for the support and guidance during my PhD period in Tübingen. Especially Prof. Dr. Nikos K. Logothetis, for providing me an opportunity to work in his research group, providing his support and funding. I would like to say few words about Prof. Dr. Martin E. Maier for his throughout supervision, teaching the basic chemistry through his Wednesday seminars and countless suggestions on number of projects during last four years.

I would like to express my gratitude to my supervisor Priv.-Doz. Dr. Goran Angelovski not only for the endowed confidence, freedom in the choice of my research and the execution of my own ideas, but also for his competent advices, constant encouragement and limitless patience during the course of interesting research projects of my doctoral thesis.

I would like to express my deepest gratitude to Dr. Matteo Placidi for his generous advices, constructive feedbacks during preparation of manuscripts and this thesis, which have been incorporated here.

I am also thankful to my project collaborators, Dr. Jörn Engelmann for performing MRI experiments and Dr. Tatjana Verbić for helping to obtain the conditional stability constants.

I would like to thank all my colleague and group members of our bioconjugate group for scientific discussions, help and friendly working atmosphere: Dr. Ilgar Mamedov, Dr. Pascal Kadjane, Dr. Fatima Oukhatar, Dr. Karolina Jankonska, Dr. Aneta Brud, Dr. Rajendra Joshi, Dr. Sven Gottschalk, Serhat Gündüz and Ms. Hildegard Schulz. Furthermore I thank to the all members of the group of Prof. Dr. Martin Maier for their help as well as Dr. Dorothee Witsuba for performing ESI-HRMS experiments.

I would like to thank members of the exam committee, Prof. Dr. Hermann A. Mayer and Prof. Dr. Thomas Ziegler too.

I should thank Prof. Dr. U. B. More, Prof. Dr. S. S. Swami, Prof. Dr. D. D. Patil, and all my college and school teachers for encouraging me to learn chemistry and laboratory skills during my studies in India.

Finally, I thank my sweet wife Snehal who stood beside me, also for her infinite love, understanding, encouragement and support to achieve this milestone. Last, but not least, baby ‘Shlok’ for entering in our life during the last phase of this thesis preparation and not disturbing during writing this thesis. I am very thankful to my parents and sisters, Akka, Mina and Uma, for their sacrifices, love and support through life as well as all members of Vibhute, Kandre and Yelmar families for their care and affection.

I thank all of my friends and well wishers for their help who could not find separate name here particularly all the friends from my schools, colleges, Ranbaxy research laboratories, Jubilant Chemsys and AMRI Singapore.

At last, I thank Babaji for assigning this duty to me which was accomplished with the wish of the mighty God.

Abstract

Die in der Magnetresonanztomographie (MRI) verwendeten Kontrastmittel werden weitestgehend in der Diagnose oder in der Grundlagenforschung als bildgebende Methode eingesetzt. Meistens um den MRI-Kontrast positiv zu verstärken, dabei werden hauptsächlich Gd^{3+} basierte Systeme verwendet. Um ein besseres Verständnis von biologischen Prozessen zu erhalten, wurden intelligente Kontrastmittel (*engl.* SCAs: smart contrast agents) entwickelt, welche in der Lage sind physiologische Veränderungen durch Veränderung des MR-Signals sichtbar zu machen. Um die Herausforderungen zu überwinden, welche sich während einer *in vivo* Routineuntersuchung mit SCAs ergeben, wie die Lokalisierung , Quantifizierung, niedrige MR-Signale etc., besteht eine mögliche Strategie darin, solche Kontrastmittel mit verschiedenen funktionellen Molekülen, wie Dendrimeren, Nanopartikeln, Proteine oder Fluoreszenzmarker, zu verknüpfen. Um an bekannte SCAs funktionelle Moleküle anzuheften, kommt es darauf an bei der Modifizierung solcher SCAs die physikalisch-chemischen Eigenschaften beizubehalten die für deren Funktion essentiell sind.

Der erste Teil dieser Dissertation beschreibt die Synthese und die Charakterisierung von pH sensitiven SCAs, an denen entweder ein aliphatischer ($\mathbf{GdL^1}$) oder ein aromatischer ($\mathbf{GdL^2}$) Linker angeheftet ist, mit angehängten Phosphatarm. Die longitudinale Relaxation von $\mathbf{GdL^1}$ und $\mathbf{GdL^2}$ wird um 146% beziehungsweise um 31% verstärkt, falls der pH-Wert von 9 auf 5 abnimmt. Diese beiden SCAs wurden zu einem biotinylierten System umgesetzt, $\mathbf{GdL^3}$ und $\mathbf{GdL^4}$, und deren Wechselwirkungen mit Avidin untersucht. Über die Untersuchungsmethoden, des "fluorescence displacement"-Assay und der MRI E-Titration, konnte ein 3:1 Bindungsmode von $\mathbf{GdL^{3\text{-}4}}$ zu Avidin mit einer genauso hohen Bindungsaffinität gezeigt werden, wie bei dem ursprünglichen Avidin-Biotin-Komplex. Diese hohe Bindungsaffinität konnte über einen kompetitiven Assay mittels MRI bestätigt werden. Der Avidin-$\mathbf{GdL^{3\text{-}4}}$-Komplex der folglich erhalten wurde, zeigte Unterschiede in r_1 als auch r_2 im Bezug auf die pH-Abhängigkeit. Diese Ergebnisse zeigen neue Möglichkeiten für die Modifikation und Verbesserung von SCAs um diese geeigneter für die *in vivo* Anwendung zumachen.

Der zweite Teil dieser Dissertation beschäftigt sich mit der Modifikation von bereits beschrieben Ca^{2+} ansprechbaren bismakrozyklischen Kontrastmitteln. Das modifizierte SCA ($\mathbf{Gd_2L^5}$) wurde über die Insertion von aromatischen Linkern erhalten, die funktionelle Gruppen mit primären Aminen tragen, die für eine weitere Derivatisierung geeignet sind. Mit 1.2 Äquivalenten an Ca^{2+} konnte gezeigt werden, dass $\mathbf{Gd_2L^5}$ eine um 97% höhere

longitutinalen Relaxation erreicht. Dies deutet daraufhin, dass die Eigenschaften für die Relaxation in **Gd_2L^5** gut erhalten blieben. Die Aminogruppe des Linkers **L^5** wurde außerdem in eine Isothiocyanat-Gruppe umgewandelt und so **L^6** erhalten. Dies erweitert die Nutzung der Liganden, da die reaktive Gruppe dazu genutzt werden kann, um zu einer effizienten Funktionalisierung von **L^6** zu führen. Diese Sonde bietet neue Möglichkeiten, diese an funktionelle Moleküle anzuheften, welche geeignet sind für eine *in vivo* Anwendung mit Hilfe der Linker.

Im letzten Kapitel wird die Synthese von **L^5** beschrieben, wobei eine Methode der Festphasensynthese angewendet wurde, benutzt wurde dabei die Phthalamid/*tert*-Butyl-Chemie. Dies ist der erste Bericht bei dem Bismakrozyklen mit Hilfe einer Festphasenmethode erhalten wurden. Diese Strategie wurde angewandt um den Zeitaufwand zu minimieren, welcher durch die Aufreinigung von polaren Intermediaten in wässriger Phase anfällt. Nach der erfolgreich demonstrierten Synthesen von **L^5**, wurde der Ca^{2+} ansprechbare bismakrozyklische Ligand **L^7**, der zwei aromatische Linker an jedem Makrozyklus trägt, erfolgreich synthetisiert.. Diese Synthesestrategie erlaubt es prinzipiell innerhalb einer kurzen Zeit eine große Anzahl analoger Moleküle zu synthetisieren und so eine Molekülsammlung zu erstellen. Zudem erlaubt die strukturelle Modifikation an der Festphase die Insertion verschiedener Linker, sowie das Anbringen geeigneter Marker um die *in vivo* Anwendung zu verbessern.

Abbreviations

ArH	Aromatic
Boc	*tert*-butoxycarbonyl
Bz	Benzoyl
Bn	Benzyl
CBz	Benzyloxycarbonyl
CA	Contrast agent
CPP	Cell penetrating peptide
cyclen	1,4,7,10-tetraazacyclododecane
δ	Chemical shift
CDCl3	Chloroform deuterated
DCC	Dicyclohexylcarbodimide
DCM	Dichloromethane
DIPEA	N,N'-diisopropylethylamine
DMAP	4-Dimetylaminopyridine
DMF	Dimethylformamide
DOTA	1,4,7,10-tetraazacyclododecane-N,N',N'',N'''-tetraacetic acid
DO3A (*tris*-*t*-Bu ester)	1,4,7,10-tetraazacyclododecane-1,4,7-*tris*(acetic acid-*tert*-butyl ester)
D_2O	Deuterium oxide
DTPA	Diethylene triamine pentaacetic acid
EDC	1-Ethyl-3-(3'-dimethylaminopropyl) carbodiimide
EGTA	Ethylene glycol *bis*(2-aminoethylether)-N,N,N',N'-tetraacetic acid
ESI-MS	Electrospray ionization mass spectrometry

Eq	Equation
Et	Ethyl
EtOAc	Ethyl acetate
$EuCl_3$	Europium trichloride
Fig	Figure
Fmoc	9-fluorenylmethoxycarbonyl
g	Gram (s)
$GdCl_3$	Gadolinium chloride
h	Hour(s)
H_2	Hydrogen
HATU	2-(1-H-7-azabenzotriazol-1-yl)-1,1,3,3-tetramethyluronium hexafluorophosphate
HBTU	2-(1H-benzotriazol-1-yl)-1,1,3,3-tetramethyluronium hexafluorophosphate
HBr	Hydrobromic acid
HCl	Hydrochloric acid
HOBt	1-hydroxybenzotriazole
HPLC	High performance liquid chromatography
Hz	Hertz
J	Coupling constant
Ln	Lanthanide
Me	Methyl
mmol	Millimol
mM	Millimolar
MeOH	Methanol
MR	Magnetic resonance
MRI	Magnetic resonance imaging

NMR	Nuclear magnetic resonance
NMM	N-methylmorpholine
Pd-C	Palladium carbon
PMB	*p*-methoxybenzyl
R_f	Retention factor (TLC)
RP-HPLC	Reverse phase high performance liquid chromatography
R_t	Retention time (HPLC)
SCA	Smart contrast agent
^{t}Bu	*tert*-butyl
T	Tesla (MRI)
TFA	Trifluoroacetic acid
THF	Tetrahydrofuran
TLC	Thin layer chromatography
Trt	Trityl
UV	Ultraviolet
rt	Room temperature

Table of Contents

Chapter 1: Introduction 1
1.1 Imaging 3
1.2 Basics of MRI 3
1.3 Classification of CAs 8
1.3.1 Superparamagnetic contrast agents 8
1.3.2 Paramagnetic contrast agents 9
1.4 Tunable molecular parameters contributing to longitudinal relaxivity 13
1.4.1 Hydration number, q 13
1.4.2 Rotational correlation time, $\boldsymbol{\tau R}$ 15
1.4.3 Residence time of the coordinated water/proton, $\boldsymbol{\tau m}$ 16
1.5 Smart Contrast Agents 18
1.5.1 pH activated smart contrast agents 18
1.5.2 Cation sensitive smart contrast agents 19
1.5.3 Enzyme activated smart contrast agents 22
1.6 Aim of Project 24
Chapter 2: Synthesis and characterization of pH-sensitive, biotinylated MRI contrast agents and their conjugates with avidin 27
2.1 Introduction 29
2.2 Ligand design 32
2.3 Results and Discussion 33
2.3.1 Synthesis of complexes GdL^1 and GdL^2 33
2.3.2 Relaxometric experiments 37
2.3.3 Luminescence emission experiments 37
2.4 Biotinylation of GdL$^{1-2}$ 39
2.5 Fluorescence displacement assay 40
2.6 MRI phantom experiments 42
2.7 Competitive MRI assay 43
2.8 Conclusions 44
Chapter 3: Synthetic modification of Ca^{2+} responsive bismacrocyclic contrast agent and study of its response towards Ca^{2+} 47
3.1 Introduction 49
3.2 Ligand design 53
3.3 Results and discussions 55
3.3.1 Retrosynthetic analysis of L^5 55
3.3.2 Synthesis of L^5, strategy 1 56

3.3 Synthesis of L^5, strategy 2 61
3.4. Relaxometric Ca^{2+} titration in HEPES buffer 66
3.5 Conclusions 67
Chapter 4: Synthetic modification of Ca^{2+} sensitive smart contrast agent using solid phase synthesis 69
4.1 Introduction 71
4.1.1 Solid phase synthesis (SPS) 71
4.2 Ligand design and retrosynthetic plan 73
4.3 Results and discussion 77
4.3.1 Synthesis of L^5 77
4.3.2 Synthesis of L^8 81
4.4 Conclusions 87
Chapter 5: Summary, conclusions and outlook 89
Chapter 6: Materials and methods 95
6.1 Materials and Methods 97
6.1.1 Chemicals and working techniques 97
6.1.2 Reverse phase high performance liquid chromatography (RP-HPLC) 97
6.1.3 NMR-spectroscopy 98
6.1.4 Mass spectrometry 98
6.1.5 Chromatographic methods 98
6.1.6 Luminescence lifetime measurement 99
6.2 Preparation of Ln^{3+} complexes 99
6.3 Relaxometric experiments 99
6.4 Fluorescence displacement assay 100
6.5 MRI phantom experiments 102
6.6 Competitive MRI assay 104
6.7 Experimental synthetic procedures 105

Chapter 1: Introduction

1.1 Imaging

The information about molecular abnormalities that ultimately result in disease or certain critical physiological events are of paramount importance in medical research and clinics. In order to understand the mechanism of these processes as well as to plan therapy, precise and truthful evaluations are necessary, which is the goal of molecular imaging. This key discipline of biomedical sciences is essential in monitoring the biological processes at cellular and subcellular level facilitating diagnosis, therapy monitoring, drug discovery and development. More specifically one could say it helps in understanding protein-protein interactions and enzymatic conversions. In addition it can be used to provide more detailed information regarding the structure of proteins and enzymatic function or its activity. By creating 2D or 3D images of tissues in live subjects, various properties of a potential pharmaceutical such as efficacy, metabolism, excretion and toxicity can be investigated, in a short time causing a minimal amount of disturbance to the system. This stream involves the use of highly sensitive instrumentation and contrast mechanism. The different techniques or modalities are summarized with their advantages and limitations in Table 1.[1]

Among all modalities listed below; MRI is unique due to its ability to non-invasively produce high spatiotemporal resolved images of the soft tissues, without the use of ionizing radiation. This allows imaging without damaging or destroying tissues in living animals in real time. A single MRI experiment can extract enormous amounts of information compared with other modalities. Today MRI has become the modality of choice in number of diseases such as stroke, neurodegenerative disorders and cardiovascular diseases. This technique involves measuring the change in signal originating mainly from water protons in large magnetic field.

1.2 Basics of MRI

MRI operates on the principle of nuclear magnetic resonance (NMR, well known technique to analyze the organic molecules and few inorganic species too). Nuclei can be studied in NMR if they have a nuclear spin quantum number, $\boldsymbol{I}$ more than zero ($\boldsymbol{I} \neq 0$) in other words the nuclei having unequal number of protons or neutrons. Commonly studied nuclei with spin quantum number $\boldsymbol{I} = \frac{1}{2}$ (e.g. ^{1}H, ^{13}C, ^{19}F, ^{31}P). ^{1}H is the most favorable nucleus for MRI because of its great abundance in biological materials present in water. Nuclei having spin angular momentum behave as small tiny magnets rotating around their center, producing

Table 1-1: Key modalities used in molecular imaging approaches.

Imaging Technique	**Advantages**	**Disadvantages**
Positron emission tomography (PET)	High sensitivity; isotopes can substitute for naturally occurring atoms; quantitative; translational research	PET cyclotron or generator needed; relatively low spatial resolution; exposure of subject to harmful radiation; expensive
Single photon emission computed tomography (SPECT)	Many molecular probes available; can image multiple probes simultaneously; may be adapted to clinical imaging systems; excellent sensitivity	Relatively low spatial resolution; ionizing radiation; semi-quantitative; relatively expensive
Optical imaging	Can be used repeatedly without harm; High sensitivity; quick, easy, inexpensive, and relatively high output; user friendly	Limited depth of penetration; current 2D imaging only; clinical translation very limited
Magnetic resonance imaging (MRI)	Highest spatial resolution; no ionizing radiation burden	Relatively low sensitivity; high cost; Contrast agent may be needed
Computed tomography (CT)	Bone and tumor imaging; anatomic imaging	Limited 'molecular' applications; limited soft tissue resolution; radiation
Ultrasound	Images can be generated in real time; Inexpensive; high temporal resolution; quantitative; no radiation; clinical utility	Low spatial resolution; difficult to image extravascular targets; limited depth penetration; only anatomical information

magnetic fields. The direction of this field is random, but when placed in a large external magnetic field, B_0, the population of spins split into a number of discrete energy levels determined by ***I***. Nuclei having **I** = 1/2 only have two energy levels; When the angular moment aligns into the direction of B_0 it is called as lower energy state, N^+, while when alignment is against B_0 it is called as higher energy state, N^-. Boltzmann's equation provides the relationship between these two states (Eq.1-1) where ΔE is the energy difference between the spin states, k is Boltzmann's constant, 1.3805x10^{-23} J/K and T is temperature in Kelvin. This equation indicates the population of spins in each energy state is dependent on the temperature.

$$\mathrm{N}^{-}/N^{+} = e^{-E/kT} \qquad \text{Eq. (1-1)}$$

In an external magnetic field, torque is created due to coupling between the nuclear spin and angular momentum. As a result spinning nuclei precess around the direction of the B_0. Known as the frequency of precession, or Larmour frequency, ω is directly proportional to strength of B_0 (Eq. 1-2) where γ is the gyromagnetic ratio, in MHz/Tesla and is characteristic of each nuclei.

$$\omega = \gamma B_0 \qquad \text{Eq. (1-2)}$$

There is always excess number of spins in lower energy state at equilibrium (although number is very small) hence the net magnetization is in the direction of B_0. When B_0 is perpendicular to x- and y-axis and parallel to z-axis, then at equilibrium net magnetization will be in the direction of z-axis which is also called as longitudinal magnetization and $M_z \neq 0$, magnitude of M_z can be obtained by Curie law which shows that macroscopic magnetization is directly proportional to the magnetic field strength B_0 while M_x and M_y components or transverse components of magnetization will not be present at this time, $M_x = 0$, $M_y = 0$. If electromagnetic energy, of the same magnitude as the difference in energy between the spin levels, is emitted near the spins, in the form of radio frequency (RF pulse), it generates an extra magnetic field B_1 in the direction perpendicular to the B_0. As a result the net magnetization component M_z turns away from the z-axis. When RF signal is turned off, the displaced M_z-component returns to its equilibrium value slowly, this mechanism is called as longitudinal relaxation or T_1-relaxation (T_1 is time required to return to the initial value of M_z) or spin-lattice relaxation because of its origin in the interactions of the spins with their surroundings (Eq. 1-3 and Figure 1-1)

$$M_z = M_0(1 - e^{-t/T_1}) \qquad \text{Eq. (1-3)}$$

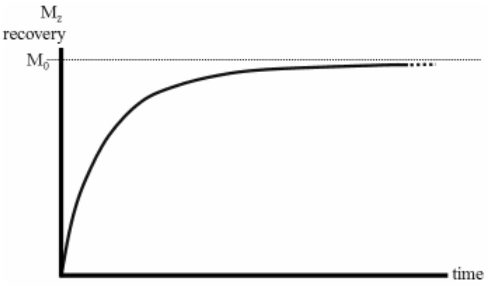

Figure 1-1: Graphical representation of T_1 recovery curve.

At the same time after the RF pulse or signal, M_{xy} component present in the xy-plane decreases to its equilibrium value of zero due to dephasing of the signal; this process is called transverse or spin-spin relaxation because its origin in the spin-spin characterized by T_2, the time required for the M_{xy} component to return to its initial value of zero (Eq. 1-4 and Figure 1-2) where TR is the time between two successive RF pulses and $e^{-t/T2}$ is the spin-spin decay factor characterized by the time constant T_2.

$$M_{xy} = M_0(1 - e^{-TR/T_1})e^{-t/T_2} \qquad \text{Eq. (1-4)}$$

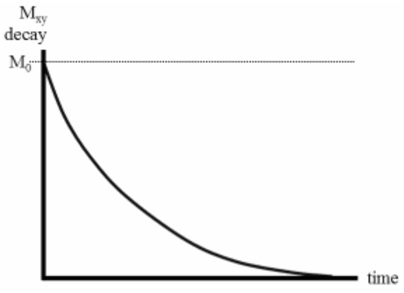

Figure 1-2: Graphical representation of T_2 decay curve.

In practice there are two factors which contribute to the decay of transverse magnetization, molecular interactions and distortions in the homogeneous external magnetic field B_0. Combination of these two is called as time constant T_2* (Eq. 1-5).

$$\frac{1}{T_2^*} = \frac{1}{T_2} + \frac{1}{T_{2inhomo.}} \qquad \text{Eq. (1-5)}$$

Thus the contrast observed in MRI is dependent on the combined magnetic moment M and hence on the spin density of nuclei under study, T_1 and T_2 (T_2*).[2]

Despite having a number of advantages MRI has low sensitivity, which can be overcome by using the contrast agents (CAs), paramagnetic diagnostic magneto-pharmaceuticals. The pioneering work of Bloch and Lauterbur began the use of contrast agents in the MRI to enhance the image contrast for a better understanding of physiological and pathophysiological events.[3, 4] Over the last couple of decades the field has matured with a significant number of applications in humans. Up to 45% of all clinical MRIs were performed using CAs.[5] This also generated a tremendous amount of interest in the scientific community regarding the function of these agents and their application *in vivo*.

Paramagnetic CAs alter the relaxation rate of local water protons which is reflected by a change in the intensity of the MRI signal. The signal intensity increases with an increase in longitudinal relaxation rate, R_1, ($R_1=1/T_1$) and decreases with increasing transverse relaxation rate, R_2, ($R_2=1/T_2$). The T_1-weighted images are obtained by using the pulse sequences which focuses on R_1 at the same time T_2-weighted images are obtained from R_2. CAs are categorized according to the extent by which they alter R_1 as well as R_2. Gd and Mn based agents have a more profound effect on R_1 hence they are used to enhance T_1 weighted images, where as systems such as iron oxide nanoparticles are used to enhance T_2 weighted images.

1.3 Classification of CAs

CAs can be classified different ways according to their biodistribution and image enhancement properties. In terms of biodistribution agents can be classified as extracellular, blood pool or organ specific, they are also categorized according whether they predominantly shorten T_1 or T_2 times as T_1 and T_2 agents respectively.[2] Furthermore, according to their magnetic properties they can be categorized as i) superparamagnetic and ii) paramagnetic contrast agents.

1.3.1 Superparamagnetic contrast agents

Water soluble crystals of iron oxide such as Magnetite (Fe_3O_4) or Maghemite (γ-Fe_3O_4) have been used as superparamagnetic CAs. The core diameter is in the range of 4–10 nm. In such crystals iron ions (Fe^{2+} or Fe^{3+}) are magnetically ordered and contribute to the net magnetic moment of particle. Known as superparamagnetism, this leads to a remarkable shortening of T_2 or T_2* relaxation times resulting into darkening of the MR image (T_1 is also shortened but focus remains on T_2 effects because of larger change in magnitude). These CAs are generally used as intravascular or blood pool agents as they mainly reside into the intravascular space. To avoid aggregation and to enhance their biodistribution, particles are coated with biodegradable and non-toxic material. Iron oxide particles can be further subdivided as monocrystaline iron oxide nanoparticles (MION) with a mean diameter less than 20 nm, ultrasmall iron oxide particles (USPIO) with mean diameter less than 50 nm and superparamagnetic iron oxide (SPIO) refers to iron oxide cores with mean diameter greater than 50 nm.[2, 6-8]

These particles are popular because of two main reasons 1) In T_2-weighted images they give the most change in signal per unit of metal ion $Fe^{2+}/Fe^{3+}$and 2) the presence of biodegradable iron leads to non-toxic CA for *in vivo* imaging since the iron can be metabolized in the biochemical pathways of the cells. In addition, easy synthesis by controlled precipitation of iron oxide in an aqueous solution of Fe^{2+}/Fe^{3+} and coating material can produce quantitative amounts of material. Long vascular half-life and the absence of extravascular leakage are also attractive features of these agents. Using different coating material, particles can be manipulated for specific functions and targets. Dextran coated iron oxide particles are used for the visualization of the vascular or central nervous system as well as to identify malignant lymph nodes, liver tumors and brain tumors. *In vivo* monitoring of gene-expression, stem cells is possible using superparamagnetic iron oxide nanoparticles.[9] Feridex, I. V. is the contrast agent approved by U.S. Food and Drug Administration (US-FDA) for clinical usage for the evaluation of lesions of the liver.[10, 11]

1.3.2 Paramagnetic contrast agents

Generally gadolinium (Gd^{3+}) and manganese (Mn^{2+}) complexed in organic multidentate ligands are used as paramagnetic CAs. They are chosen because of their useful magnetic properties arising due to presence of unpaired electrons in their outermost shell. Mn^{2+} has five unpaired electrons while Gd^{3+} has seven unpaired electrons in 3d and 4f orbitals respectively. Long electronic relaxation time, τ_{1e}, plays critical role in selection of these metals and the presence of high number of unpaired electrons in outer electronic shell provides enough long electronic relaxation time. Compared to Mn^{2+} complexes, Gd^{3+} complexes have been extensively used in research and clinics. Gd^{3+} is favored over other lanthanide metal ions such as Dy^{3+} or Ho^{3+} despite having higher magnetic moment, due to their asymmetric ground state. Approximately 95% of total contrast enhancement MRI experiments in clinics were performed using Gd^{3+} based CAs.[12] But Gd^{3+} ion have high toxicity, uncontrolled biodistribution as well as involvement in blocking of certain ion channels which prohibit being administered directly *in vivo*. For example, aqueous Gd^{3+} has LD_{50} (LD_{50} = is the measure of toxicity, dose that causes death in 50% of the animals) in the range of 0.1–0.2 mmol/Kg to small animals. Toxicity arises due to the comparable ionic radii of Gd^{3+} to Ca^{2+} (1.2 and 1.1 Å respectively)[13] which interferes with the Ca^{2+} signaling channels. Therefore it is necessary to administer Gd^{3+} in the form of complexes formed with multidentate organic ligands with a coordination number of either eight or nine (CN 8 or 9), to ensure high stability and reduce toxicity dramatically.[2, 13] Few Gd^{3+} based CAs have been approved by US-FDA over the years in clinical application. These are low molecular weight, and non-specific extracellular agents. Gd^{3+} encapsulated in polyaminocarboxylate containing organic molecules such as DTPA (diethylenetriaminepentacetate), DOTA (1,4,7,10-tetraazacyclododecane-1,4,7,10-tetraacetate) and their derivatives (Figure 1-3). DTPA and DOTA form thermodynamically and kinetically stable complexes with Gd^{3+}. The thermodynamic stability constant for Gd-DTPA and Gd-DOTA are $\log K_{GdL}$ = 22.1 and 25.6 respectively.[14] Normally derivatization of DTPA reduces its stability but it is still considered safe *in vivo*. Kinetic inertness is also crucial, Gd(DTPA-BMA) has a high stability at logK_{GdL}>18, but it is kinetically labile especially in acidic environment and has resulted in conditions such as nephrogenic systemic fibrosis.[15]

In addition to optimal contrast enhancement an ideal CA should possess additional properties such as high water solubility, rapid clearance from body, high thermodynamic and kinetic stability, suitable pharmacokinetics, low toxicity etc. These all essential constraints should be considered while designing a paramagnetic contrast agent.[16] The ability of CA to shorten T_1 and T_2 is expressed in terms of relaxivity r_1 and r_2 respectively. This is direct measure of efficiency of the CAs (Eq. 1-6) where $T_{1,2dia.}$ is relaxation time of the solvent (water) in absence of paramagnetic species generally called as diamagnetic contribution which is constant for water, C is concentration of paramagnetic probe.

$$\frac{1}{T_{1,2}} = \frac{1}{T_{1,2dia.}} + r_{1,2} \bullet C \qquad \text{Eq. (1-6)}$$

If one plots a $1/T_{1,2}$ versus concentration of paramagnetic species, a straight line is obtained with slope equal to relaxivity r_1/r_2, with units $mM^{-1}s^{-1}$. Hence relaxivity, r_1/r_2 is directly proportional to the concentration of paramagnetic probe. This is valid only for dilute solutions of the probes, in the absence of intermolecular interaction of probes. Paramagnetic chelates influence the relaxation of water protons by dipole-dipole interaction between the nuclear spins and the fluctuating local magnetic field originated from unpaired electron spin. The distance between the paramagnetic metal ion and water molecules is inversely proportional to transmitting the paramagnetic effect.

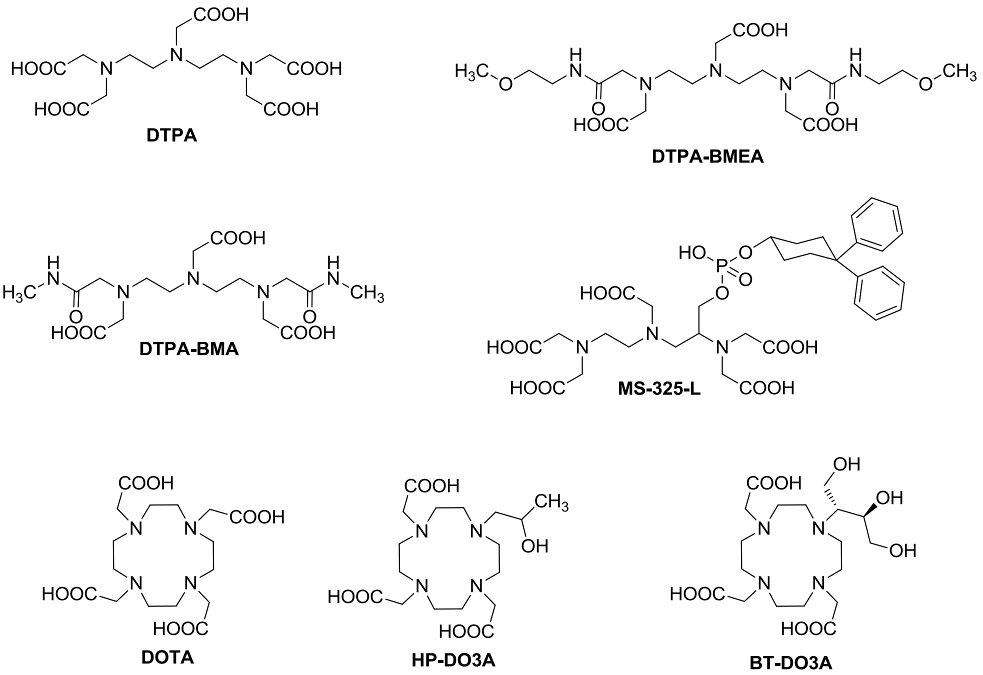

Figure 1-3: Commonly used ligands for Gd^{3+} chelation for clinically approved Gd(III) contrast agents.

Three different types of interaction between the paramagnetic species and water molecules contribute to the total relaxation.The inner sphere water molecules which directly bind to the metal ion in the inner coordination sphere and exchange with the bulk solvent. Some hydrophilic parts of the chelate form hydrogen bonds with water molecules and increase their residence time in second coordination sphere. Moreover water molecules of bulk experience paramagnetic effect, when they diffuse in the surroundings of paramagnetic species in outer coordination sphere. This effect is called as outer-sphere relaxation. Therefore relaxivity is expressed as the combined effect of inner sphere and outer sphere relaxation (Eq. 1-7). where *IS, SS* and *OS* in superscripts stands for inner sphere, second sphere and outer sphere respectively.[17]

$$r_{1,2} = r^{IS} + r^{ss} + r^{OS} \qquad \text{Eq. (1-7)}$$

The longitudinal inner-sphere relaxation rate can be obtained from Eq. 1-8; in this equation P_m is the mole fraction of solvent coordinated to the metal ion, τ_m is mean water residence time and T_{1m} is relaxation time of the bound water protons.

$$\frac{1}{T_1} = P_m \frac{1}{T_{1m} + \tau_m} \qquad \text{Eq. (1-8)}$$

The value T_{1m} can be obtained by using Solomon-Bloembergen-Morgan (SBM) [18-20] theory by following Eq. 1-9, where γ is the proton gyromagnetic ratio, g is the electronic g-factor, *S* is the total electron spin of the metal ion, μ_B is the Bohr magneton, *r* is the proton-metal ion distance, ω_S and ω_H are the electronic and proton Larmor precession frequencies, respectively.

$$\frac{1}{T_{1m}} = \frac{2\gamma^2 g^2 S(S+1)\mu_B^2}{15r^6}\left[\frac{3\tau_{c1}}{1+\omega_H^2\tau_{c1}^2} + \frac{7\tau_{c2}}{1+\omega_S^2\tau_{c2}^2}\right] \qquad \text{Eq. (1-9)}$$

The molecular correlation time, τ_c, is determined by following parameters: rotational correlation time τ_R, the electronic correlation time τ_{ie}, and the proton residence time τ_m (Eq. 1-10) where *i* = 1, 2.

$$\frac{1}{\tau_{ci}} = \frac{1}{\tau_R} + \frac{1}{\tau_{ie}} + \frac{1}{\tau_m} \qquad \text{Eq. (1-10)}$$

The theory in the abovementioned equations demonstrates that optimizing a number of microparameters is necessary to obtain high relaxivities r_1/r_2, such as increasing the hydration number *q*, optimization of distance between metal ion and proton, decreasing the proton residence time, increasing the rotational correlation time, electronic relaxation times and strength of applied magnetic field. These parameters directly or indirectly contribute in inner- and outer-sphere relaxation mechanism (Figure 1-4). Optimization of such parameters would increase the efficacy of the CA, lowering required dose for the same signal. In addition to enhancing the signal, tuning of parameters allowed scientists to design smart or responsive contrast agents (SCA) (see below). Among all the parameters the hydration number *q*, rotational correlation time τ_R, and residence time of the proton τ_m can be most readily altered.

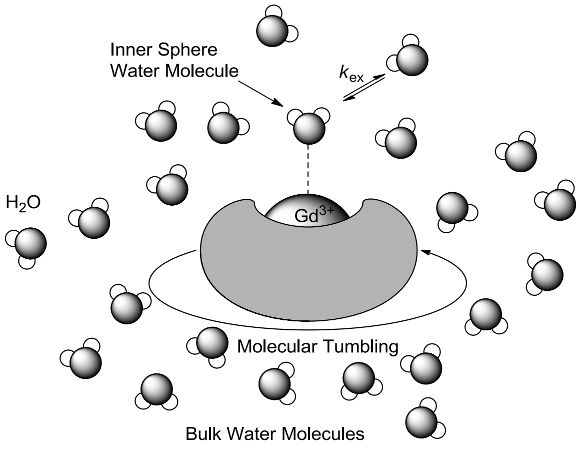

Figure 1-4: Schematic representation of factors contributing towards the relaxivity of CA. Monoaqua complex of Gd^{3+} is shown; $q = 1$ and $\tau_m = 1/k_{ex}$.

1.4 Tunable molecular parameters contributing to longitudinal relaxivity

1.4.1 Hydration number, *q*

Hydration number q is the number of water molecules directly bond to the paramagnetic metal ion. It has profound influence on inner-sphere relaxation mechanism as relaxivity increases with increase in q. But increasing hydration number may have adverse effect on the thermodynamic and/or kinetic stability of complex. In addition formation of ternary complexes with endogenous anions (carboxylates or phosphates, present in high concentrations *in vivo*) significantly reduces the signal from of bishydrated complexes. Hence it is necessary to balance both stability and q while designing CA. Note all clinically approved CAs are mono-hydrated, for example $[Gd(DTPA)(H_2O)]^{2-}$ and $[Gd(DOTA)(H_2O)]^{-}$. Despite these issues, Raymond and co-workers introduced new bishydrated ligands based on TREN-HOPO (tris(2-aminoethyl)amine-hydroxypyridinone).[21] This type of complexes have q =3 with good stability and low affinity towards the endogenous anions. Aime *et al*. reported novel heptadentate ligand the 6-amino-6-methylperhydro-1,4-diazepine-1,4,N^6,N^6-tetraacetate (AAZTA) (Figure 1-5).[22]

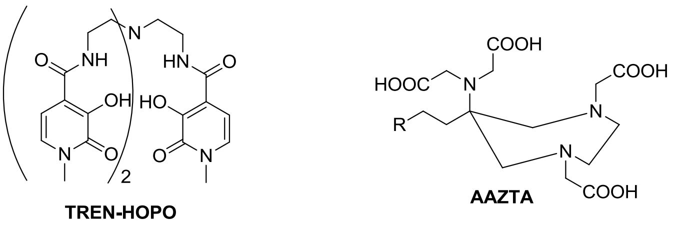

Figure 1-5: Structure of ligands for Gd(III) complexes with q=2.

In research, a derivative of DOTA, DO3A (1,4,7,10-tetraazacyclododecane-1,4,7-tricarboxylic acid) is widely used for Gd^{3+} chelation, where the free amine site could be utilized to install a number of useful linkers to modify the application of agent. The stability is good ($\log K_{GdL} > 20$) with hydration number q=2.[23] Formation of ternary complexes with endogenous anions such as carbonate, phosphate, citrate or even coordinating functionalities of proteins reduces the *in vivo* relaxivity of these type of complexes.[24]

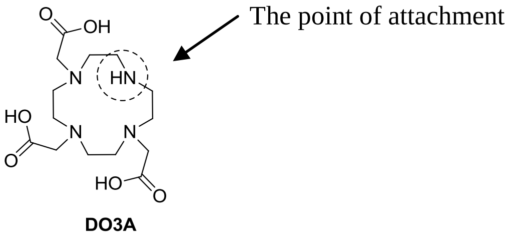

Figure 1-6: Structure of DO3A ligand.

The determination of hydration number provides an insight to understanding the mechanism of relaxivity change. Many experimental techniques are extensively used for this purpose. Joop Peters and co-workers[25] reported Dy^{3+} induced shifts of ^{17}O in directly bond $H_2{}^{17}O$ in NMR. The slope of straight line in between ^{17}O shift and chelate concentration directly measures the q. The authors used $[Dy(H_2O)_8]^{3+}$ as reference with known number of directly bond water molecules for calculations.

In another approach Horrocks *et al*[26, 27] devised the laser-induced luminescence method to determine hydration number. They have obtained hydration number; relating difference in luminescence life time measurement in H_2O and D_2O solution of Tb^{3+} or Eu^{3+} complexes. The equation used in this technique is recently revised[28, 29] with correction factor for outer sphere effects which is 0.25 for Eu^{3+} (Eq. 1-11) where A' is proportionality constant specific to given lanthanide ion and τ is luminescence lifetime. They have also correlated the number of directly bound water molecules from the crystal structure with the difference in the lifetimes in H_2O and D_2O

$$q = A'(\tau_{H_2O}^{-1} - \tau_{D_2O}^{-1} - 0.25) \qquad \text{Eq. (1-11)}$$

These methods are indirect as Ln^{3+} complexes were investigated other than Gd^{3+} complexes. More recently Caravan *et al.*[30] investigated new method with use of pulsed ^{17}O Mims electron–nuclear double resonance (ENDOR) spectroscopy for the direct determination q of Gd^{3+} complexes. Spectra of metal complexes in frozen aqueous solutions at approximately physiological concentrations can be obtained either in the presence or absence of protein targets.

1.4.2 Rotational correlation time, τ_R

The longitudinal relaxivity values of Gd^{3+} complexes increases with increase in the τ_R. But this phenomenon is field dependant and occurs most efficiently between the Larmor frequencies of 10–70 MHz when τ_m is in between 10–50 ns. Above this field strength (>100 MHz) different mechanism follows. Here shorter τ_m is more important (<10 ns) with intermediate values of τ_R.[31] Different types of strategies are used to slow down the rotation of Gd^{3+} complexes such as i) covalently attachment of complexes to macromolecules such as spherical dendrimers, linear polymers etc. In one of the example Gd^{3+} complexes conjugated to PAMAM(polyamidoamine) dendrimers of 1st to 4th generation were studied. The relaxivities were almost doubled over 1st generation to 4th generation of dendrimer but to a lesser extent than expected.[32] In another study a Gd^{3+} complex attached to the modified dextran polymer revealed minimal increase in the relaxivity despite the large increase in molecular weight. This could be caused due to movement of the polymer chain or flexibility of linear polymer. Hence more rigid macromolecules are required to achieve optimum value of relaxivity.[33] ii) In different approach non-covalent bonding of the complex to protein like serum albumin is used to slow down the rotation. Clinically used MS-325 (Figure 1-3) attached to human serum albumin (HSA) using a hydrophobic diphenylcyclohexyl moiety increases the relaxivity up to 8 fold at 20 MHz and 37 °C.[34] Merbach and coworkers reported longitudinal relaxivity 15.8 $mM^{-1}s^{-1}$ at 200 MHz, 37 °C. Self-assembled $Fe[Gd_2bpy(DTTA)_2(H_2O)_4]_3^{4-}$ agent displayed four times higher *in vivo* relaxivity than commercially available GdDOTA (Figure 1-7).[35] Even though it is crucial parameter, there is no direct method to measure τ_R. It can be obtained by fitting the data from ^1H NMRD (nuclear magnetic relaxation dispersion) curves. ^2D or ^{13}C relaxation measurement on the ligands or electron paramagnetic resonance (EPR) spectra of vanadyl (VO^{2+}) can also be used.[2]

1.4.3 Residence time of the coordinated water/proton, τ_m

The residence time of water and proton is same at around neutral pH. Increasing acidity or basicity of the solution catalyses proton exchange faster and enhances it.[36, 37] Optimal value of τ_m is dependent on magnetic field strength and τ_R of the complex. τ_m should be as short in the range of 10–30 ns for macromolecular CAs at 60 MHz or 1.5 T. For higher field applications 1–10 ns will be more suitable.[31] This phenomenon can be determined by variable temperature or pressure ^{17}O NMR relaxation rate measurements.[2]

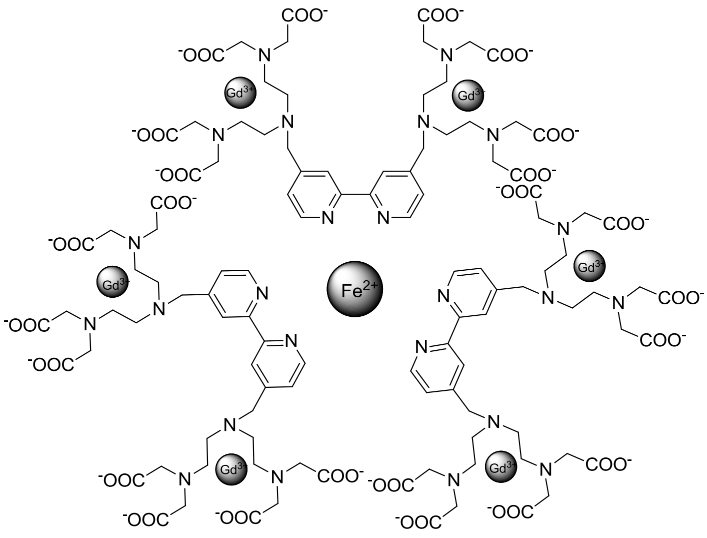

1-1

Figure 1-7: Schematic structure representation of mettalostar $[Fe[Gd_2bpy(DTTA)_2(H_2O)_4]_3]^{4-}$.

Complex charge, solvent accessibility, steric effects around water binding site of complexes, abundance of isomers are key factors that affect the value of τ_m. Negatively charged Gd^{3+} complexes of DOTA or DTPA-like ligands demonstrate shorter τ_m than corresponding neutral or positively charged species. The amide substituent also influences τ_m. Square antiprismatic (SAP) or twisted square antiprismatic (TSAP) isomers observed in Ln(DOTA) complexes and their derivative have different τ_m values. Reports display 10–100 times faster water exchange for TSAP isomer over SAP. Therefore structures that favor one isomer over the other will have consequences for the residence time.[2, 17, 38]

The mechanism of exchange of water involves either an associative, dissociative process or interchange processes too. In case of bishydrated ligands the associative mechanism shortens the τ_m. For example HOPO or AAZATA based complexes have τ_m in the range of nanoseconds.[22, 39]

Besides these parameters second-sphere parameters has significant role in relaxivity. There are examples of complexes without inner-sphere water complexes that show relaxivity as high as monohydrated commercial agents. DOTA like complexes with four phosphoric acid arms have second-sphere as well as outer-sphere water which contributes to the relaxivity.[40] This phenomenon was proved in many phosphoric acid containing DO3A based Gd^{3+} complexes which display higher relaxivity than DOTA analogue.[41] But it is difficult to predictively alter outer-sphere water hence it was not utilized in designing responsive contrast agents.[2]

In order to generate new types of contrast agents which not only will enhance anatomical images but also report the molecular or cellular events *in vivo*, smart (responsive) contrast agents (SCAs) are currently being developed that alter their MR signal, through modification of one or more of the abovementioned parameters.

1.5 Smart Contrast Agents

SCAs display changes in relaxivity with changes in its microenvironment. This change in relaxivity r_1 can be obtained by tuning one of the previously mentioned parameters such as q, τ_m or τ_R. Field independent large relaxivity changes can be achieved by altering hydration number. The functional group of the ligand interacts differentely causing change in hydration number leads to changes in relaxivity value. In another approach researchers slowed down the rotation of CAs in solution attaching them to macromolecules such as peptides, proteins, dendrimers, different biomolecules etc. Here special attention is essential as slower rotation would result in decrease in τ_m which would compensate the relaxivity change. Few examples of the SCAs are demonstrated in following sections with more detail discussion in case of pH activated and Ca^{2+} responsive SCAs in following chapters.

1.5.1 pH activated smart contrast agents

Change in the local pH in living organism is generally sign of pathological disorders. Tumor tissues display slightly acidic pH (pH 6.8—6.9) when compared to normal tissues.[42] This necessitates the development of different methods to accurately measure pH in living animals for early diagnosis of the malignant tissues. Acid/base ionization properties of certain functional groups of organic molecules attached to the ligand are utilized in a general approach to design pH-sensitive CA. Depending on protonation state of these functional groups; they are coordinate or decoordinates with Gd^{3+} metal center resulting into relaxivity change. Several pH responsive contrast agents have been reported by number of research groups.[23, 43, 44] Sherry and coworkers published the first pH sensitive MRI contrast agent **1-2** in 1999 (Figure 1-8).[45] Following it, a number of pH sensitive CAs were studied in *in vivo* model environments. Evolution and application of these agents is discussed in detail in chapter 2 (see below).

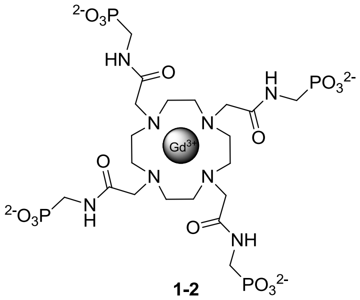

1-2

Figure 1-8: Chemical structure of pH sensitive contrast agent.

1.5.2 Cation sensitive smart contrast agents

Metal ions play crucial role in growth and development of living organisms. But irregularities cause number of acute diseases such as diabetes, certain neurodegenerative diseases. To better understand a number of physiological events particularly in the brain it is essential to understand the metal ion concentration *in vivo*. Number of MRI based probes to detect metal ions such as Ca^{2+}, Zn^{2+},$Cu^{+/2+}$, $Fe^{2+/3+}$ have been developed and studied.[23, 46-48] Selectivity for one particular metal ion over others, endogenous anions or biomolecules is most important criteria which should be considered while designing such probes. Binding affinity of metal ion to CA or its biocompatibility are other critical aspects to consider when designing CA. Incorporating calcium binding unit (DOPTA ligand system) in between two Gd-DO3A macrocycles, T. Meade and coworkers published the first Ca^{2+} sensitive in 1999.[49] Relaxivity increased from 3.3 $mM^{-1}s^{-1}$ to 5.8 $mM^{-1}s^{-1}$(75%, at 500 MHz, 25 °C, **1-3**). In the absence of Ca^{2+} carboxylic acid arms of BAPTA or APTRA derivatives

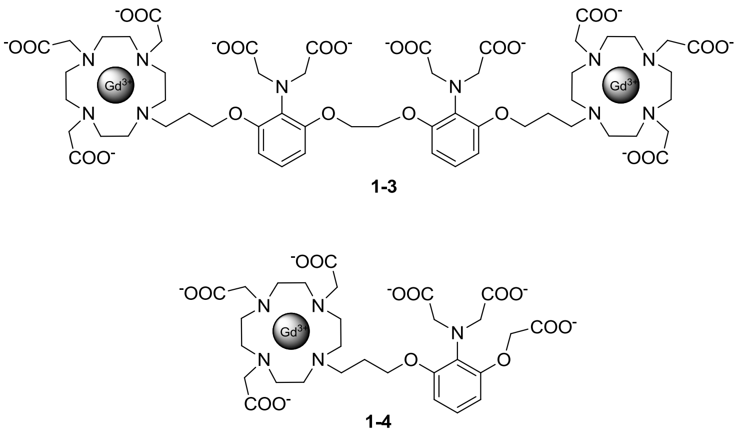

1-3

1-4

Figure 1-9: Representative example of Ca^{2+} sensitive contrast agents

coordinate to the Gd^{3+}, hindering the access of metal ion to water. But in presence of Ca^{2+} these carboxylates coordinate to Ca^{2+} leaving open access to water to Gd^{3+}. This phenomenon yielded changes in *q*, and hence relaxivity. Moreover our laboratory reported excellent changes in relaxivity exploring different types of ligand system to bind Ca^{2+}.[50-56] Ca^{2+} ion sensitive CAs are discussed in more detail in following chapter 3 (see below).

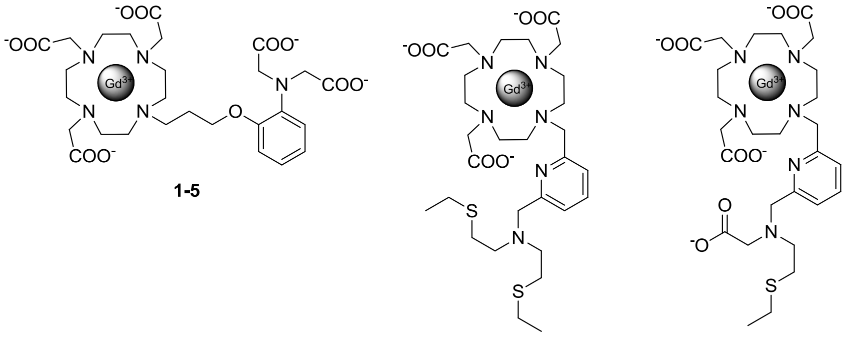

1-5

1-6

1-7

Figure 1-10: Representative examples of Cu$^{+/2+}$ sensitive contrast agents

A number of copper sensitive CAs have been studied by the group of Christopher Chang. Gd-DO3A derivatives with Cu$^{2+/+}$ binding moieties such as iminodiacetate derivative or thioether derivatives are utilized (Figure 1-10). Gd-DO3A with iminodiacetate derivative **1-5** displayed a 41% increase in longitudinal relaxivity from 3.76 mM^{-1}s^{-1} initial to 5.29 mM^{-1}s^{-1} (400 MHz, 25 °C) on addition of Cu^{2+}. The binding affinity to Cu^{2+} was in the micromolar range (K_d = 167 µM). This agent has selectivity to Cu^{2+} over other biological relevant metal ions except Zn^{2+}. With the addition of a 10 fold excess of Zn^{2+} authors observed change in relaxivity which is important finding since *in vivo* Zn^{2+} will interfere in assigning of Cu^{2+} ion concentration.[57] In an attempt to improve the selectivity over Zn^{2+}, incorporation of thioethers in Gd-DO3A **1-6** for binding to copper ions resulted not only in better selectivity over Zn^{2+} to Cu^{+} but relaxivity increased from r_1 = 1.5 mM^{-1}s^{-1} to 6.9 mM^{-1}s^{-1} (60 MHz, 37 °C) upon addition of one equivalent of Cu^{+}. The K_d values are reported in the picomolar range. Change in q from 0 to 2 was the responsible for relaxivity change revealed from dysprosium induced ^{17}O shift experiments and NMRD fitting profiles. Incorporation of one carboxylate on copper binding unit, **1-7**, led to binding affinity of Cu^{2+} over Cu^{+} in femtomolar range.[58]

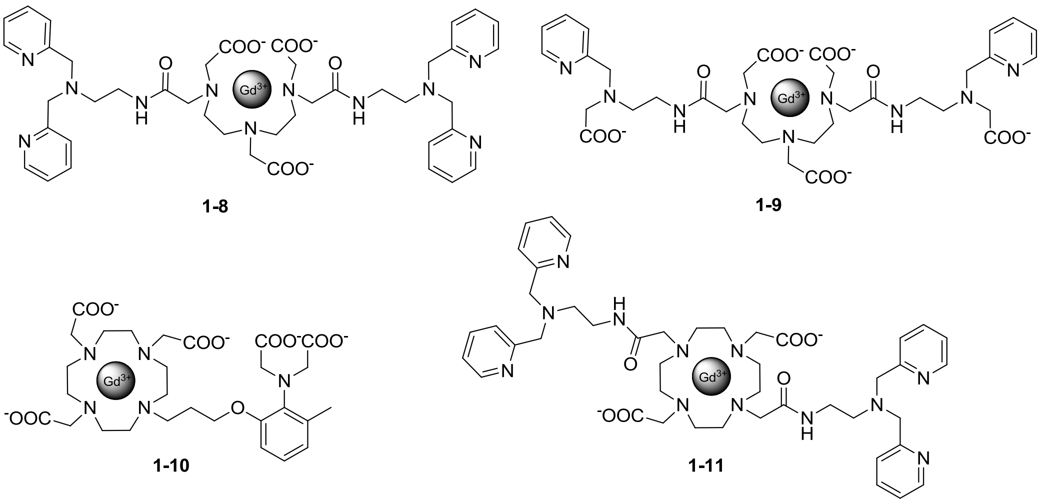

Figure 1-11: Representative examples of Zn^{2+} sensitive contrast agents.

A series of Zn^{2+} sensors were synthesized and studied by number of research groups. Initially Nagano's group reported two Gd-DTPA based Zn^{2+} sensors. These sensors have good selectivity over other metal ions. These are based on the turn-off principle means as upon addition of Zn^{2+} metal ion the relaxivity decreases from its initial value. A probe was reported with a DTPA derivatives in between two picolylamine units (Figure 1-11). In **1-8** the relaxivity decreases from 6.06 to 3.98 $mM^{-1}s^{-1}$ (300 MHz, 25 °C, pH 8, 33% decrease) with addition of one equivalent of Zn^{2+} and returns to its initial value with further addition of another equiv. of Zn^{2+} ion. In **1-9** two picolyl units were replaced by acetate group. Here the relaxivity decrease is 30% with addition of one equiv. of Zn^{+2}. However the stability of these complexes was too low for further studies.[59] In another strategy a Gd-DO3A derivative with an iminodiacetate moiety was linked via propyl and ethyl linkers. The results revealed an increase in r_1 from 2.3 to 5.1 $mM^{-1}s^{-1}$ (60 MHz at 37 °C, 121%) with addition of one equivalent of Zn^{2+} in the complex with propyl linker **1-10**. This agent was sensitive towards Cu^{2+} too, since upon addition of 1 eq. of Cu^{2+} there was change in relaxivity from 3.1 $mM^{-1}s^{-1}$ to 5.1 $mM^{-1}s^{-1}$ (60 MHz, 37 °C). Sensitivity to Ca^{2+}, Mg^{2+} was not observed. The observed relaxivity change was a direct outcome of an increase in q from 0.3 to 1.0 in absence and presence of Zn^{+2} respectively. Moreover the binding constant ($\log K_A = 3.6$) was in suitable range to utilize the agent *in vivo*.[60] The complex with ethyl linker was almost insensitive to the addition of Zn^{2+}. Sherry and coworkers used Gd-DOTA-BPEN **1-11** as a Zn^{2+} sensor. At 23 MHz and 37 °C, a 20% change in relaxivity was displayed with binding constant $\log K_A = 7.5$. Titrations in the presence of HSA showed a 165% change in r_1 at 23 MHz, a result of binding to HSA in presence of Zn^{2+} which increases the τ_R value. There are reports of potassium and magnesium responsive probes too.[61, 62] Supramolecular heterobimetallic Fe-Gd complexes have been reported.[63-66] These CAs have not designed as responsive CAs but to increase the relaxivity decreasing rotational correlation time τ_R (see above).

1.5.3 Enzyme activated smart contrast agents

Enzymes are highly specific biomolecules which catalyze a number of biochemical processes. It is of profound importance to understand where specific enzymes localize and how they function within the body or cells. Extensive attempts have been made to understand a number of enzyme processes such as bond cleavage which in turn results into change in relaxivity of CA. The general approach exploited was either q change or change in affinity towards specific proteins such as HSA to slow down tumbling of CA. The first example was studied by Meade and coworkers. A Gd-DOTA complex bearing a β-galactopyranose unit was synthesized and studied in the presence of β-galactosidase enzyme. β-galactopyranose serves as umbrella over the Gd^{3+} inhibiting the interaction of water in absence of enzyme. β-galactopyranose is then cleaved irreversibly by the enzyme allowing water to interact with the metal ion. Hence a change in relaxivity was observed (low to high) as result of change in q during the process.[67] This complex with a slight modification was successfully employed in visualization of gene expression *in vivo* using MRI.[68] The same group also extensively studied oncologically significant β-glucuronidase activated Gd-DO3A type of CA.[69] A Gd-DO3A based complex **1-12** carrying pendant acetoxymethyl esters, sensitive to procine liver esterase was studied by Lowe and coworkers. This SCA showed an 84% change in relaxivity r_1 (20 MHz at 25 °C) when procine liver esterase cleaves the esters complex and transforms CA into negatively charged species, which also suppresses the carbonate binding and increases the hydration states hence relaxivity.[70] The q change was assessed by lifetime measurement of corresponding Eu^{3+} complexes. Another approach is to increase rotational correlation time τ_R using enzyme catalyzed HSA binding or polymerization known as receptor-induced magnetization enhancement (RIME). For this endeavor a Gd-DTPA conjugate with tri-lysine peptide, **1-13** and a human carboxypeptidase, thrombin activatable fibrinolysis inhibitor (TAFI) were investigated. TAFI cleaves the lysine residues and converts the complex such to bind strongly with HSA. This increased the relaxivities over 100% (20 MHz at 24 °C) by the RIME phenomenon.[71] Recently a Gd-DOTA complex with galactose protected tyrosine −OH functionality was investigated. β-galactosidase promoted cleavage of sugar moiety; the complex was polymerized by tyrosinase activated melanin which increases relaxivity in the field range of 0.5–1.5T.[72]

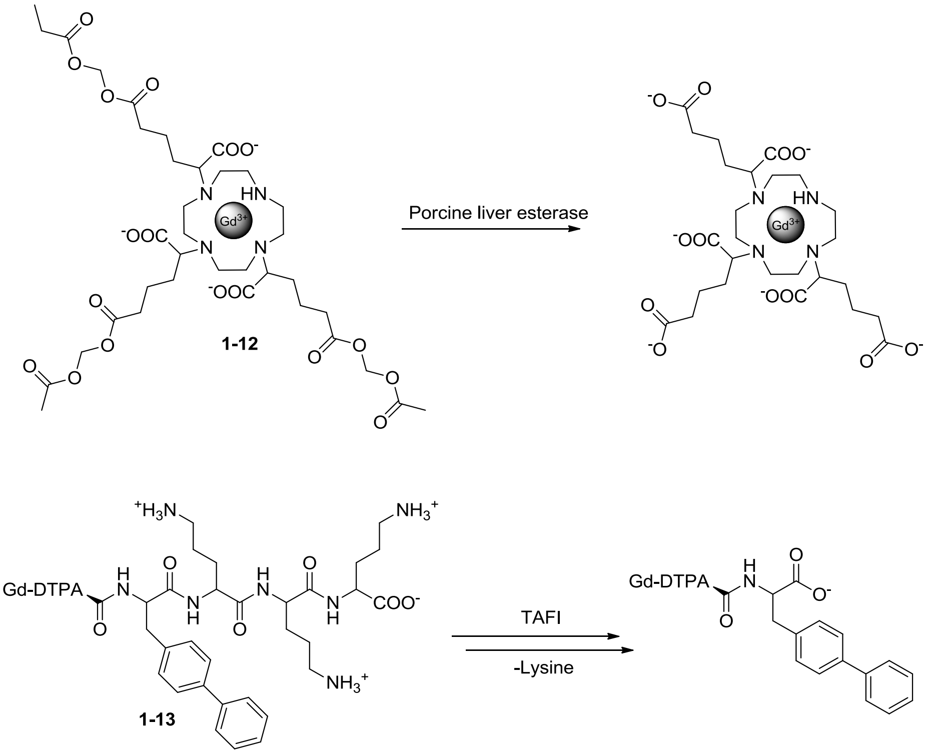
Porcine liver esterase
Gd^{3+}
1-12
TAFI
-Lysine
Gd-DTPA
1-13

Figure 1-12: Representative examples of enzyme activated contrast agent.

1.6 Aim of Project

A number of SCAs have shown remarkable signal changes in *in vitro* analysis. Despite this there are few that can proceed to the *in vivo* applications. The real challenges in this progression are a result of a more complex *in vivo* environment. Firstly, endogenous anions such as carbonate, phosphates, citrate decrease the relaxivity extensively in DO3A based SCAs forming ternary complexes.[23] Some coordinating moieties of proteins decrease free access of water unlike in *in vitro* conditions through a similar mechanism. Furthermore the diffusion over time through extracellular space of SCAs decreases its local concentration resulting in a corresponding decay of MRI signal over time. In such circumstances it is not possible to assess if the changes in the MRI signal are a direct outcome of response to biological event or simply a change in concentration of SCA or interference of endogenous anions/proteins. Moreover low target recognition, agglomeration and non-specific accumulation of SCAs in different tissues are other major obstacles in *in viv*o application of SCAs. In addition to this single imaging modality, MRI is unable to provide information on all aspects of structural and functional targeted biological phenomenon.

These obstacles could be overcome by using conjugates of SCAs with different types of functional molecules such as nanoparticles, dendrimers, liposomes, viruses, fluorescent tags, peptides, targeting vectors, antibodies etc. Another strategy can be combination of different imaging modalities such as optical or PET to assess *in vivo* concentration or structural and functional changes of probes. This approach allows the confirmation of observed biological phenomenon using an independent measurement. Most importantly in order to attach SCAs to functional molecules it is necessary to modify the current *in vitro* analyzed and potential SCAs without affecting its physico-chemical properties in particular its smart activity.

The aim of this project is to synthetically modify the recentely developed, potential SCAs without changing their physicochemical properties in order to introduce coupling unit and attach of them to the functional molecules utilizing a new coupling unit. Furthermore this hybrid will be evaluated *in vivo* in rodents and primates to track down the physiological events such as change in concentration in Ca^{2+} ion during neuronal signaling. The attempts to fulfill the aim are discussed in this thesis.

The chapter 2 focuses on the synthetic modification and characterization of DO3A based pH sensitive contrast agents appended with a phosphonate pendant arm by inserting two different types of linking units either with an aliphatic or aromatic linker with primary amine as functional group. The general idea of this project was to design a common synthetic strategy to majority of DO3A based smart contrast agents to further functionalize with ones choice. The pH sensitive agents were resynthesized with linking units, and studied its physicochemical properties using different analytical techniques such as NMR or fluorescence spectroscopy. Using newly introduced linking units, modified pH responsive agents were further attached to biotin to obtain biotinylated agents and studied with and without avidin at different pH in MRI scanner.

Chapter 3 deals with the use of newly developed synthetic strategy from chapter 2 to insert linking unit in one of Ca^{2+} sensitive agent. DO3A based bismacrocyclic complex carrying EGTA derivative in between two macrocycles as Ca^{2+} chelator has the potential for Ca^{2+} detection in neuronal signaling. This molecule has a high relaxivity response with Ca^{2+} as result of change in hydration number and selectivity over other endogenous metal ions such as Mg^{2+}. This SCA was successfully modified by the introduction of linker moiety in one of the macrocycles to couple it to functional molecules. A number of synthetic strategies were attempted to optimize the unique synthetic strategy to produce synthetically challenging bismacrocyclic ligand in large amounts with highest purity. The synthesis of complex and study of change in longitudinal relaxivity with Ca^{2+} of modified Ca^{2+} responsive agent is discussed in this chapter.

The chapter 4 describes the utilization of well established synthetic strategy by peptide chemists, solid phase peptide synthesis (SPPS) for modification of Ca^{2+} sensitive bismacrocyclic complex with two coupling units on macrocycle. This method enables the delivery of synthetically challenging ligand in a short time avoiding the difficult and time consuming purifications of intermediate compounds. Moreover this synthetic strategy would be more useful to synthesize the different synthetic analogues with slight structural changes for optimization of potential contrast agent. In this attempt aromatic linkers were added on both macrocycles that could be attached to various functional molecules for further *in vivo* application.

Chapter 2: Synthesis and characterization of pH-sensitive, biotinylated MRI contrast agents and their conjugates with avidin

2.1 Introduction

The critical role of pH in many physiological and pathophysiological events in living organisms is well established. Many of the major deadly diseases are associated with a variation in pH such as stroke, inflammation, infection, tumors, kidney failure, cancer etc. For instance many malignant tissues have a slightly acidic pH in the range of 5.85–7.68 in humans while in rodents the range is 5.80–7.52.[73] This change in pH is direct consequence of oxygen deficiency and many other essential nutrients that cause the uncontrolled growth of cells. This leads to the production of lactic acid under anaerobic conditions and the hydrolysis of ATP (adenosine-5′-triphosphate) in an energy-deficient microenvironment. Combined this leads to the acidic pH in tumors.[74, 75] Furthermore the pharmacokinetic properties of many drugs depend on the local pH that they experience.[76] Therefore, it has become of paramount importance to accurately determine the local pH in live human tissues. Many efforts have been made in this direction; some involve the use of a pH electrode by inserting it directly into tissues under study.[77] This approach is invasive and only restricted to *in vitro* analysis since such measurements in *in vivo* are complicated by an unknown component from damaged cells and blood from the ruptured capilarries.[78] Another approach is non-invasive and particularly useful for *in vivo* measurements using molecular probes that are weak acids or bases.[42, 79] These probes change their spectral properties in different pH environments which can be traced by spectroscopic techniques. Optical pH indicator dyes, EPR sensitive probes or ^{31}P NMR are generally utilized in such applications.[79-82] Although these are non-invasive, they have many limitations such as low resolution, lack of sensitivity, low depth of penetration etc.[83]

In light of the above limitations attention was moved towards the MRI technique which combines the highest spatiotemporal resolution with non invasive measurement to overcome these issues. Therefore, significant efforts have been undertaken by researchers to develop pH responsive MRI contrast agents. These SCAs contain functional groups which change their protonation state around neutral pH, such as phosphonates or arylsulphonamides. As mentioned earlier (Chapter 1), Sherry and coworkers developed the first pH responsive agent for MRI based on a tetraamide phosphonate derivative of DOTA (DOTA-4AMP), **GdL^{1}**, was reported more than a decade ago followed by DO3A derivative containing sulphonamide pendant arm (DO3A-SA, **2-1**) with different substituents on benzene ring (Figure 2-1). These SCAs contain functional groups which change their protonation state around neutral pH, the general mechanism reported involves alteration of the coordination environment around the metal center at different pH, which affects the number of proximate water molecules, resulting in a change in signal. In **1-2**, hydrogen bonds formed after protonation of the phosphonate play a crucial role catalyzing the exchange of protons between inner and outer sphere water, resulting in a change in signal as a function of pH. The mechanism of action of DO3A-SA **2-1**, is different: at acidic pH the protonation of the nitrogen allows water to approach Gd^{3+}, whereas at basic pH deprotonation of nitrogen results in its coordination to the metal center, reducing hydration number *q* and hence relaxivity by hindering the access of water molecules to the inner sphere.[84] However there is an upmost need for SCAs with a response that can be combined with additional properties such as controlled biodistribution or determination of its exact local concentration *in vivo*. Such requirements necessitate additional synthetic modifications to SCAs and therefore special attention should be given towards the changes in the physico-chemical properties of SCAs, to ensure their relaxivity changes, while crucial issues such as the kinetic and thermodynamic stability are retained. For instance, the *in vivo* biodistribution of probes varies considerably with slight changes in their structures.[85, 86]

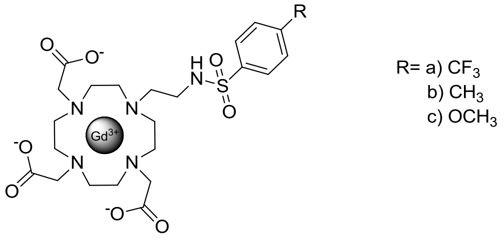

2-1

Figure 2-1: pH sensitive agent with sulphonamide pendant arm.

Proceeding in this direction, Sherry and co-workers attached a modified version of SCA **2-2** to a PAMAM G5 dendrimer to improve the MR signal by increasing the molecular weight of the conjugate (Figure 2-2).[87]

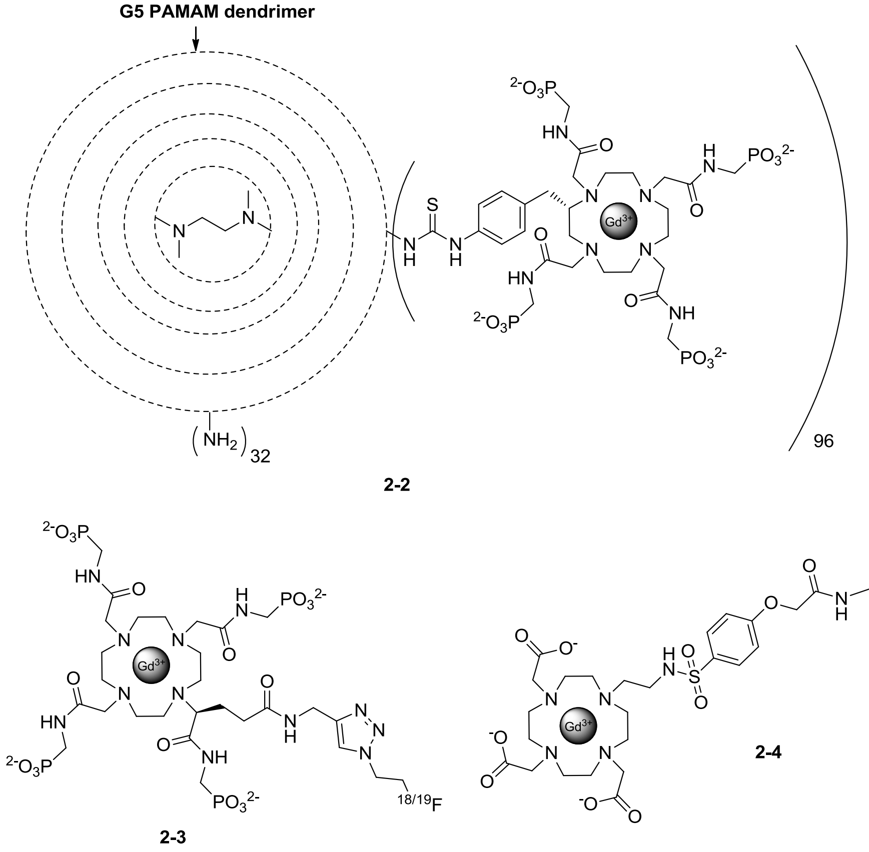

2-2

2-3

2-4

Figure 2-2: Few examples of early modifications of pH responsive probes.

The relaxivity of the conjugate increased 100% from pH 6 to pH 9.6 due to the increase in τ_R. However, due to its isoelectric point at pH ~6, this dendrimeric SCA precipitates from solution. In another approach, a dual-modal MR-PET agent **2-3** was prepared in which quantification of the local probe concentration was accomplished by the presence of the PET active ^{18}F nucleus, within the phosphonate-containing SCA, enabling pH mapping.[83] Other attempts involved modification of the sulfonamide based pH sensitive agent. Namely, the accessibility of its phenolic oxygen allowed the coupling of the functional molecule to a poly-β-cyclodextrin containing ^{19}F reporter. Here an adamantane derivative was introduced on the phenolic oxygen to achieve an effective non-covalent coupling to the poly-β-cyclodextrin, where the ^{19}F signal intensity is used to quantify the amount of SCA (Figure 2-2, **2-4**).[88] Our group recently reported a DO3A based, pH responsive probe appended with a phosphonate arm **2-5** (DO3APP, Figure 2-3).[41] It was shown that coordination of the phosphonate arm to the metal center results on a decrease in pH. In this work, we report further synthetic modifications on the propylphosphonate containing SCAs which involve the introduction of a side linker to allow the coupling of SCAs to a diverse range of functional molecules such as dendrimers, nanoparticles, proteins, peptides or fluorescent tags. Most significantly the physico-chemical properties of SCAs, in particular its response (the pH dependent r_1 changes), must be retained after coupling to the linker. Consequently, the properties of SCAs and the other functional molecules could be used together to further characterize the function of the SCAs *in vitro* and *in vivo*, broadening the scope of their application.

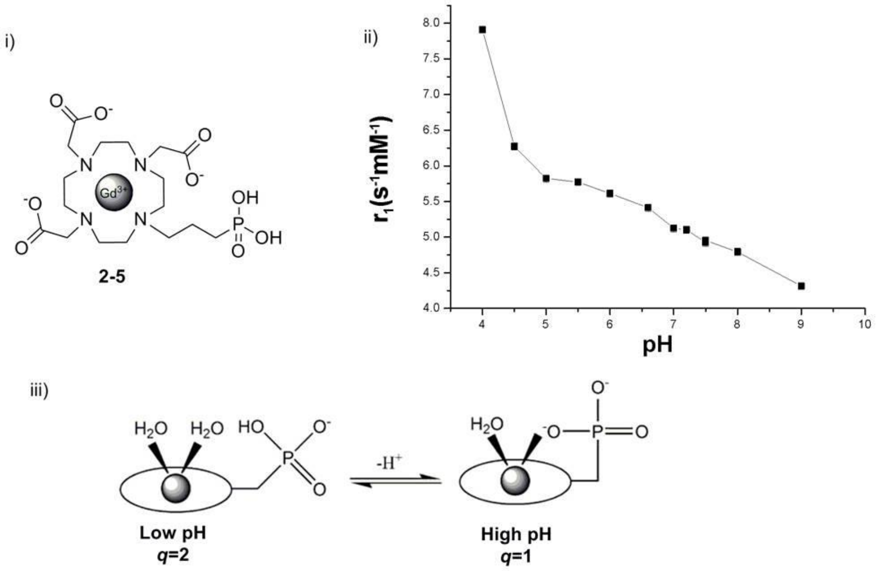

Figure 2-3: i) Structure, ii) relaxivity response to pH and iii) mechanism of action of DO3APP.

2.2 Ligand design

Keeping these objectives in mind we wanted to develop a common synthetic strategy to modify the majority of DO3A based SCAs to further functionalize them easily without losing their essential properties. Therefore we have chosen the 1,7-bis(*tert*-butoxycarbonylmethyl)-1,4,7,10-tetraazacyclododecane (bis-*tert*-butyl DO2A) derivative of cyclen in which one of the secondary amines was alkylated with linking moiety keeping the other free for the attachment of a sensor unit (Figure 2-4, top). Here we have chosen the contrast agent containing a phosphonate pendant arm as pH sensor (DO3APP). Thus we have designed two novel cyclen based ligands **L^1** and **L^2** (Figure 2-4). Their synthesis involved incorporating aliphatic (derivative of 6-aminohexanoic acid) and aromatic linkers (derivative of 4-(*p*-amino phenyl) butyric acid) onto cyclen derivatives ultimately producing ligands **L^1** and **L^2** respectively. These linkers were added on the cyclen nitrogen positioned *trans* to the propylphosphonate pendant arm, thus keeping these two pendant moieties as distant as possible to avoid any interference in the desired activity. Both linkers possess a primary amine as the terminal group, suitable for coupling to molecules containing free carboxylic acids, or electrophilic groups.

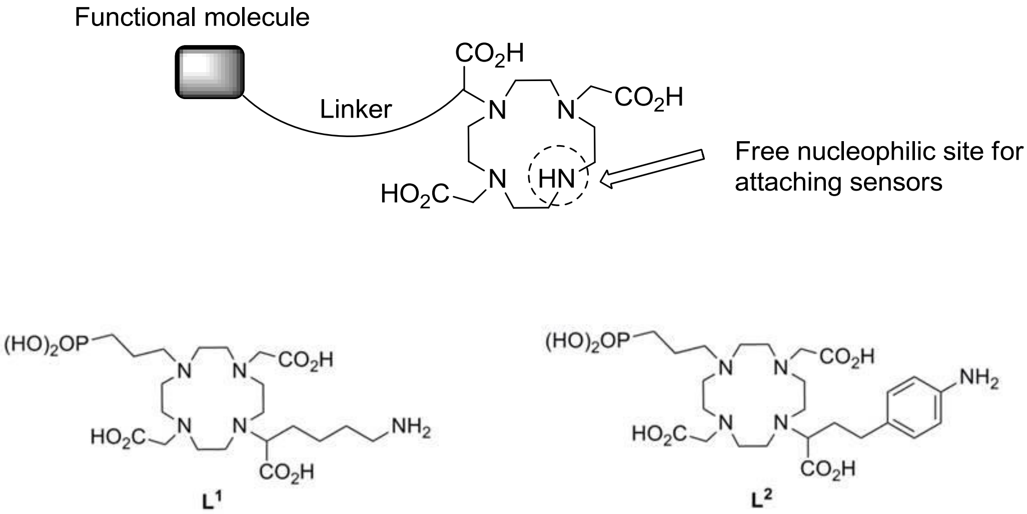

Figure 2-4: i) Schematic representation of DO3A derivative containing linker ii) Structures of designed ligands with linking units.

Moreover, the aniline group in **L^2** can be converted to an isothiocyanate to enable further coupling to molecules with free amines. To demonstrate the applicability of the newly developed SCAs, we incorporated biotin and studied the properties of the biotinylated SCAs and their avidin conjugates regarding a pH-response. The biotin-avidin system has a specific interaction with an extraordinary affinity, being stable over larger range of pH and temperatures *in vivo*.[89] This system is thus an excellent tool for the targeted delivery or accumulation of the SCA *in vivo* to boost the signal.

2.3 Results and Discussion

2.3.1 Synthesis of complexes GdL^1 and GdL^2

The preparation of **L^1** was accomplished by synthesizing aliphatic linking unit **2-8** (Scheme 2-1). 6-amino hexanoic acid **2-6** was heated with phthalic anhydride at 170 °C for 2 h which provided phthalimide protected amine with free acid **2-7**.[90] Acid **2-7** was subjected to an α–bromination in thionyl chloride and *tert*-butyl protection to afford **2-8** using an established procedure.[91] 1,7-Bis(*tert*-butoxycarbonylmethyl)-1,4,7,10-tetraazacyclododecane (bis-*tert*-butyl DO2A) **2-10** was prepared following the procedure reported previously.[92] The key reaction of the synthesis was the selective mono-alkylation of **2-10** with the newly synthesized bromide **2-8** to obtain the tris-alkylated cyclen derivative **2-11**, achieved under high dilution conditions in acetonitrile, with sodium bicarbonate. The final alkylation of **2-11** was accomplished using diethyl (3-bromo propyl) phosphonate in acetonitrile in the presence of potassium carbonate to afford **2-12** in good yields. The deprotection of amine was attempted with ethelenediamine in 2-propanol with reflux conditions and the reaction was monitored by ESI-MS analysis. A number of attempts were made to purify the resulting product **2-13** with silica, basic and neutral alumina column chromatography but due to highly polar nature of product as well as formation of number of side products, we were unable to isolate **2-13** in high purity. Therefore we have decided to change the amine protecting group, starting with the commercially available H-Lys(Z)-OH with Cbz protected amine. This was diazotized with sodium nitrite, and brominated using potassium bromide and *tert*-butyl protection of carboxylic acid with 2,2,2-trichloroacetimidate gave us similar linker **2-15** with required protected form of the amine (Scheme 2-2).[93]

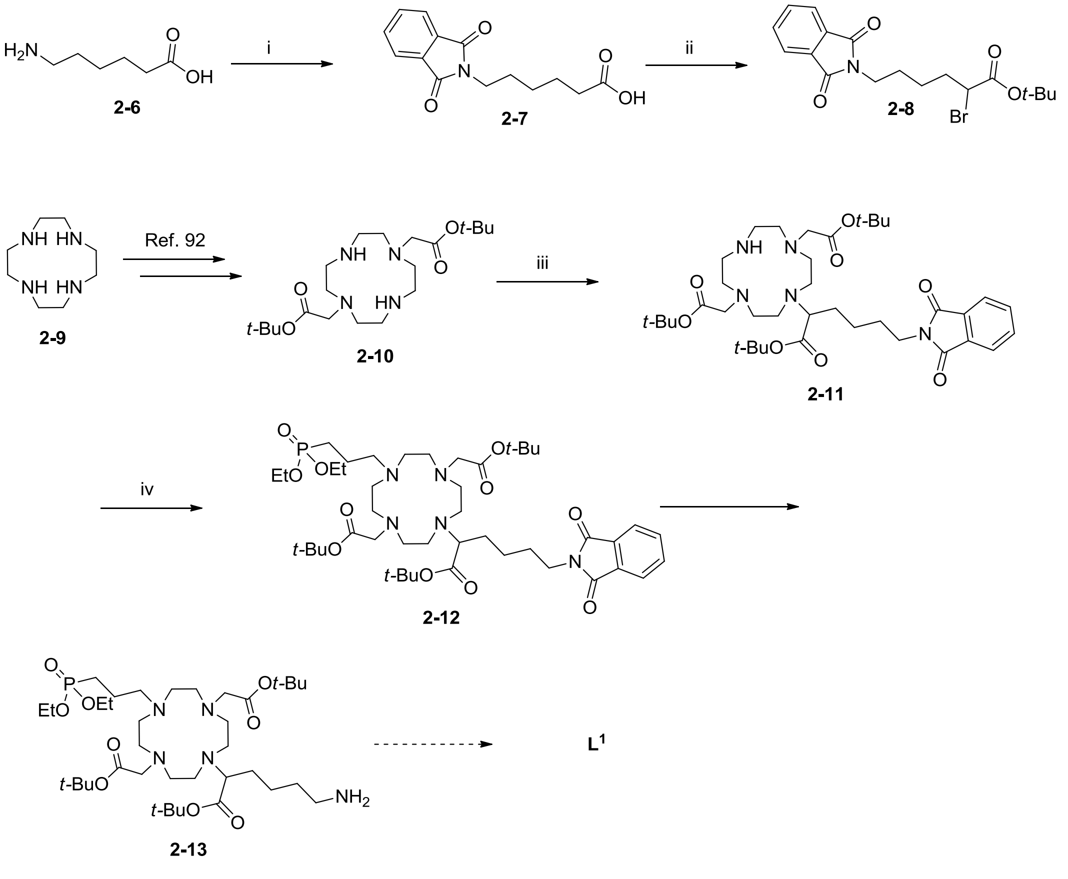
H2N
O
OH
2-6
i
O
N
O
O
OH
2-7
ii
O
N
O
O
Ot-Bu
2-8
Br
NH HN
NH HN
2-9
Ref. 92
NH N
N HN
Ot-Bu
O
O
t-BuO
2-10
iii
NH N
N N
Ot-Bu
O
O
t-BuO
t-BuO
O
O
N
O
2-11
iv
O
P
EtO OEt
N N
N N
Ot-Bu
O
O
t-BuO
t-BuO
O
O
N
O
2-12
O
P
EtO OEt
N N
N N
Ot-Bu
O
O
t-BuO
t-BuO
O
NH2
2-13
L1

Scheme 2-1: Synthesis of **LnL^1** **Reagents and conditions:** (i) Phthalic anhydride, 170 °C; (ii) $SOCl_2$, Br_2, *tert*-BuOH, TEA; (iii) **3**, $NaHCO_3$, CH_3CN; (iv) Diethyl(3-bromopropyl)phosphonate, K_2CO_3, CH_3CN; (v) Ethylenediamine, *iso*-PrOH, reflux.

At the same time the aromatic linker **2-17** was prepared according to a modified literature procedure,[70] achieving a higher yield (77% vs. 48%) than previously reported.[94] After isolating the two linkers; **L^1** and **L^2** were obtained successfully in high yields by using two similar synthetic routes. Selective mono alkylation of **2-10** in both the cases was achieved following the same procedure as already described for aliphatic linker with phthalamide protecting group. Similarly the final alkylation with diethyl (3-bromo propyl) phosphonate in acetonitrile at 70 °C on **2-18** and **2-21** gave rise to **2-19** and **2-22** respectively. Hydrogenation of **2-19** with Pd/C in ethanol provided free amine **2-20**. Treatment of **2-20** with bromotrimethylsilane and subsequently formic acid at 60 °C, yielded the ligand **L^1**. Similarly the nitro group of **2-22** was converted into the amine to produce **2-23** by hydrogenation using Pd/C as a catalyst in ethanol. Deprotection was carried out as described for **L^1** to afford **L^2**, except that TFA is used instead of formic acid. Both ligands **L^2** and **L^2** were characterized by means of ^{1}H, ^{13}C, ^{31}P NMR and HR-ESI mass spectrometry.

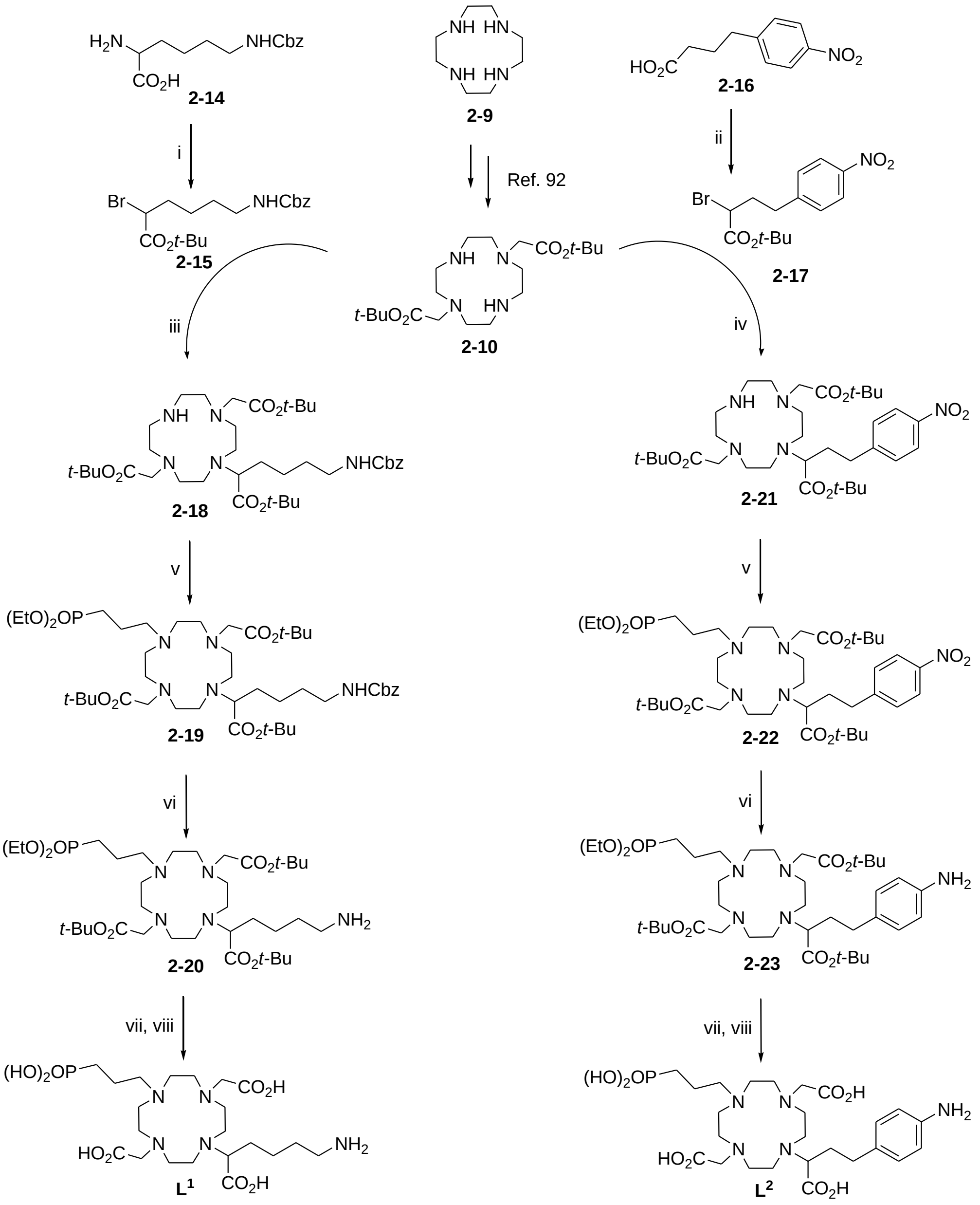
2-14
2-9
2-16
i
Ref. 92
ii
2-15
2-10
2-17
iii
iv
2-18
2-21
v
v
2-19
2-22
vi
vi
2-20
2-23
vii, viii
vii, viii
L1
L2

Scheme 2-2: Synthesis of **L**[1] and **L**[2]. **Reagents and conditions:** i) $NaNO_2$, KBr, 1N HBr, *tert*-butyl 2,2,2-trichloroacetimidate, $CHCl_3$; ii) $SOCl_2$, Br_2, *tert*-butyl 2-2-2-trichloroacetimidate, $CHCl_3$; iii) $NaHCO_3$, CH_3CN; iv) $NaHCO_3$, CH_3CN; v) Diethyl(3-bromopropyl)phosphonate, K_2CO_3, CH_3CN; vi) H_2, Pd/C, EtOH; vii) $BrSi(CH_3)_3$, CH_2Cl_2, viii) formic acid (for **L**[1]) or TFA (for **L**[2]), CH_2Cl_2.

Complexation of ligands **L**[1], **L**[2] with lanthanide chlorides ($GdCl_3$•$6H_2O$, $EuCl_3$•$6H_2O$) was carried out using a standard procedure (see materials and methods section) to obtain the desired complexes at neutral pH. The successful formation of complexes was confirmed by means of ESI-MS and the spectra contained appropriate isotope pattern distribution, characteristic for Gd^{3+} or Eu^{3+} complexes.

2.3.2 Relaxometric experiments

A relaxometric study of complexes **GdL$^{1-2}$** was performed at 7 T (300 MHz) and 25 °C. The T_1 relaxation times were recorded at pH 9, 7 and 5 using different concentrations of complexes ranging from 3 mM to 1 mM. The pH was adjusted using solid lithium hydroxide and *para*-toluenesulfonic acid to avoid dilution of **GdL$^{1-2}$** solutions, the exact concentration of which was determined by the bulk magnetic susceptibility shift method.[95] The r_1 relaxivity at each pH is obtained as a slope of the linear regression curve for concentrations of **GdL$^{1-2}$** plotted against relaxation rate (R_1). The relaxivities of both **GdL$^{1-2}$** at the acidic pH were slightly higher than for the parent DO3APP compound (Figure 2-5).[41]

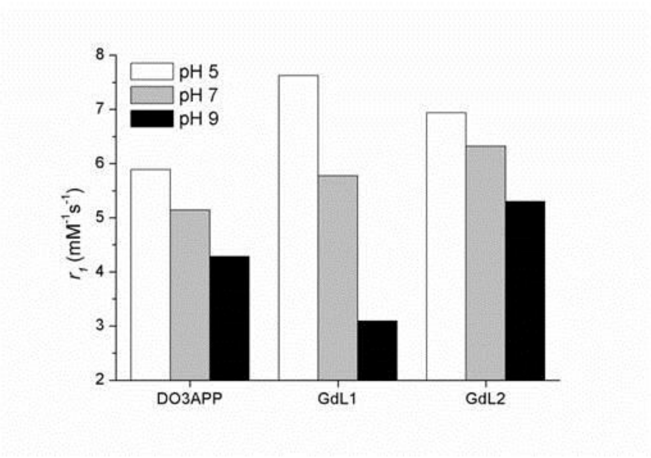

Figure 2-5: The pH dependence of the proton relaxivity (r_1) of **GdL^1** and **GdL^2** (7 T, 25 °C) compared to DO3APP (7 T, 21 °C).

In both cases we observed a continuous increase in relaxivity from pH 9 to 5. A total increase in r_1 of 147% from pH 9 to 5 was recorded for **GdL^1** (32% from pH 7 to pH 5), whilst total increase of 31% in r_1 was observed for **GdL^2** over the same pH range. The change in relaxivity with a change in pH is the same as that observed in the parent compound. Protonation of the phosphonate in acidic pH induces movement of the pendant arm and allows more water molecules to interact with the metal center resulting in a higher relaxivity.

2.3.3 Luminescence emission experiments

The two responsive complexes were characterized further by investigating their Eu^{3+} analogues. The ^{31}P NMR spectra of **EuL^1** and **EuL^2** were recorded at pD 5 and 7 (Annexure I). A pH-dependant low field chemical shift of approximately 2 ppm in both complexes indicates that a similar mechanism responsible for the r_1 changes is occurring as observed for

DO3APP.[41] Time resolved luminescence decay experiments were performed on complexes **EuL^1** and **EuL^2** to evaluate the change in the inner sphere hydration at different pH (Table 2-1). The experiments were carried out on 5 mM solutions of **EuL$^{1\text{-}2}$** in H_2O and D_2O. The hydration number was estimated using equation 1-11 where A' is 1.2 ms and the correction factor for the contribution of the second sphere is –0.25 ms^{-1}.[29]

Table 2-1: Emission lifetimes and estimated *q* values of **EuL^1** at neutral and acidic pH/pD

Compound	τ (ms) H_2O	τ (ms) D_2O	*q*
pH/pD 7	0.56	1.69	1.1
pH/pD 5	0.42	1.51	1.8

For **EuL^1** the apparent *q* value increases from 1.1 to 1.8 as the pH decreases from 7 to 5. The observed change is in good agreement with the findings of relaxivity experiments on the corresponding Gd^{3+} complex, confirming that the change in r_1 is directly influenced by changes in *q*. Determination of the *q* value for **EuL^2** was not possible due to the low intensity of emission and low solubility of the complex at high concentrations (> 3-4 mM). One of the reasons for the weak emission could be the presence of the highly electron donating aniline derivative in close proximity of metal center which quenches/deactivates the Eu emissive state,[96] whereas the hydrophobic aromatic ring of the linker might decrease the solubility but given the similar r_1 change we have assumed the mechanism is similar.

The relaxometric and luminescence emission experiments performed on the modified phosphonate complexes confirm that the synthetic modifications in close proximity of the metal centre do not negatively affect the coordination of Ln^{3+}, hence the pH responsive properties (similar to the DO3APP parent compound) are retained. This enabled us to pursue further investigations involving **L$^{1\text{-}2}$** towards their potential MRI application with other biomolecules such as proteins (see below).

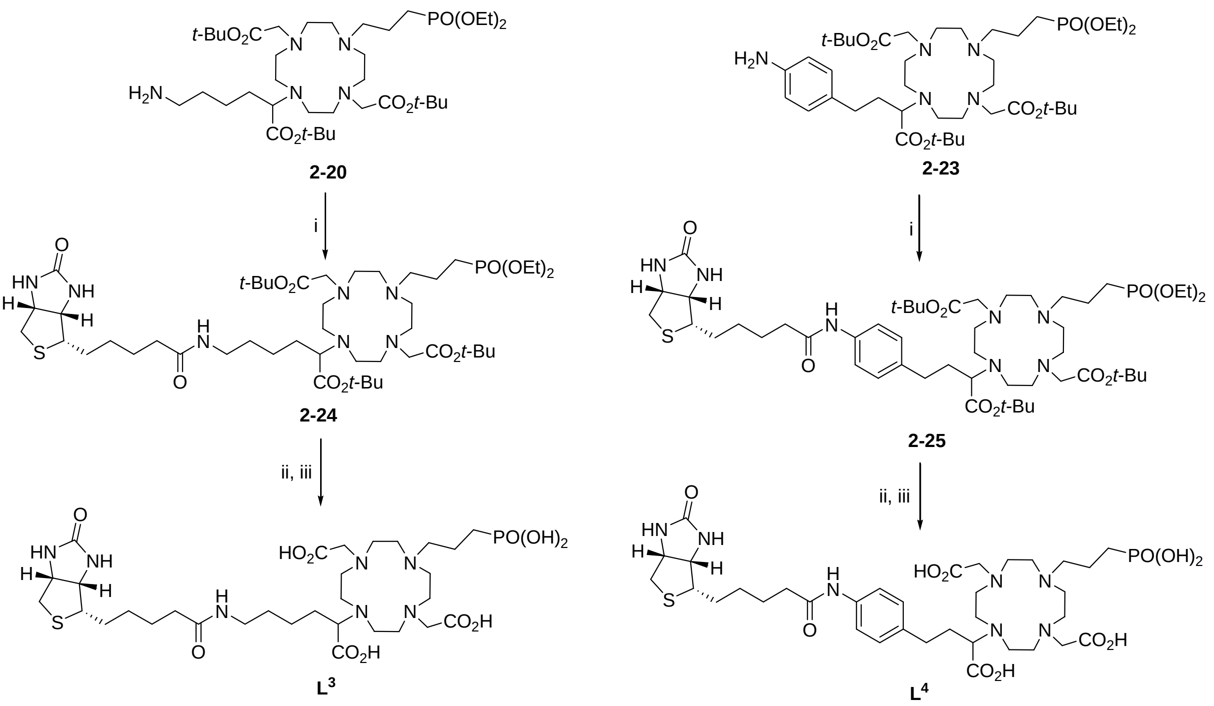

Scheme 2-3: Synthesis of **L**^{3} and **L**^{4}. **Reagents and conditions:** i) Biotin, EDCI•HCl, DMAP, DMF; ii) $BrSi(CH_3)_3$, CH_2Cl_2; iii) TFA, CH_2Cl_2.

2.4 Biotinylation of GdL$^{1\text{-}2}$

The high affinity avidin-biotin conjugate is a widely studied system used in many therapeutic, diagnostic, and pharmacological applications.[97-99] Avidin is a tetrameric protein with a high molecular mass (66k Dalton) and has an extremely high binding affinity towards biotin ($K_d \sim 1.7\times10^{-15}$) over wide pH range.[89] Once biotinylated, the avidin conjugate of our SCAs can be delivered to specific regions *in vivo*, or the biotinylated SCAs alone could be used for selective cell-targeting.[100] Hence, we have synthesized two biotinylated molecules **L**^{3}and **L**^{4} in a two step procedure commencing with the ester-protected ligands **2-20** and **2-23** (Scheme 2-3). They were coupled to biotin using EDCI•HCl and DMAP in DMF at room temperature, where the reaction was monitored by ESI-MS. The ligands were obtained following the deprotection of phosphonate and carboxylic acids using bromotrimethylsilane and trifluoroacetic acid respectively. Following the characterization of the ligands, their Gd^{3+} complexes were prepared as described previously (see materials and methods section).

2.5 Fluorescence displacement assay

The binding affinity of the newly synthesized molecules **GdL$^{3\text{-}4}$** to avidin was measured using a fluorometric assay based on the displacement of the fluorescent probe 2-anilinonaphthalene-6-sulfonic acid (ANS), employing the method developed by Horowitz and coworkers.[101] Briefly, ANS is strongly fluorescent when attached to avidin whereas the unbound dye has only a low fluorescence intensity. Since the binding affinity of ANS to avidin is lower than binding affinity of biotin to avidin, the addition of biotin displaces ANS from the avidin binding pocket resulting in the quenching of the fluorescence in the sample. The fluorescence displacement assay was performed in parallel on biotin, **GdL^{3}** and **GdL^{4}**. Upon addition of biotin or a biotinylated probe to the mixture of avidin and ANS, the fluorescence intensity decreased reaching a sharp inflection point at 3 equivalents of biotin or **GdL$^{3\text{-}4}$** (Figure 2-6). After this point there was no further drop in intensity observed even after the addition of several equivalents of biotin or **GdL$^{3\text{-}4}$**. The measured stoichiometry is in line with the results previously reported by Horowitz and can be associated with the affinity-purified avidin obtained from commercial sources.[101]

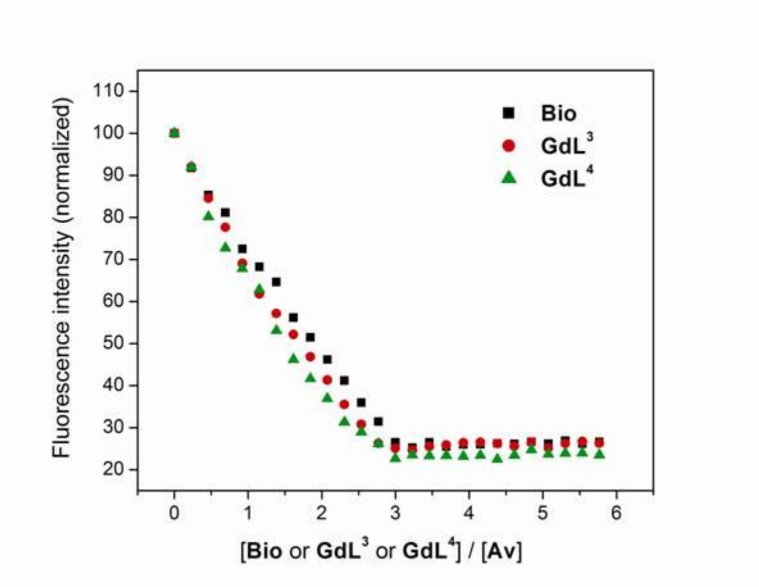

Figure 2-6: Fluorescence titration of the avidin-ANS complex with biotin and **GdL$^{3\text{-}4}$**.

This assay shows that only three binding sites are available in the studied avidin to interact with ANS and these three molecules of dye can be replaced by biotin or biotinylated SCAs. However, the titration curves of **GdL$^{3\text{-}4}$** are comparable to biotin indicating the binding affinities of both compounds are as strong as biotin. The calculated stability constants (see Materials and methods section) with K_s values $5.1\text{x}10^{13}$, $7.1\text{x}10^{13}$ and $8.0\text{x}10^{13}$ for biotin,

GdL^3 and **GdL^4**, respectively, suggest that the binding affinities of biotin and biotinylated SCAs are not significantly different from each other.

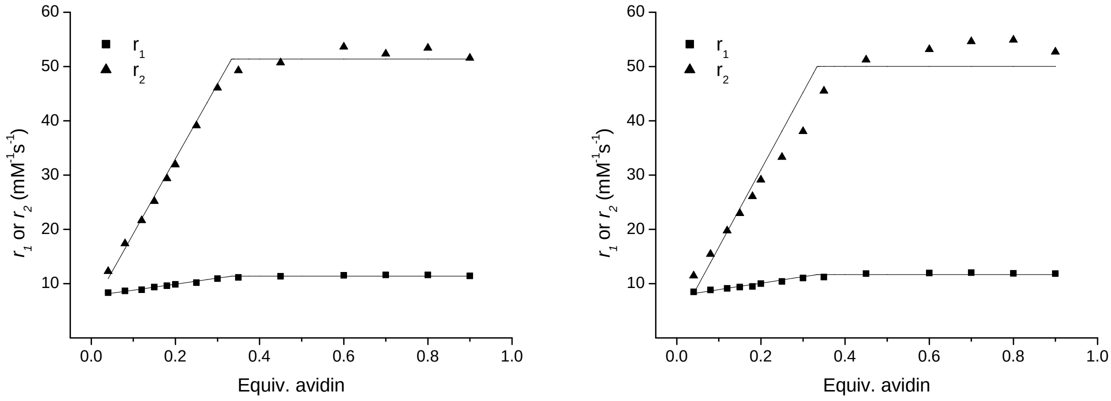

Figure 2-7: E-titrations of **GdL^3** (left) and **GdL^4** (right) with avidin at 3T MRI scanner (21 ^{o}C, HEPES, pH 7.4). The lines correspond to the fit assuming n=3 and K_s^{II}(Av(**GdL^3**)$_3$)=7.1x10^{13} or K_s^{II}(Av(**GdL^4**)$_3$)=8.0x10^{13} obtained from the fluorescence displacement assay. The R^2 values were 0.9817 and 0.9924 for r_1 and r_2 respectively for **GdL^3**, whereas 0.9583 and 0.9438 for r_1 and r_2 respectively for **GdL^4**. A better fit (R^2=0.9936 and 0.9963 for r_1 and r_2 respectively) for **GdL^4** could be obtained when n is also fitted (n=2.4 and 2.3 for r_1 and r_2 respectively).

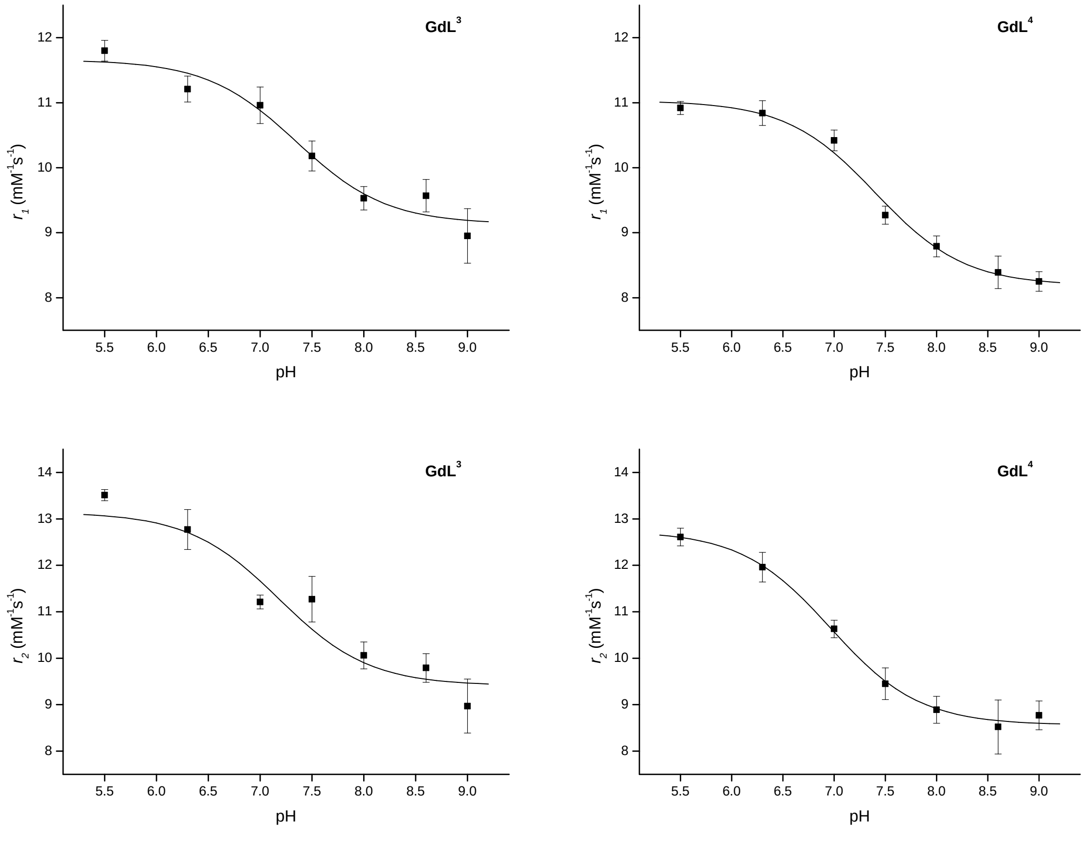

Figure 2-8: pH-dependant r_1/r_2 response of **GdL^3** (left) and **GdL^4** (right) in the absence of avidin (3T MRI scanner, 21 ^{o}C). Values are presented as mean ± SEM of five independent experiments. The lines represent the result of the sigmoidal fit and are displayed to aid a better visualization of the pH dependent r_1/r_2 decrease.

2.6 MRI phantom experiments

To confirm the observations of the fluorescence displacement assays, we followed the longitudinal and transverse relaxation rates (R_1, R_2) in samples with a constant concentration of **GdL$^{3-4}$** in HEPES buffer and varying concentrations of avidin in a method known as an E-titration.[102] These mixtures were incubated at 37 °C for 2 h and their relaxation times T_1 and T_2 were measured using a 3T (123 MHz) MRI scanner following the procedure and parameters as described in materials and methods section. A linear increase in r_1/r_2 with the addition of avidin compared to the unbound probe was observed until all biotinylated complexes are bound to avidin. A further increase in avidin concentration has no further effect on r_1/r_2 (Figure 2-7). The MRI phantom experiments confirm that biotinylated complexes bind to avidin. The increase in the r_1/r_2 of conjugates is the direct consequence of the τ_R increase, which is commonly observed for macromolecular contrast agents at magnetic fields relevant for clinics.[103] The plateaus of r_1/r_2 values were observed at 0.3–0.4 equiv of avidin which matches our observations from the fluorometric assay, indicating three of the binding sites are occupied in avidin.

In the subsequent step we studied the pH response of **GdL$^{3-4}$** in the absence and presence of avidin. We mixed **GdL$^{3-4}$** and avidin in a 3:1 ratio. The pH was adjusted over a wide range from 5.5 to 9.0 using buffers like MES, HEPES and CHES with 25 mM concentration. Longitudinal T_1 and transverse T_2 relaxation times were again obtained at 25 ºC in a 3T MRI scanner. A decrease in relaxation times T_1 and T_2, hence an increase in r_1 and r_2, was observed for both complexes when the pH decreased from 9 to 5.5 (Figure 2-9). The **GdL^3**-avidin conjugate showed an increase from 10.2 to 13.1 mM^{-1}s^{-1} (28%) and from 38.9 to 60.6 mM^{-1}s^{-1} (56%) of r_1 and r_2 respectively. Within the same pH range, the **GdL^4**–avidin conjugate showed an increase from 11.1 to 12.4 mM^{-1}s^{-1} (12%) and from 41.2 to 55.5 mM^{-1}s^{-1} (35%) of r_1 and r_2 respectively. When comparing these values with those obtained under same conditions (3T scanner, pH 5.5–9) for **GdL$^{3-4}$** in absence of avidin, the relative changes in relaxivities are comparable, except that the absolute r_2 values are much higher in the **GdL$^{3-4}$**–avidin conjugates (Figure 2-8). The results suggest that the investigated SCAs remained responsive not only by the further synthetic modifications (biotinylation of **GdL$^{1-2}$** to **GdL^{3-}**

^{4}), but **GdL$^{3-4}$** are capable of a specific and strong binding to the avidin while retaining their MR activity. Finally, the observed r_1/r_2 changes are the most pronounced from the weakly acidic to weakly basic pH making **GdL$^{3-4}$** promising prototype SCAs for further investigations *in vivo* in the physiological pH range.

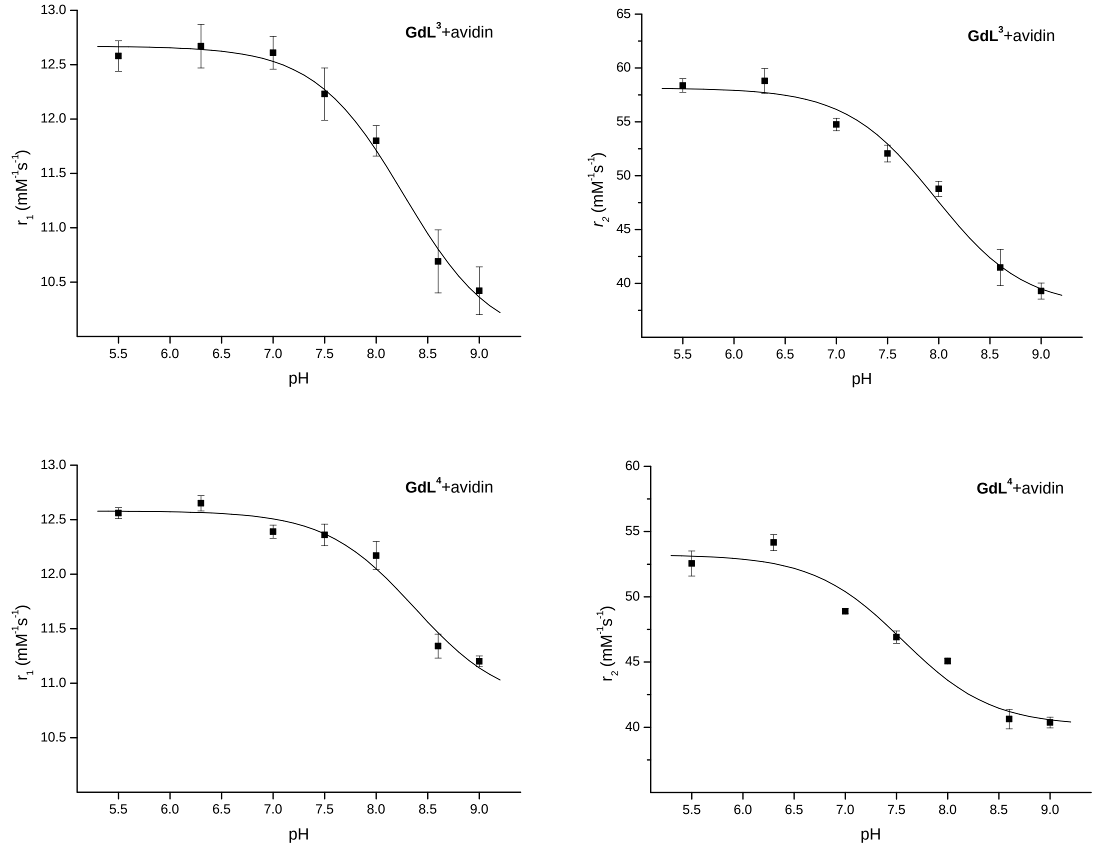

Figure 2-9: pH-dependant r_1 (left) and r_2 (right) response of **GdL^{3}** (top) and **GdL^{4}** (bottom) with avidin at 3T MRI scanner (21 °C). The avidin:**GdL$^{3-4}$** molar ratio was 1:3. Values are presented as mean ± SEM of five independent experiments. The lines represent the result of the sigmoidal fit and are displayed to aid a better visualization of the pH dependent r_1/r_2 decrease.

2.7 Competitive MRI assay

We performed a competitive assay with biotin to further characterize the binding affinity of the biotinylated SCAs towards avidin and estimate their *in vivo* potency. **GdL$^{3-4}$** were mixed with avidin in a fixed 3:1 ratio (HEPES buffer, pH 7.4). Different concentrations of biotin were added and the mixtures were incubated for five hours (for detail see Materials and Methods section). If the binding affinity of SCA is lower than biotin, **GdL$^{3-4}$** should be displaced by biotin from the avidin binding pocket, resulting in a decrease in relaxivity, in particular r_2. Following the incubation, the longitudinal and transverse relaxation times were measured in a 3T MRI scanner. We observed a minor decrease in relaxivities only after addition of 100 times excess of biotin whereas the r_1/r_2 did not change at lower concentrations of biotin (Figure 2-10). Such results are expected given the equilibrium exchange of biotinylated **GdL$^{3-4}$** at high concentrations of biotin. However, these findings confirm that the binding affinity of **GdL^3** and **GdL^4** to avidin is as high as of biotin. Furthermore, they imply the stability of MRI signal changes caused by SCAs either in its premixed solution with biotin, or in the presence of endogenous biotin *in vivo*.

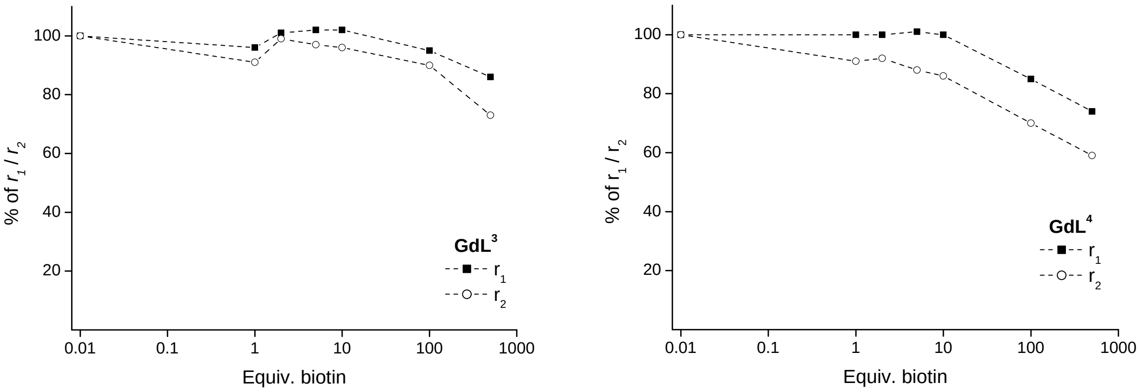

Figure 2-10: Competitive MRI assay of avidin:**GdL^3** (1:3, 125 µM **GdL^3**, left) and avidin:**GdL^4** (1:3, 125 µM **GdL^4**, right) with varying concentrations of biotin at 3T MRI scanner (21 ^{o}C).

2.8 Conclusions

We have synthesized and characterized two novel macrocyclic gadolinium based pH responsive contrast agents with an aliphatic or aromatic linker. Relaxometric and luminescence studies at different pH confirmed that for both agents the main physicochemical properties related to the pH dependant MRI response were retained after inserting the linking unit and are comparable to their parent compound. Furthermore, they were coupled to biotin and the response of the newly prepared responsive MRI agents was studied in more detail. The binding affinity of these complexes with avidin was showed to be as effective as biotin itself through fluorescence displacement or competitive MRI assays. MRI phantom experiments in the presence of avidin revealed the relaxivity was changing along with the change in pH at physiologically relevant values. These complexes offer a useful pathway towards target-specific SCA for *in vivo* applications. The major aim of the project was achieved since enabling to modify the DO3A type pH sensor for further functionalization. Future directions will involve applying this strategy in introducing various functional molecules such as proteins, peptides, receptor ligands or fluorescent tags to SCAs of various kinds (e.g. pH- or ion-responsive) making them suitable for their application *in vivo*.

Chapter 3: Synthetic modification of Ca^{2+} responsive bismacrocyclic contrast agent and study of its response towards Ca^{2+}

3.1 Introduction

Metal ions such as Cu^+/Cu^{2+}, Fe^{2+}/Fe^{3+}, Zn^{2+} and Ca^{2+} are essential for the growth and development of living organisms. The deficiencies of such ions may cause acute diseases such as diabetes, neurodegenerative disorders or cancer. Therefore, it is crucial to precisely determine fluctuations in concentration of these metal ions during physiological and pathological events *in vivo*. In particular Ca^{2+} plays key role in cellular processes since thousands of processes rely on calcium influx. Its dual task as secondary messenger as well as an electric current carrier in brain makes it a more valuable metal ion over others in describing cognitive function. Neuronal activities lead to critical changes in Ca^{2+} concentration.[104] Basic aspects of neuronal regulation and abnormalities in signaling in diseased states could be investigated further by understanding Ca^{2+} signaling pathways in neurons. Ca^{2+} not only influences gene expression, neurotransmitter release, neuronal functions but also neuronal growth, its development, survival and death.[105] Several signaling pathways in the brain increase cytosolic Ca^{2+} concentration up to 0.5–1.0 mM, drawing it from the endoplasmic reticulum (ET) or extracellular space inducing large concentration gradients across their membranes. Various voltage-sensitive Ca^{2+} channels and ligand-ligand cation channels such as nicotinic receptor, methyl-d-aspartate receptor or IP_3 triggered redistribution from intracellular stores help Ca^{2+} influx inside the cell. Ca^{2+} acts as second messenger by modulating the activity of number of mediators such as calmodulin. The Ca^{2+}-calmodulin conjugate activates more than 20 eukaryotic enzymes like cyclic nucleotide PDEs, adenylate cyclase etc. The conventional interaction of calmodulin requires a rise in Ca^{2+} concentration since four binding sites of Ca^{2+} should be occupied to activate it. Hypoxia and ischemia induce a large elevation in intracellular Ca^{2+} concentrations in some cerebral neurons.[106]

Hence understanding the Ca^{2+} concentration in real time would add immense value in the neuroscientific application in tracking dynamic changes in it during neuronal signaling. With this aim, a number of research groups developed Ca^{2+} sensitive fluorescent dyes[107] for optical imaging. As mentioned previously optical imaging has limiting depth penetration as well as limitations such as the production of photobleaching side products of the fluorescent probes restricting their application *in vivo*. MRI has advantage over optical imaging since it has unlimited depth of penetration and several MRI probes are stable *in vivo*. Therefore MRI could be the potential tool to follow *in vivo* concentration changes in Ca^{2+} with better spatiotemporal resolution using Ca^{2+} sensitive CAs.

To this end, Li *et al* proposed first potential MRI contrast agent (Figure 1-9) which is based on Gd^{3+} and DOPTA ligand system, with a Ca^{2+} dissociation constant of 0.96 µM, where the relaxivity of the complex increases by approximately 80% when Ca^{2+} is added.[49] Even though it is a potential candidate for *in vivo* imaging till date there are no further reports from the authors of its *in vivo* utilization. Our laboratory proceeds in this direction, synthesizing and applying Ca^{2+} sensitive CAs in rodents and ultimately primates to directly detect and quantify Ca^{2+} concentration, and hence neuronal activity using MRI. With this aim in one of early report Dhingra *et al* reported a Gd^{3+}–DOPTRA derivative (Figure 1-9). This agent shows around a 100% change in relaxivity upon addition of Ca^{2+}. Further relaxivity studies in physiological fluids such as ACSF and AECM proved that agent would be potential candidate for *in vivo* application even though there is considerable drop into the change in relaxivity due to anion binding to Gd which blocks water access considerably.[52]

Furthermore Mamedov *et al* published detailed study of DO3A based Gd^{3+} complex appended with bisphosphonate unit[56] which are known to be effective Ca^{2+} chelators with formation constants in the high micromolar to low millimolar range.[108, 109] This agent displays unusual behavior with Ca^{2+} addition as its relaxivity decreases. This is explained as the outcome of a Ca^{2+} ion assisted aggregation which is commonly observed phenomenon in probes carrying such functional groups.[110] Further *in vivo* evolution of this agent demonstrated that the complex strongly interacted with brain parenchyma limiting its diffusivity. Moreover bismacrocyclic Gd^{3+} complexes were studied, [53, 111] which are either two DO3A type macrocyles bridged by a BAPTA bisamide or EDTA/DTPA bisamide Ca^{2+} chelators (Figure 3-1). These agents have been investigated thoroughly, although most of these have low sensitivity towards the Ca^{2+} ion (10–30% change in relaxivity with Ca^{2+} addition until saturation of signal) as well as low selectivity over other metal ions. The Gd^{3+} complex containing two macrocycles connected by modified EGTA linker along with an ethyl or propyl spacer provided the best results, with more than an 80% (propyl spacer) overall change in relaxivity with addition of one equivalent of Ca^{2+} ion in HEPES buffer (11.75 T, 25 °C, Figure 3-2). The association constants for both complexes, $\log K_A$ is around 4–5 which suggests that reversible interaction of the agent is possible during the Ca^{2+} fluctuations *in vivo*. This was confirmed using EDTA since addition of EDTA to a solution of CA saturated with Ca^{2+} retains the increased relaxivity to the initial value. Unlike other SCAs this has better selectivity over other endogenous metal ion Mg^{2+}. Moreover, the study of complexes in brain extracelluar matrix (BEM) was encouraging as a change in relaxivity in relevant range of Ca^{2+} in brain (0.8–1.2 mM) displayed 10% change in relaxivity.

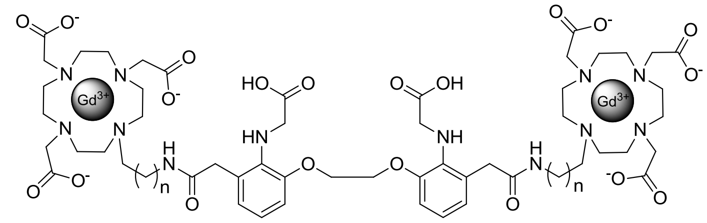

n = 1 or 2

3-1

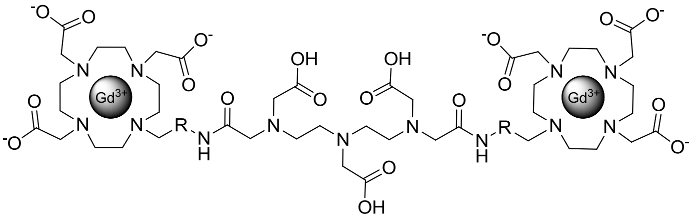

R = $-CH_2-$ or $-C_6H_4$

3-2

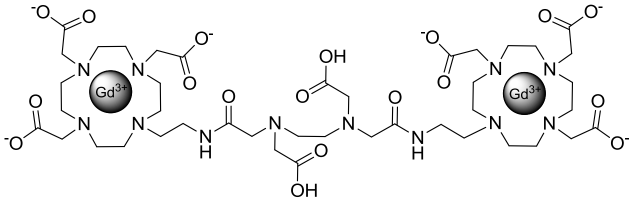

3-3

Figure 3-1: Few examples of Ca^{2+} responsive contrast agents.

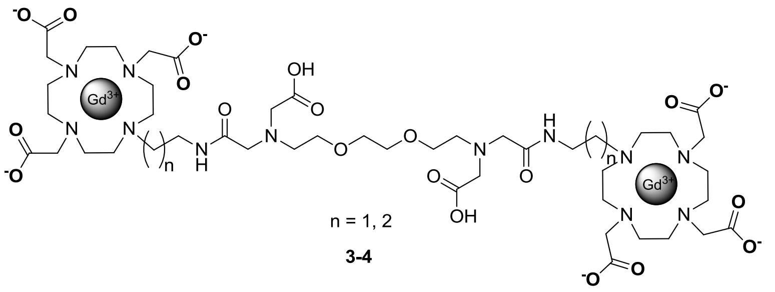

3-4

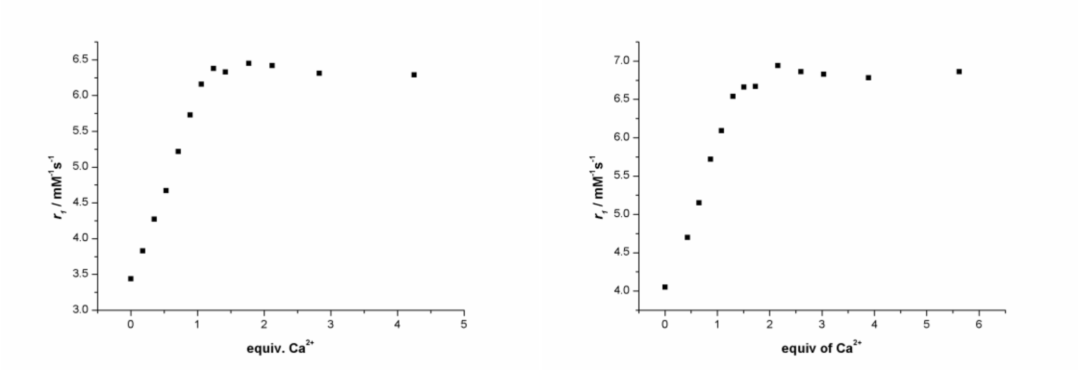

Figure 3-2: Structure of bis-macrocycles containing modified EGTA linker (top). Relaxometric Ca^{2+} titration in the buffer with ethyl spacer (n = 1, left) and with propyl spacer (n = 2, right) at 11.75 T and 25°C.

With such promising *in vitro* results, an assessment of its function *in vivo* was attempted. It was found that major issues hinders its ability to report changes with higher spatiotemporal resolution, faster onsets, greater spatial or structure specificity. Namely, MRI signal is dependent on Ca^{2+} concentration as well as concentration of SCA. To assess the concentration of SCA one needs to measure the diffusion of molecule in tissues and correlate the observed signal. Therefore it is necessary to have enough concentration of SCA for long time scale or its diffusion should be decreased substantially. The other issues are determination of the exact concentration SCA *in vivo* as well as localization to demonstrate the changes in MR signal are due to change in Ca^{2+} concentration rather than a change in SCA concentration.

To increase the concentration and/or decrease diffusion this agent can be delivered with a high pay load on functional molecules such as dendrimers, nanoparticles or delivery vectors. For tracking the exact *in vivo* concentration, the SCA can be attached to a ^{19}F containing moiety. Here dual frequency ^{1}H and ^{19}F MRI can be utilized. ^{19}F MRI signal will allow the exact concentration of SCA *in vivo* to be determined, independent of Ca^{2+} ion concentration. Furthermore, if ^{18}F is introduced through this linker, one could follow the probe concentration using PET signal. Another strategy would be the conjugation of the SCA with USPIO nanoparticles to convert it into ratiometric probe, where T_2 from iron oxide nanoparticle will remain constant and T_1 from probe which will change as a function of Ca^{2+} concentration, thus rendering the MR signal independent of probe concentration therefore, to attach such functional molecules to the SCA one needs to synthetically modify the existing responsive bismacrocycles without changing their physico-chemical properties particularly their response to Ca^{2+} ions (Figure 3-3).

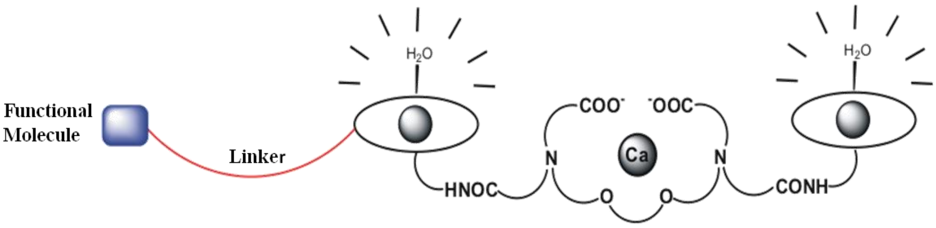

Figure 3-3: Schematic representation of Ca^{2+} sensitive CA with linker molecule.

3.2 Ligand design

With this objective in mind we have decided to synthetically modify the above mentioned molecule with a propyl spacer inserting a linking unit and studying the response to Ca^{2+} ions before attaching it to a functional molecule. We had already developed and utilized two different types of linking units (Chapter 2) in pH responsive agents. With similar synthetic approach we have decided to insert one of the linker in Ca^{2+} sensitive agent (Figure 3-4).

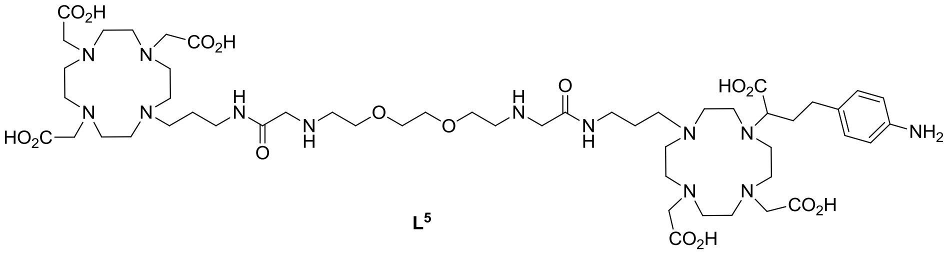

L^5

Figure 3-4: Structure of designed ligand **L^5**.

The choice for aromatic linking unit over aliphatic linker was made on following basis:

i) aromatic amine could be used to couple to carboxylic acids using simple acid amine coupling reaction with coupling agents such as EDC, DCC etc,

ii) the aromatic amine can also be converted to more reactive and stable nucleophilic isothiocynate group, which can react with amines at high pH. Therefore one amine gives us the potential to attach this molecule to a variety of functional molecules,

iii) aromatic linker would provide a suitable chromophore for spectroscopic detection during HPLC purification,

iv) aromatic linker provide more rigidity to the molecule which would help to ensure the functional molecules are at a suitable distance from the Ca^{2+} chelator or Gd^{3+} centers to minimize the interference of functional molecules in sensor moieties. Namely, flexible linker like aliphatic linker may allow the functional molecule and Gd^{3+} centers to come closer by conformational changes which might obstruct the relaxivity change.

3.3 Results and discussions

3.3.1 Retrosynthetic analysis of L^5

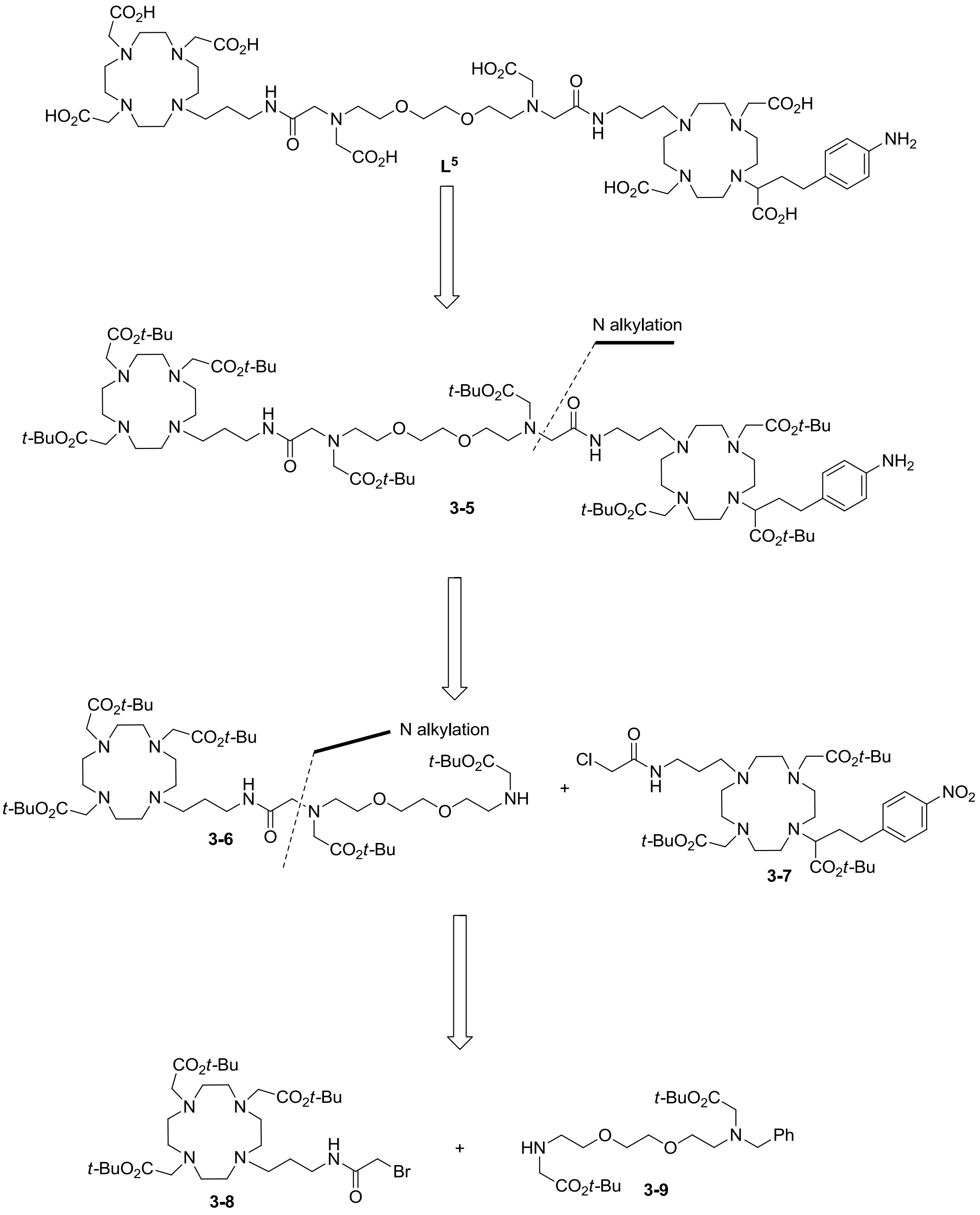
L^5
N alkylation
3-5
N alkylation
3-6
3-7
3-8
3-9
+
+

Figure 3-5: Retrosynthetic analysis of **L^5** containing alkylation reactions.

Retrosynthetic analysis of ligand **L**^{5} is shown as the figure 3-5. It suggests the preparation of three distinct units and later their union by sequential N-alkylation reactions. This led to the synthesis of three different building blocks, **3-7**, **3-8** and **3-9**.

3.3.2 Synthesis of L^{5}, strategy 1

Bromide **3-8** was synthesized following the same pathway as reported in literature.[50] Amine **3-9** was prepared by selective mono protection of diamine **3-10** on one of the symmetric secondary amine using benzyl chloride in acetonitrile at room temperature with a moderate yield. The mono protection of diamine **3-10** with benzyl chloroformate to give amine **3-12** was attempted, however with too low yield. Compound **3-13** was investigated with the objective to increase the yield as well to explore the different deprotection conditions but no significant improvement was achieved in case of yield (Figure 3-6). Hence we proceeded with benzyl protected amine **3-9**. Alkylation of amine **3-9** with bromide **3-8** in acetonitrile and potassium carbonate at 70 °C produced **3-11**. Reductive debenzylation of amine with $Pd(OH)_2$ in ethanol under a H_2 atmosphere produced scaffold **3-6** with good yield (Scheme 3-1).

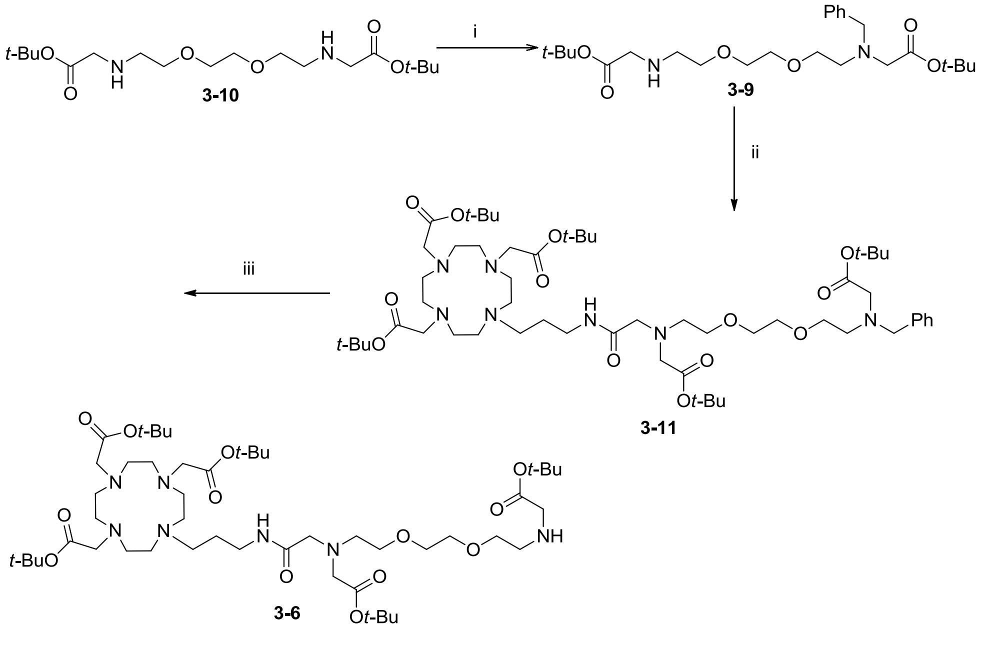

Scheme 3-1: Synthesis of scafold **3-6**. **Reagents and Conditions**: i) BnCl, Cs_2CO_3, CH_3CN; ii) **3-8**, K_2CO_3, CH_3CN; iii) H_2, $Pd(OH)_2$, NH_4OH(aq.), EtOH.

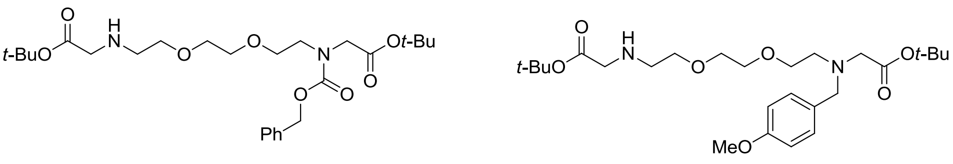

3-12 **3-13**

Figure 3-6: Examples of monoprotected EGTA derivatives.

The synthesis of scaffold **3-7** commenced with the alkylation of *tris* alkylated derivative **2-21** (chapter 2) with N-(3-bromopropyl)phthalimide to afford *tetra* alkylated derivative **3-14**. The deprotection of phthalamide gave rise to amine **3-15**. Treatment of acetic anhydride to primary amine **3-15** produced the desired scaffold **3-7** (Scheme 3-2). With the enough amounts of scaffolds in hand we were set to carry out the final alkylation to obtain ligand in fully protected form.

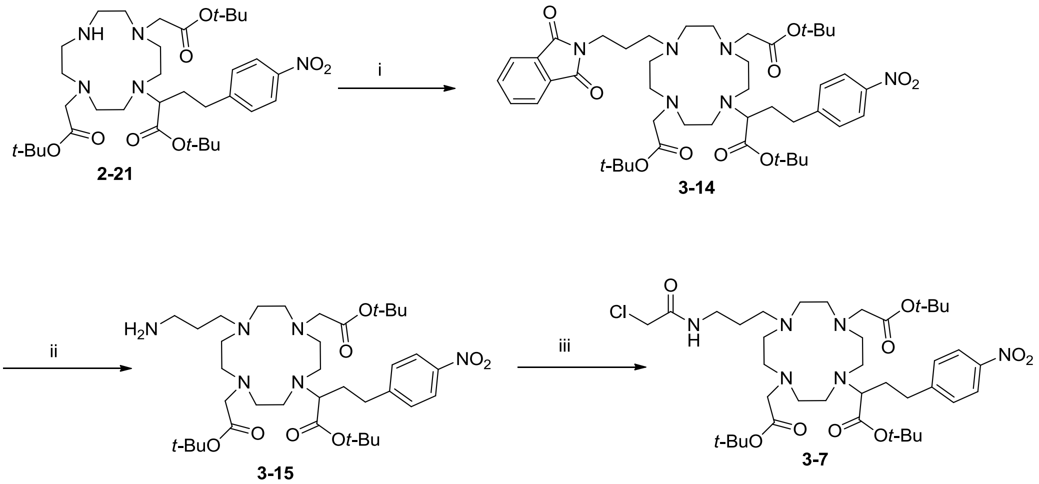

Scheme 3-2: Synthesis of scafold **3-7**. **Reagents and conditions:** i) N-(3-bromopropyl)phthalimide, K_2CO_3, CH_3CN; ii) Ethylenediamine, iso-PrOH, 90 °C; iii) Chloroacetic anhydride, $NaHCO_3$, dioxane, water.

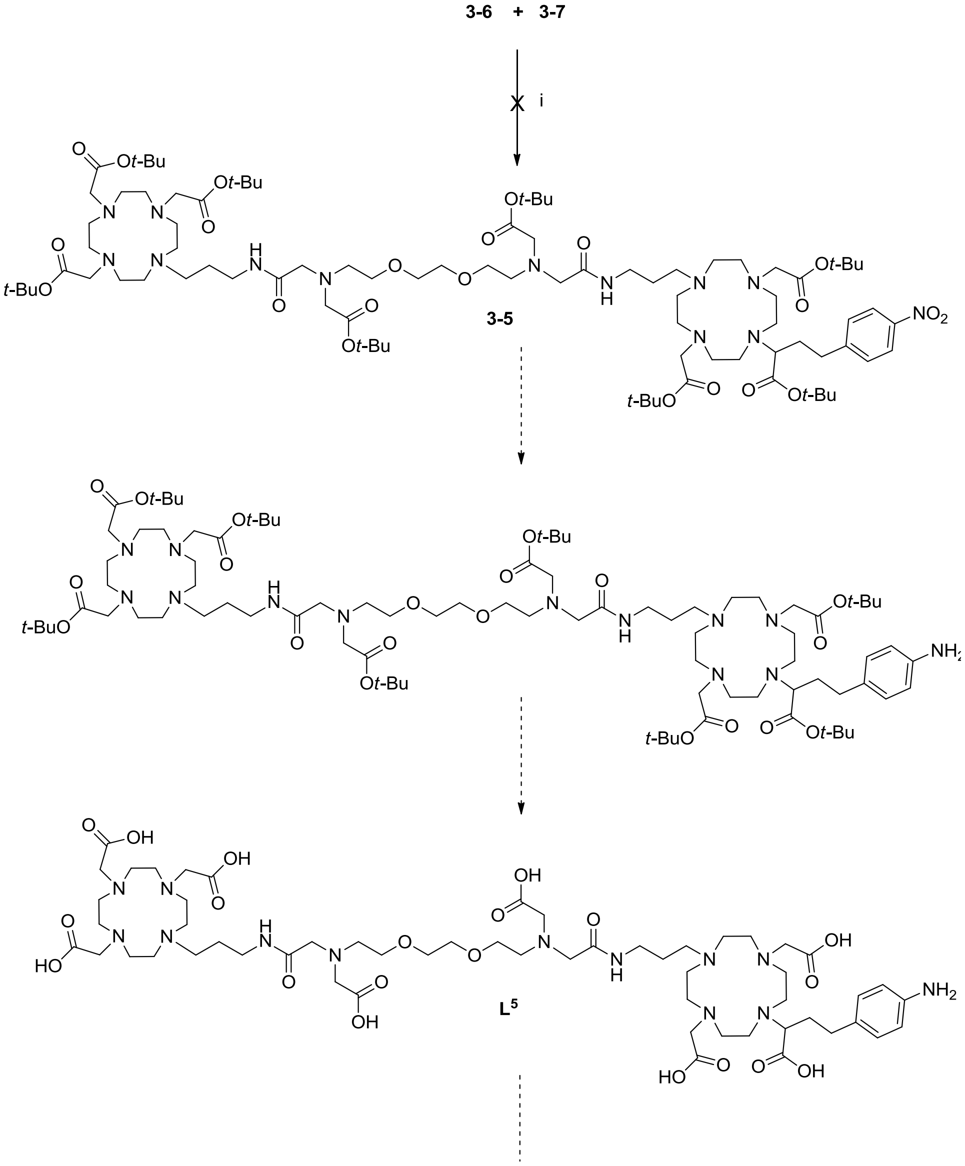

Scheme 3-3: Synthesis of **Gd_2L^5**. **Reagents and conditions:** i) K_2CO_3, CH_3CN, 70 °C.

We have treated scaffold **3-6** and **3-7** in acetonitrile with K_2CO_3 as base (Scheme 3-3). These conditions did not provide any appreciable amount of desired product. We believe this is due to an intramolecular alkylation of scaffold **3-6** to give product **3-16** (Figure 3-7), resulting in no desired product. This was confirmed by ESI-MS analysis. This may be due to the highly electron withdrawing nitro group present at *para* position of benzylic methylene making this carbon center more acidic. In the presence of a base this is acting as better nucleophile than the secondary amine of **3-7**. Furthermore, due to steric reasons the intramolecular reaction is favored over the intermolecular reaction.

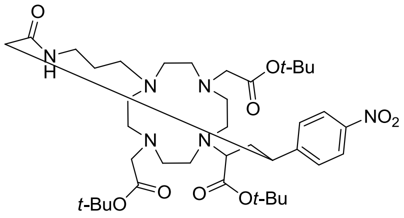

3-16

Figure 3-7: Structure of undesired product formed in Scheme 3-3.

Therefore we decided to inhibit the withdrawing effect of *para*-nitro group in scaffold **3-6** by converting it into a Boc protected amine. The synthesis was accomplished by reducing nitro group of already synthesized intermediate **3-14** into amine **3-17** using Pd/C catalyzed reduction under H_2 atmosphere (Scheme 3-4).

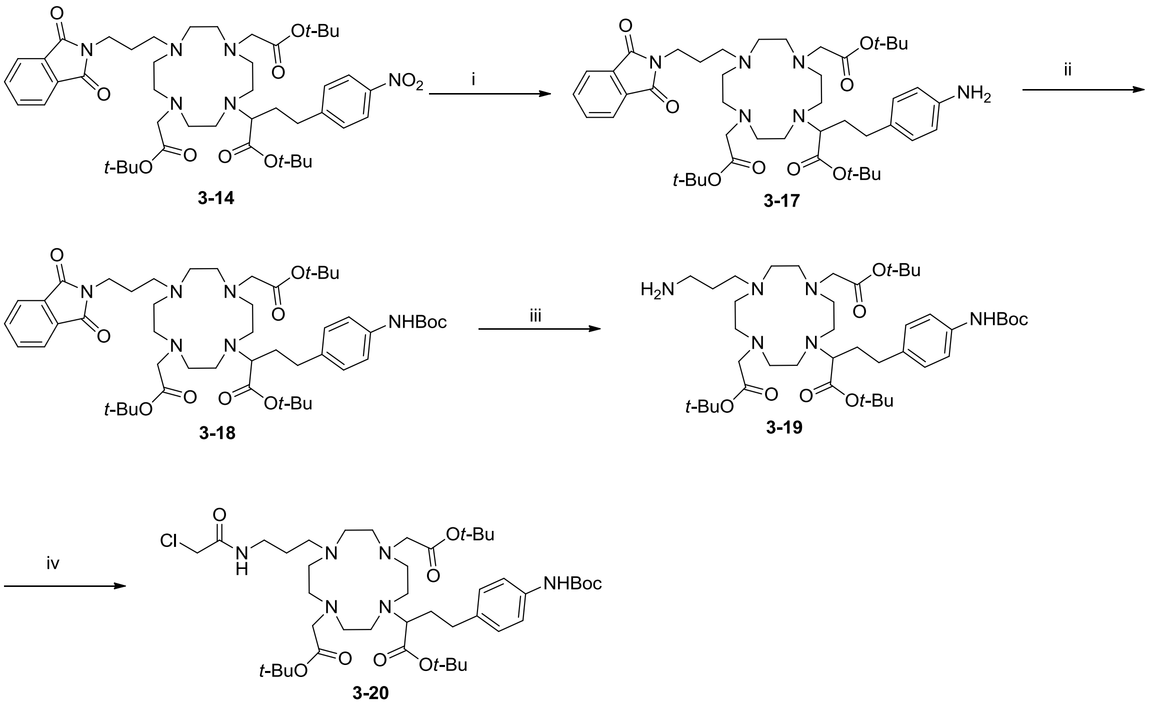

Scheme 3-4. Synthetic modification of scafold **3-7** to **3-20**. **Reagents and Conditions:** i) H_2, Pd/C, EtOH; ii) $(Boc)_2O$, $NaHCO_3$, dioxane water; iii) Ethylenediamine, *i*-PrOH, 90 °C; iv) Chloroacetic anhydride, $NaHCO_3$, dioxane, water.

The amine **3-17** was protected using Boc anhydride in a dioxane and water mixture at room temperature to afford **3-18**. The primary amine **3-19** was obtained after pthalamide deprotection of **3-18** with ethylenediamine in refluxing *iso*-propanol. A number of attempts were made to purify intermediates **3-18** and **3-19** using silica gel and alumina column chromatography, but due to the highly polar nature of compounds as well as the comparable polarity between products and side products separation was not possible. Therefore we proceeded with the subsequent acylation without purification. Chloroacetic anhydride used for acylation of primary amine **3-19** yielded the desired scaffold **3-20**. With suitable quantities of the reagents **3-6** and **3-20** we proceeded with the N-alkylation reaction in acetonitrile. The desired compound **3-21** was obtained in a moderate yield, where traces of undesired product **3-16** were not observed. The ligand precursor was subjected to simultaneous deprotection of all the acids and amine in a mixture of trifluroacetic acid and dichloromethane at room temperature to yield $\mathbf{L^5}$. Purification of the product appeard tedious because of highly polar nature of bismacrocycle. The possible reason may be presence of many *tert* amines which favours more thermodynamically stable salt formation as well as formation of some conformationally more stable undesired products. This synthetic strategy therefore proved to be less suitable to produce the ligand in reasonable amount and purity. Therefore a new synthetic pathway was designed with the appropriate retrosynthetic plan (Figure 3-8).

3.3 Synthesis of L^5, strategy 2

The final ligand is anticipated to be obtained by coupling the previously synthesized amine intermediate **3-19** and carboxylic acid scaffold **3-22** using coupling agents such as DCC, HATU, or HBTU.

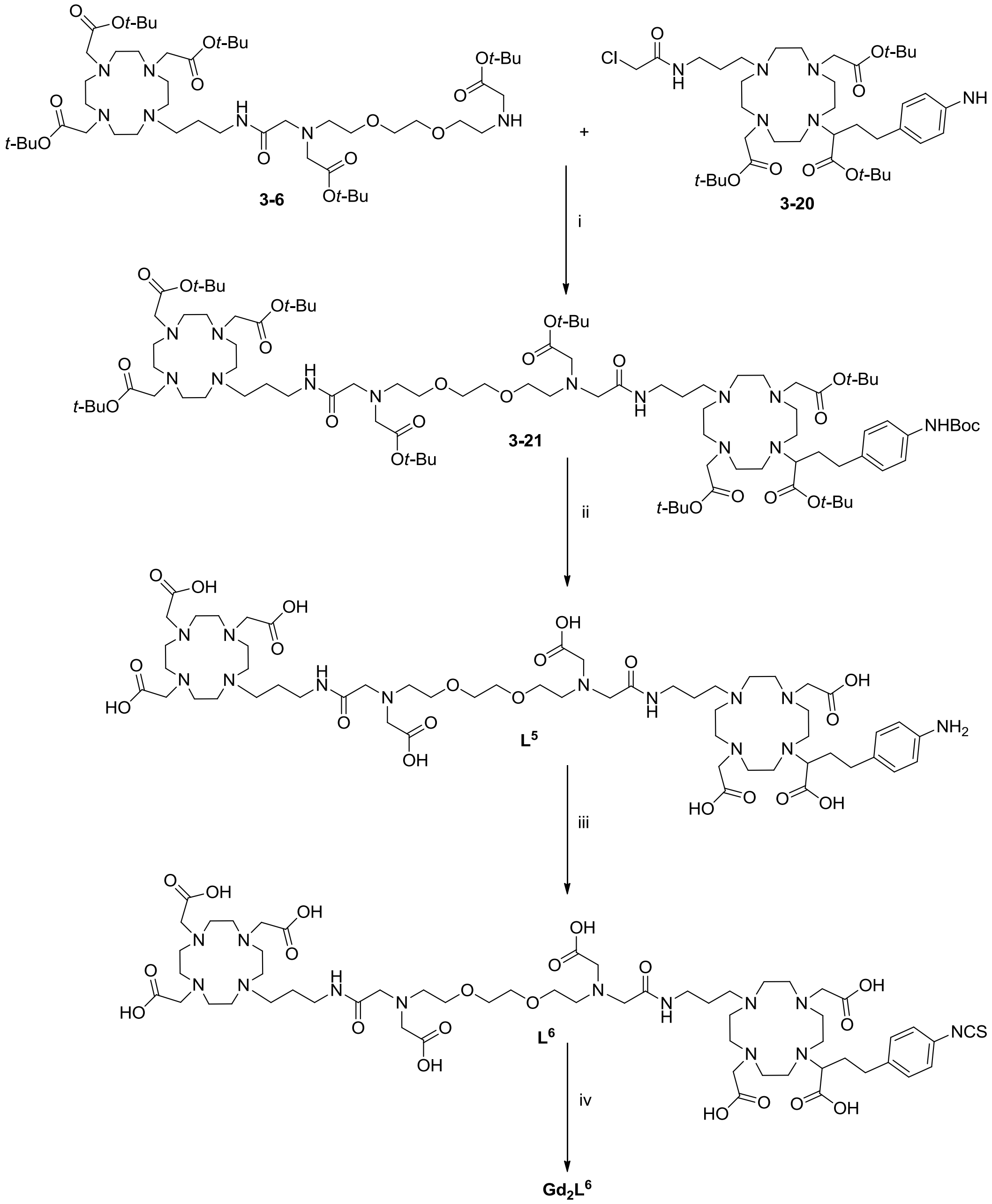

Scheme 3-5. Synthesis of bismacrocyclic complex **Gd_2L^6**. **Reagents and Conditions:** i) K_2CO_3, KI, CH_3CN, 70 °C, 16h; ii) TFA, CH_2Cl_2, 16h; iii) $CSCl_2$, CCl_4, H_2O, pH 2–3, 30 min.; iv) $GdCl_3$•$6H_2O$, H_2O, pH 6–7, 60 °C, 16h.

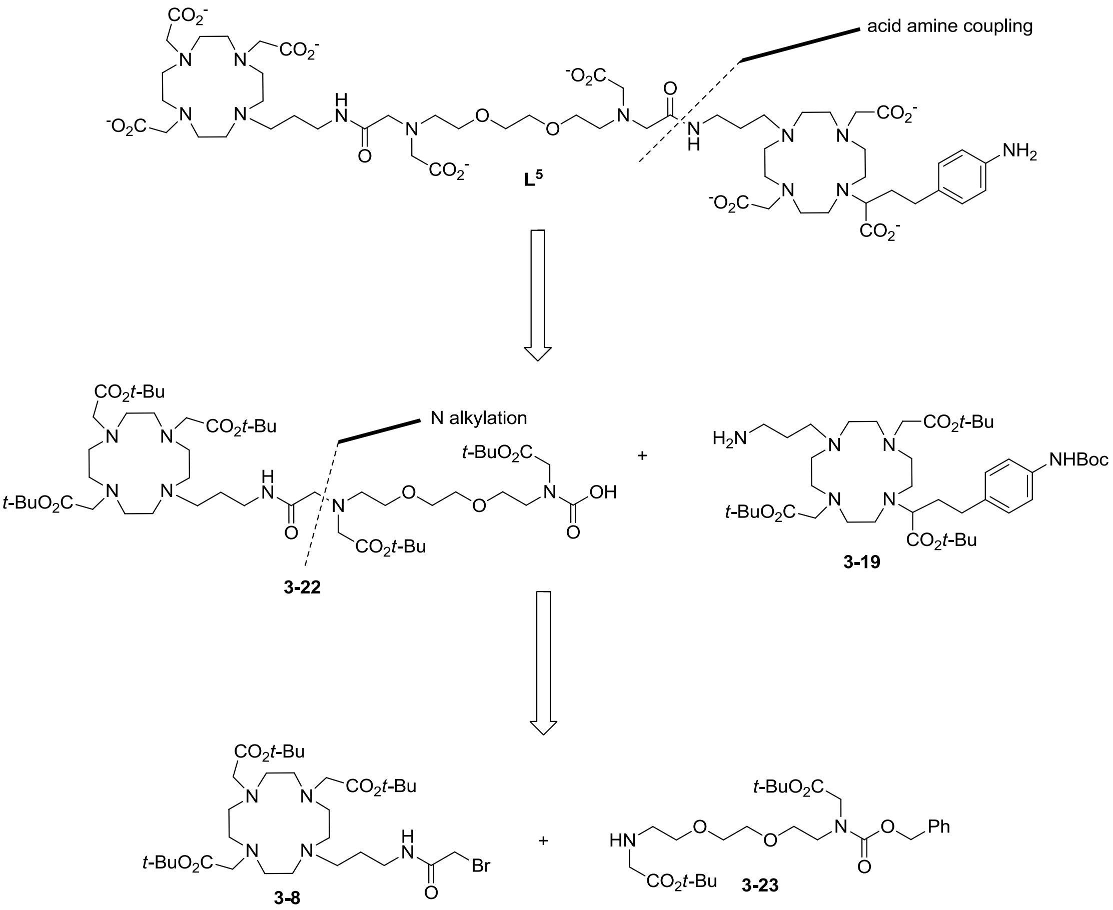
acid amine coupling
L5
N alkylation
3-22
3-19
3-8
3-23

Figure 3-8: Retrosynthetic analysis of **L**^{5} using coupling reaction

The synthesis of scaffold **3-22** commenced with the selective monoalkylation of diamine **3-10** with benzyl bromoacetate and cesium carbonate in acetonitrile for three days at room temperature.

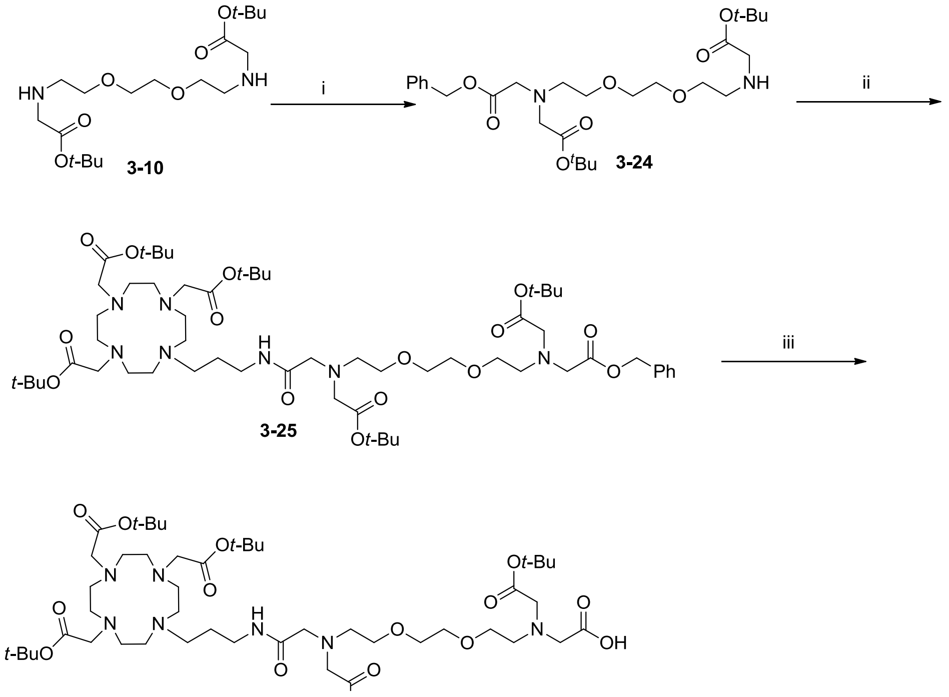

Scheme 3-6: Synthesis of acid **3-22**. **Reagents and Conditions:** i) Benzyl bromoacetate, Cs_2CO_3, CH_3CN, 72h; ii) **3-8**, K_2CO_3, CH_3CN, 70 °C; iii) H_2, Pd/C, EtOH, 16h.

Treatment of monoalkylated secondary amine **3-24** with **3-8** in the presence of potassium carbonate, and in acetonitrile at 70 °C gave the benzyl protected acid **3-25**. The acid **3-22** was obtained by hydrogenation of **3-25** catalyzed by Pd/C in ethanol (Scheme 3-6). The acid **3-22** and amine **3-19** were treated with HBTU in DMF at room temperature for 16 h yielding the ligand precursor **3-26**. The reaction mixture was washed multiple times with water after removal of DMF under reduced pressure, followed by multiple attempts to purify using silica gel or different types of alumina column chromatography. Unfortunately none of abovementioned efforts resulted into pure product **3-26**. Therefore, we continued to the next reaction with trifluroacetic acid to obtain ligand in dichloromethane. Herein we used RP-HPLC to purify ligand but unfortunately product and impurities exhibited same retention time, $R_{t,}$ on C18 column. With careful observation of the analytical data it was revealed that the excess of amine **3-19** was necessary for completion of reaction. This excess amine was eluting with product through normal phase and reverse phase column chromatography.

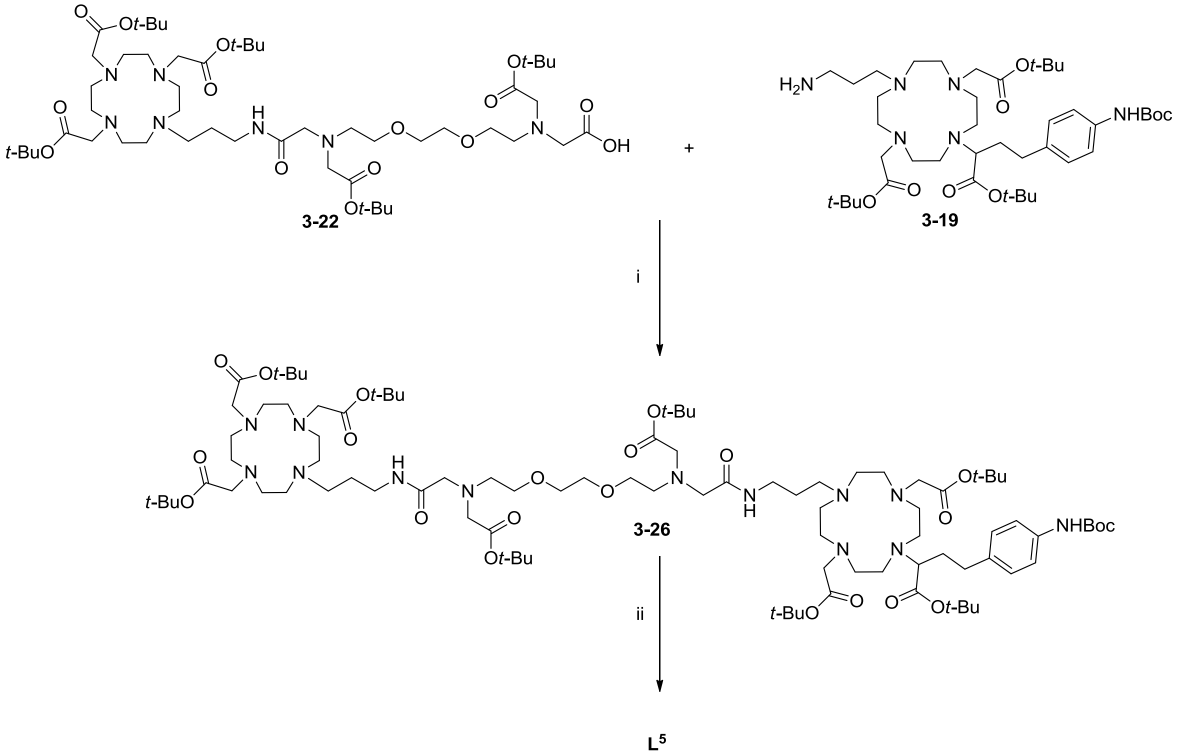

Scheme 3-7: Synthesis of bismacrocyclic ligand **L^5**. **Reagents and Conditions:** i) HBTU, DMF, 16 h ii) TFA, CH_2Cl_2, 16 h.

Therefore we decided to replace the amine **3-19** that we coupled with **3-22**. We have simply removed phtalamide protection on nitro derivative **3-14** to afford required amine **3-27** by heating it in isopropyl alcohol at 90 °C with nitro group. With present approach we decreased the number of synthetic steps to produce **3-19** by two, avoiding the reduction of nitro group, as well as protection of obtained amine (Scheme 3-8).

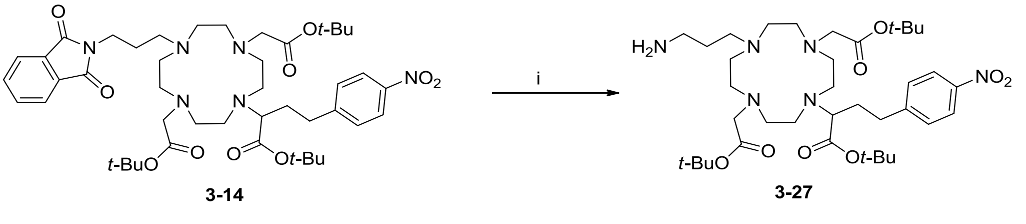

Scheme 3-8: Synthesis of amine **3-27**. **Reagents and Conditions:** i) Ethylenediamine, *iso*-PrOH, 90 °C, 16 h, reflux.

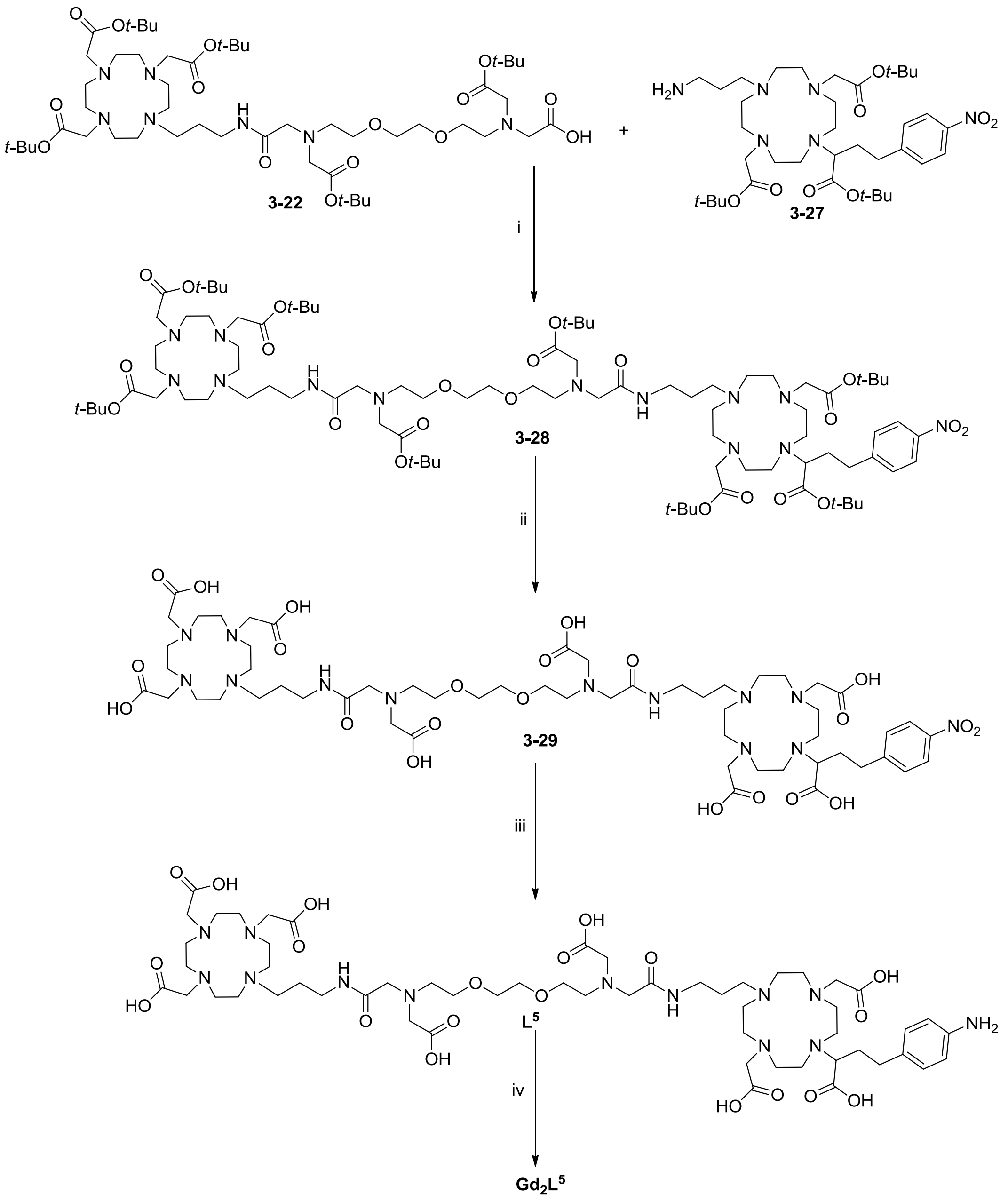

Scheme 3-9: Synthesis $\mathbf{Gd_2L^5}$. **Reagents and Conditions:** i) HBTU, DMF, 30 min; ii) TFA, CH_2Cl_2; iii) H_2, Pd/C, EtOH, H_2O, 16 h; iv) $GdCl_3$•$6H_2O$, pH 6–7, H_2O, 60 °C.

The coupling of acid **3-22** and amine **3-27** was carried out in DMF in presence of HBTU at room temperature to yield bismacrocycle **3-28**. The attempted purification was unsuccessful hence **3-28** was subjected to deprotection in trifluroacetic acid and dichloromethane to give the nitro derivative **3-29**. RP-HPLC was carried out to purify **3-29**. The product was hydrogenated in ethanol and water mixture catalyzed by Pd/C to afford $\mathbf{L^5}$ (Scheme 3-9). $\mathbf{L^6}$ was afforded by reaction with thiophosgene in water at room temperature to while maintaining pH between 2–3 for 20 minutes. The gadolinium complexation of the ligand was carried out as described in the materials and methods section. This synthetic approach provides us with a reasonable and reproducible amount of ligand $\mathbf{L^5}$ with the highest purity.

3.4. Relaxometric Ca^{2+} titration in HEPES buffer

A relaxometric study of complex $\mathbf{Gd_2L^5}$ was performed at 7 T (300 MHz) and 25 °C. The T_1 relaxation times were recorded at pH 7.4 using 3.0 mM Gd^{3+} solution of complex in 100 mM HEPES buffer. An aqueous solution of Ca^{2+} (in 0.1 eq. portions) was added until 2.0 equivalents with respect to $\mathbf{Gd_2L^5}$. In the absence of Ca^{2+} the initial relaxivity observed was 3.6 $mM^{-1}s^{-1}$ which increased by 97% with stepwise addition of Ca^{2+} to 7.1 $mM^{-1}s^{-1}$. The r_1 enhancement was maximal at 1.2 equiv of Ca^{2+} and remains constant with further Ca^{2+} addition. The observed r_1 increase demonstrates the high sensitivity of the agent to Ca^{2+}. The reversibility of the $\mathbf{Gd_2L^5}$–Ca^{2+} interaction was checked by the addition of an equimolar amount of EDTA with respect to the Ca^{2+}. The addition of EDTA re-established the relaxivity to its initial value, proving the reversible binding of the agent to the Ca^{2+}. A strong chelator such as EDTA removes the Ca^{2+} bound to the low affinity chelator system (Figure 3-9 and Table 3-1).

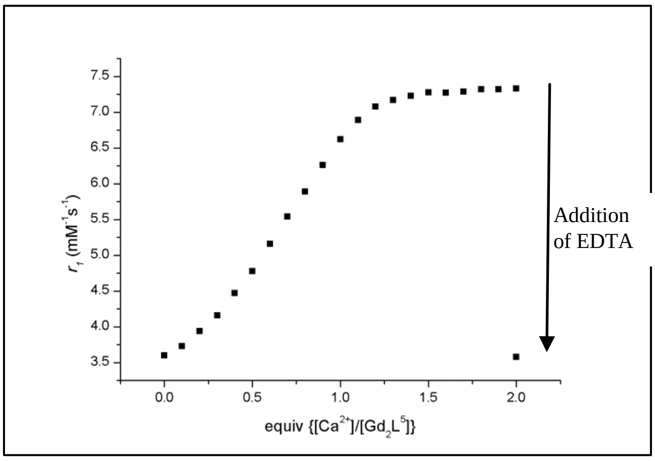

Figure 3-9: The Ca^{2+} dependent relaxivity response of $\mathbf{Gd_2L^5}$ in HEPES buffer (7T, 25 °C).

It has already been established that the mechanism involved in this change in relaxivity involves a change in hydration number with addition of Ca^{2+} ions. Increase in inner sphere-hydration number q with addition of Ca^{2+} is responsible for change in relaxivity in this class of complexes. The parent europium complex has demonstrated increase in q with addition of Ca^{2+} from 0.5 to 0.9. Therefore we assume that the same mechanism of activity is involved here for change in relaxivity.

Table 3-1: Titration of $\mathbf{Gd_2L^5}$ with Ca^{2+}.

[SCA]mM	$[Ca^{2+}]$/mM	$[Ca^{2+}]$/[SCA]	T_1/ms	r_1/$mM^{-1}s^{-1}$
1.50	0.00	0.0	89.68	3.60
1.49	0.15	0.1	86.92	3.73
1.49	0.30	0.2	82.78	3.94
1.48	0.44	0.3	78.90	4.16
1.48	0.59	0.4	73.88	4.47
1.47	0.74	0.5	69.44	4.78
1.46	0.88	0.6	64.63	5.16
1.46	1.02	0.7	60.51	5.54
1.45	1.16	0.8	57.27	5.89
1.45	1.30	0.9	54.14	6.26
1.44	1.44	1.0	51.39	6.62
1.44	1.58	1.1	49.60	6.89
1.43	1.72	1.2	48.51	7.08
1.43	1.85	1.3	48.11	7.17
1.42	1.99	1.4	47.88	7.23
1.42	2.12	1.5	47.74	7.28
1.41	2.26	1.6	47.97	7.27
1.40	2.39	1.7	48.03	7.29
1.40	2.52	1.8	48.02	7.32
1.39	2.65	1.9	48.15	7.32
1.39	2.78	2.0	48.27	7.33

3.5 Conclusions

In summary, we have successfully introduced a linker unit in a bismacrocyclic Ca^{2+} sensitive contrast agent. The synthetic strategy produced the ligand successfully in over 20 reaction steps. The other feature of the synthesis includes the optimization of key reaction like the mono alkylation of one of the secondary amine. Unification of two macrocyles with bridging modified EGTA was successfully achieved using a peptide coupling reaction. The response of SCA to Ca^{2+} ion was retained in the modified contrast agent without loss of stability. The modified SCA shows a 97% increase in relaxivity with the addition of 1.2 equivalents of Ca^{2+} with respect to the SCA which proves insertion of linker in the bismacrocylce doesn't have negative impact on its activity towards the Ca^{2+} metal ion. This synthetic strategy is encouraging for use in different responsive or anatomical probes based on DO3A macrocycle for further functionalization. This synthetic modification can provide a new pathway to attach this type of SCAs to number of functional molecules for the *in vivo* applications of obtained multifunctional hybrids.

Chapter 4: Synthetic modification of Ca^{2+} sensitive smart contrast agent using solid phase synthesis

4.1 Introduction

The inspirational Nobel Prize winning idea of Prof. Bruce Merrifield was to use solid support[112] to carry out the synthesis of peptides, which revolutionized the field of organic synthesis since the 1960s. Lately, many synthetic laboratories ranging from academia as well as to industry have started to develop new strategies suitable for use with solid support. The popularity of solid phase synthesis in the organic synthetic community is due to the efficacy of the method and obtaining product without the laborious intermediate purification steps. All the synthetic steps are carried out under heterogeneous conditions, between soluble reagents in the liquid phase and soluble peptide on solid support. Using this technique more than 100 amino acids can be coupled in very short time to deliver peptides with high purities.

4.1.1 Solid phase synthesis (SPS)

The SPS technique comprises the anchoring of first building block on a solid support with suitable protecting groups, followed by removal of one protecting group and the addition of the second reactant. These two steps are repeated until the desired product is constructed and finally it is cleaved from the solid support. The reactions can be carried out simply by mixing and shaking of the reagents in suitable solvents in the presence of suitable activators/catalysts. This leads to an exploration of combinatorial synthesis to produce libraries of peptides or small organic molecules for screening and to develop structure-activity relationship in medicinal chemistry.[113, 114] The major advantages of using solid phase synthesis are as follows:

i) Ease of method. Since the synthesis is occurring on the solid support; excess reagents can be used to drive the reaction to completion. Excess reagent can be washed from product (which is immobilized on solid support) with suitable solvent, where simple filtration is enough to remove excess reagent as well as some by-products.

ii) No intermediate purification and analysis. The entire reaction sequence can be carried out without isolation, purification and analysis of intermediate steps; only final product needs to be purified. In turn, this eliminates many time consuming and laborious processes used in traditional liquid phase synthesis.

iii) Low mechanical loss. All reaction sequences can be carried out in the same reaction container which minimizes the mechanical loss of reaction product.

iv) Automation. The simple synthetic technique can be automated using a computer assisted synthesizer.

Although there are a number of advantages, the success of solid phase synthesis depends on the appropriate selection of the solid support, linker that anchors the first reactant on the solid support, the combination of different protection/deprotection strategies and purification of final product after cleavage from the solid support.

Merrifield first synthesized a tetrapeptide using SPPS methodology.[112] The first amino acid was attached to the solid support through ester linkage of carboxylic acid group of the C-terminal amino acid. In the subsequent step the amine group was deprotected and coupled to second amino acid using DCC coupling agent, followed by deprotection and coupling to the next amino acid. This cycle was repeated until the desired tetrapeptide on solid support was obtained, which was cleaved in the final step by saponification or using HBr. Polystyrene cross linked with 2% divinyl benzene was used as solid support and DMF as solvent. Subsequently an automatic peptide synthesizer was developed which delivered a protected linear polypeptide of 124 amino acid residues with the sequence of bovine pancreatic ribonuclease A (RNase A).[115, 116] Following these reports, scientists attempted synthesis on solid support with varying supports,[117, 118] linkers,[119-122] conditions,[120, 123, 124] different protection-deprotection approaches[125] and various peptide bond formation strategies.[126-128]

Furthermore there are number of reports published in last decade on the use of SPPS in attachment of macrocycles such as NOTA, DOTA to peptides where peptides are selected with a specific role to act as a carrier or targeting vector of the macrocycle with metal ion.[129-139] Despite the large number of advantages, to the best of our knowledge there is no report of formation and functionalization of a bismacrocyclic DO3A derivative on solid support. As mentioned in the previous section (Chapter 3), there were significant challenges involved in the synthesis of the modified Ca^{2+} responsive agent, primarily due to the challenging purifications of intermediates and products, despite the efficiency of the transformations. To circumvent the above mentioned issues, we chose to use solid support for the synthesis of these types of bismacrocycles. Using SPS we could exclude time consuming intermediate purifications and further functionalize the ligand with peptides, fluorescent tags etc. Hence we designed the ligand structure for the bismacrocyclic compound (**L^7**) containing two linker units on each macrocycle which will be utilized to attach them to different tags.

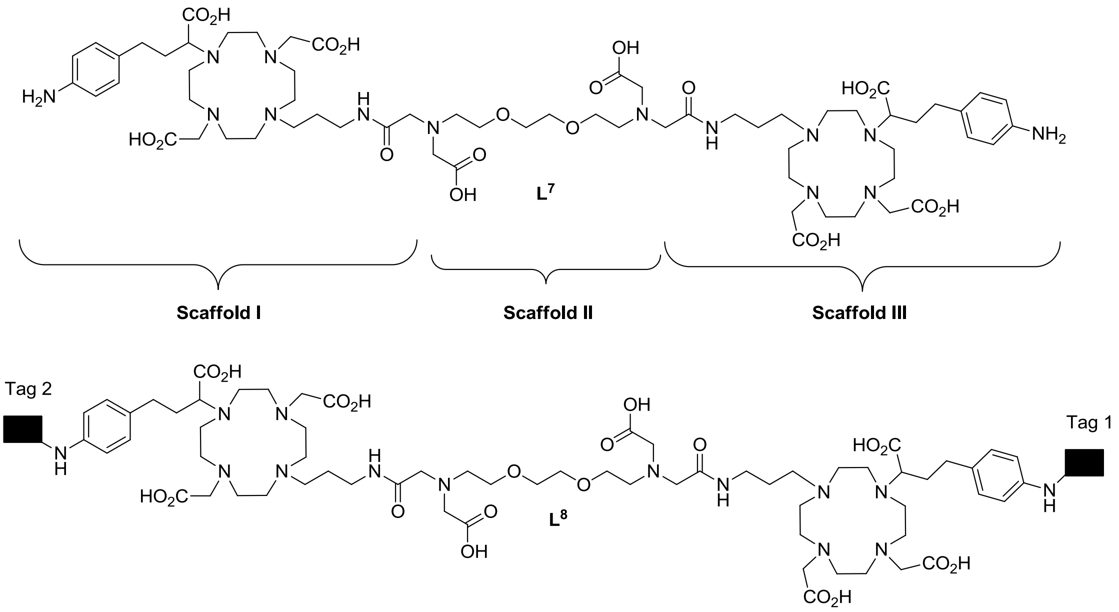

Figure 4-1: Schematic representation of ligand $\mathbf{L^7}$ and its modified version $\mathbf{L^8}$ carrying two different tags on each macrocycle.

4.2 Ligand design and retrosynthetic plan

We have designed a novel synthetic strategy which would yield the Ca^{2+} sensitive bismacrocycle with two identical linkers on each macrocycle on a solid support. In addition this strategy would enable us to produce a number of bismacrocyclic analogues in a very short period of time. The first retrosynthetic plan was straight forward since three scaffolds are added one after another in the following order, the first macrocycle on solid phase, then the Ca^{2+} chelator (a derivative of EGTA), finally the second macrocycle (Figure 4-3). The unification of all three scaffolds will be achieved with a peptide coupling reaction in presence of agents such as EDC, DCC, DIC, or HATU.

As mentioned earlier the few of the most crucial aspects are the choice of resin and linker. Since the resin is regarded as co-solvent in SPS, it should meet two important requirements: i) It should be compatible with the reagents and solvents used in the sequence of reactions to avoid premature cleavage of intermediates from the solid support and ii) It should provide the required functional group on the final molecule after deprotection. Other requisites include insolubility; swelling, loading, low price etc. Following a search of the literature we found the commercially available 2-(3,5-dimethoxy-4-formylphenoxy)ethyl polystyrene resin with backbone amide linker (BAL)[140, 141] having an aldehyde functional group (Figure 4-2). The main advantage of this approach is that, the aromatic primary amine group from the scaffold **I** can be attached to the resin via reductive amination. Thus the formed amine would be stable throughout the following acid amine coupling and deprotection steps involved in synthesis. Finally the molecule can be detached by using 50% mixture of TFA and dichloromethane retaining the primary amine. However 2-chlorotrityl chloride resin can also be used for the similar purpose since the anchoring of first scaffold containing aromatic primary amine can be achieved by alkylation reaction in presence of bases such as DIPEA, TEA, collidine and can be cleaved using TFA at the end. In order to choose more suitable resin for this project, small screening was carried out in two above mentioned resins by anchoring scaffold **I** and subsequent deprotection of pthalimide. In both cases complete conversion was observed but we decided to continue further with 2-chlorotrityl chloride resin since the anchoring of scaffold **I** is easier as compared to BAL resin.

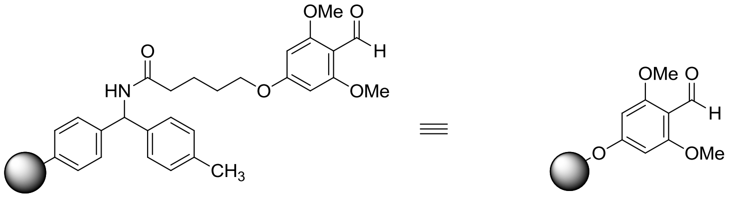

BAL resin

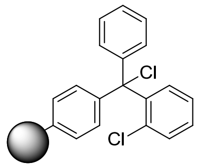

2-chlorotrityl chloride resin

Figure 4-2: Schematic presentation of resins.

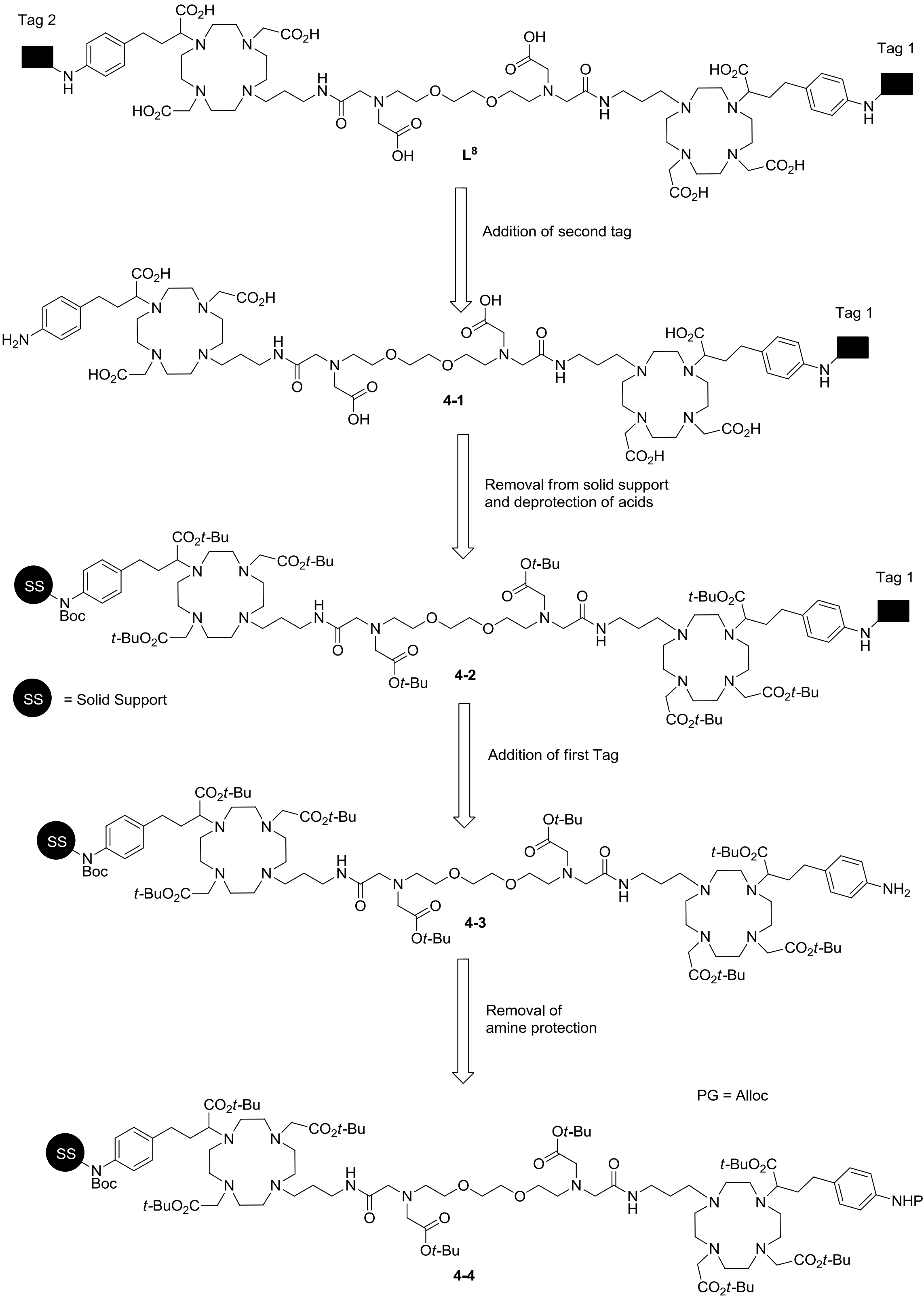
Tag 2
Tag 1
L8
Addition of second tag
4-1
Removal from solid support
and deprotection of acids
4-2
SS = Solid Support
Addition of first Tag
4-3
Removal of
amine protection
PG = Alloc
4-4

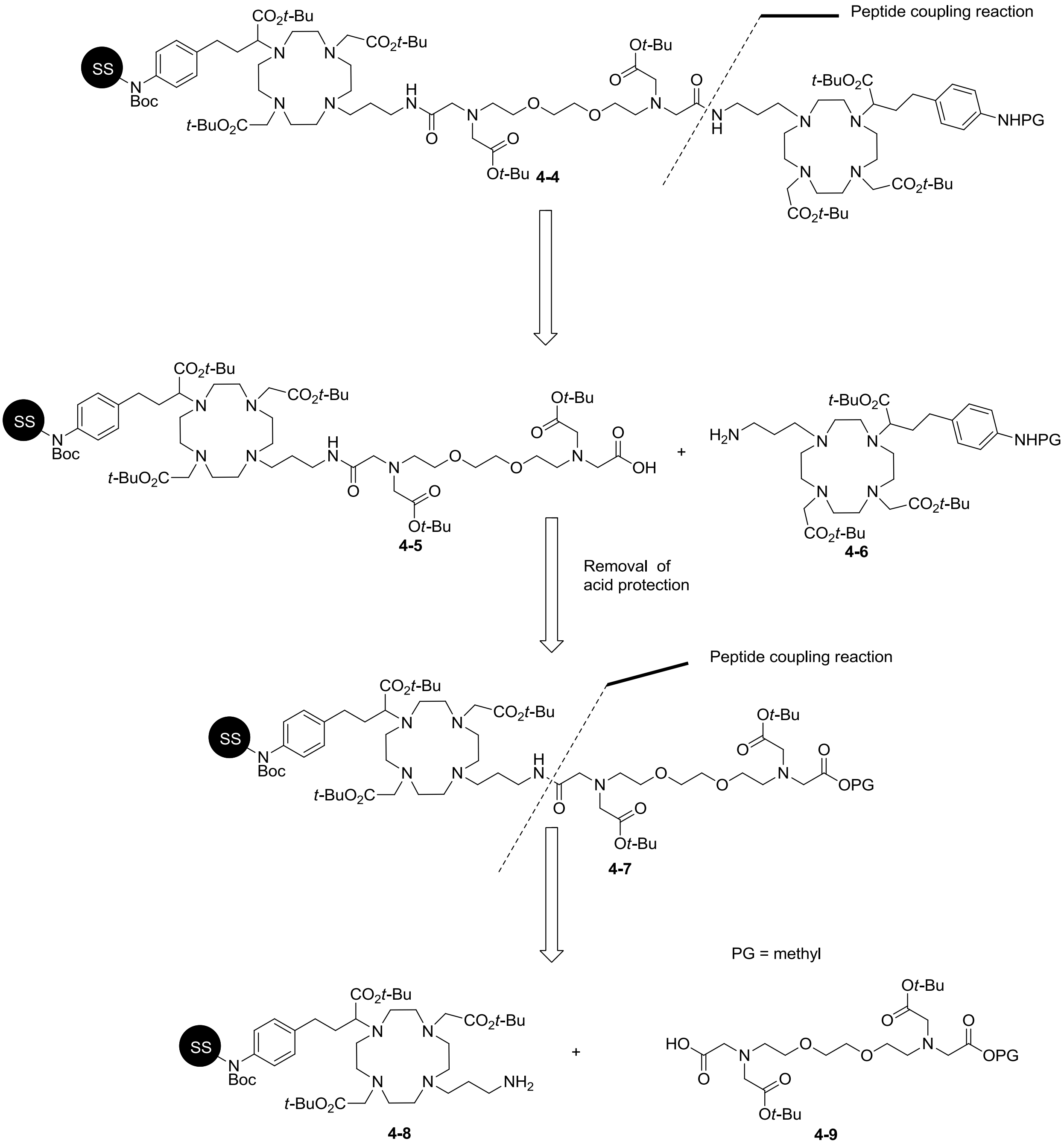
Peptide coupling reaction
4-4
4-5
4-6
Removal of acid protection
Peptide coupling reaction
4-7
4-8
4-9
SS
Boc
NHPG
OPG

PG = methyl

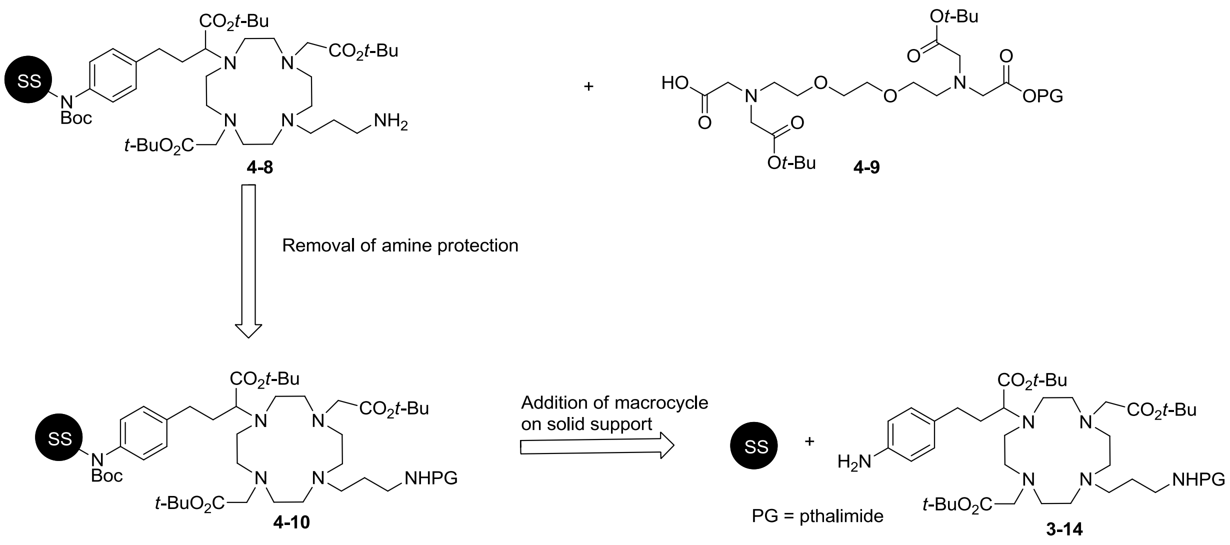

Figure 4-3: Retrosynthetic analysis of bismacrocycle containing two different tags on each macrocycle attached through aromatic linkers

After selection of resin the main task was to synthesize the required scaffolds in sufficient quantities to complete the synthesis on solid phase. Intermediate **3-14** from the previous chapter 3 can be used as scaffold **I**. We note that the aliphatic amine was masked as a pthalimide (despite of Fmoc or other base labile protecting group alternatives), although it is known that strong conditions are needed to remove pthalimide protection. Fmoc strategy was avoided since entirely new synthetic pathway would be required to prepare the scaffold.

As a proof of principle we decided to synthesize ligand $\mathbf{L^5}$ on solid support. Retrosynthetic plan would be anchoring of first macrocycle on solid support followed by removal of aliphatic amine protection and then coupling of amine and acid (scaffold **II**) using coupling agent. Finally detachment of product from solid support as well as removal of acid protection would yield $\mathbf{L^5}$ (Figure 4-4).

4.3 Results and discussion

4.3.1 Synthesis of $\mathbf{L^5}$

Synthesis of $\mathbf{L^5}$ was accomplished by using the intermediate **3-14** as scaffold **I** and intermediate **3-22** (both from previous chapter 3) as scaffold **II (**Scheme 4-1). Scaffold **I** which is primary amine was incorporated on swollen 2-chloro trityl chloride resin in

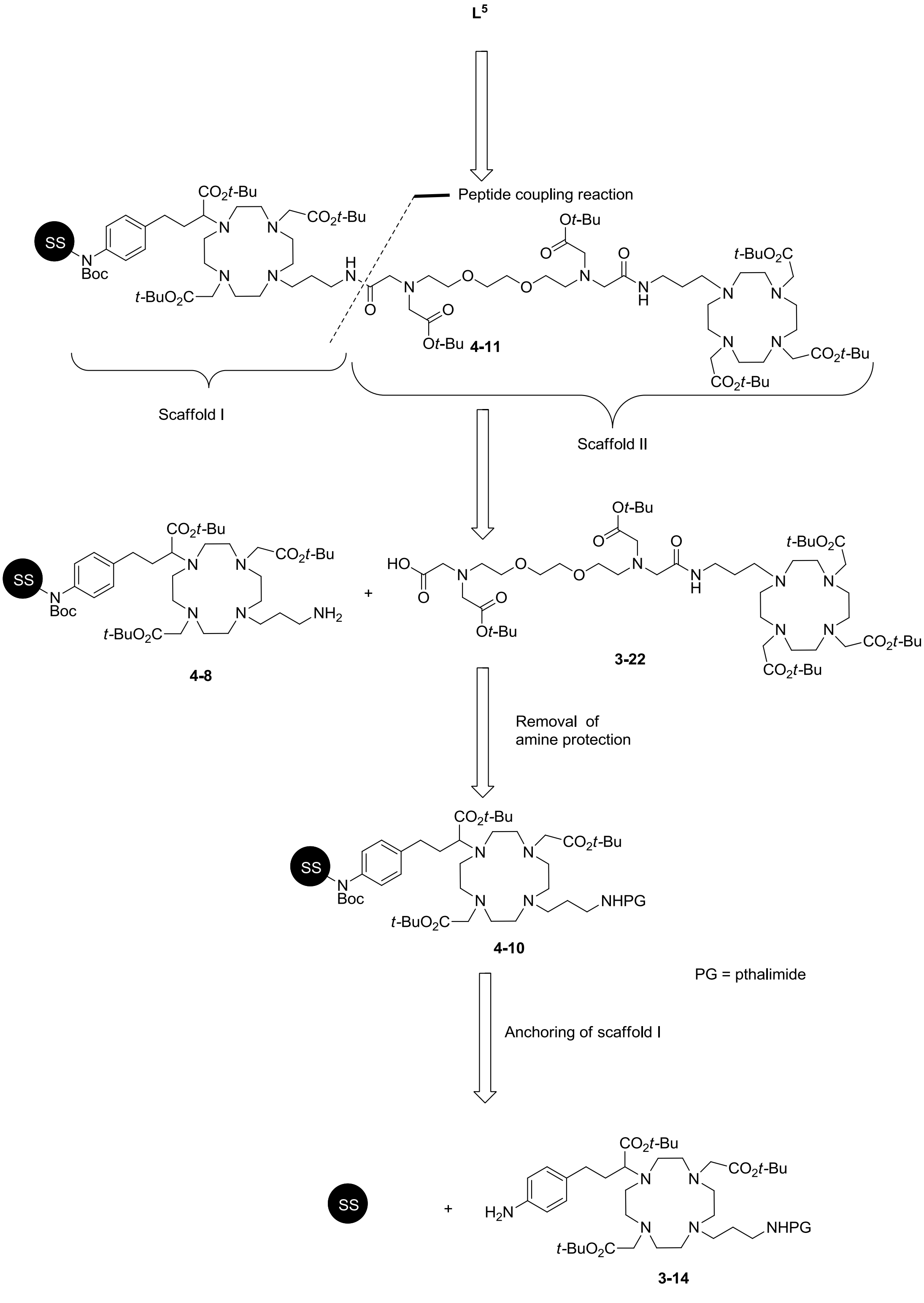
L5
Peptide coupling reaction
4-11
Scaffold I
Scaffold II
4-8
3-22
Removal of amine protection
4-10
PG = pthalimide
Anchoring of scaffold I
3-14
SS
Boc

Figure 4-4: Retrosynthetic analysis of **L**^{5} on solid support.

dichloromethane and DIPEA as base by substitution reaction. In order to maximize the loading of the macrocycle, the procedure was repeated twice. The successful loading of the first macrocycle on the resin was confirmed by ESI-MS which, was performed after coupling and extensive washing of the resin using DMF and dichloromethane followed by deprotection of few solid beads in 50% TFA in dichloromethane. The formed secondary amine of **4-12** was blocked by Boc protection in presence of excess trimethylamine and Boc anhydride in DMF at room temperature to obtain **4-10**. This additional protection was necessary to diminish the formation of side products with the excess of activated acid used in coupling conditions. The success of this reaction is difficult to determine as deprotection with TFA will also remove Boc group resulting in the same mass of the deprotected molecule **4-12**. The removal of pthalimide was accomplished by the same procedure as described before (Chapter 2) in presence of ethylendiamine in refluxing *iso*-propanaol to yield **4-8**. The conversion was efficient since we observed only the product peak after washing and deprotection on an analytical control. Coupling of **4-8** to acid **3-22** was achieved with the coupling agent HBTU and base DIPEA in DMF for 16 h, to obtain ligand precursor **4-11**. This reaction was carried out twice to maximize the conversion. ESI-MS confirmed the formation of product and absence of starting material. Deprotection of *tert*-butyl and Boc was achieved using 50% TFA in dichloromethane. Ligand $\mathbf{L^5}$ was obtained after precipitation of obtained crude from cold diethyl ether. The NMR analysis is consistent with the analysis of $\mathbf{L^5}$ obtained in liquid phase (Chapter 3). This led us to conclude that the applied synthetic strategy is successful. After that we moved to the synthesis of $\mathbf{L^8}$

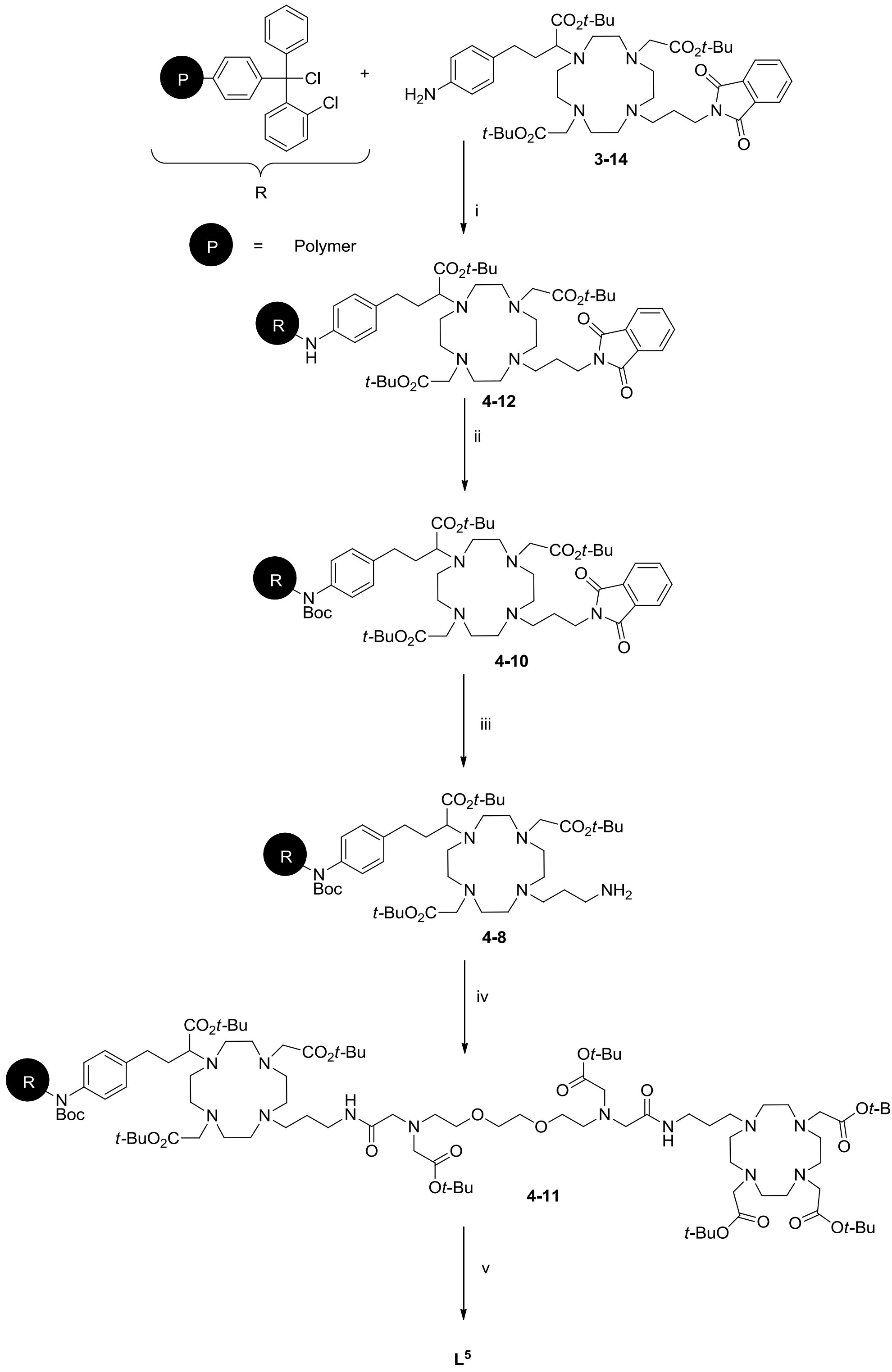
P
Cl
Cl
+
R
P = Polymer
H2N
CO2t-Bu
t-BuO2C
3-14
i
4-12
ii
Boc
4-10
iii
NH2
4-8
iv
Ot-Bu
t-BuO
4-11
v
L5

Scheme 4-1: Synthesis of **L**^{5} on solid support. **Reagents and conditions:** i) DIPEA, CH_2Cl_2, 16h; ii) $(Boc)_2O$, DIPEA, CH_2Cl_2, 16h; iii) Ethylenediamine, *iso*-PrOH, 90 °C, 16h; iv) **3-22**, HBTU, DIPEA, DMF, 16h; v) 50% TFA, CH_2Cl_2, 16h.

4.3.2 Synthesis of L^8

As mentioned earlier the main task was to synthesize required scaffolds (**II** and **III**) in sufficient quantity. The EGTA derivative acting as the Ca^{2+} chelator and bridging the two macrocycles was obtained from the synthetic pathway as shown in Scheme 4-2. The previously used diamine **3-10** was selectively monoalkylated using benzyl bromoacetate and cesium carbonate in acetonitrile at room temperature over two days to yield the amine **4-13**. The dialkylated derivative **4-14** was obtained by alkylating **4-13** with methyl bromoacetate and potassium carbonate at 70 °C. Hydrogenation in ethanol catalyzed by Pd/C produced the required acid **4-15** (scaffold **II** of $\mathbf{L^8}$).

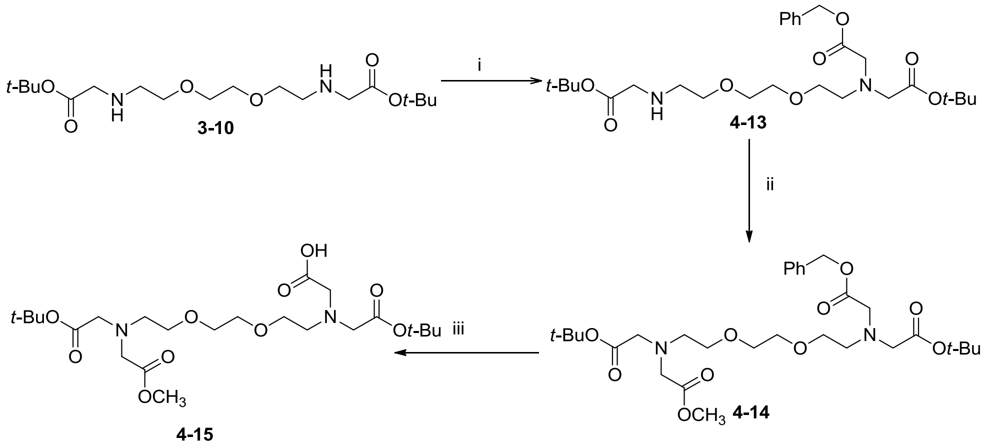

Scheme 4-2: Synthesis of EGTA derivative as scaffold **II** (**4-15**). **Reagents and conditions:** i) Benzyl bromoacetate, Cs_2CO_3, CH_3CN, 48h; ii) Methyl bromoacetate, K_2CO_3, CH_3CN, 70 °C; iii) H_2, Pd/C, EtOH, 16h.

Scaffold **III** is the extension of intermediate **3-14,** protected with allyl chloroformate. Deprotection of pthalimide using a previously described protocol afforded scaffold **III** (**4-17)** (Scheme 4-3).

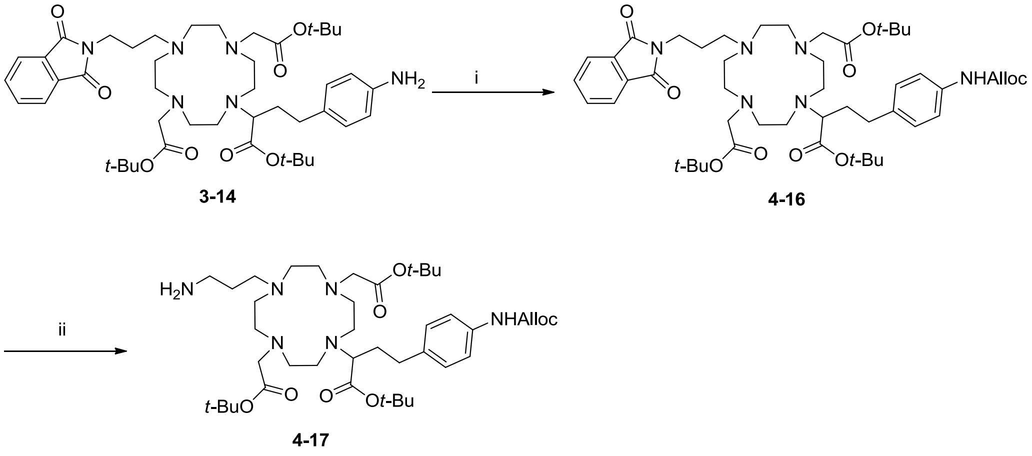

Scheme 4-3: Synthesis of amine **4-17**. **Reagents and conditions:** i) Allyl chloroformate, $NaHCO_3$, Dioxane, water; ii) Ethylenediamine, *iso*-PrOH, 90 °C, 16h.

With scaffolds **II** and **III** on hand, we attempted the synthesis of target molecule on resin. The coupling of intermediate **4-8** and scaffold **4-15** was achieved with the coupling agent HBTU and base DIPEA in DMF for 16 h, to obtain ester **4-7**. This reaction was carried out twice to maximize the conversion. ESI-MS confirmed the formation of product and absence of starting material (Scheme 4-4).

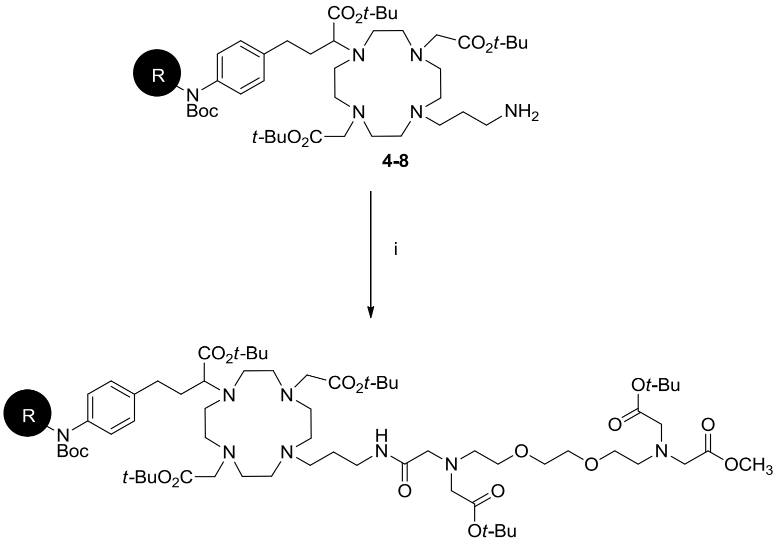

4-8

4-7

Scheme 4-4: Synthesis of methyl ester **4-7** on solid support. **Reagents and conditions:** i) **4-15**, HBTU, DIPEA, DMF, 16h.

The saponification of methyl ester to produce acid **4-7** (Scheme 4-7) was attempted by number of methods (Table 4-1).

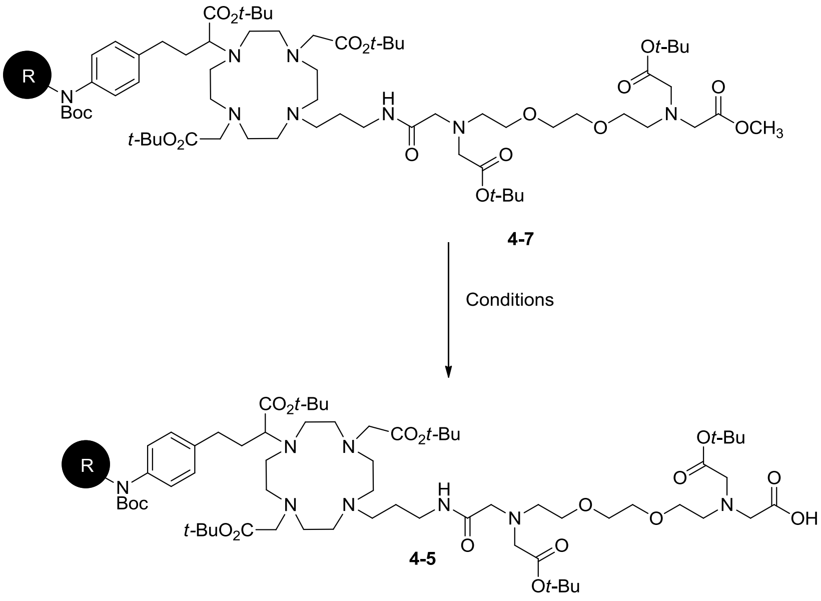

Scheme 4-5: Synthesis of an acid **4-21** on resin.

Table 4-1: Summary of attempts made to hydrolyze methyl ester **4-7**.

Reagents and Conditions	**Results**
1. LiOH, THF, Methanol, H_2O (2:2:1), rt, 16h	Complete conversion, shrinking of resin
2. LiOH (sat.aq.), THF, Methanol, rt, 16h	Complete conversion, shrinking of resin
3. NaOH, Methanol, rt, 16 h	Moderate conversion, shrinking of resin
4. K_2CO_3(sat. aq.), THF, Methanol, rt, 16h	Complete conversion, shrinking of resin
5. K_2CO_3, THF, Methanol, rt, 16h.	No conversion
6. LiOH, THF, Methanol, rt, 16h	No conversion

Each reaction summarized in Table 4-1 was monitored by ESI-MS after cleavage of product with 50% TFA in dichloromethane. In all attempts whenever water was used shrinking of resin was observed with almost complete loss of product from resin. In addition, no conversion was observed using a number of bases in absence of water. However with the obtained resin bound acid we proceed to next reaction which is coupling of carboxylic acid **4-5** from resin and amine of scaffold **III** (**4-17**).

We attempted number of conditions to achieve the coupling to get the desired compound **4-4**, none of which were successful (Table 4-2).

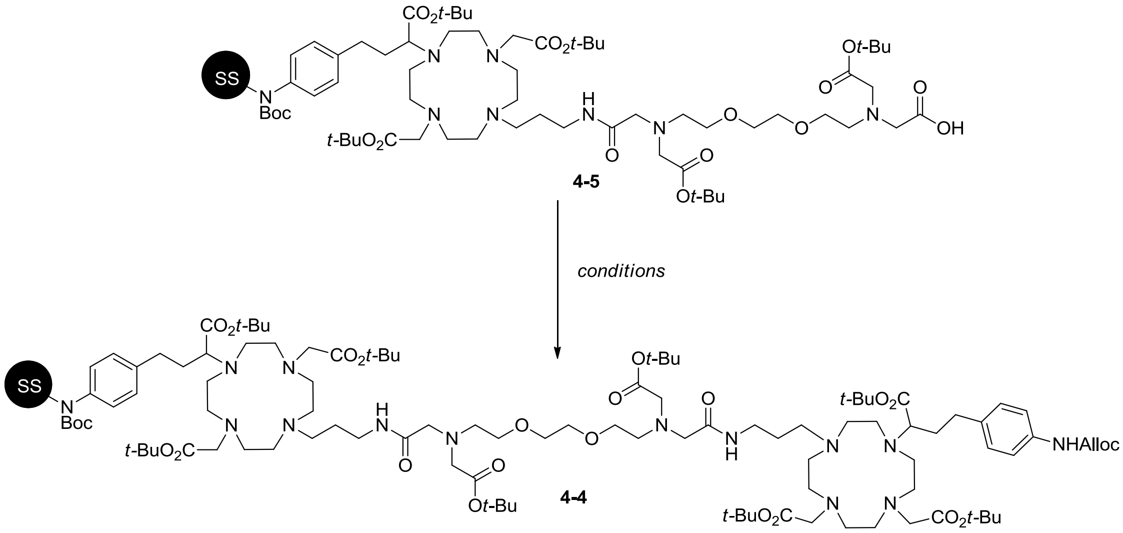

Scheme 4-6: Synthesis of fully protected bismacrocycle with linkers on solid support.

Table 4-2: Summary of attempts made to couple acid **4-5** and amine **4-17**.

Reagents and Conditions	Results
1. HATU, HOBt, DIPEA, DMF, rt, 16h	No conversion.
2. HBTU, HOBt, DIPEA, DMF, rt, 16h	No conversion.
3. EDC•HCl, DMAP, DMF, rt, 16 h	No conversion
4. DCC, CH_2Cl_2, rt, 16h	No conversion.
5. DIC, CH_2Cl_2, rt, 16h	No conversion.
6. PyBOP, DIPEA, CH_2Cl_2, rt, 16h	No conversion.
7. PyBrOP, DIPEA, CH_2Cl_2, rt, 16h	No conversion.

The reason for this failure might be that the growing chain on the solid support sterically hinders carboxylic acid, which inhibits its coupling to the amine. Therefore, we proposed new synthetic strategy to obtain the bismacrocycle. In this, we could couple the EGTA derivative and second macrocycle (scaffolds **II** and **III**), followed by the deprotection of methyl ester in solution phase and coupling to the first macrocycle **4-8** on solid support.

We accomplished the synthesis of acid **4-19** with two scaffolds **II** and **III** in solution phase (Scheme 4-7). Mono-methyl protected acid **4-9** was coupled with amine **4-17** in the presence of HBTU in DMF at room temperature to afford **4-18**. Saponification of methyl ester **4-18** to produce acid or scaffold **4-19** was achieved using lithium hydroxide in a mixture of THF, methanol and water. Due to highly polar nature of products, number of attempts were failed to purify intermediates as well as products using existing purification techniques. Hence we proceed with crude mixture of **4-19** for further reactions.

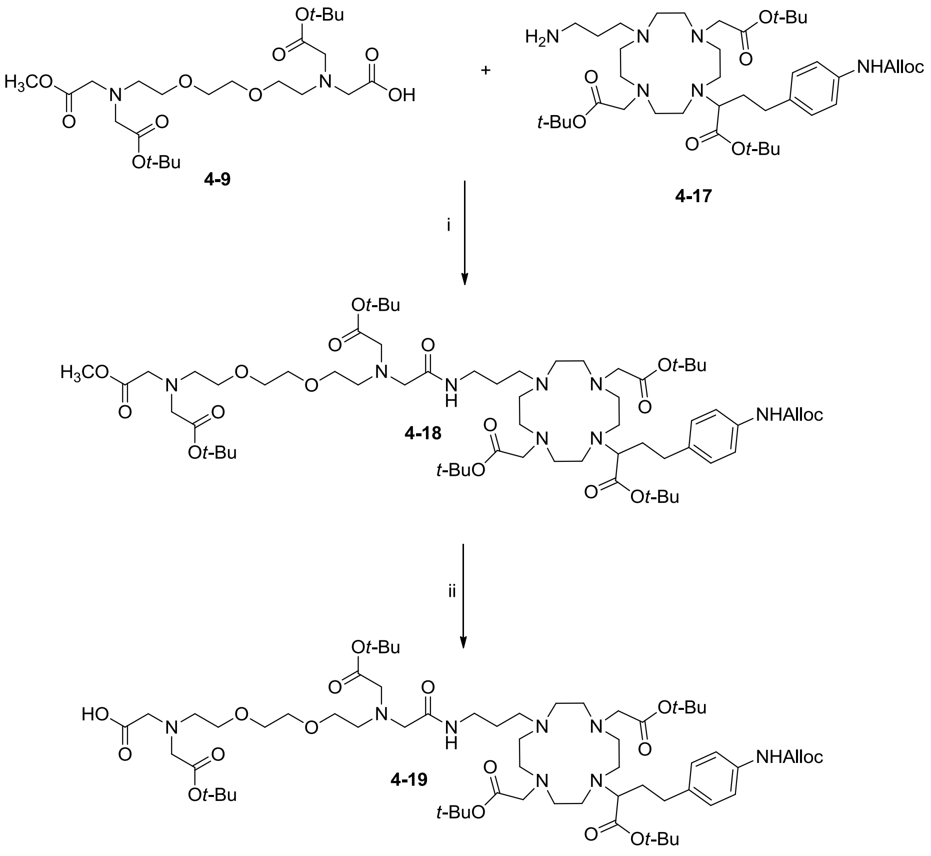
4-9
4-17
i
4-18
ii
4-19
+
Ot-Bu
H3CO
HO
OH
H2N
t-BuO
NHAlloc
N
O
H

Scheme 4-7: Synthesis of acid **4-19. Reagents and conditions**: i) HBTU, DMF, 16h; ii) LiOH, THF, methanol, H_2O, 16h.

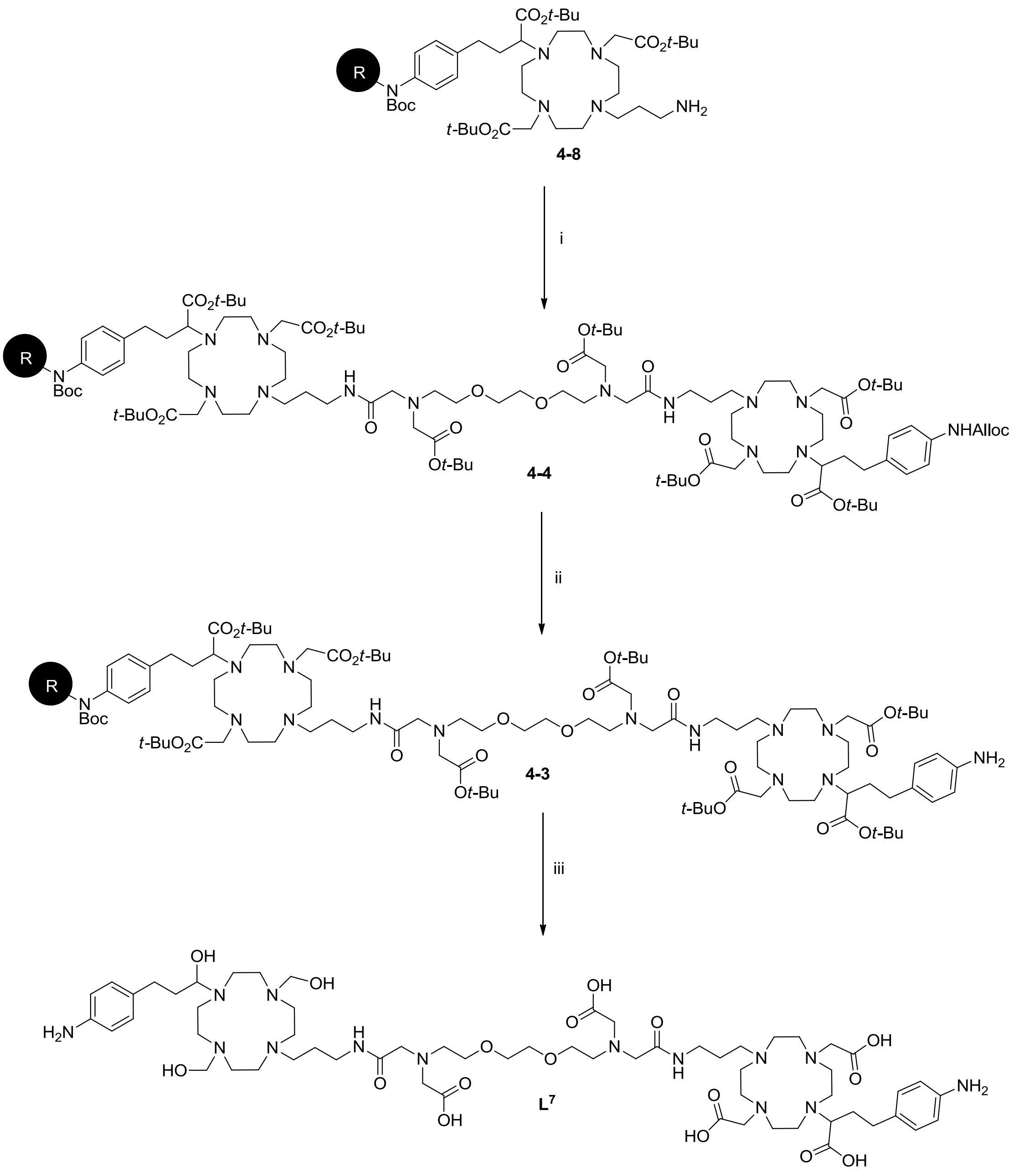

Scheme 4-8: Synthesis of **L**^{7}. **Reagents and conditions:** i) **4-19**, HBTU, DIPEA, DMF, 16h; ii) Pd(PPh_3)$_4$, morpholine, DMF, 16h; ii) 50% TFA, CH_2Cl_2, 16h.

With acid **4-19** on hand, we completed the synthesis of the bismacrocycle on 2-chlorotrityl chloride resin (Scheme 4-8) following a scheme similar to scheme 4-1. Acid **4-19** was coupled in DMF to amine **4-8** on solid support using HBTU as coupling agent. Deprotection of Alloc with Pd(PPh_3)$_4$ in DMF and morpholine as a cation scavenger provided amine **4-3** on solid support for further addition of functional molecule such as dyes, cell penetrating peptides or cargo molecules (Tag 1). This is the most important intermediate of the sequence to further functionalize the bismacrocycle using amine coupling chemistry on solid support.

To prove the success of desired synthetic strategy, we carried out deprotection of the bismacrocycle from the resin as well as concomitant deprotection of *tert*-butyl and Boc in 50% trifluroacetic acid and dichloromethane to afford **L^7**. Every reaction step in the sequence was confirmed by ESI-MS after cleavage in trifluroacetic acid and dichloromethane mixture. ESI-MS confirmed the formation of the final ligand **L^7**. Final analysis of **L^7** showed small impurities even after RP-HPLC purification and yield is also poor which could be because of crude mixture of acid **4-19** (Scheme 4-7) used in final coupling. Hence further attempts are necessary to get pure **4-19** in order to get pure **L^7**.

4.4 Conclusions

In conclusion, we have developed a facile route to modify a Ca^{2+} responsive contrast agent. The ligand **L^5** consisting of a bismacrocycle appended with aromatic linker unit was synthesized on a 2-chloro trityl chloride resin. This is the first attempt to use solid support to synthesize a bismacrocycle. The key feature of this approach is the successful demonstration of phthalimide-strategy for amine protection. Phthalimide was successfully removed using ethtylenediamine in refluxing *iso*-propanol on solid support. Importantly, after reflux, phthalimide protected reactant was not observed in ESI-MS leading to the conclusion that the deprotection went almost to completion. Further **L^7** bismacrocycle appended with two aromatic linker units on each cyclen backbone and free aniline as functional group were synthesized successfully. This strategy will enable us to deliver series of analogues of Ca^{2+} responsive agents as well as other bismacrocyclic responsive agents in a short period just by changing the building blocks. The technique is simple and useful exploiting combinatorial chemistry to potentially deliver libraries of molecules. Further functionalization of the agents could be done more easily than through solution phase techniques.

Chapter 5: Summary, conclusions and outlook

The aim of work presented in this thesis was to synthetically modify responsive MRI contrast agents by appending with linker moieties comprising appropriate functional groups on it to further couple with various functional molecules.

The first part of thesis presented synthetic modifications of DO3A based phosphonate side arm appended pH sensitive CA. With convenient similar multistep synthetic routes lanthanide complexes of **L**^{1} (with aliphatic linker) and **L**^{2} (with aromatic linker) were prepared. Key feature of the synthesis was the selective monoalkylation of bis-*tert*-butyl DO2A with linkers. The relaxometric study of **GdL**$^{1–2}$ at different pH (basic, neutral and acidic) revealed that the pH response in **GdL**$^{1–2}$ is retained. **GdL**^{1} showed 147% change in longitudinal relaxivity r_1 (with change in pH from 9 to 5) while 31% change in r_1 of **GdL**^{2} observed within same range of pH change. The change in r_1 of **GdL**^{1} is observed due to change in hydration number q at different pH which was confirmed using time resolved emission lifetime measurement. Biotin was introduced in modified agents to obtain biotinylated contrast agents **GdL**^{3} (with aliphatic linker) and **GdL**^{4} (with aromatic linker) for targeted imaging. The binding affinity of **GdL**$^{3–4}$ towards avidin was studied using two independent methods. Fluorescence displacement assay performed using ANS dye displayed only three binding sites were present in studied avidin for coupling with biotinylated complexes. Conditional stability constant Ks of biotin and biotinylated complexes showed binding affinities are as comparable as biotin obtained using titration curves of avidin and biotin/**GdL**$^{3–4}$. These results were further confirmed by E-titrations performed in following r_1 and r_2.

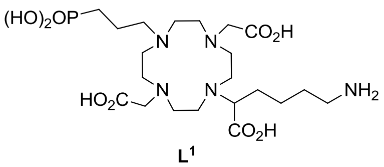

L^{1}

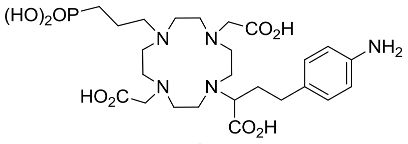

L^{2}

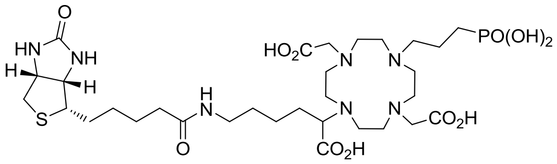

L^{3}

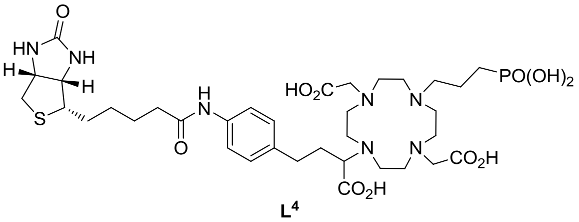

L^{4}

MRI phantom experiments of **GdL**$^{3–4}$ with and without avidin following r_1 and r_2 were carried out at different pH ranging from acidic to basic. **GdL**$^{3–4}$ in the presence and absence of avidin exhibited increase in r_1 and r_2 with decreasing pH from 9 to 5.5. **GdL**^{3}-avidin conjugate showed 21% and 49% increase in r_1 and r_2 respectively. While **GdL^4**-avidin conjugate displayed 12% and 30% increase in r_1 and r_2 respectively. The competitive MRI assay indicated an excess of biotin would not replace the biotinylated complexes from avidin which confirms the feasibility of complexes *in vivo* conditions. This study is pathway for development of target specific SCAs for *in vivo* application. The strategy can be used to modify the majority of DO3A based responsive MRI probes.

Chapter 3 described synthetic modification of bismacrocyclic Ca^{2+} sensitive probe inserting the aromatic linker on one of the cyclen backbone of it. Synthesis of ligand **L^5** has been accomplished in more than 20 reaction steps. Key step of synthesis involved selective mono protection of one of amine from identical secondary amines of EGTA derivative. Terminal amino group from the linker was successfully converted into isothiocynate group to obtain ligand **L^6**. **Gd$_2$L^5** displayed 97% change in relaxivity towards Ca^{2+} which proved the preservation of Ca^{2+} response after synthetic modification (complete retention in relaxivity property).

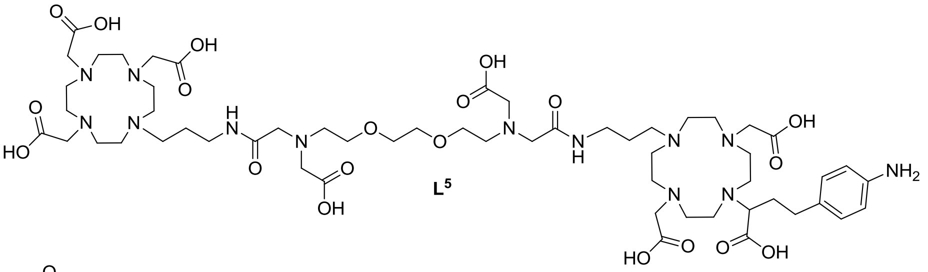
L^5

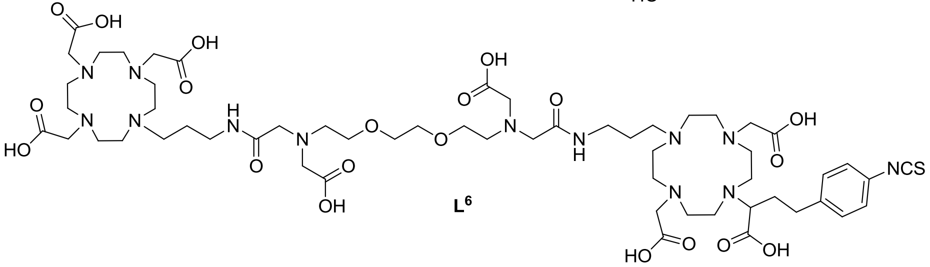
L^6

Gd$_2$L^5 opens the door to form new conjugated systems with several functional molecules including dendrimers, peptides, fluorescent tags, and nanoparticles according to the desired application.

In many *in vivo* applications one of the biggest obstacles to use such probes routinely is its diffusion over time from region of interest and hence decreases in signal intensity during measurement. In order to decrease the diffusion and to increase the local concentration, use of conjugates of probes with dendrimers of higher generations will be helpful. To facile formation of such conjugates, **Gd$_2$L^5** would be better since it can be attached to dendrimer more efficiently via newly introduced linker and assess its applicability *in vitro* and *in vivo* models.

Furthermore, the modified agent can be attached to the USPIO nanoparticles, well known as T_2 agents to form ratiometric probe of T_1/T_2 since T_2 from nanoparticle would remain constant and T_1 will change as a function of Ca^{2+} concentration. This will provide a MRI signal independent of probe concentration

Alternatively, newly introduced linker from SCA can be utilized to attach NMR active atom containing molecules such as perfluorocarbons or their derivatives where ^{19}F can be served to quantify the SCA *in vivo*. In such diverse applications modified SCA $\mathbf{Gd_2L^5}$ would serve as excellent probe to further functionalization.

Chapter 4 reported synthesis of $\mathbf{L^5}$ on solid support applying phthalimide/*tert*-butyl chemistry. This is first report of synthesis of bismacrocycle on solid support. Furthermore ligand $\mathbf{L^7}$ which is modified version of $\mathbf{L^5}$ comprising two aromatic linkers on each macrocycle was successfully synthesized. Further optimizations are needed such as coupling conditions, purification procedure to obtain the ligand in sufficient quantity with high purity.

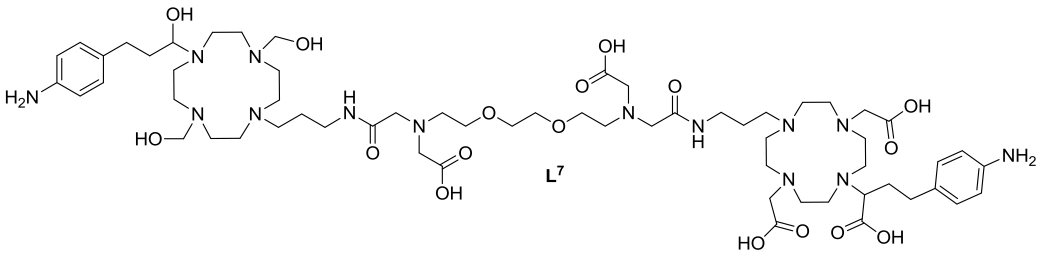

$\mathbf{L^7}$

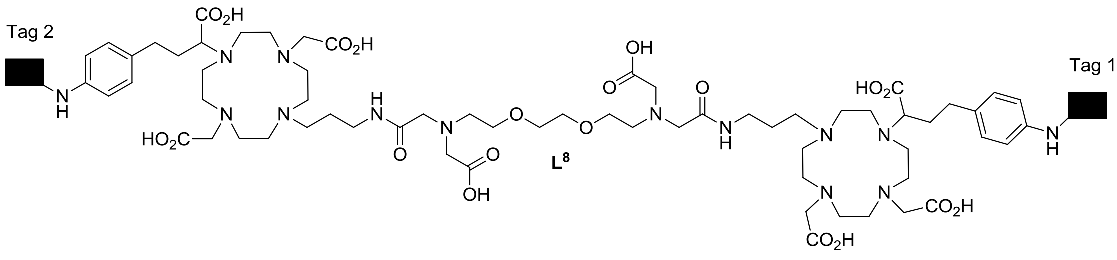

$\mathbf{L^8}$

This is one of convenient strategy to obtain and attach the Ca^{2+} responsive agent to a functional molecule which will, in conjugation with agent, report useful information *in vivo*. Addition of two different dyes as tag 1 and tag 2 will yield excellent conjugate to study the FRET (fluorescence resonance energy transfer) response with a change in Ca^{2+} concentration. This approach would provide easy way to obtain multimodal targeted probe. Moreover, in order to make the probe target specific facile attachment of delivering or targeting vectors would be affordable using described methodology.

Overall, we have successfully modified DO3A based multi targeted responsive contrast agents by inserting linking units in it. Efficient and easy labeling of such agents with wide range of functional molecules are possible using aforementioned strategies. Furthermore the demonstrated methodology would be excellent tool to obtain multimodal imaging probes for biomedical applications.

Chapter 6: Materials and methods

6.1 Materials and Methods

6.1.1 Chemicals and working techniques

All chemicals and reagents were purchased from commercial sources and were used without further purifications. The anhydrous solvents dichloromethane, acetonitrile, methanol, dimethylformamide were purchased from Acros Organics. H-Lys(Z)-OH (**2-14**), 4-(4-nitro phenyl butyric acid (**2-16**) and biotin were purchased from Sigma-Aldrich, Germany. Cyclen (**2-9**) was purchased from CheMatech, France. Avidin was purchased from Merck, Germany. ANS was purchased from Life Technologies GmbH, Germany. bis-*tert*-butyl DO2A (**2-10**) and DO3A-propyl amine bromide (DO3A-PA bromide) was synthesized using reported procedure.[142] Unless otherwise mentioned all reactions were carried out under a nitrogen atmosphere, all glass wares were washed with mixed acid solution and rinsed with distilled water and acetone prior to use and the flasks were dried in hot oven (60 °C). Air and water sensitive reagents were kept under an inert atmosphere of nitrogen. Distilled water was used for the reaction work up and milliQ water was used after the last deprotection steps. The compounds are not described in the experimental sections were synthesized according to reported procedures.

6.1.2 Reverse phase high performance liquid chromatography (RP-HPLC)

HPLC was performed at room temperature on a Varian PrepStar Instrument, Australia, equipped with PrepStar SD-1 pump heads. UV absorbance was measured using ProStar 335 photodiode array detector at 214 nm and 254 nm. This detector is equipped with a dual-path length flow cell which enables measurement of absorbance of analytical and preparative samples without changing the flow cell. All solvents used were of HPLC grade and were bought from different commercial sources and used without further purification.

Reversed phase analytical HPLC was performed in a stainless steel Atlantis C18 column (4.6 mm × 150 mm, particle size 5 µm) with a flow rate of 1mL/min.

Reverse phase semi-preparative HPLC was also performed on similar type of column but with bigger size (19 mm × 150 mm, particle size 5 µm) with flow rate of 10 mL/min.:

The following elution methods of 30 minutes were used, *Method A*

80% solvent A (water, 0.1% HCOOH and 20% solvent B (acetonitrile, 0.1% HCOOH) isocratic for 5 minutes to 80 % solvent B until 17 minutes, isocratic till 23 minutes then again 20% till 27 minutes and isocratic till 30 minutes.

Method B

Method B was same as Method *A* except solvent B was methanol with 0.1% HCOOH.

Method C

80% solvent A (water, 0.1% HCOOH and 20% solvent B (acetonitrile, 0.1% HCOOH) isocratic for 5 minutes to 95 % solvent B until 17 minutes, isocratic till 23 minutes then again 20% till 27 minutes and isocratic till 30 minutes.

6.1.3 NMR-spectroscopy

^{1}H, ^{13}C, ^{31}P NMR of all ligands and intermediates as well as ^{31}P NMR of Eu^{3+} complexes NMR analysis were carried out using a Bruker 300MHz. ^{1}H, ^{13}C and ^{31}P NMR spectra were performed in deuterated solvents and chemical shifts were assigned by comparison with the residual proton and carbon resonance of the solvents and tetramethylsilane as the internal reference ($\delta = 0$). ^{31}P NMR was done using 85% H_3PO_4 ($\delta = 0$) as external reference. Data are reported as follows: chemical shift (multiplicity: s = singlet, d = doublet, t = triplet, dd = double of doublet, br = broadened, *J* = coupling constant (Hz), integration, peak assignment in italic form).

6.1.4 Mass spectrometry

ESI low resolution mass spectra (ESI-MS) were recorded on a SL 1100 system (Agilent, Germany) with ion trap detection in positive and negative mode. ESI high resolution mass spectras (ESI-HRMS) were performed on a Bruker Daltonics Apex II FT-ICR-MS (Bruker, Germany). MS values were reported as ESI-MS: calculated for the related compound by found mass.

6.1.5 Chromatographic methods

Flash column chromatography was performed using flash silica gel 60 (70-230 mesh) and alumina (basic and neutral) from commercial sources. Analytical thin layer chromatography (TLC) was performed on aluminum sheet silica gel plates with 0.2 mm thick silica gel 60

F254 (E. Merck, Germany) using different mobile phase. The compounds were visualized by UV at 254 wavelength light and TLC plates were developed in Iodine chamber, and different staining agents such as ninhydrin solution, Dragendorff reagent etc.

6.1.6 Luminescence lifetime measurement

Luminescence steady-state and time resolved measurements were performed on QuantaMasterTM 3 PH fluorescence spectrometer from Photon Technology International, Inc. (USA). The steady state measurements were performed in H_2O **(**25 °C, at pH 7 and 5) at a concentration of 5 mM for **EuL**$^{\mathbf{1,\,2}}$. Excitation and emission slits were set to 2 nm and 1 nm. Datasets are an average of 15 scans. The time resolved measurements were performed in H_2O and D_2O **(**25 °C, at pH 7 and 5). Excitation and emission slits were set to 15 and 5 nm bandpass respectively, with 10 µs resolution. Datasets are recorded with a 100 µs delay and are an average of 10 scans. Each reported value is the mean of three independent measurements and obtained curves are fitted to the first order exponential decay with $R^2 > 0.99$.

6.2 Preparation of Ln^{3+} complexes

GdL$^{\mathbf{1\text{-}4}}$ and **EuL**$^{\mathbf{1\text{-}2}}$ were prepared from the respective solution of the ligand (1.0 equiv) and the aqueous solution of $GdCl_3•6H_20$ for **L**$^{\mathbf{1\text{-}4}}$ or $EuCl_3•6H_20$ (1.0 equiv) for **L**$^{\mathbf{1\text{-}2}}$. For each complex the lanthanide salt solution was added portion wise over 6 h. Once the ligand could no longer be observed by ESI-MS, the reaction mixture was stirred at 60 °C for an additional 16 h. The pH value of the solution was periodically checked and adjusted to 6.5-7.0 by using an aqueous solution of sodium hydroxide (0.5 M). The solutions were then treated with Chelex® 100 sodium form for 4 h at room temperature to remove any excess lanthanide ion. The absence of free Gd^{3+}/Eu^{3+} was confirmed with the xylenol orange test. The complexes were characterized by ESI-LRMS in negative mode and the appropriate isotope pattern distribution for Gd^{3+} and Eu^{3+} was obtained. **GdL**$^{\mathbf{5}}$ was also prepared by the same method except an aqueous solution of 2 equiv of $GdCl_3•6H_20$ was added to **L**$^{\mathbf{5}}$.

6.3 Relaxometric experiments

The relaxivities of the complexes **GdL**$^{\mathbf{1\text{-}2}}$ are an average of three measurements at concentrations ranging from 1-3 mM in H_2O. The solution pH was adjusted with solid LiOH and *p*-TsOH. For each measurement the exact concentration of the Gd^{3+} complex was determined using the bulk magnetic susceptibility shift technique.[95] While relaxivities of complex **GdL^5** as well as relaxivities with Ca^{2+} titration are at 1.5 mM concentration of probe.

6.4 Fluorescence displacement assay

Stock solutions of avidin and ANS were prepared at concentrations 4 µM and 40 µM, respectively, in 0.15 M sodium phosphate buffer at pH 7. Buffered solutions of avidin (1 mL, 4 µM) and ANS (1 mL, 40 µM) were mixed 1:1 (v/v) and the resulting conjugate was titrated with biotin/ **GdL^3**/**GdL^4** (320 µM) in 5 µL aliquots. All measurements were performed at 25 °C with the excitation and emission wavelengths of 328 and 408 nm respectively, and excitation and emission slits at 2 nm bandpass.

The corrected and normalized fluorescence signal is plotted as a function of the ratio of added biotin/**GdL$^{3-4}$** to avidin (Fig. 2-6). Since three, rather than four binding sites are available on the avidin tetramer, this stoichiometry was used to develop a linear relationship used to determine the conditional stability constant value K_s for the reaction of avidin-2,6-ANS complex with biotin (Eq. 6-1), as well as with **GdL^{3,4}**.

$$\mathrm{Av(ANS)_3 + 3Bio \rightleftharpoons Av(Bio)_3 + 3ANS}, \qquad K_\mathrm{s} = \frac{\mathrm{[Av(Bio)_3][ANS]^3}}{\mathrm{[Av(ANS)_3][Bio]^3}} \qquad \text{Eq. (6-1)}$$

If the basic avidin-ANS and avidin-biotin reactions are considered:

$$\mathrm{Av + 3ANS \rightleftharpoons Av(ANS)_3}, \qquad K_\mathrm{s}^\mathrm{I} = \frac{\mathrm{[Av(ANS)_3]}}{\mathrm{[Av][ANS]^3}} \qquad \text{Eq. (6-2)}$$

$$\mathrm{Av + 3Bio \rightleftharpoons Av(Bio)_3}, \qquad K_\mathrm{s}^\mathrm{II} = \frac{\mathrm{[Av(Bio)_3]}}{\mathrm{[Av][Bio]^3}} \qquad \text{Eq. (6-3)}$$

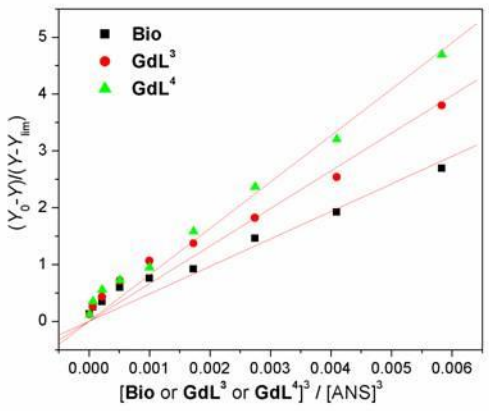

Figure 6-1: Conditional stability constant (K_s) determination according to Eq. 6-6.

Table 6-1: Conditional stability constant values (K_s) obtained as the slope of the linear fit based on Eq. 6-1

Sample fluorescence Titration		K_s ± SD	
	Av-Bio	Av-**GdL**^{3}	Av-**GdL**^{4}
1.	302 ± 11	413 ± 24	464 ± 19
2.	417 ± 16	735 ± 30	618 ± 22
3.	527 ± 22	541 ± 21	751 ± 29
4.	379 ± 12	625 ± 23	676 ± 16
5.	487 ± 18	662 ± 33	818 ± 29
$<K_s>$ ± SD	$(4.2 \pm 0.9)\text{x}10^2$	$(6 \pm 1)\text{x}10^2$	$(7 \pm 1)\text{x}10^2$

then K_s from Eq. 6-1 can be rearranged:

$$K_s = \frac{[\mathrm{Av(Bio)_3}][\mathrm{ANS}]^3}{[\mathrm{Av(ANS)_3}][\mathrm{Bio}]^3} \times \frac{[\mathrm{Av}]}{[\mathrm{Av}]} = \frac{K_s^{\mathrm{II}}}{K_s^{\mathrm{I}}} \qquad \text{Eq. (6-4)}$$

to give the linear dependence:

$$\frac{[\mathrm{Av(Bio)_3}]}{[\mathrm{Av(ANS)_3}]} = K_s \times \frac{[\mathrm{Bio}]^3}{[\mathrm{ANS}]^3} \qquad \text{Eq. (6-5)}$$

where [ANS] represents the fixed concentration of ANS (experimental details given in the Experimental section), [Bio] is the concentration of added biotin in each titration point, and [Av(Bio)$_3$] and [Av(ANS)$_3$] are the concentrations of avidin-biotin and avidin-ANS complexes, respectively. As these concentrations are proportional to measured fluorescence intensities,[143] the obtained experimental data (Figure 6-6) can be used for conditional stability constant determination:

$$\frac{Y_0 - Y}{Y - Y_{\mathrm{lim}}} = K_s \times \frac{[\mathrm{Bio}]^3}{[\mathrm{ANS}]^3} \qquad \text{Eq. (6-6)}$$

where Y_0 is the fluorescence intensity at the beginning of titration (no biotin added), Y_{lim} is an average value of all measured fluorescence intensities after the equivalence point was reached, and Y stands for measured fluorescence intensities during the titration (as reaction (1) proceeds). The measured fluorescence intensities were corrected for inner-filter effects[144] and normalized. The conditional stability constant values K_{s} for avidin-biotin, avidin-**GdL^3** and avidin-**GdL^4** are obtained as slopes from the linear fit based on Eq. 6-6, with $R^2>0.98$ (Figure 6-1). K_{s} values are obtained as mean values of five times repeated titrations. Results are shown in Table 5-2. As the dissociation constant of the avidin(monomer)-ANS was already reported (K_{d}=203 µM)[3], K_s^{I} value (Eq. 5-2) is calculated ($K_{\mathrm{s}}^{\mathrm{I}} = \frac{1}{(K_{\mathrm{d}})^3} = 1.2\mathrm{x}10^{11}$), and used for the overall stability constants $K_{\mathrm{s}}^{\mathrm{II}}$ (Eq. 5-4) calculation, resulting in $K_{\mathrm{s}}^{\mathrm{II}}$(Av(Bio)$_3$)=5.1x10^{13}, $K_{\mathrm{s}}^{\mathrm{II}}$(Av(**GdL^3**)$_3$)=7.1x10^{13}, $K_{\mathrm{s}}^{\mathrm{II}}$(Av(**GdL^4**)$_3$)=8.0x10^{13}.

6.5 MRI phantom experiments

MR imaging of the samples was performed at 3T (123 MHz, 21 °C) on a clinical human MR scanner (MAGNETOM Tim Trio, Siemens Healthcare, Germany). Stock solutions of **GdL$^{3\text{-}4}$** (0.25 mM) and avidin (0.225 mM) were prepared in HEPES buffer (25 mM, pH 7.4) and water, respectively. The concentration of **GdL$^{3\text{-}4}$** was kept constant (0.125 mM) while the concentration of avidin varied up to a ratio of 0.9 avidin:**GdL$^{3\text{-}4}$** . The mixtures were kept for 3 h at 37 °C for incubation, followed by the measurement in 3T MRI scanner. For the subsequent pH-dependant MRI experiments of **GdL$^{3\text{-}4}$** with avidin, the following buffers were used to adjust pH: MES buffer for pH 5.5 and 6.3, HEPES buffer for pH 7.0, 7.5 and 8.0, and CHES buffer for pH 8.6 and 9.0.

Longitudinal relaxation times (T_1) were measured using an inversion recovery sequence to obtain images from an axial slice of 1 mm thickness through the samples. The inversion time (*Ti*) was varied from 23 ms to 3000 ms in 12 steps. Images were read out with a turbo spin echo technique, acquiring 5 echoes per scan. The repetition time (TR) was 10,000 ms to ensure complete relaxation. Six averages per *Ti* were possible within 18 min. For T_2, a home-written spin-echo sequence was used with echo times varying from 25 ms to 275 ms in 10 steps and a repetition time of 8 s. Diffusion sensitivity was reduced by minimizing the crusher gradients surrounding the refocusing pulse. A matrix of 256 x 256 voxels was used over a field-of-view of 110 x 110 mm^2 resulting in a voxel volume of $0.43 \times 0.43 \times 1\ mm^3$. Data analysis was performed by fitting of relaxation curves with self-written routines under MATLAB 7.1 R14 (The Mathworks Inc., United States). The series of T_1 (with varying t = TI) and T_2 (with varying t = TE) relaxation data were fitted to the equations 6-7 and 6-8.

$$S = S_0 (1 - exp(-t / T_1)) + S_{(TI = 0)} exp(-t / T_1) \qquad \text{Eq. (6-7)}$$

$$S = S_0 exp(-t / T_2) \qquad \text{Eq. (6-8)}$$

Nonlinear least-squares fitting of three parameters S_0, $S_{(TI = 0)}$, and T_1/T_2 was done for manually selected regions of interest with the Trust-Region Reflective Newton algorithm implemented in MATLAB. The quality of the fit was controlled by visual inspection and by calculating the mean errors and residuals. The obtained T_1/T_2 values of the samples were converted to R_1 (= $1/T_1$) and R_2 (= $1/T_2$).

$$r_{1,2} = (\mathrm{R}_{1,2\mathrm{obs}} - \mathrm{R}_{1,2\mathrm{dia}})/[\mathrm{SCA}] \qquad \text{Eq. (6-9)}$$

Relaxivities r_1/r_2 were calculated by using equation 6-9, where $\mathrm{R}_{1,2\mathrm{obs}}$ – observed relaxation rate, $\mathrm{R}_{1,2\mathrm{dia}}$ – diamagnetic contribution to the relaxation rate and [SCA] – applied concentration of SCA. The curves obtained from the MRI E-titrations were fitted based on the previously published formula[145], however they were slightly modified to use relaxivity values instead of relaxation rates (Eq. 6-10).

$$r_{1,2}^{obs} = 1000 \times \left\{ \left(L_0 \times r_{1,2}^{f}\right) + 0.5 \times \left(r_{1,2}^{b} - r_{1,2}^{f}\right) \times \left((n \times c_{Av}) + L_0 + {K_a}^{-1} - \sqrt{\left((n \times c_{Av}) + L_0 + {K_a}^{-1}\right)^2 - 4 \times n \times L_0 \times c_{Av}} \right) \right\} \qquad \text{Eq. (6-10)}$$

where:

$r_{1,2}^{obs}$: observed longitudinal or transversal relaxivity

L_0 : concentration of SCA in M (set to 0.001 M since relaxivities are used)

$r_{1,2}^{f}$: longitudinal or transversal relaxivity of the free SCA

$r_{1,2}^{b}$: longitudinal or transversal relaxivity of the avidin bound SCA

n: number of binding sites on the avidin tetramer (set to n=3 as obtained from fluorescence displacement assay)

c_{Av}: normalized concentration of avidin in M

K_a: binding constant of respective SCA (set to 7.1×10^{13} and 8.0×10^{13} for **GdL^3** and **GdL^4**, respectively, as obtained from the fluorescence displacement assay).

6.6 Competitive MRI assay

Stock solutions of avidin and **GdL^3**/**GdL^4** were prepared at 0.225 mM and 0.250 mM respectively in HEPES buffer (25 mM, pH 7). A series of different concentrations of biotin were prepared from 250 mM to 1 mM also in HEPES buffer. Avidin (66.7 µL) was mixed with **GdL^3**/**GdL^4** (200 µL) and samples with a 0 to 500 times excess of biotin were obtained by adding different volumes of biotin stock solutions 10 min after the preparation of avidin-**GdL^3**/**GdL^4** mixture. The volume was adjusted to 400 µL by adding HEPES buffer. Mixtures were incubated at 37 °C for 5 h. Longitudinal and transverse relaxations times were recorded on the 3T MRI scanner.

6.7 Experimental synthetic procedures

6-(1,3-dioxoisoindolin-2-yl) hexanoic acid (2-7)

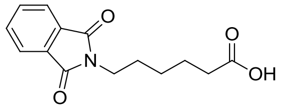

6-amino hexanoic acid (5.00 g, 38.16 mmol) and phthalic anhydride (5.64 g, 38.16 mmol) were mixed and stirred at 170 °C for 5 h. Reaction mixture was cooled to room temperature and dissolved into dichloromethane (200 mL). Organic layer was washed with 0.1 M HCl (2 × 50 mL), dried over Na_2SO_4 and concentrated to get pure white solid of acid **2-7** after triturating with diethyl ether (9.50 g, 95%).

^{1}H NMR (300 MHz, $CDCl_3$), δ (ppm):1.26-1.47 (m, 2H) 1.53- 1.77 (m, 4H) 2.31 (t, *J* = 7.5 Hz, 2H), 3.64 (t, *J* = 7.5 Hz, 2H), 7.66 (dd, *J* = 3, 3 Hz, 2H, Ar*H*) 7.79 (dd, *J* = 3, 3 Hz, 2H, Ar*H*).

^{13}C{1H} NMR (75 MHz, $CDCl_3$), δ (ppm): 24.0, 28.1, 33.7, 37.6, 123.1, 132.0, 133.8, 168.3, 179.4.

ESI-MS for $C_{14}H_{14}NO_4$ [$(M - H)^-$] *m/z* calcd. 260.1, found 259.9.

tert-butyl-2-bromo-6-(1,3-dioxoisoindolin-2-yl)hexanoate (2-8)

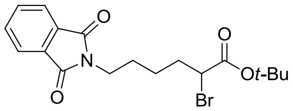

Acid **2-7** (2.00 g, 7.66 mmol) was dissolved in thionyl chloride (2.20 mL, 30.65 mmol) and stirred at 75 °C for 24 h. Bromine (450 µL, 8.42 mmol) was slowly added to the mixture at 70 °C over 30 min. and the reaction mixture was stirred at same temperature for another 16 h. The volatiles were removed under reduced pressure. Diethyl ether (3 × 20 mL) was added and removed under reduced pressure to remove traces of volatiles. The residue was dissolved into diethyl ether (20 mL) and added to the mixture of *tert*-butanol (1.10 mL, 11.49 mmol) and triehtyl amine (1.60 mL, 11.49 mL) in anhydrous diethyl ether (80 mL). The mixture was stirred at room temperature for 16 h. Reaction mixture was diluted with diethyl ether (150 mL) and water (50 mL). Organic layer was separated washed with water (3 × 50 mL), brine (50 mL) and concentrated under reduced pressure. The resultant residue was purified by silica gel column chromatography (2% ethyl acetate/hexanes) to afford the title phthalimide **2-8** as orange oil (2.0 g, 66%).

^{1}H NMR (300 MHz, CDCl$_3$), δ (ppm): 1.29-1.60 (m, 11H, C(C*H*$_3$)$_3$), 1.60- 1.84 (m, 2H), 1.84-2.18 (m, 2H), 3.67(t, *J* = 7.5 Hz, 2H, NC*H*$_2$), 4.08 (t, *J* = 7.5 Hz, 1H, C*H*BrCH$_2$), 7.69 (dd, *J* = 3, 3 Hz, 2H, Ar*H*),7.82 (dd, *J* = 3, 3 Hz, 2H, Ar*H*).

^{13}C{1H} NMR (75 MHz, CDCl$_3$), δ (ppm): 24.5, 27.6 (C(*C*H$_3$)$_3$), 27.8, 34.3, 37.5, 47.3, 82.3 (*C*(CH$_3$)$_3$), 123.1, 132.0, 133.9 (Ar*C*), 168.2, 168.6 (*C*=O).

Compound 2-11

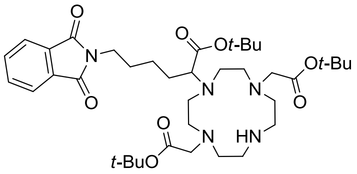

To a mixture of bis-*tert*-butyl DO2A **2-10** (0.50 g, 1.25 mmol) and K$_2$CO$_3$ (0.40 g, 1.00 mmol) in anhydrous acetonitrile (40 mL) was added solution of phthalimide **2-8** (84 mg, 1.00 mmol) in acetonitrile (20 mL) slowly over 30 minutes. The resultant solution was stirred at room temperature for 2 days. A residue was obtained after filtration and concentration of the reaction mixture under reduced pressure which was purified by silica gel column chromatography (3% methanol/dichloromethane) provided pure white solid of amine **2-11** (0.55 g, 61%).

^{1}H NMR (300 MHz, CDCl$_3$), δ (ppm): 1.08-1.49 (m, 29H, C(C*H*$_3$)$_3$), 1.53-1.78 (m, 4H), 1.86-3.90 (m, 23H, C*H*$_2$ ring, C*H*, C*H*$_2$ acetate arm, NC*H*$_2$CH$_2$), 7.65 (dd, *J* = 3, 3 Hz, 2H, Ar*H*), 7.77(dd, *J* = 3, 3 Hz, 2H, Ar*H*), 9.42 (br., 1H, N*H*).

^{13}C{1H} NMR (75 MHz, CDCl$_3$), δ (ppm): 23.7, 28.0 (C(*C*H$_3$)$_3$), 28.1, 29.1, 37.3 (N*C*H$_2$CH$_2$), 46.6, 49.4, 50.7, 51.1 (*C*H$_2$ ring), 56.3(*C*H$_2$'s acetate arm), 61.5(*C*H acetate arm), 81.3, 81.6 (*C*(CH$_3$)$_3$), 123.0, 131.9, 133.8, 168.3 (Ar*C*), 170.2, 171.2 (*C*=O).

ESI-MS for $C_{38}H_{62}N_5O_8$ [(M + H)$^+$] *m/z* calcd. 716.5, found 716.4.

Compound 2-12

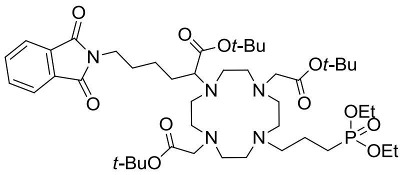

Amine **2-11** (0.40 g, 0.55 mmol) was dissolved into anhydrous acetonitrile (10 mL), potassium carbonate (0.15 g, 1.12 mmol) and diethyl(3-bromopropyl)phosphonate (214 µL, 1.12 mmol) were added under nitrogen atmosphere at room temperature. The reaction was heated at 70 °C for 16 h. The insoluble solids were removed by filtration; filtrate was concentrated to obtain a residue, which was purified by silica gel column chromatography (1:1:0.1 Methanol/dichloromethane/ammonia solution). Removal of solvents yielded light yellow oil of phthalimide **2-12** (0.39 g, 78%).

^{1}H NMR (300 MHz, CDCl$_3$), δ (ppm): 1.27 (t, J = 6 Hz, OCH$_2$CH_3), 1.32-1.52 (m, 27H, C(CH_3)$_3$), 1.53-1.87 (m, 8H), 1.94-3.97 (m, 27H, CH_2 ring, CH, CH_2 acetate arm, NCH_2CH$_2$), 3.92-4.18 (m, 4H, OCH_2CH$_3$), 7.71 (dd, J = 3, 3 Hz, 2H, ArH), 7.81 (dd, J = 3, 3 Hz, 2H, ArH).

^{13}C{1H} NMR (75 MHz, CDCl$_3$), δ (ppm): 16.4 (d, J = 6 Hz, CH$_2$$CH_3$), 19.2 (d, J = 5.3 Hz), 23.6, 23.9, 26.3, 28.4, 37.4, 44.7, 47.2, 48.5, 49.3, 49.3, 50.7, 52.5, 53.2, 54.7, 55.0, 56.1, 57.1, 61.4 (d, J = 6 Hz), 61.5(CH acetate arm), 82.2, 82.5, 83.0 (C(CH$_3$)$_3$), 123.1, 131.9, 134.2 (ArC), 168.4, 173.3, 174.2, 174.6 (C=O).

^{31}P NMR (75 MHz, CDCl$_3$), δ (ppm): 31.0(s).

ESI-MS for $C_{45}H_{77}N_5O_{11}P$ [(M + H)$^+$] *m/z* calcd. 894.5, found 894.6.

***tert*-butyl-6-(((benzyloxy)carbonyl)amino)-2-bromohexanoate (2-15)**

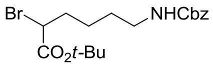

Potassium bromide (2.96 g, 12.50 mmol) was added to the solution of H-Lys(Z)-OH (2.00 g, 7.13 mmol) in HBr (16 mL, 1N). The resultant mixture was cooled to 0 °C, sodium nitrite (0.59 g, 8.56 mmol) was added portion wise over 1 h and the mixture was stirred for a further 2 h. Conc. sulfuric acid (1 mL) was added slowly at 0 °C and the solution was allowed to reach room temperature. The mixture was extracted with diethyl ether (3 × 150 mL). The combined organic layers were dried over anhydrous sodium sulphate and concentrated to afford bromo derivative of acid as slight yellow syrup. This acid (0.50 g, 1.45 mmol) was suspended in chloroform (5 mL) and *tert*-butyl-2, 2, 2-trichloroacetimidate (0.64 g, 2.90 mmol) in chloroform (5 mL) was added drop wise. After 10 minutes a catalytic amount of trifluoroborane diethyl etherate (10 µL) was added and the resultant mixture was stirred at room temperature for 16 h under a nitrogen atmosphere. Sodium bicarbonate (1.00 g) was added to the mixture and stirred for another 10 minutes. The insoluble salts were removed by filtration and residue was obtained after concentration of filtrate. The residue was purified using silica gel column chromatography (6% ethyl acetate/hexane) to obtain light yellow oil of bromide **2-15** (0.30 g, 51%).

^{1}H NMR (300 MHz, CDCl$_3$) δ (ppm): 1.41-1.63 (m, 13H, $CH_2CH_2CH_2CH_2$, $(CH_3)_3C$), 1.87-2.12 (m, 2H, $CH_2CHBrCO$), 3.19 (t, J = 6 Hz, 2H, $NHCH_2CH_2$), 4.10 (t, J = 6 Hz, 1H, $CH_2CHBrCO$), 4.84 (br. s, 1H, NHCH$_2$), 5.10 (s, 2H, PhCH$_2$OCO), 7.37- 7.32 (m, 5H, Ar*H*).

^{13}C{1H} NMR (75 MHz, CDCl$_3$) δ (ppm): 24.4 ($NHCH_2CH_2CH_2$), 27.7 ($(CH_3)_3C$), 29.2 ($CHBrCH_2CH_2$), 34.4 ($NCH_2CH_2CH_2$), 40.6 ($CHBrCH_2CH_2$), 47.4 (COCHBrCH$_2$), 66.6 (PhCH$_2$OCO), 82.4 ($(CH_3)_3C$) 128.1, 128.5, 136.5, (Ar*C*) 156.3, 168.7 (*C*=O).

ESI-HRMS for $C_{18}H_{26}BrNNaO_4$ [M+Na$^+$]$^+$, *m/z* calcd. 422.0937, found 422.0937.

tert-butyl-2-bromo-4-(4-nitrophenyl)butanoate (2-17)

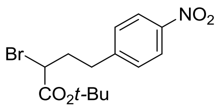

4-(4-nitrophenyl)-butyric acid (3.00 g, 14.34 mmol) was dissolved in thionyl chloride (4.16 mL, 57.36 mmol) and the mixture was stirred at 75 °C for 16 h. Bromine (0.82 mL, 15.78 mmol) was added drop wise at the same temperature and mixture was again stirred for 16 h. The reaction was cooled to room temperature and the mixture was poured over ice and stirred for 2 h. The aqueous layer was extracted with diethyl ether (3 x 200 mL). The combined organic phases were washed with brine (200 mL), dried over Na_2SO_4 and concentrated under reduced pressure. The residue was redissolved in chloroform (30 mL) and a solution of *tert*-butyl-2, 2, 2-trichloro acetimidate (6.27 g, 28.68 mmol) in chloroform (20 mL) was added slowly followed by boron trifluoride etherate (100 µL). The resultant mixture was stirred at room temperature for 16 h. Sodium bicarbonate (2.00 g) was added and stirred for 30 minutes. The inorganic impurities were removed by filtration, the filtrate was concentrated and the residue was purified by silica gel column chromatography (2% ethyl acetate/hexane) to afford light yellow oil of bromide **2-17** (3.80 g, 77%).

^{1}H NMR (300 MHz, CDCl$_3$) δ (ppm): 1.49 (s, 9H, $(CH_3)_3C$), 2.21-2.43 (m, 2H, CH_2CH_2CHBr), 2.77-3.00 (m, 2H, CH_2CH_2CHBr), 4.07 (dd, J= 9, 6 Hz, 1H, CH_2CH_2CHBr), 7.38 (d, J= 9 Hz, 2H, Ar*H*), 8.18 (d, J= 9 Hz, 2H, Ar*H*).

$^{13}C\{1H\}$ NMR (75 MHz, $CDCl_3$) δ (ppm): 27.7 ((*C*H_3)$_3$C), 33.1 (ArCH_2*C*H_2CHBr), 35.7 (Ar*C*H_2CH_2CHBr), 46.4 (ArCH_2CH_2*C*HBr), 82.8 (CH_3)$_3$*C*), 123.9, 129.3, 146.7, 147.9 (Ar*C*), 168.3 (*C*=O).

ESI-HRMS for $C_{14}H_{18}BrNO_4$ $[M+Na]^+$, *m/z* calcd. 366.0311, found 366.0307.

Compound 2-18

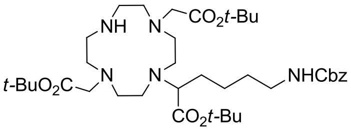

A solution of *tert*-butyl DO2A **2-10** (2.00 g, 5.00 mmol) in anhydrous acetonitrile (50 mL) was added drop wise over 2 h to the mixture of bromide **2-15** (2.50 g, 6.25 mmol) and sodium bicarbonate (0.42 g, 5.00 mmol) in anhydrous acetonitrile (100 mL) at room temperature. The resultant mixture was stirred at room temperature for 2 days. The insoluble salts were removed by filtration and the filtrate was concentrated under reduced pressure. Pure product was afforded by silica gel column chromatography (3% methanol/dichloromethane) to give amine **2-18** as off-white solid (1.65 g, 46%).

^1H NMR (300 MHz, $CDCl_3$) δ (ppm): 1.43 (m, 27H, (C*H_3*)$_3$C), 1.56-1.68 (m, 4H, CH_2C*H_2*C*H_2*CH_2), 2.32-3.53 (br, 21H, C*H_2* ring, C*H*COO*t*Bu and C*H_2*COO*t*Bu), 5.06 (s, 2H, PhC*H_2*CO), 5.79 (br s, 1H, CH_2N*H*COOCH_2), 7.19-7.39 (m, 5H, Ar*H*), 9.49 (br s, 1H, N*H* ring).

$^{13}C\{1H\}$ NMR (75 MHz, $CDCl_3$) δ (ppm): 23.8, 28.1, 28.2 ((*C*H_3)$_3$C), 29.2, 30.0, 40.4 (NH*C*H_2CH_2), 45.6 48.5, 49.9, 50.9 (*C*H_2 ring), 56.1 (*C*H_2COO*t*Bu), 61.9 (*C*HCOO*t*Bu), 66.1 (Ph*C*H_2OCO), 81.5, 81.7, ((CH_3)$_3$*C*), 127.7, 127.8, 128.3, 136.9, (Ar*C*), 156.6, 170.1, 171.4 (*C*=O).

ESI-HRMS for $C_{38}H_{66}N_5O_8$ $[M+H^+]^+$, *m/z* calcd. 720.4911, found 720.4901.

Compound 2-19.

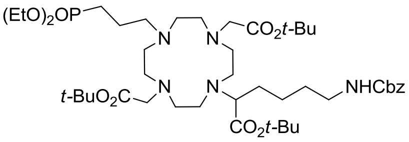

Potassium carbonate (0.27 g, 1.99 mmol) and diethyl(3-bromopropyl)phosphonate (0.38 mL, 1.99 mmol) were added to the solution of amine **2-18** (1.30 g, 1.80 mmol) in anhydrous acetonitrile (15 mL). The reaction was heated to 70 °C for 16 h. The insoluble solids were removed by filtration, the filtrate was concentrated under reduced pressure and the residue was purified by silica gel column chromatography (50% methanol/dichloromethane/10% ammonia). Removal of solvents yielded light yellow oil of carbamate **2-19** (1.20 g, 74%).

^{1}H NMR (300 MHz, $CDCl_3$) δ (ppm): 1.29 (t, *J* = 6 Hz, 6H, OCH_2CH_3), 1.36-1.80 (m, 37H, CH_2CH_2PO, $(CH_3)_3C$), 2.28-2.94 (br, 18H, CH_2 ring), 3.12-3.22 (m, 7H, C*H*COO*t*Bu and $CH_2COOtBu$), 4.94-4.17 (m, 4H, $P(O)CH_2$), 5.07 (s, 2H, $PhCH_2OC(O)$), 5.46 (br s, 1H, CH_2NHCbz), 7.21-7.42 (m, 5H, Ar*H*).

^{13}C{1H} NMR (75 MHz, $CDCl_3$) δ (ppm): 16.3 (d, *J* = 6 Hz, OCH_2CH_3), 20.2 (d, *J* = 4.5 Hz, $POCH_2CH_2$), 23.3 (d, $^1J_{PC}$ = 141 Hz, $P(O)CH_2CH_2$), 23.3, 28.1, 28.2, 29.3, 29.5, 40.7 (CH_2CH_2NHCOO), 49.5 (NCH_2CH_2), 52.3, 52.5, 52.6, 56.0 (CH_2 ring), 61.2, 61.2 ($CH_2COOtBu$), 64.1 (*C*HCOO*t*Bu), 66.2 (OCH_2CH_3), 80.4, 80.5 ($(CH_3)_3C$), 127.8, 128.0, 128.3, 136.7 (Ar*C*), 156.3, 170.8, 172.8 (*C*=O).

^{31}P{^{1}H} NMR (122 MHz, $CDCl_3$) δ (ppm): 32.9 (s).

ESI-HRMS for $C_{45}H_{81}N_5O_{11}P$ $[M+H]^+$, *m/z* calcd. 898.5670, found 898.5659.

Compound 2-20

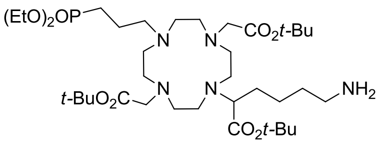

Carbamate **2-19** (0.68 g, 0.75 mmol) was dissolved in absolute ethanol (20 mL) and 10% Pd-C (70 mg, 10% w/w) was added. The heterogeneous mixture was shaken for 16 h under a hydrogen atmosphere (35 psi) in a Parr hydrogenator apparatus. The catalyst was removed by filtration through the celite and the filtrate was concentrated to obtain light yellow oil of the amine **2-20** (0.50 g, 86%).

^{1}H NMR (300 MHz, $CDCl_3$) δ (ppm): 1.31 (t, *J* = 6 Hz, 6H, OCH_2CH_3), 1.37-1.95 (br, 37H, $P(O)CH_2CH_2CH_2$, $NHCH_2CH_2CH_2CH_2$, $(CH_3)_3C$), 2.15-3.45 (br, 25H), 3.95-4.20 (m, 4H, OCH_2CH_3).

^{13}C{1H} NMR (75 MHz, $CDCl_3$) δ (ppm): 16.5 (d, *J* = 6 Hz, OCH_2CH_3), 20.0 (d, *J* = 4.5 Hz, $P(O)CH_2CH_2$), 23.5 (d, $^1J_{PC}$ = 140 Hz,$P(O)CH_2CH_2$), 23.6, 28.2, 28.3 ($(CH_3)_3C$), 29.9,

33.5, 42.1 (CH$_2$*C*H$_2$NH$_2$), 49.6 (N*C*H$_2$CH$_2$), 52.3, 52.3, 52.7, 56.2 (*C*H$_2$ ring), 61.3, 61.4 (*C*H$_2$COO*t*Bu, O*C*H$_2$CH$_3$), 64.2 (*C*HCOO*t*Bu), 80.5, 80.6 (CH$_3$)$_3$*C*), 171.0, 172.9 (*C*=O).
^{31}P{^{1}H} NMR (122 MHz, CDCl$_3$) δ (ppm): 31.0 (s), 32.9 (s).
ESI-HRMS: for $C_{21}H_{41}N_5O_9P$ [M+H]$^+$, *m/z* calcd. 764.5296, found 764.5294.

Ligand L^1

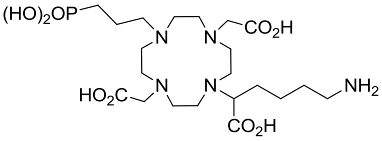

Bromotrimethylsilane (0.62 g, 3.90 mmol) was added slowly at 0 ^{o}C to the solution of the amine **2-20** (0.30 g, 0.39 mmol) in anhydrous dichloromethane (20 mL). The reaction mixture was stirred for 12 h at room temperature. The solvent was removed under reduced pressure and the residue was dissolved in formic acid (4 mL) and stirred at 60 °C for 16 h. The reaction mixture was cooled to room temperature and excess volatiles were removed under reduced pressure. The residue was dissolved in water (2 mL) and added slowly to acetone (200 mL) under vigorous stirring. The solution was cooled to -20 °C for 12 h. The solid product was isolated by filtration, dried under reduced pressure to afford an off-white solid of **L^1** (0.30 g, quant.)
^{1}H NMR (300 MHz, D$_2$O) δ (ppm): 1.40-2.15 (br, 10H), 2.80-3.35 (br, 23H, C*H*$_2$ ring, C*H*$_2$ acid arm), 4.09 (m, 1H, NC*H*(COOH)CH$_2$).
^{13}C{1H} NMR (75 MHz, D$_2$O) δ (ppm): 17.2, 23.6, 23.6 (d, $^1J_{PC}$ = 137 Hz, PO*C*H$_2$CH$_2$), 24.8, 26.5, 39.0, 46.9, 47.2, 48.3, 49.6, 49.9, 50.0, 50.1, 53.3, 54.2, 54.4, 63.1 (*C*HCOOH), 170.8, 173.6, 174.58 (*C*=O).
^{31}P{^{1}H} NMR (122 MHz, D$_2$O) δ (ppm): 27.2 (s).
ESI-HRMS for $C_{21}H_{41}N_5O_9P$: [M-H$^+$]$^-$, *m/z* calcd. 538.2647, found 538.2648.

Compound 2-21

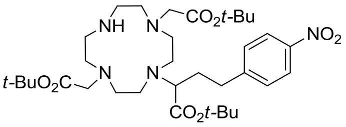

Sodium bicarbonate (0.37 g, 4.40 mmol) and a solution of bromide **2-17** (1.51 g, 4.40 mmol) in anhydrous acetonitrile (50 mL) were added slowly to a solution of bis-*tert*-butyl DO2A **2-10** (2.20 g, 5.50 mmol) in anhydrous acetonitrile (100 mL) over 3 h at room temperature. The resultant mixture was stirred at room temperature for 2 days. The inorganic impurities were removed by filtration, the filtrate was concentrated under reduced pressure and the residue was purified with silica gel column chromatography (3% methanol/dichloromethane). The amine **2-21** was isolated as an off-white solid after recrystallization from cold diethyl ether (1.90 g, 65%).

^{1}H NMR (300 MHz, CDCl$_3$) δ (ppm): 1.40 (s, 9H, (C*H*$_3$)$_3$C) 1.49 (s, 18H, (C*H*$_3$)$_3$C), 1.93-2.25 (br, 2H, CHC*H*$_2$CH$_2$), 2.38 (d, *J*= 12 Hz, 2H, ArC*H*$_2$CH$_2$), 2.53-3.37 (br, 21H, C*H*COO*t*Bu and C*H*$_2$COO*t*Bu, C*H*$_2$ ring), 7.63 (d, *J* = 9 Hz, 2H, Ar*H*), 8.17 (d, *J* = 9 Hz, 2H, Ar*H*).

^{13}C{1H} NMR (75 MHz, CDCl$_3$) δ (ppm): 28.0, 28.3 ((*C*H$_3$)$_3$C), 31.6 (ArCH$_2$C*H*$_2$), 32.3 (ArC*H*$_2$CH$_2$), 45.8, 48.2, 49.5, 50.8 (*C*H$_2$ ring), 55.5 (*C*H$_2$COO*t*Bu), 60.3 (*C*HCOO*t*Bu), 81.6, 82.2 ((CH$_3$)$_3$*C*), 123.7, 130.1, 146.6, 148.9 (Ar*C*), 170.04, 170.9 (*C*=O).

ESI-HRMS for $C_{34}H_{57}N_5O_8$ $[M+H]^+$, *m/z* calcd. 664.4279, found 664.4282.

Compound 2-22

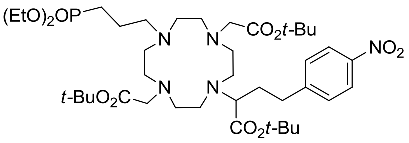

Amine **2-21** (0.93 g, 1.40 mmol) was dissolved into anhydrous acetonitrile (20 mL) and potassium carbonate (0.23 g, 1.68 mmol), diethyl-(3-bromopropyl) phosphonate (0.32 mL, 1.68 mmol) and catalytic amount of potassium iodide were added at room temperature. The resultant mixture was stirred at 70 °C for 16 h. After cooling to room temperature, the insoluble materials were removed by filtration, the filtrate was concentrated under reduced pressure to afford a residue which was purified by silica gel column chromatography (50% methanol/dichloromethane/2% ammonia) to obtain nitro **2-22** as light yellow oil (0.75 g, 63%).

^{1}H NMR (300 MHz, CDCl$_3$) δ (ppm): 1.30 (t, *J*= 7.5 Hz, 6H, P(O)OCH$_2$C*H*$_3$)$_2$), 1.37-1.56 (m, 27H, (C*H*$_3$)$_3$C), 1.61-2.22 (br, 6H, ArC*H*$_2$C*H*$_2$, P(O)CH$_2$C*H*$_2$CH$_2$), 2.31-3.05 (br, 20H, C*H*$_2$ ring), 3.10-3.35 (m, 5H, C*H*COO*t*Bu, C*H*$_2$COO*t*Bu), 3.96-4.18 (m, 4H, OC*H*$_2$CH$_3$), 7.38 (d, *J*= 7.5 Hz, 2H, Ar*H*), 8.13 (d, *J* = 7.5, 2H, Ar*H*).

^{13}C{1H} NMR (75 MHz, CDCl$_3$) δ (ppm): 16.5 (d, *J*= 5.3 Hz, P(O)OCH$_2$*C*H$_3$), 20.1 (d, *J* = 2.3 Hz, P(O)CH$_2$*C*H$_2$), 23.5 (d, $^1J_{PC}$ = 140 Hz, P(O)*C*H$_2$CH$_2$), 28.2, 28.3 ((*C*H$_3$)$_3$C), 31.4, 32.6 (Ar*C*H$_2$-*C*H$_2$-CH-), 49.8 (N*C*H$_2$CH$_2$), 52.5, 52.5, 52.7, 56.2 (*C*H$_2$ ring), 61.3, 61.4 (*C*H$_2$COO*t*Bu, O*C*H$_2$CH$_3$), 64.1 (*C*HCOO*t*Bu), 80.7, 81.0 ((CH$_3$)$_3$*C*), 123.6, 129.3, 146.3, 150.2 (Ar*C*), 170.8, 172.3 (*C*=O).

^{31}P{^{1}H} NMR (122 MHz, D$_2$O) δ (ppm): 32.8 (s).

ESI-HRMS for $C_{41}H_{72}N_5O_{11}P$ [M+H]$^+$, *m/z* calcd. 842.5038, found 842.5038.

Compound 2-23

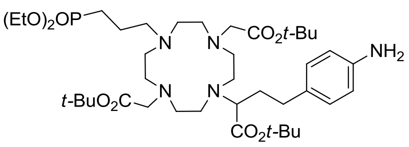

A mixture of nitro **2-22** (0.45 g, 0.53 mmol) and 10% Pd-C (90 mg, 20% w/w) in absolute ethanol (20 mL) was shaken under a hydrogen atmosphere (35 psi) in a Parr hydrogenator. After completion of the reaction, the catalyst was removed by filtration through celite and the solvent was removed under reduced pressure. The residue was purified through alumina column chromatography (3% methanol/dichloromethane) to obtain a pure light yellow oil of amine **2-23** (0.37 g, 78%).

^{1}H NMR (300 MHz, CDCl$_3$) δ (ppm): 1.29 (t, *J*= 7.5 Hz, 6H, P(O)OCH$_2$C*H*$_3$), 1.35-1.47 (br, 27H, (C*H*$_3$)$_3$C), 1.60-1.87(br, 6H, ArC*H*$_2$C*H*$_2$CHBr, P(O)CH$_2$C*H*$_2$CH$_2$), 2.36-2.95 (br, 20H, C*H*$_2$ ring), 3.10-3.33 (m, 5H, C*H*COO*t*Bu, C*H*$_2$COO*t*Bu) 3.55 (br s, 2H, ArN*H*$_2$), 3.93-4.16 (m, 4H, OC*H*$_2$CH$_3$), 6.60 (d, *J*= 7.5 Hz, 2H, Ar*H*), 6.97 (d, *J* = 7.5, 2H, Ar*H*).

^{13}C{1H} NMR (75 MHz, CDCl$_3$) δ (ppm): 16.4 (d, *J* = 6 Hz, P(O)OCH$_2$*C*H$_3$), 20.0 (d, *J* = 4.5 Hz, P(O)CH$_2$*C*H$_2$CH$_2$), 23.4 (d, $^1J_{PC}$ = 140 Hz, P(O)*C*H$_2$CH$_2$CH$_2$), 28.1, 28.3 (*C*H$_3$)$_3$C), 29.6 (P(O)CH$_2$*C*H$_2$CH$_2$), 31.8 (ArCH$_2$*C*H$_2$), 32.3 (Ar*C*H$_2$CH$_2$), 49.7 (N*C*H$_2$CH$_2$), 52.2, 52.3, 52.8, 53.3, 55.6, 55.9 (*C*H$_2$ ring), 56.13 (*C*H$_2$COO*t*Bu), 61.3 (d, *J* = 3 Hz,-P(O)O*C*H$_2$CH$_3$), 61.3, 64.5 (*C*HCOO*t*Bu), 80.5, 80.5 ((CH$_3$)$_3$*C*), 115.1, 129.1, 132.0, 144.2 (Ar*C*), 171.0, 172.8(*C*=O).

^{31}P{^{1}H} NMR (122 MHz, CDCl$_3$) δ (ppm): 32.9 (s), 31.0 (s).

ESI-HRMS for $C_{41}H_{74}N_5O_9P$ [M+H]$^+$, *m/z* calcd. 812.5296, found 812.5296.

Ligand L^2

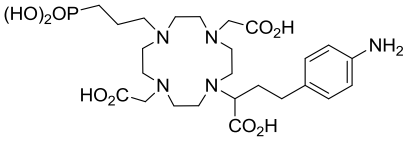

Bromotrimethylsilane (0.57 mL, 4.31 mmol) was added to a solution of amine **2-23** (0.35 g, 0.431 mmol) in anhydrous dichloromethane (15 mL) cooled at 0 °C. The reaction was allowed to warm up to room temperature and was stirred for 16 h. The reaction mixture was concentrated under reduced pressure to remove excess reagent and solvent. The residue was suspended in anhydrous dichloromethane (15 mL), trifluoroacetic acid (10 mL) was added at 0 °C and the solution was stirred at room temperature for 16 h. The reaction mixture was concentrated under reduced pressure, the residue was dissolved in methanol and added to diethyl ether under vigorous stirring. After filtration and drying, **L^2** was obtained as off-white solid (0.21 g, 84%).

^{1}H NMR (300 MHz, D$_2$O) δ (ppm): 1.53-2.50 (br, 8H, ArC*H*$_2$C*H*$_2$, P(O)C*H*$_2$C*H*$_2$CH$_2$), 2.50-4.0 (br, 23H, C*H*$_2$ ring, C*H*$_2$COOH and C*H*COOH, NC*H*$_2$CH$_2$CH$_2$P(O)), 7.34 (d, *J*= 7.5 Hz, 2H, Ar*H*), 7.42 (d, *J* = 7.5 Hz, 2H, Ar*H*).

^{13}C{1H} NMR (75 MHz, D$_2$O) δ (ppm): 17.4, 23.9 (d, $^1J_{PC}$ = 135 Hz), 26.4, 31.7, 47.0, 47.3, 47.4, 48.1, 49.4, 49.6, 49.8, 50.2, 53.6, 54.2, 54.5, 61.3, 123.4, 128.3, 130.6, 141.3 (Ar*C*), 171.3, 173.3, 174.5 (*C*=O). ^{31}P{^{1}H} NMR (122 MHz, D$_2$O) δ (ppm): 26.6 (s).

ESI-HRMS for $C_{25}H_{42}N_5O_9P$:[M-H]$^-$, *m/z* calcd. 586.2647, found 586.2643.

Compound 2-24

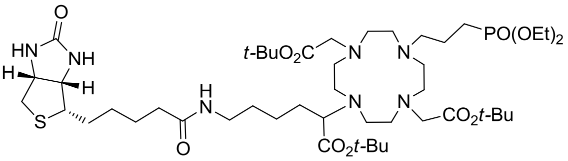

1-ethyl-3-(3-dimethylaminopropyl) carbodiimide (58 mg, 0.301 mmol) was added to a suspension of biotin (88 mg, 0.36 mmol) and 4-dimethylamino pyridine (76 mg, 0.60 mmol) in anhydrous dimethylformamide (8 mL) at room temperature. The solution of amine **2-20** (0.23 g, 0.30 mmol) in anhydrous dimethylformamide (6 mL) was added slowly over 10 minutes, and the mixture was stirred for another 16 h. The reaction mixture was concentrated under reduced pressure and resultant residue was dissolved in dichloromethane (100 mL) and water (100 mL). The organic layer was separated and aqueous layer was extracted with dichloromethane (2 × 75 mL). The combined organic layers were washed by brine, dried over Na_2SO_4 and concentrated under reduced pressure. The residue was purified by silica gel column chromatography (10% methanol/dichloromethane) to yield product biotinylated ester **2-24** as off-white solid (0.16 g, 54%).

^{1}H NMR (300 MHz, $CDCl_3$) δ (ppm): 1.20 (t, *J* = 6 Hz, 6H, ($P(O)OCH_2CH_3$), 1.26 -1.44 (br, 33H,), 1.44-1.84 (br, 12H), 1.87-2.60 (br, 13H), 2.61-3.40 (br, 16 H,), 3.81-4.06 (m, 4 H, OCH_2CH_3), 4.24 (m, 1 H, C*H*), 4.39 (m, 1H, C*H*), 5.91 (br s, 1H, N*H*), 6.33 (br s, 1H, N*H*), 8.48 (br s, 1H, N*H*).

^{13}C{1H} NMR (75 MHz, $CDCl_3$) δ (ppm): 16.2 (d, *J* = 5.3 Hz, $P(O)OCH_2CH_3$), 18.9, 22.5, 24.4, 25.6,26.2, 27.6, 27.6, 27.8, 29.0, 35.44, 4.34, 40.4, 44.5, 47.0, 48.1, 49.0, 50.6, 52.3, 53.2, 54.6, 54.8, 55.3, 55.8, 57.0, 59.9, 61.2, 61.3, 61.5, 82.2, 82.2, 83.0, 172.80, 173.6, 173.8, 174.9.

^{31}P NMR (75 MHz, $CDCl_3$) δ (ppm): 26. 6 (s).

ESI-HRMS for $C_{47}H_{89}N_7O_{11}PS$:[M-H]$^-$, *m/z* calcd. 990.6072, found 990.6080.

Compound 2-25

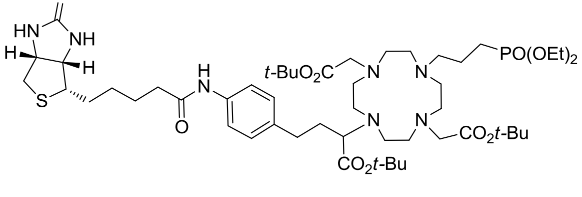

Following the same procedure as described for biotinylated ester **2-24**, biotinylated ester **2-25** was isolated as light yellow solid (98 mg, 56%).

^{1}H NMR (300 MHz, $CDCl_3$) δ (ppm): 1.28 (t, *J* = 6 Hz, 6H, OCH_2CH_3), 1.40 -1.53 (br, 27H, $(CH_3)_3C$), 1.54 - 3.73 (br, 39H), 3.91-4.18 (br, 5 H, C*H*COO*t*Bu, OCH_2CH_3), 4.30 (s, 1H, NHC*H*(CH)CH_2), 4.48 (s, 1H, NHC*H*(CH)CH_2), 5.42-5.88(m, 2H, SCH_2CH), 7.01 (d, *J* = 6 Hz, 2H, Ar*H*), 7.53 9d, *J* = 6 Hz, 2H, Ar*H*), 8.34 (br, 1H, -N*H*).

^{13}C{1H} NMR (75 MHz, $CDCl_3$) δ (ppm): 14.1, 16.3 (d, *J* = 6 Hz, P(O)O$CH_2$$CH_3$), 18.9, 23.4(d, $^1J_{PC}$ = 135 Hz, P(O)$CH_2CH_2CH_2$), 25.5, 27.7, 27.8, 28.0 ($(CH_3)_3C$), 29.6, 33.4, 36.6, 40.2, 43.9, 47.0, 47.8, 48.5, 50.7, 52.5, 54.6, 54.9, 55.4, 55.9, 56.5, 58.9, 60.4, 61.47, 61.5, 61.9, 82.2, 82.5, 82.9 ($(CH_3)_3C$), 120.3, 129.0, 135.9, 137.0 (Ar*C*), 164.5, 172.5, 173.0, 174.3, 175.0 (*C*=O).

^{31}P{^{1}H} NMR (122 MHz, $CDCl_3$) δ (ppm): 31.1 (s).

ESI-HRMS for $C_{51}H_{89}N_7O_{11}PS$:[M-H]$^-$, *m/z* calcd. 1038.6072, found 1038.6073.

Ligand L^3

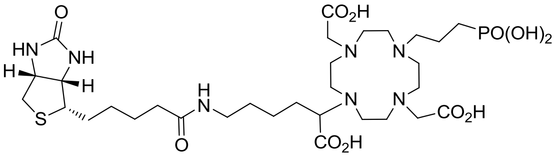

L^3 was synthesized from ester **2-24** following the same procedure as described for **L^2**. The purification was accomplished by RP-HPLC, following the method *C* (0.16 g, 49%).

^{1}H NMR (300 MHz, D_2O) δ (ppm): 1.01-2.43(br, 18H), 2.49-4.06 (br, 28H), 4.35 (s, 1H), 4.53 (s, 1H).

^{13}C{1H} NMR (75 MHz, D_2O) δ (ppm): 17.4, 24.1, 25.0 (d, $^1J_{pc}$ = 134 Hz, P(O)CH_2CH_2), 25.2, 25.4, 27.7, 28.0, 28.3, 35.5, 38.6, 39.8, 47.9, 48.2, 49.5, 52.5, 53.1, 53.8, 54.0, 54.3, 54.5, 55.4, 60.2, 62.1, 64.6, 165.2, 172.0, 173. 7, 174.6, 176.5(*C*=O).

^{31}P{^{1}H} NMR (122 MHz, D_2O) δ (ppm): 23.6 (s), 24.0 (s).

ESI-HRMS for $C_{31}H_{56}N_7O_{11}PS$:[M-H]$^-$, *m/z* calcd. 764.3423, found 764.3422.

Ligand L^4

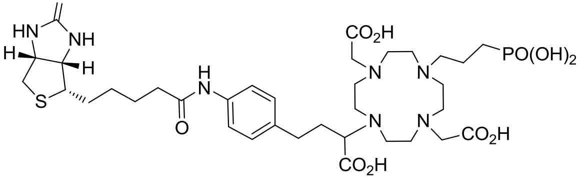

L^4 was synthesized from ester **2-25** following the same procedure as described for **L^2**. The purification was accomplished by RP-HPLC, following the method *C* (68 mg, 58%).

^{1}H NMR (300 MHz, D_2O) δ (ppm): 1.00-2.00 (br, 12H), 2.00-3.85 (br, 30H), 4.31 (s, 1 H), 4.51 (s, 1H), 7.29 (m, 4H).

^{13}C{1H} NMR (75 MHz, D2O) δ (ppm): 16.8, 24.8 (d, *J* = 134 Hz, PO$CH_2$$CH_2$), 25.1, 27.7, 28.0, 29.1, 31.6, 36.2, 39.7, 46.8, 48.7, 48.9, 49.3, 49.5, 50.3, 53.5, 53.8, 55.3, 56.4, 57.5, 60.2, 62.0, 63.5, 122.2, 129.4, 135.2, 137.6 (Ar*C*), 165.2, 173.1, 175.2, 175.2, 175.4 (*C*=O).

^{31}P{^{1}H} NMR (122 MHz, D_2O) δ (ppm): 23.0 (s), 23.7(s).

ESI-HRMS: for $C_{35}H_{56}N_7O_{11}PS$ $[M-H]^-$, *m/z* calcd. 812.3423, found 812.3426.

Compound 3-6

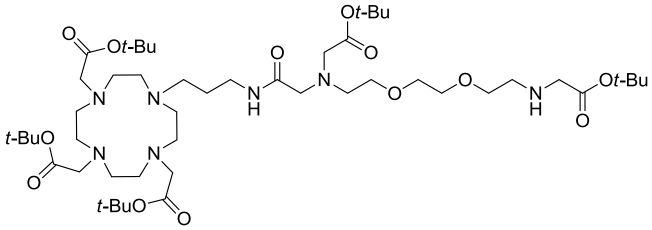

Benzyl amine **3-11** (0.65 g, 0.60 mmol) was dissolved in ethanol (15 mL) with 10% Pd-C (65 mg, 10% w/w) and shaken for 16 h in a Parr apparatus under H_2 (50 psi). The residue was obtained after reaction mixture was filtered and solvent was evaporated under reduced pressure. The residue was purified by silica gel column chromatography to obtain the pure amine **3-6** as white fluffy powder (0.54 g, 91%).

^{1}H NMR (300 MHz, $CDCl_3$), δ (ppm): 1.25-1.55 (m, 45H, C(C*H*)$_3$), 1.59-1.87 (m, 2H, $NCH_2CH_2CH_2$), 1.94-3.84 (m, 44H), 8.09(br. s, 1H, N*H*).

ESI-HRMS for $C_{49}H_{94}N_7O_{13}$ $[(M + H)^+]$ *m/z* calcd. 988.690413, found 988.690172.

Compound 3-7

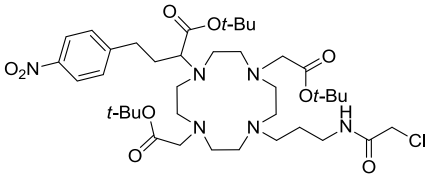

To a mixture of amine **3-15** (0.65 g, 0.90 mmol) and triethylamine (0.15 mL, 1.08 mmol) in dichloromethane (10 mL) a solution of chloroacetic anhydride (0.19 g, 1.08 mmol) dichloromethane (5 mL) at 0 °C was added slowly. The resultant mixture was stirred at 0 °C to room temperature for 2 h. This was diluted with dichloromethane (100 mL), and washed by water (2 × 100 mL). The organic layer was dried over sodium sulphate, and concentrated under reduced pressure to obtain a residue which was purified by alumina column chromatography (4% methanol/dichloromethane) to afford chloride **3-7** as light yellow oil (0.48 g, 67%).

^{1}H NMR (300 MHz, $CDCl_3$), δ (ppm): 1.30-1.52 (br., 27H, C(C*H*)$_3$), 1.57-1.72 (m, 2H, NCH$_2$C*H*$_2$CH$_2$), 1.74-2.07 (m, 2H, ArCH$_2$C*H*$_2$CH), 2.32-3.01 (m, 20H), 3.03-3.52 (m, 7H, C*H* and C*H*$_2$'s acetate arm, NHC*H*$_2$CH$_2$CH$_2$), 3.96 (s, 2H, ClC*H*$_2$CO), 7.33 (d, *J* = 7.5 Hz, 2H, Ar*H*), 7.73 (br., s, N*H*COCH$_2$Cl), 8.10 (d, *J* = 7.5 Hz, 2H, Ar*H*).

^{13}C{1H} NMR (75 MHz, $CDCl_3$), δ (ppm): 25.97, 28.16, 28.30 (C(*C*H)$_3$), 31.43, 32.58, 38.97, 42.74, 49.99 (NC*H*$_2$-CH$_2$), 52.24, 53.08, 53.23, 53.37 (*C*H$_2$ ring), 56.44 (*C*H$_2$ acetate arm), 64.00 (*C*H acetate arm), 80.84, 81.05 (*C*(CH)$_3$), 123.58, 129.25, 146.32, 150.10 (Ar*C*), 166.09, 170.66, 172.22 (*C*=O).

ESI-HRMS for $C_{39}H_{66}N_6O_9$ [(M + H)$^+$] *m/z* calcd. 797.457432, found 797.457079.

Compound 3-9

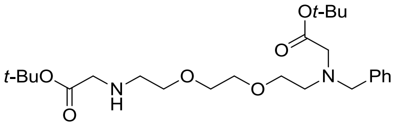

To a mixture of amine **3-10** (2.0 g, 5.32 mmol) and cesium carbonate (1.36 g, 4.26 mmol) in anhydrous acetonitrile (100 mL) at room temperature was added slowly a solution of benzyl chloride (85 mM solution in acetonitrile, 4.26 mmol). The resultant solution was stirred at room temperature for 2 days. The Insoluble salts were removed by filtration and the filtrate was concentrated under reduced pressure. The residue was dissolved into dichloromethane (200 mL) and water (100 mL). Organic layer was separated; the aqueous phase was extracted with dichloromethane (2 × 100 mL). The combined organic layers were dried over sodium sulphate, filtered through cotton plug, and concentrated under reduced pressure. Purification of the residue by silica gel column chromatography (3% methanol/dichloromethane) gave the mono benzyl amine derivative **3-9** as light yellow oil (1.00 g, 45%).

^{1}H NMR (300 MHz, $CDCl_3$), δ (ppm): 1.46 (s, 18H, C(C*H*$_3$)$_3$), 2.68-3.01 (m, 5H, N*H*C*H*$_2$CH$_2$), 3.21-3.39(m, 4H, NC*H*$_2$COO^{t}Bu), 3.59 (br., 8H, C*H*$_2$'s next to oxygen), 3.85 (s, 2H, NC*H*$_2$Ph), 7.10-7.44 (m, 5H, Ar*H*).

^{13}C{1H} NMR (75 MHz, CDCl$_3$), δ (ppm): 27.9, 28.1 (C(*C*H$_3$)$_3$), 48.5, 51.3, 52.9, 55.6, 58.5, 69.8, 70.0, 70.1, 70.2, 80.6, 81.0 (*C*(CH$_3$)$_3$), 126.9, 128.1, 128.8, 138.9 (Ar*C*), 170.9, 171.1(*C*=O).

ESI-MS for $C_{25}H_{43}N_2O_6$ [(M + H)$^+$] *m/z* calcd. 467.311564, found 467.311887.

Compound 3-11

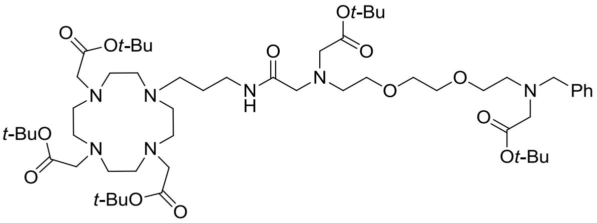

To a solution of amine **3-9** (0.70 g, 1.50 mmol) and potassium carbonate (0.25 g, 1.80 mmol) in anhydrous acetonitrile (20 mL) at room temperature was added slowly into the solution of DO3A-PA-bromide (1.24 g, 1.80 mmol). The resultant solution was stirred at 70 °C for 4 h. The insoluble materials were removed by filtration and the filtrate was concentrated under reduced pressure. Residue was dissolved into dichloromethane (100 mL) and water (50 mL) was added. The organic layer separated, washed by water (2 x 40 mL). The organic layer was dried over sodium sulphate, filtered, and concentrated under reduced pressure. Purification of the residue by silica gel column chromatography (4% methanol/dichloromethane) gave benzyl amine **3-11** as a white flocculent powder (1.25 g, 77%).

^{1}H NMR (300 MHz, CDCl$_3$), δ (ppm): 1.31-1.56 (m, 45H, C(C*H*)$_3$), 1.56-1.87 (m, 2H, NCH$_2$-C*H*$_2$-CH$_2$-), 1.97-3.88 (m, 46H), 7.27 (br., 5H, Ar*H*), 8.31(br. s, 1H, N*H*).

^{13}C{1H} NMR (75 MHz, CDCl$_3$), δ (ppm): 27.65, 27.85, 28.00 (C(*C*H)$_3$), 29.48, 37.40, 50.08, 51.84, 52.54, 52.89, 53.37, 54.23, 55.01, 55.47, 56.49, 56.71, 58.46, 58.83, 59.18, 59.59, 67.01, 67.09, 69.05, 69.15, 70.05, 81.51, 82.12, 82.25, 82.51(*C*(CH)$_3$), 127.74, 128.47, 129.68, 135.56(Ar*C*), 169.81, 170.20, 171.41, 172.24, 172.33, 172.43(*C*=O).

ESI-HRMS for $C_{56}H_{100}N_7O_{13}$ [(M + H)$^+$] *m/z* calcd. 1078.737363, found 1078.736514.

Compound 3-12

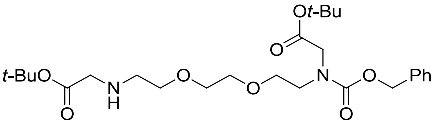

To a mixture of amine **3-10** (0.35 g, 0.93 mmol) in 1,4-dioxane (20 mL) and 10% acetic acid (20 mL, pH 3.5–4) at room temperature was added slowly benzyl chloroformate (133 µL, 0.93 mmol), pH was maintained in between 3.5-4 1N NaOH. The resultant solution was stirred at room temperature for 16 days. Reaction mixture was concentrated under reduced pressure on rotary evaporator. Residue was dissolved into dichloromethane (70 mL) and water (70 mL). Organic layer was separated; the aqueous phase was extracted by dichloromethane (2 × 50 mL). The combined organic layers were dried over sodium sulphate, filtered through cotton plug, and concentrated under reduced pressure. Purification of the residue by silica gel column chromatography (3% methanol/dichloromethane) gave mono Cbz protected carbamate **3-12** as light yellow oil (50 mg, 10%).

^{1}H NMR (300 MHz, $CDCl_3$), δ (ppm): 1.30-1.48(s, 18H), 1.97 (br s, 1H), 3.27 (s, 2H), 3.39-3.68 (m, 10H), 3.90-4.02 (d, 2H), 5.04-5.15 (s, 2H), 7.19-7.36 (m, 5H, Ar*H*).

^{13}C{1H} NMR (75 MHz, $CDCl_3$), δ (ppm): 27.9, 28.0, 47.7, 48.4, 48.6, 50.7, 51.6, 67.1, 67.3, 70.0, 70.1, 70.2, 70.3, 70.4, 70.6, 70.7, 76.6, 80.9, 81.3, 81.4, 127.6, 127.6, 127.8, 127.9, 128.3, 128.4, 136.4, 136.5, 156.0, 156.2, 168.9, 171.4.

ESI-HRMS for $C_{26}H_{43}N_2O_8$ $[(M + H)^+]$ *m/z* calcd. 511.301393, found 511.301221.

Compound 3-13

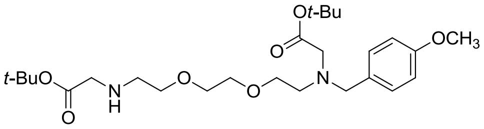

To a mixture of amine **3-10** (0.3 g, 0.80 mmol) and cesium carbonate (0.21 g, .64 mmol) in anhydrous acetonitrile (15 mL) at room temperature was added slowly a solution of 4-methoxybenzyl chloride (85 µL, 4.26 mmol) in acetonitrile (7 mL). The resultant solution was stirred at room temperature for 2 days. The insoluble salts were removed by filtration; the filtrate was concentrated under reduced pressure. The residue was dissolved in dichloromethane (50 mL) and water (50 mL) was added. The organic layer was separated and the aqueous phase was extracted by dichloromethane (2 × 50 mL). The combined organic layers were dried over sodium sulphate, filtered through cotton plug, and concentrated under reduced pressure. Purification of the residue by silica gel column chromatography (3% methanol/dichloromethane) gave mono *para* methoxy benzyl amine **3-13** as light yellow oil (0.17 g, 39%).

^{1}H NMR (300 MHz, CDCl$_3$), δ (ppm): 1.46 (s, 18H, C(C*H*$_3$)$_3$), 2.68-3.01 (m, 5H, N*H*C*H*$_2$CH$_2$), 3.21-3.39(m, 4H, NC*H*$_2$COO^{t}Bu), 3.59 (br., 8H, C*H*$_2$'s next to oxygen), 3.85 (s, 2H, NC*H*$_2$Ph), 7.10-7.44 (m, 5H, Ar*H*).

Compound 3-14

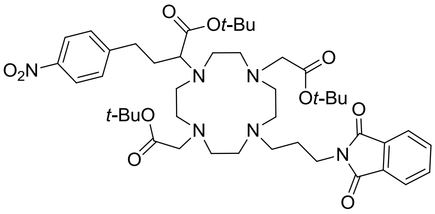

To a mixture of amine **2-21** (1.00 g, 1.50 mmol) and K$_2$CO$_3$ (0.46 g, 3.31 mmol) in anhydrous acetonitrile (15 ml), N-(3-bromopropyl)phthalamide (0.48 g, 1.80 mmol) was added and reaction mixture was stirred at 70 °C for 16 h. It was then cooled to room temperature and volatiles were removed under reduced pressure. Water (70 mL) was added and the resultant mixture was extracted with dichloromethane (3 × 100 mL). The organic layer was dried over anhydrous sodium sulphate, filtered, and evaporated to obtain yellow oil. The crude product was purified by alumina column chromatography (4% methanol/dichloromethane) to obtain phthalimide **3-14** as white flocculent powder (1.80 g, 66%).

^{1}H NMR (300 MHz, CDCl$_3$), δ (ppm): 1.43 (br., 27H, C(C*H*)$_3$), 1.66-2.06 (m, 4H, NCH$_2$C*H*$_2$CH$_2$, ArC*H*$_2$CH$_2$), 2.25-3.91 (m, 27H), 7.28 (d, *J* = 6 Hz, 2H, Ar*H*), 7.54.7.87 (m, 4H, phthamide Ar*H*), 8.03 (d, *J* = 6 Hz, 2H, Ar*H*).

^{13}C{1H} NMR (75 MHz, CDCl$_3$), δ (ppm): 26.29, 28.17, 28.28 (C(*C*H)$_3$), 31.48, 32.64, 36.62, 49.85 (NC*H*$_2$CH$_2$), 52.45, 52.75, 52.84, 53.06 (*C*H$_2$ ring), 56.09 (*C*H$_2$ acetate arm), 64.27(*C*H acetate arm), 80.57, 80.88 (*C*(CH)$_3$), 122.96, 123.46, 129.19, 132.05, 133.73, 146.13, 150.33 (Ar*C*), 168.15, 170.84, 172.33 (*C*=O).

ESI-HRMS for $C_{45}H_{67}N_6O_{10}$ [(M + H)$^+$] *m/z* calcd. 851.491319, found 851.491835.

Compound 3-15

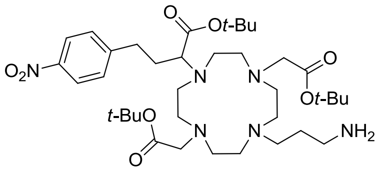

To a solution of phthalimide **3-14** (0.81 g, 0.95 mmol) in 2-propanol (10 mL) was added ethylenediamine (0.32 mL, 4.76 mmol) and reaction was heated to reflux for 16 h. A residue was obtained after filtration and concentration of the filtrate under reduced pressure. This was dissolved into 30% dichloromethane/diethyl ether and insolubles were removed by filtration. Concentration of filtrate under reduced pressure yielded amine **3-15** as light yellow oil (0.65 g, 95%).

^{1}H NMR (300 MHz, CDCl$_3$), δ (ppm): 1.34-1.49 (br., 27H, C(C*H*)$_3$), 1.49-1.66 (m, 2H, NCH$_2$C*H*$_2$CH$_2$), 1.76-2.07 (m, 2H, ArCH$_2$C*H*$_2$CH), 2.32-3.07 (m, 22H), 3.11-3.39 (m, 5H, C*H* and C*H*$_2$'s acetate arm), 7.37 (d, *J* = 7.5 Hz, 2H, Ar*H*), 8.13 (d, *J* = 7.5 Hz, 2H, Ar*H*).

^{13}C{1H} NMR (75 MHz, CDCl$_3$), δ (ppm): 27.99, 28.18, 28.33 (C(*C*H)$_3$), 31.46, 32.67, 40.38, 49.80 (NC*H*$_2$CH$_2$), 52.30, 52.56, 52.76, 53.05 (*C*H$_2$ ring), 56.29 (*C*H$_2$ acetate arm), 64.38 (*C*H acetate arm), 80.79, 81.09 (*C*(CH)$_3$), 123.59, 129.34, 146.30, 150.24 (Ar*C*), 170.82, 172.49 (*C*=O).

ESI-HRMS for $C_{37}H_{65}N_6O_8$ [(M + H)$^+$] *m/z* calcd. 721.485840, found 721.485209.

Compound 3-17

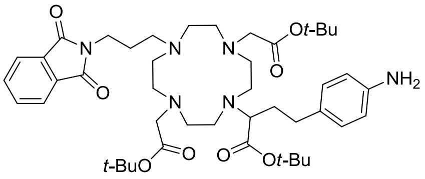

A mixture of pthaimide **3-14** (0.55 mg, 0.65 mmol) and 10% Pd-C (0.10 g, 20% w/w) in absolute ethanol (25 mL) was shaken under a hydrogen atmosphere (35 psi) in a Parr hydrogenator. After completion of the reaction, the catalyst was removed by filtration through celite and the solvent was removed under reduced pressure to obtain pure light yellow oil of amine **3-17** (0.50 g, 78%).

^{1}H NMR (300 MHz, CDCl$_3$) δ (ppm): 1.26-1.58 (m, 27H, (C(C*H*$_3$)$_3$), 1.57-2.10 (m, 4H), 2.10-3.18 (br, 21H, C*H*$_2$ ring, C*H*COO^{t}Bu and C*H*$_2$COO^{t}Bu), 6.52 (d, *J* = 7.5 Hz, 2H, Ar*H*), 6.91 (d, *J* = 7.5 Hz, 2H, Ar*H*).

^{13}C{1H} NMR (75 MHz, CDCl$_3$) δ (ppm): 26.1, 28.1 (C(*C*H$_3$)$_3$), 31.9, 32.2, 36.5, 49.7, 52.1, 52.3, 52.8, 53.0,(*C*H$_2$ ring), 56.1 (*C*H$_2$COO^{t}Bu), 64.4 (*C*HCOO^{t}Bu), 80.3, 80.4, (*C*(CH$_3$)$_3$), 115.1, 122.9, 129.0, 131.9, 132.0, 133.6, 144.1 (Ar*C*), 168.1, 171.0, 172.8 (*C*=O).

ESI-HRMS for $C_{45}H_{69}N_6O_8$ [M+H]$^+$, *m/z* calcd. 821.517140, found 821.516412.

Compound 3-20

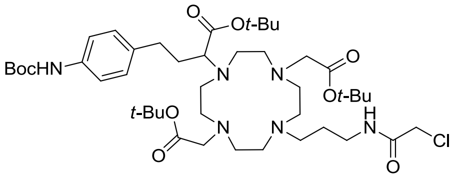

To a solution of the amine **3-19** (0.25 g, 0.32 mmol) in of dichloromethane (10 mL) was added drop wise at 0 °C N,N-diisopropylethylamine (62 µl, 0.38 mmol) followed by chloroacetic anhydride (64 mg, 0.38 mmol) in dichloromethane (10 mL). The solution was stirred at 0 °C for 45 min and at room temperature for 2 h. The reaction mixture was diluted with dichloromethane (50 mL) and water (30 mL). The aqueous layer was separated and extracted with dichloromethane (3 × 20ml) and the combined organic layers were dried over sodium sulfate. The solvent was evaporated *in vacuo* and the resultant oil was purified by alumina column chromatography (4% methanol/dichloromethane) to yield chloride **3-20** as white flocculent powder (0.16 g, 94%).

^{1}H NMR (300 MHz, CDCl$_3$), δ (ppm): 1.31-1.58 (br., 36H, C(C*H*$_3$)$_3$), 1.58-1.72 (m, 2H, NCH$_2$C*H*$_2$CH$_2$), 1.72-2.11 (m, 2H, ArCH$_2$C*H*$_2$CH), 2.30-3.69 (m, 27H), 3.85-4.27 (s, 2H, ClC*H*$_2$CO), 6.63 (br., s, N*H*Boc), 7.09 (d, *J* = 6 Hz, 2H, Ar*H*), 7.86 (br s, 1H, N*H*COCH$_2$Cl), 7.27 (d, *J* = 6 Hz, 2H, Ar*H*).

^{13}C{1H} NMR (75 MHz, CDCl$_3$), δ (ppm): 23.8, 28.1, 28.2 (C(*C*H$_3$)$_3$), 31.9, 32.0, 38.9, 42.7, 49.9 (NC*H*$_2$CH$_2$), 51.9, 52.0, 53.0, (*C*H$_2$ ring), 56.3 (*C*H$_2$ acetate arm), 64.2 (*C*H acetate arm), 80.1, 80.6, 80.7 (*C*(CH$_3$)$_3$), 118.7, 128.8, 136.2, 136.5 (Ar*C*), 152.8, 166.2, 170.7, 172.5 (*C*=O).

ESI-HRMS for $C_{44}H_{76}ClN_6O_9$ [(M + H)$^+$] *m/z* calcd. 867.535682, found 867.536426.

Compound 3-21

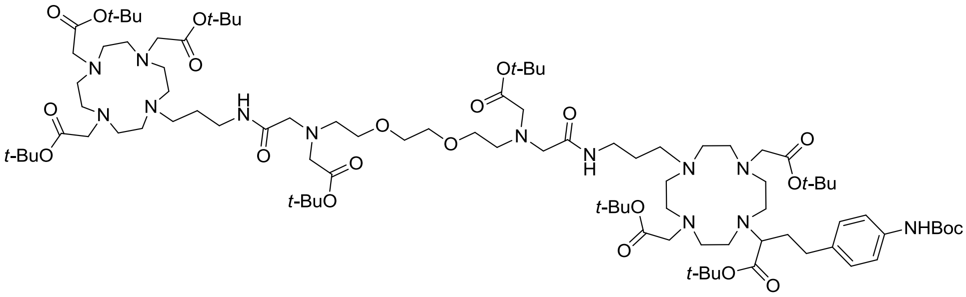

To a solution of amine **3-6** (0.30 g, 0.30 mmol) and potassium carbonate (62 mg, 1.03 mmol) in anhydrous acetonitrile (8 mL) was added chloride **3-20** (0.29 g, 0.33 mmol). The resultant solution was stirred at 70 °C for 16 h. The insoluble material was removed by filtration and the filtrate was concentrated under reduced pressure to get brown oil, which was purified by silica gel column chromatography (12% methanol/dichloromethane) to afford light yellow flocculent powder of ester **3-21** (0.25 g, 45%).

^{1}H NMR (300 MHz, $CDCl_3$), δ (ppm): 1.28-1.54 (br., 81H, $(C(C\mathit{H}_3)_3)$, 1.55-1.87 (m, 6H, $NCH_2C\mathit{H}_2CH_2$, $ArCH_2C\mathit{H}_2CH$), 1.89-3.94 (m, 73H), 6.70 (br., s, N*H*Boc), 6.93-7.16 (m, 2H, Ar*H*), 7.21-7.43 (m, 2H, Ar*H*), 8.03 (br.s, 2H, $N\mathit{H}CH_2CH_2$).

^{13}C{1H} NMR (75 MHz, $CDCl_3$), δ (ppm): 24.2, 25.5, 29.2, 33.1, 37.1, 44.2, 46.8, 47.4, 47.9, 48.5, 49.8, 50.4, 50.6, 50.9, 51.6, 52.3, 55.3, 55.4, 55.6, 56.3, 56.8, 57.9, 58.2, 58.6, 58.6, 66.9, 68.9, 80.0, 81.2, 81.3, 82.0, 82.3, 82.4, 118.5, 128.7, 134.5, 136.6, 152.4, 169.5, 169.6, 170.9, 171.1, 171.4, 172.0, 172.4, 173.2, 173.9, 174.3.

ESI-HRMS for $C_{93}H_{169}N_{13}O_{22}$ $[(M+2H)+Na]^{2+}$ *m/z* calcd. 614.41288, found 614.41377.

Compound 3-22

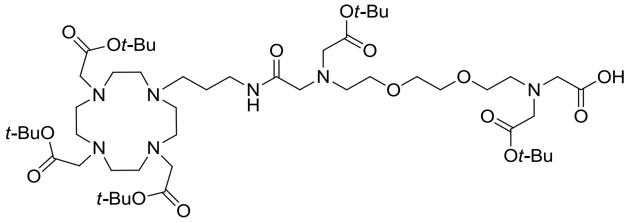

A mixture of ester **3-35** (0.50 g, 0.57 mmol) and 10% Pd-C (50 mg, 10% w/w) in ethanol (15 mL) was stirred under a H_2 atmosphere (35 psi) for 16 h. The reaction mixture was filtered through a celite bed and concentrated under reduced pressure to obtain light brown oil. The residue was dissolved in dichloromethane (50 mL) and water (30 mL). The organic layer was separated washed by brine, dried over sodium sulphate and concentrated under reduced pressure to afford a white flocculent powder of acid **3-22** (0.46 g, 99%).

^{1}H NMR (300 MHz, $CDCl_3$), δ (ppm): 1.26-1.57 (m, 45H, $C(C\mathit{H})_3$), 1.57-3.79 (m, 48H).

^{13}C{1H} NMR (75 MHz, $CDCl_3$), δ (ppm): 27.5, 27.7, 27.8, 37.1, 47.5, 49.8, 49.9, 51.2, 51.6, 52.4, 52.6, 53.3, 55.2, 55.4, 56.3, 56.5, 57.6, 57.9, 58.14, 58.4, 58.5, 67.4, 67.7, 69.1, 81.3, 82.1, 82.4, 169.8, 170.1, 171.2, 171.4, 172.1, 173.2, 174.0.

ESI-HRMS for $C_{51}H_{96}N_7O_{15}$ $[(M+H)^+]$ *m/z* calcd. 1046.695892, found 1046.696059.

Compound 3-24

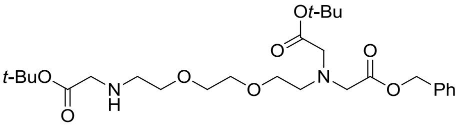

To a solution of amine **3-10** (2.0 g, 5.32 mmol) and cesium carbonate (1.36 g, 4.26 mmol) in anhydrous acetonitrile (100 mL) at room temperature was added slowly solution of benzyl bromoacetate (85 mmol solution in acetonitrile, 4.26 mmol). The resultant solution was stirred at room temperature for 2 days. The insoluble materials were removed by filtration and the filtrate was concentrated under reduced pressure. The residue was dissolved in dichloromethane (200 mL) and water (100 mL). The organic layer was separated; the aqueous phase was extracted by dichloromethane (2 × 100 mL). The combined organic layer was dried over sodium sulphate, filtered, and concentrated under reduced pressure. Purification of the residue by silica gel column chromatography (3% methanol/dichloromethane) gave ester **3-24** as light yellow oil (1.00 g, 36%).

^{1}H NMR (300 MHz, CDCl$_3$), δ (ppm): 1.38-1.54 (s, 18H, (C(C*H*$_3$)$_3$), 1.95 (br., s, 1H, N*H*), 2.74 (t, *J* = 6 Hz, 2H), 2.95 (t, *J* = 6 Hz, 2H), 3.29, 3.31(s, 2H, N*H*COOBn), 3.44-3.71 (m, 12H), 5.12, 5.17 (s, 2H, C*H*$_2$ benzyl), 7.29-7.41 (m, 5H, Ar*H*).

^{13}C{1H} NMR (75 MHz, CDCl$_3$), δ (ppm): 28.0, 28.1 (C(*C*H$_3$)$_3$), 48.7, 51.6, 53.5, 55.8, 56.6, 66.1, 70.2, 70.3, 70.6, 80.9, 80.9(*C*(CH$_3$)$_3$), 128.2, 128.5, 135.7 (Ar*C*), 170.6, 171.3, 171.4 (*C*=O).

ESI-HRMS for $C_{27}H_{44}N_2O_8Na$ [(M + Na)$^+$] *m/z* calcd. 547.298987, found 547.298984.

Compound 3-25

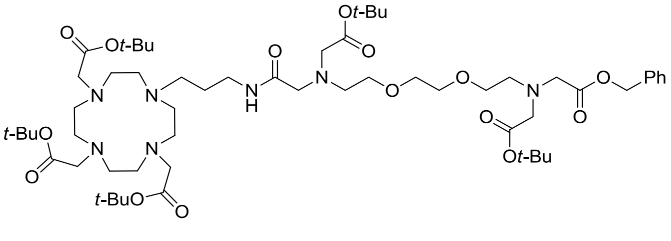

To a solution of amine **3-24** (0.70 g, 1.50 mmol) and potassium carbonate (0.25 g, 1.80 mmol) in anhydrous acetonitrile (20 mL) at room temperature was added slowly to a solution of DO3A-PA-bromide (1.24 g, 1.80 mmol). The resultant solution was stirred at 70 °C for 4 h. The insoluble materials were removed by filtration; the filtrate was concentrated under reduced pressure. The residue was dissolved into dichloromethane (100 mL) and water (50 mL). The organic layer separated and washed by water (2 x 40 mL). The organic layer was dried over sodium sulphate, filtered, and concentrated under reduced pressure. Purification of the residue by silica gel column chromatography (4% methanol/dichloromethane) gave ester **3-25** as a white flocculent powder (1.25 g, 77%).

^{1}H NMR (300 MHz, CDCl$_3$), δ (ppm): 1.29-1.58 (m, 45H, C(C*H*)$_3$), 1.58-1.86 (m, 2H, NCH$_2$C*H*$_2$CH$_2$), 1.88-3.88 (m, 46H), 5.11 (s, 2H), 7.15-7.42 (br., 5H, Ar*H*).

^{13}C{1H} NMR (75 MHz, CDCl$_3$), δ (ppm): 27.5, 27.6, 27.8, 37.1, 47.4,49.7, 49.8, 49.9, 50.0, 50.4, 50.6, 51.5, 52.3, 53.2, 55.3, 56.2, 56.4, 58.5, 66.1, 69.1, 69.7, 69.8, 81.3, 82.0, 82.3, 127.8, 128.0, 128.2, 135.2, 169.6, 170.0, 171.2, 172.2, 173.3.

ESI-MS calculated for $C_{58}H_{102}N_7O_{15}$ [(M + H)$^+$] m/z: 1136.7, found 1136.7.

Compound 3-29

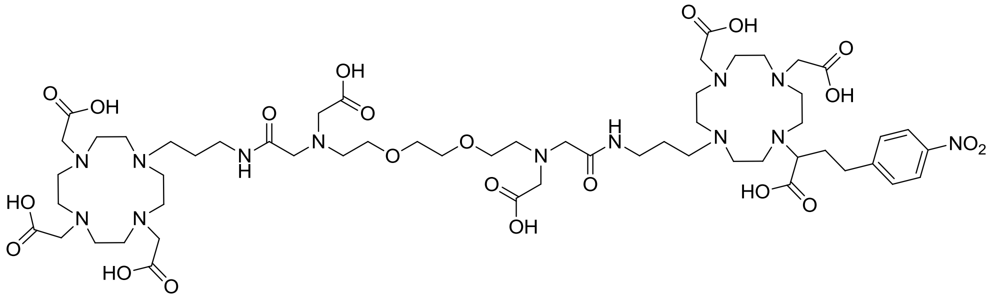

To **3-28** (0.12 g, 0.07 mmol) was added with formic acid (30 mL) and resultant mixture was stirred at 60 °C for 16 h. The volatiles were removed under reduced pressure and methanol (3 × 20 mL) was added and again concentrated. The residue was purified by RP-HPLC using method B to obtain nitro **3-29** (27 mg, 13 % over two steps).

^{1}H NMR (300 MHz, D$_2$O), δ (ppm): 1.58-2.49 (m, 8H), 1.58-4.02 (m, 65H), 4.15 (br. s, 4H), 7.49 (d, *J* = 7.5 Hz, 2H), 8.16 (d, *J* = 7.5 Hz, 2H).

ESI-MS for $C_{56}H_{92}N_{13}O_{22}$ [(M - H)$^-$] *m/z* calcd. 1298.6, found 1298.6.

Ligand L^5

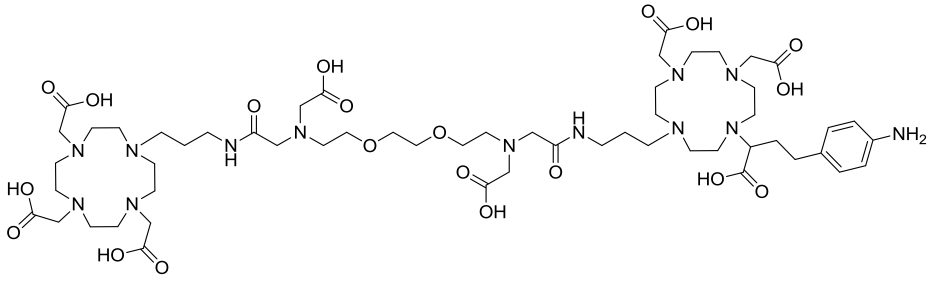

A mixture of nitro **3-29** (27 mg, 0.02 mmol) and 10% Pd-C (10 mg, 40% w/w) in water (15 mL) was shaken under H_2 (35 psi) for 16 h. The reaction mixture was filtered through a celite bed. The filtrate was concentrated under reduced pressure to obtain pure ligand **L^5** (27 mg, quant.).

^{1}H NMR (300 MHz, D_2O), δ (ppm): 1.14-2.40 (m, 10H), 2.40-4.20 (m, 69H), 4.15 (br. s, 4H), 6.95 (d, J = 7.5 Hz, 2H), 7.18 (d, J = 7.5 Hz, 2H).

ESI-MS for $C_{56}H_{94}N_{13}O_{20}$ [(M - H)$^-$] *m/z* calcd. 1268.7, found 1268.6.

Ligand L^6

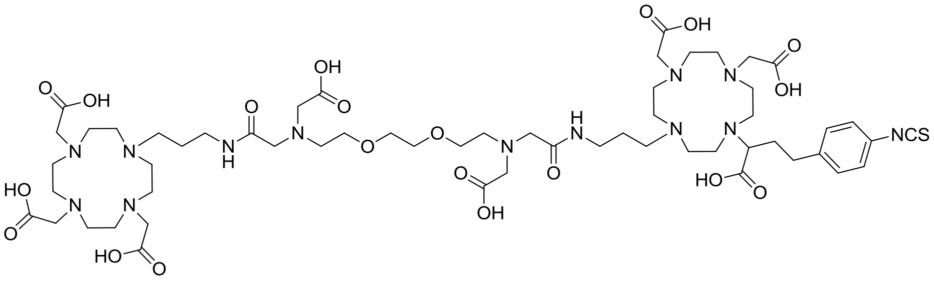

A mixture of **L^5** (75 mg, 0.06 mmol) in water (7 mL) and chloroform (7 mL) was added with thiophosgene (9 µl, 0.18 mmol) and stirred at room temperature for 30 minutes. Organic layer was removed and aqueous layer was washed with chloroform (3 × 15 mL). Aqueous layer was concentrated to afford **L^6** (27 mg, quant.).

^{1}H NMR (300 MHz, D_2O), δ (ppm): 1.46-2.37 (m, 6H), 2.41-2.41 (m, 73H), 6.91 (d, J = 7.5 Hz, 2H), 7.07 (d, J = 7.5 Hz, 2H).

^{13}C{1H} NMR (75 MHz, D_2O), δ (ppm): 25.5, 28.7, 34.3, 39.2, 49.4,49.5, 49.6, 50.6, 51.1, 52.3, 52.6, 54.6, 55.6, 56.0, 57.0, 58.0, 58.6, 58.9, 63.6, 67.2, 72.2, 128.7, 131.3, 132.8, 136.6, 142.0, 167.5, 170.5, 170.7, 171.2, 172.9, 175.8, 176.7, 177.0.

ESI-MS for $C_{57}H_{92}N_{13}O_{20}S$ [(M - H)$^-$] *m/z* calcd. 1310.6, found 1310.7.

Compound 4-3

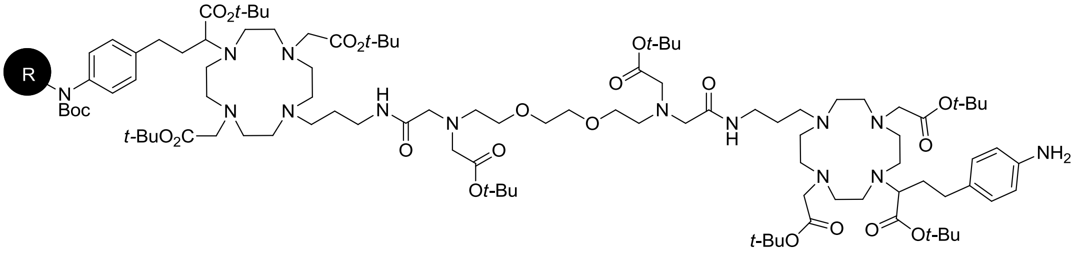
R
N
Boc
CO2t-Bu
CO2t-Bu
t-BuO2C
N
H
O
Ot-Bu
Ot-Bu
O
H
Ot-Bu
O
NH2
t-BuO
O
O
Ot-Bu

To a suspension of alloc **4-14** (0.06 mmol) in degassed DMF by nitrogen gas (5 mL) was added $Pd(PPh_3)_4$ (14 mg, 0.012 mmol) and morpholine (26 mg, 0.30 mmol). The resultant mixture was again degassed with nitrogen gas for 10 minutes and agitated for 16 h. The solvents were drained out and resin was washed with DMF (3 mL × 3) dichloromethane (3 mL × 3), methanol (3 mL × 3) ending with a final washing with dichloromethane (3 mL) to accomplish resin bound amine 4-3.

Compound 4-4

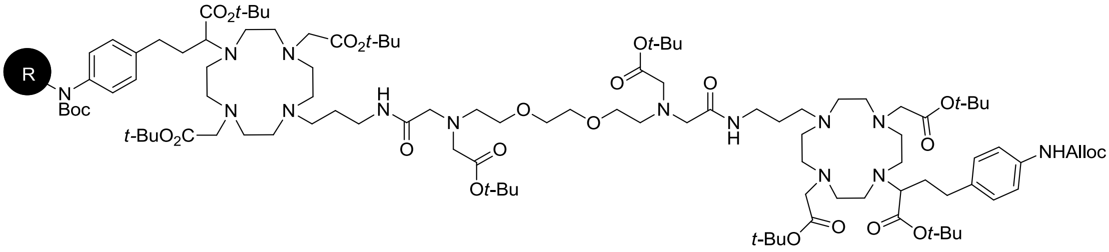
R
N
Boc
CO2t-Bu
CO2t-Bu
t-BuO2C
N
H
O
Ot-Bu
Ot-Bu
O
H
Ot-Bu
O
NHAlloc
t-BuO
O
O
Ot-Bu

To a suspension of the resin-bound amine **4-8** (0.06 mmol) in DMF (3 mL) was added pre-made (10 minute before addition) mixture of acid **4-19** (0.15 g, 0.12 mmol), HBTU (46 mg, 0.12 mmol) and N,N-diisopropylethylamine (21 µl, 0.12 mmol) and gently shaken for 18 h at room temperature. The solution was filtered through a phase extraction frit cartridge and washed with DMF (3 mL × 3) dichloromethane (3 mL × 3), methanol (3 mL × 3), alternatively, ending with a final washing with dichloromethane (3 mL). The procedure was repeated for two more times to afford alloc **4-4**.

Compound 4-7

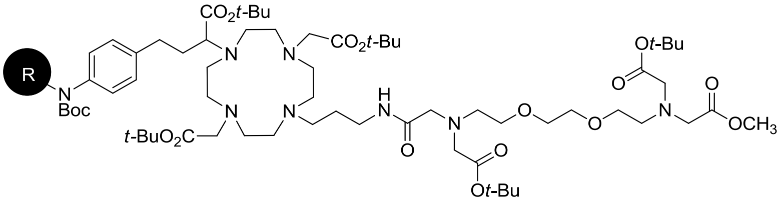

To a suspension of the resin-bound amine **4-8** (0.06 mmol) in DMF (3 mL) was added pre-made (10 minute before addition) mixture of acid **4-15** (61 mg, 0.12 mmol), HBTU (45 mg, 0.12 mmol) and N,N-diisopropylethylamine (21 µl, 0.12 mmol) and gently shaken for 18 h at room temperature. The solution was filtered through a phase extraction frit cartridge and washed with DMF (3 mL × 3) dichloromethane (3 mL × 3), methanol (3 mL × 3), alternatively, ending with a final washing with dichloromethane (3 mL). The procedure was repeated for two more times to afford ester **4-7**.

Compound 4-8

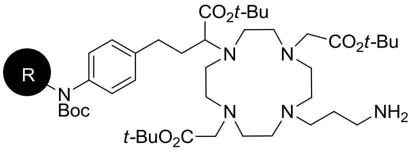

A resin-bound protected amine **4-10** (0.06 mmol) was suspended in *iso*-propanol (7 mL) in the 25 mL round bottom flask and the mixture was added with ethylenediamine (32 µl, 0.5 mmol) and heated to reflux for 16 h. Reaction mixture was transferred into a phase extraction frit and extensively washed by methanol (10 × 5 mL), DMF (10 × 5 mL) and dichloromethane (10 × 5 mL) to afford resin bound amine **4-8**.

Compound 4-10

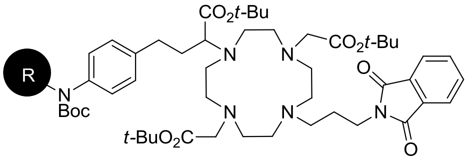

The resin bound amine **4-12** (0.06 mmol) was swelled in CH_2Cl_2 (5 mL) for 1 h, and then it was washed with CH_2Cl_2 (3 × 5 mL) and DMF (3 × 5 mL). A solution of N,N-diisopropylethylamine (104 µL, 0.60 mmol) and di-*tert* butyl dicarbonate (131 mg, 0.25 mmol) in DMF (5 mL) was added and the resultant mixture was agitated on orbital shaker for 18 h. The resin was drained and washed with DMF (4 × 7 mL), methanol (4 × 7 mL), dichloromethane (4 × 7 mL) to obtain pthalimide **4-10**.

Compound 4-11

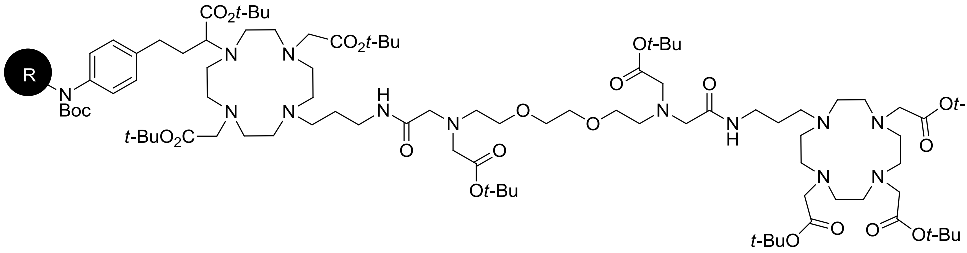

To a suspension of the resin-bound amine **4-8** (0.06 mmol) in DMF (3 mL) was added pre-made (10 minute before addition) mixture of acid **3-22** (95 mg, 0.09 mmol), HBTU (35 mg, 0.09 mmol) and N,N-diisopropylethylamine (21 µl, 0.12 mmol) and gently shaken for 18 h at room temperature. The solution was filtered through a phase extraction frit cartridge and washed with DMF (3 mL × 3) dichloromethane (3 mL × 3), methanol (3 mL × 3), alternatively, ending with a final washing with dichloromethane (3 mL). The procedure was repeated for two more times to afford ester **4-11**.

Compound 4-12

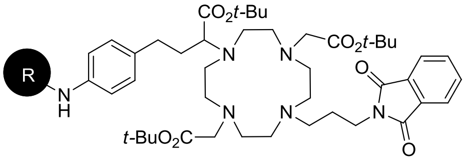

A 2-chloro trityl chloride resin (50 mg, 0.06 mmol, loading 1.22 mmol/g) was swelled in dichloromethane (7 mL) for 1 h and then it was washed with DMF (3 × 5 mL) and dichloromethane (3 × 5 mL). The resin was again suspended in dichloromethane (5 mL) and amine **3-14** (50 mg, 0.06 mmol) was added followed by N,N-diisopropylethylamine (10 µL, 0.06 mmol). After agitating the mixture for 10 minutes another portion of diisopropylethyl amine (20 ul, 0.12 mmol) was added and reaction mixture was agitated for another 18 h. The solution was filtered through a phase extraction frit cartridge and washed with DMF (3 mL × 3) and CH_2Cl_2 (3 mL × 3). The resin was added with methanol (0.5 mL) in CH_2Cl_2 (5 mL) and agitated for 30 min. to endcap reactive sites and filtered off to eliminate any remaining reactive site in resin. The resin was washed extensively with DMF (3 mL × 3) and CH_2Cl_2 (3 mL × 3) to accomplish resin bound pthalimide **4-12**.

Compound 4-13

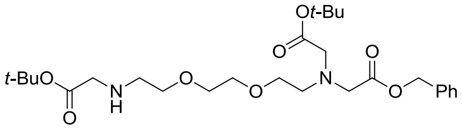

To a solution of amine **3-10** (6.0 g, 15.95 mmol) and cesium carbonate (4.10 g, 12.78 mmol) in anhydrous acetonitrile (200 mL) at room temperature was added slowly solution of benzyl bromoacetate (255 mmol solution in acetonitrile, 12.78 mmol). The resultant solution was stirred at room temperature for 2 days. The insoluble materials were removed by filtration and the filtrate was concentrated under reduced pressure. The residue was dissolved in dichloromethane (200 mL) and water (100 mL). The organic layer was separated; the aqueous phase was extracted by dichloromethane (2 × 100 mL). The combined organic layer was dried over sodium sulphate, filtered, and concentrated under reduced pressure. Purification of the residue by silica gel column chromatography (3% methanol/dichloromethane) gave the benzyl ester **4-13** as light yellow oil (3.50 g, 42%).

^{1}H NMR (300 MHz, $CDCl_3$), δ (ppm): 1.38-1.54 (s, 18H, (C(C*H*$_3$)$_3$), 1.95 (br., s, 1H, N*H*), 2.74 (t, *J* = 6 Hz, 2H), 2.95 (t, *J* = 6 Hz, 2H), 3.29, 3.31(s, 2H, N*H*COOBn), 3.44-3.71 (m, 12H), 5.12, 5.17 (s, 2H, C*H*$_2$ benzyl), 7.29-7.41 (m, 5H, Ar*H*).

^{13}C{1H} NMR (75 MHz, $CDCl_3$), δ (ppm): 28.0, 28.1 (C(*C*H$_3$)$_3$), 48.7, 51.6, 53.5, 55.8, 56.6, 66.1, 70.2, 70.3, 70.6, 80.9, 80.9(*C*(CH$_3$)$_3$), 128.2, 128.5, 135.7 (Ar*C*), 170.6, 171.3, 171.4 (*C*=O).

ESI-HRMS for $C_{27}H_{44}N_2O_8Na$ [(M + Na)$^+$] *m/z* calcd. 547.298987, found 547.298984

Compound 4-14

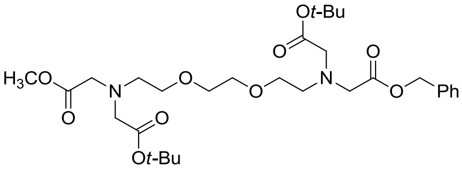

A solution of methyl bromoacetate (167 µL, 1.76 mmol) in acetonitrile (3 mL) was added drop wise to a mixture of amine **4-13** (0.77 g, 1.46 mmol), potassium carbonate (0.24 g, 1.76 mmol), and acetonitrile (10 mL) at room temperature. After 16 h of heating at 70 °C, the mixture was cooled to room temperature and concentrated under reduced pressure. The residue was partitioned between water (75 mL) and dichloromethane (75 mL), the layers were separated, and the organic phase was washed with water (3 × 50 mL) brine, dried over sodium sulphate, filtered through a plug of cotton, and concentrated under reduced pressure. Purification by silica gel column chromatography (3% methanol/dichloromethane) afforded ester **4-14** as light yellow oil (0.63 g, 72%).

^{1}H NMR (300 MHz, $CDCl_3$) δ (ppm): 1.44 (s, 18H, $(C(CH_3)_3)$), 2.94 (q, J = 6 Hz, 4H), 3.44-3.64(m, 14H), 3.66 (s, 2H), 3.68 (s, 2H), 5.13(major), 5.19 (minor) (s, 2H, $PhCH_2$), 7.29-7.37 (m, 5H, Ar*H*).

^{13}C{1H} NMR (75 MHz, $CDCl_3$) δ (ppm): 28.0, 28.1 $(C(CH_3)_3)$, 51.4, 53.4, 55.6, 55.8, 56.6, 66.0, 70.1, 70.2, 70.3, 80.8$(C(CH_3)_3)$, 128.2, 128.4, 135.7 (Ar*C*), 170.4, 170.5, 171.3, 171.9 (*C*=O).

ESI-HRMS for $C_{30}H_{48}N_2O_{10}Na$ $[M+Na]^+$, *m/z* calcd. 619.320117, found 619.320600.

Compound 4-15

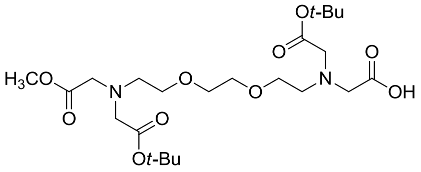

A mixture of ester **4-14** (0.63 mg, 1.06 mmol) and 10% Pd-C (0.12 g, 20% w/w) in absolute ethanol (25 mL) was shaken under a hydrogen atmosphere (35 psi) in a Parr hydrogenator. After completion of the reaction, the catalyst was removed by filtration through plug of celite and the solvent was removed under reduced pressure to obtain a pure light yellow oil of acid **4-15** (0.54 g, 78%).

^{1}H NMR (300 MHz, $CDCl_3$) δ (ppm): 1.43 (s, 18H, $(C(CH_3)_3)$), 2.90 (t, J = 6 Hz, 4H), 3.32-3.77(m, 19H).

^{13}C{1H} NMR (75 MHz, $CDCl_3$) δ (ppm): 27.7, 27.8 $(C(CH_3)_3)$, 51.6, 55.1, 56.3, 56.5, 57.1, 58.7, 60.9, 66.9, 67.3, 68.8, 68.9, 81.2, 81.3$(C(CH_3)_3)$, 171.3, 172.2, 172.5, 174.7 (*C*=O).

ESI-HRMS for $C_{23}H_{41}N_2O_{10}$ $[M-H]^-$, *m/z* calcd. 505.276121, found 505.275832.

Compound 4-16

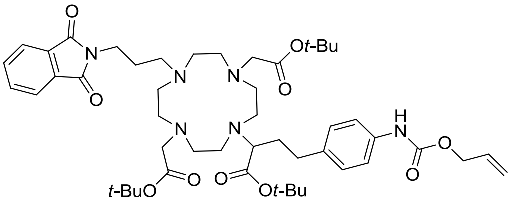

To a mixture of aime **3-14** (0.48 mg, 0.58 mmol) in dioxane (15 mL) and water (7 mL) the solution of allyl chloroformate (68 uL, 0.64 mmol) in dioxane (5 mL) was added slowly. The resultant mixture was stirred at room temperature for 16 h. The volatiles were removed under reduced pressure and residue was dissolved into dichloromethane (40 mL) and water (20 mL). The aqueous layer was removed and organic layer was washed with saturated aqueous sodium bicarbonate (20 mL) followed by water (2 × 20 mL). The organic layer was dried over sodium sulphate and concentrated to obtain light yellow syrup of alloc **4-16** (0.42 g, 79%).

^{1}H NMR (300 MHz, $CDCl_3$) δ (ppm): 1.30-1.64 (m, 27H, ($C(CH_3)_3$), 1.64-2.15 (m, 6H), 2.15-4.06 (br, 25H, C*H*$_2$ ring, C*H*COO^{t}Bu and C*H*$_2$COO^{t}Bu), 4.65 (d, *J* = 7.5 Hz, 2H), 4.98-5.49 (m, 2H), 5.74-6.14 (m, 1H), 6.77-7.92 (m, 8H, Ar*H*).

^{13}C{1H} NMR (75 MHz, $CDCl_3$) δ (ppm): 26.1, 28.1, 28.2 ($C(CH_3)_3$), 29.5, 30.2, 32.0, 36.5, 49.7, 52.2, 52.4, 52.8, 53.0,(CH_2 ring), 56.0 (CH_2COO*t*Bu), 60.2, 64.3 (*C*HCOO*t*Bu), 65.5, 80.4, 80.5, ($C(CH_3)_3$), 117.9, 118.9, 123.0, 128.8, 132.0, 132.5, 135.5, 137.1, 153.2, 144.1, 168.1, 170.9, 172.6 (*C*=O).

ESI-HRMS for $C_{49}H_{73}N_6O_{10}$ $[M+H]^+$, *m/z* calcd. 905.538269, found 905.538035.

Compound 4-17

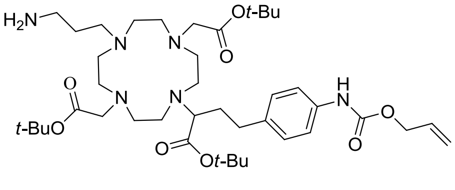

To a solution of alloc **4-16** (0.70 g, 0.77 mmol) in 2-propanol (10 mL) was added ethylenediamine (0.26 mL, 3.86 mmol) and the mixture stirred at 90 °C for 16h. The reaction mixture was cooled to room temperature and concentrated under reduced pressure. The residue was dissolved in dichloromethane (40 mL) and water (20 mL). After removal of aqueous layer, the organic layer was washed with water (2 × 25 mL) and brine (25 mL). The organic layer was dried over sodium sulphate. Pure amine **4-17** as light brown semi solid was obtained after concentration of organic layer under reduced pressure (0.46 g, 77%).

^{1}H NMR (300 MHz, CDCl$_3$) δ (ppm): 1.33-1.66 (m, 27H, (C(C*H*$_3$)$_3$), 1.67-2.29 (m, 2H), 2.32-4.13 (br, 27H, C*H*$_2$ ring, C*H*COO^{t}Bu and C*H*$_2$COO^{t}Bu), 4.65 (d, *J* = 7.5 Hz, 2H), 5.08-5.44 (m, 2H), 5.84-6.08 (m, 1H), 6.78-7.80 (m, 8H, Ar*H*).

^{13}C{1H} NMR (75 MHz, CDCl$_3$) δ (ppm): 25.2, 27.9, 28.1, 28.2 (C(*C*H$_3$)$_3$), 30.2, 31.8, 40.2, 44.5, 49.6, 52.1, 52.3, 52.8, 53.3,(*C*H$_2$ ring), 56.2 (*C*H$_2$COO^{t}Bu), 63.7, 64.4 (*C*HCOO^{t}Bu), 65.5, 80.5, 80.6, 82.1, 82.3, 82.7(*C*(CH$_3$)$_3$), 115.1, 117.8, 118.7, 123.1, 125.3, 128.8, 132.5, 133.9, 135.7, 136.9, 153.3, 168.1, 170.9, 172.8, 173.7 (*C*=O).

ESI-HRMS for $C_{41}H_{71}N_6O_8$ [M+H]$^+$, *m/z* calcd. 775.532790, found 775.532317.

Ligand L^7

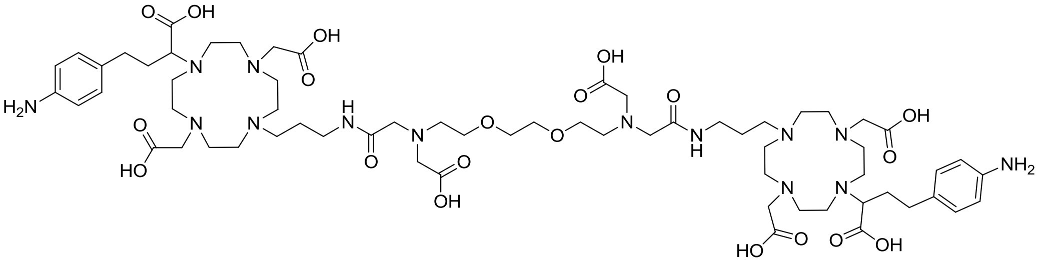

The resin-bound amine **4-29** was treated with a 90% solution of trifluoroacetic acid in CH_2Cl_2 for 16 h. The solution was drained into a round-bottom flask, and the resin was washed twice with anhydrous CH_2Cl_2. The solvents were removed under reduced pressure and the residue was dissolved into methanol (10 mL) and concentrated further. This procedure was repeated for three more times. The residue was re-dissolved into methanol (1 mL) and added drop wise to cold diethyl ether (100 mL). Mixture was stirred at room temperature for 16 h. Diethyl ether was removed using a centrifuge to obtain ligand **L^7**.

^{1}H NMR (300 MHz, D$_2$O), δ (ppm): 1.58-2.22 (m, 8H), 2.24-4.36 (m, 74H), 7.31 (d, *J* = 7.5 Hz, 2H), 7.40 (d, *J* = 7.5 Hz, 2H).

ESI-MS for $C_{64}H_{103}N_{14}O_{20}$ [(M - H)$^-$] *m/z* calcd. 1387.7, found 1387.6.

Some Important intermediates

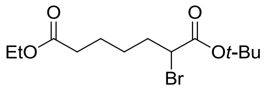

Acid (1.00 g, 5.74 mmol) was dissolved into thionyl chloride (1.67 mL, 22.98 mmol) and stirred at 75 °C for 24 h. Bromine (0.326 mL, 6.32 mmol) was added to the reaction mixture at 75 °C and stirred at same temperature for 24 h. The reaction mixture was concentrated under reduced pressure and diethyl ether (3 × 20 mL) was added and evaporated to remove traces of volatiles. The residue was dissolved into diethyl ether (20 mL) and added drop wisely to the mixture of *tert*-butanol (810 µL, 8.62 mmol) and triethylamine (1.20 mL, 8.62 mmol) also in diethyl ether (20 mL) at room temperature and the mixture was stirred at this temperature for 16 h. The reaction mixture was diluted with diethyl ether (150 mL) and washed with water (3 × 50 mL) and brine (50 mL). The organic layer was dried over sodium sulphate, filtered through cotton plug and concentrated under reduced pressure. Purification of the residue by silica gel column chromatography (4% ethyl acetate/hexanes) gave bromide (0.90 g, 50%).

^{1}H NMR (300 MHz, CDCl$_3$), δ (ppm): 1.26 (t, *J* = 9 Hz, 3H, OCH$_2$C*H*$_3$), 1.31-1.58 (m, 11H, C(C*H*$_3$)$_3$), 1.58-1.76 (m, 2H), 1.85-2.13 (m, *J* = 9 Hz, 2H), 2.30 (t, *J* = 6 Hz, 2H), 4.08-4.15 (m, 3H, OC*H*$_2$CH$_3$, C*H(*Br)CO).

^{13}C NMR (75 MHz, CDCl$_3$), δ (ppm): 14.2, 24.2, 26.7, 27.7 (C(*C*H$_3$)$_3$), 33.9, 34.49, 47.4, 60.3 (C*C*H*(*Br)CO), 82.3 (*C*(CH$_3$)$_3$), 168.7, 173.2 (*C*=O).

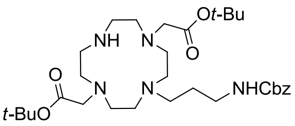

To a solution of bis-*tert* butyl ester DO2A **2-10** (1.00 g, 2.50 mmol) in anhydrous acetonitrile (50 mL) sodium bicarbonate (0.168 g, 2.00 mmol) was added followed by solution of benzy-3-bromopropyl carbamate (0.54 g, 2.00 mmol) also in anhydrous acetonitrile (20 mL) slowly at room temperature. The resultant mixture was stirred at room temperature for 2 days. The insoluble solids were removed by filtration and the filtrate was concentrated under reduced pressure to obtain a residue which was purified by silica gel column chromatography (2% methanol/dichloromethane) to obtain amine as white solid (0.57 g, 38%).

^{1}H NMR (300 MHz, CDCl$_3$), δ (ppm): 1.45 (s, 18H, C(C*H*$_3$)$_3$), 1.57-1.78 (m, 2H, CH$_2$C*H*$_2$CH$_2$), 2.43-3.47 (m, 24H,), 5.10 (s, 2H, OC*H*$_2$Ph), 5.79 (br s, , 1H, N*H*CO), 7.18-7.41 (m, 5H, Ar*H*), 10.19 (br s, 1H, N*H* ring),

^{13}C{1H} NMR (75 MHz, CDCl$_3$) δ (ppm): 24.1 (CH$_2$*C*H$_2$CH$_2$), 28.06 (C(*C*H$_3$)$_3$), 29.6 (NCO*C*H$_2$CH$_2$), 39.1 (N*C*H$_2$CH$_2$), 46.3, 48.8, 50.2, 52.2, (C*H*$_2$ ring), 57.2 (C*H*$_2$ acetate arm), 66.3 (OC*H*$_2$Ph), 81.5 (*C*(CH$_3$)$_3$), 136.6, 128.4, 128.0, 127.9 (Ar*C*), 156.7, 170.3 (*C*=O).

ESI-MS for $C_{31}H_{53}N_5O_6$ [$(M + H)^+$] *m/z* calcd. 592.4, found 592.4

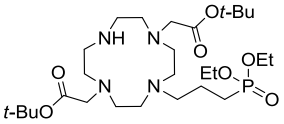

To a solution of bis-*tert* butyl ester DO2A **2-10** (2.10 g, 5.25 mmol) and sodium bicarbonate (0.35 g, 4.20 mmol) in anhydrous acetonitrile (100 mL) was added a solution of diethyl(3-bromopropyl)phosphonate (1.09 g, 4.20 mmol) in acetonitrile (40 mL) over 1 h. The resultant mixture was stirred at room temperature for 2 days. The residue obtained after filtration and concentration under reduced pressure was purified by silica gel column chromatography (3% methanol/dichloromethane) to afford amine as white solid (1.2 g, 39%)

^{1}H NMR (300 MHz, CDCl$_3$), δ (ppm): 1.28 (t, *J* = 7.5 Hz, 6H, OCH$_2$C*H*$_3$), 1.41 (s, 18H, C(C*H*$_3$)$_3$), 1.50-1.72 (m, 4H, NCH$_2$C*H*$_2$C*H*$_2$), 2.43-3.15 (m, 18H, C*H*$_2$ ring, NC*H*$_2$CH$_2$), 3.34 (s, 4H, C*H*$_2$ acetate arm), 3.95-4.16 (m, 4H, OCH$_2$C*H*$_3$), 10.17(br.s, 1H, N*H* ring),

^{13}C{1H} NMR (75 MHz, CDCl$_3$) δ (ppm): 14.5(d, *J* = 4.5 Hz ,NCH$_2$*C*H$_2$CH$_2$), 16.4(d, *J* =5.3 Hz, OCH$_2$*C*H$_3$), 23.1 (d, *J* = 141.8 Hz, P(O)*C*H$_2$CH$_2$), 28.0 (C(*C*H$_3$)$_3$), 47.4 (N*C*H$_2$CH$_2$), 48.9, 50.4, 50.8, 53.3 (*C*H$_2$ ring), 57.8 (*C*H$_2$'s acetate arm), 61.6 (d, *J* = 6 Hz, O*C*H$_2$CH$_3$), 81.5 (*C*(CH$_3$)$_3$), 170.4 (*C*=O).

ESI-MS for $C_{27}H_{56}N_4O_7P$ [$(M + H)^+$] *m/z* calcd. 579.4, found 579.4

Annexure I

^{1}H, ^{13}C and ^{31}P NMR spectra of ligands L$^{1-7}$

All spectra were recorded in D_2O

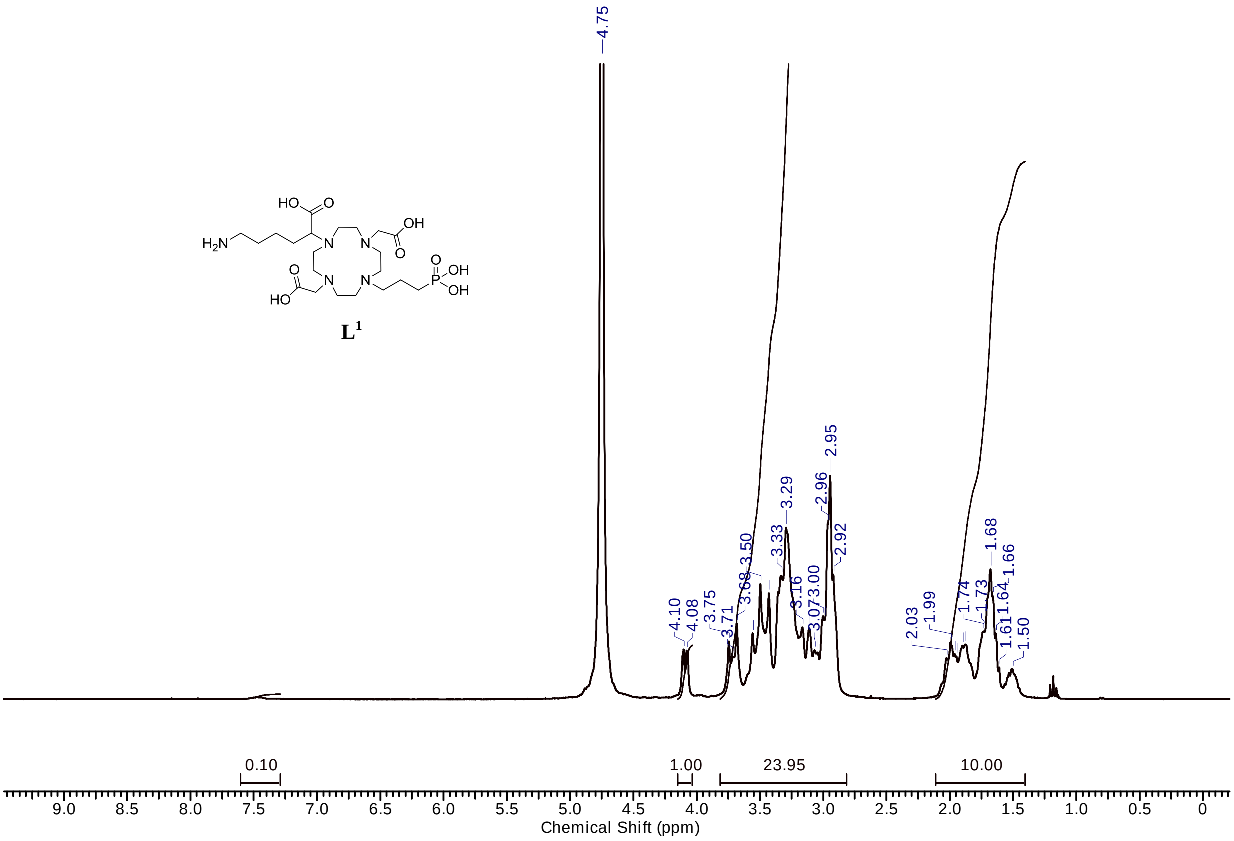
HO
O
OH
H_2N
N
O
P
OH
OH
HO
O
L^1
4.75
4.10
4.08
3.75
3.71
3.68
3.50
3.33
3.29
3.16
3.07
3.00
2.96
2.95
2.92
2.03
1.99
1.74
1.73
1.68
1.66
1.64
1.61
1.50
0.10
1.00
23.95
10.00
9.0
8.5
8.0
7.5
7.0
6.5
6.0
5.5
5.0
4.5
4.0
3.5
3.0
2.5
2.0
1.5
1.0
0.5
0
Chemical Shift (ppm)

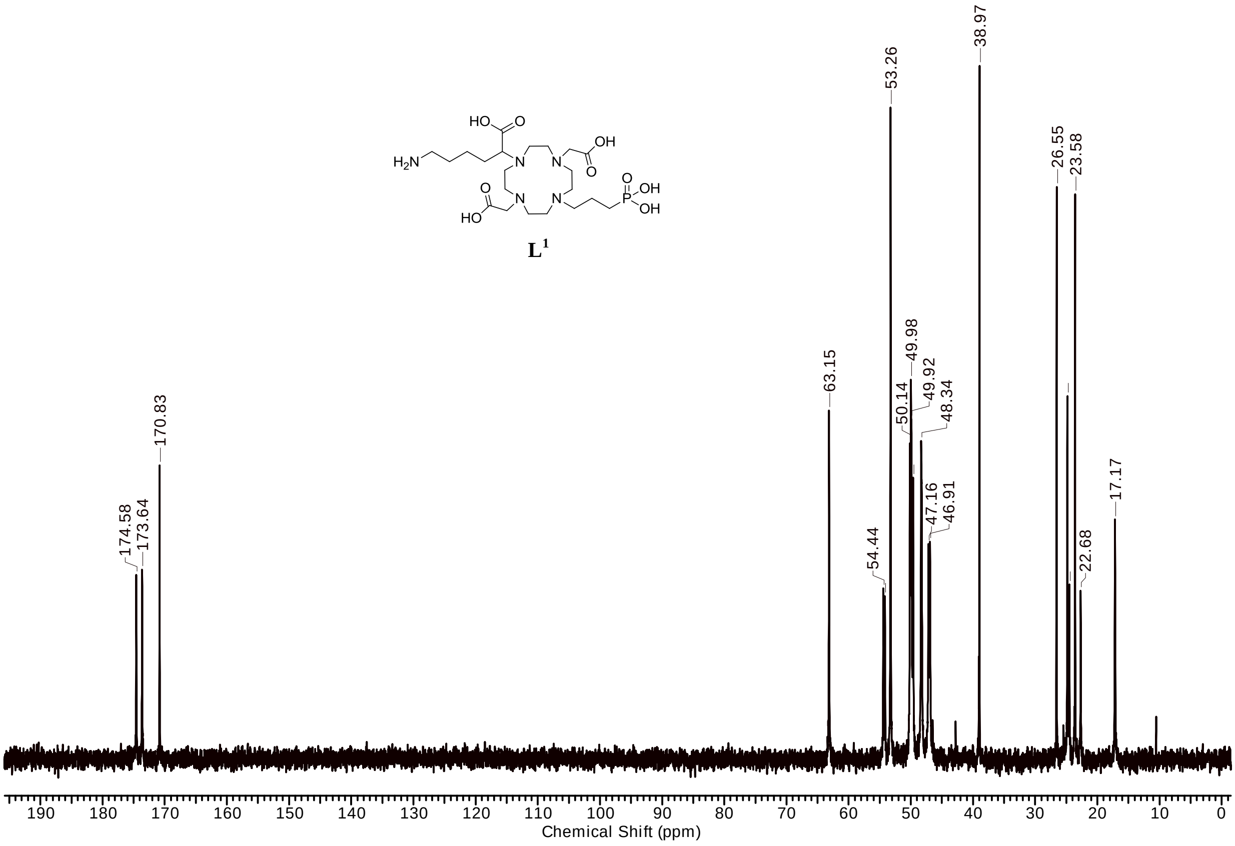
HO
O
OH
H_2N
N
O
P
OH
OH
HO
O
L^1
174.58
173.64
170.83
63.15
54.44
53.26
50.14
49.98
49.92
48.34
47.16
46.91
38.97
26.55
23.58
22.68
17.17
190
180
170
160
150
140
130
120
110
100
90
80
70
60
50
40
30
20
10
0
Chemical Shift (ppm)

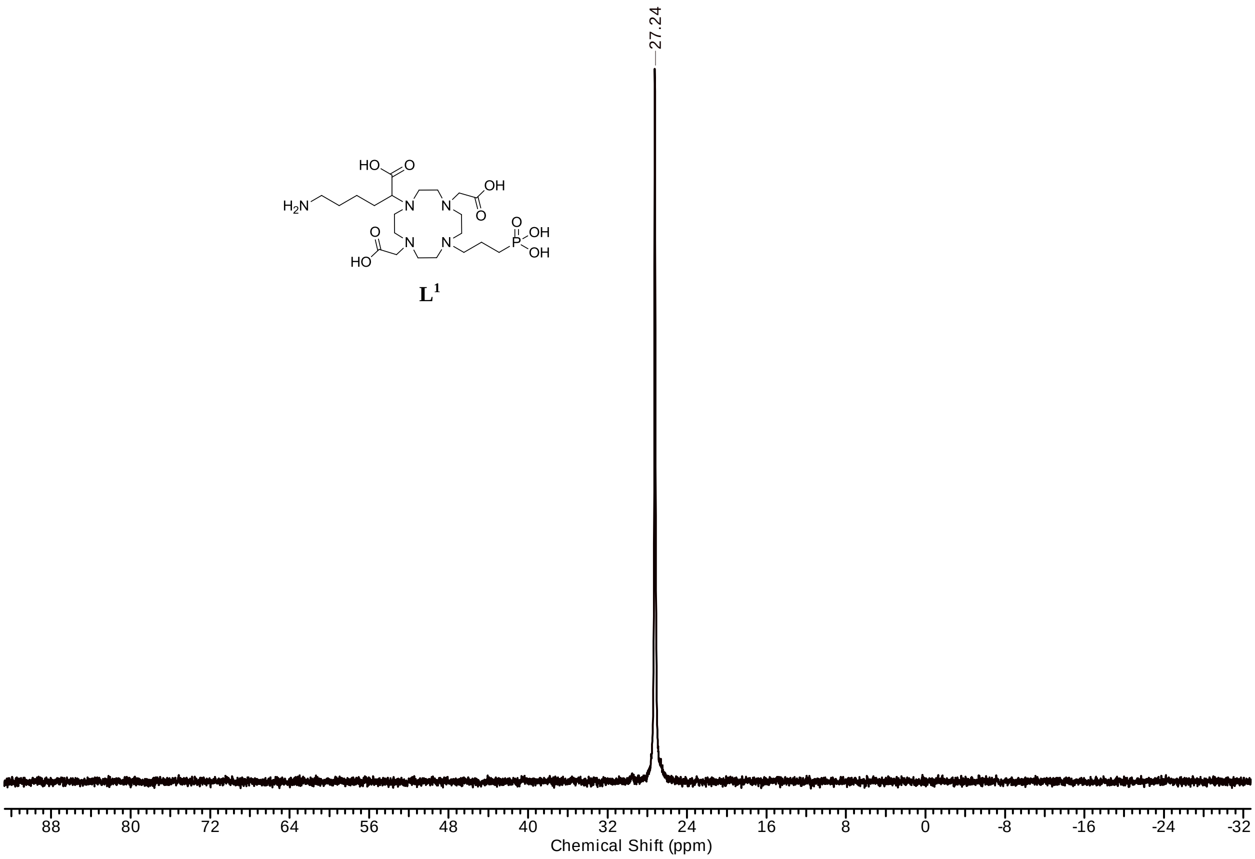
27.24
HO
O
OH
H$_2$N
N
P
88
80
72
64
56
48
40
32
24
16
8
0
-8
-16
-24
-32
Chemical Shift (ppm)

L^1

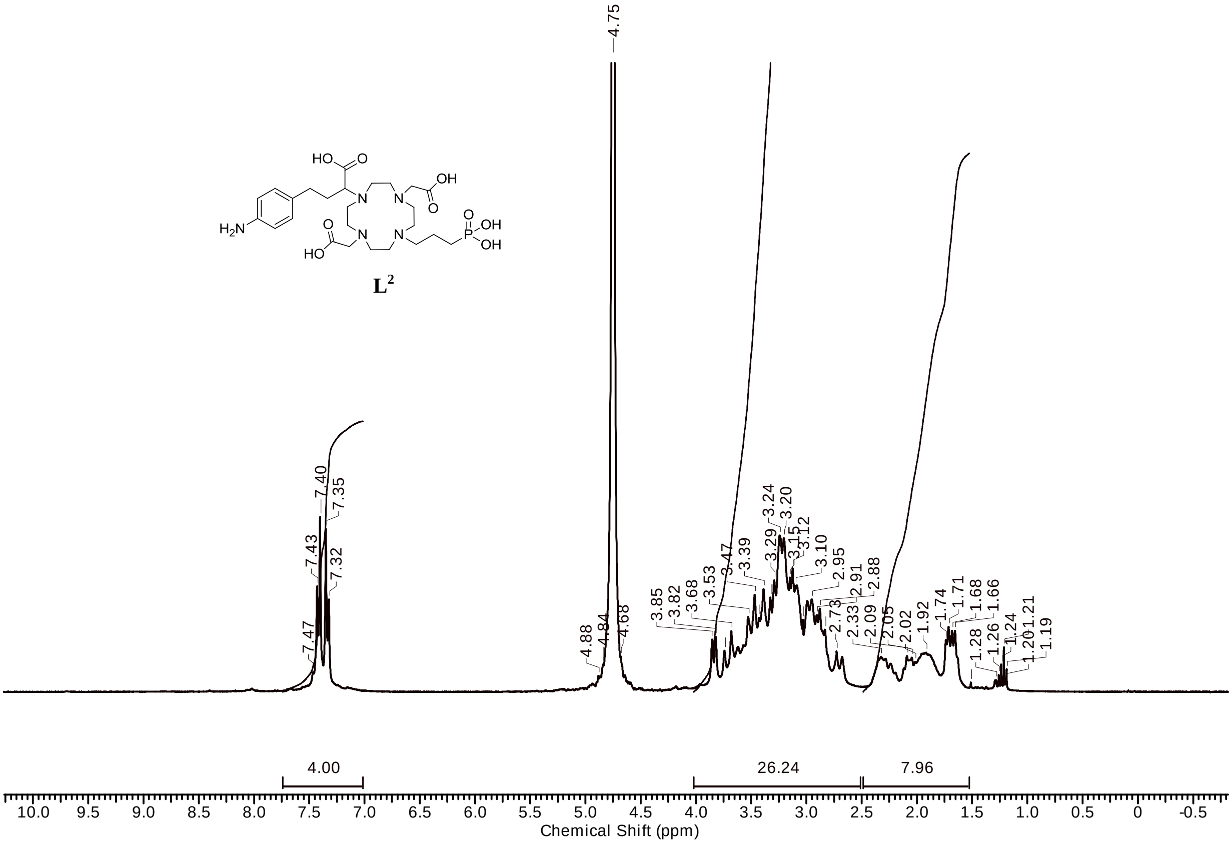
4.75
HO
O
OH
H$_2$N
N
P
7.40
7.35
7.43
7.32
7.47
4.88
4.84
4.68
3.85
3.82
3.68
3.53
3.47
3.39
3.29
3.24
3.20
3.15
3.12
3.10
2.95
2.91
2.88
2.73
2.33
2.09
2.05
2.02
1.92
1.74
1.71
1.68
1.66
1.28
1.26
1.24
1.20
1.21
1.19
4.00
26.24
7.96
10.0
9.5
9.0
8.5
8.0
7.5
7.0
6.5
6.0
5.5
5.0
4.5
4.0
3.5
3.0
2.5
2.0
1.5
1.0
0.5
0
-0.5
Chemical Shift (ppm)

L^2

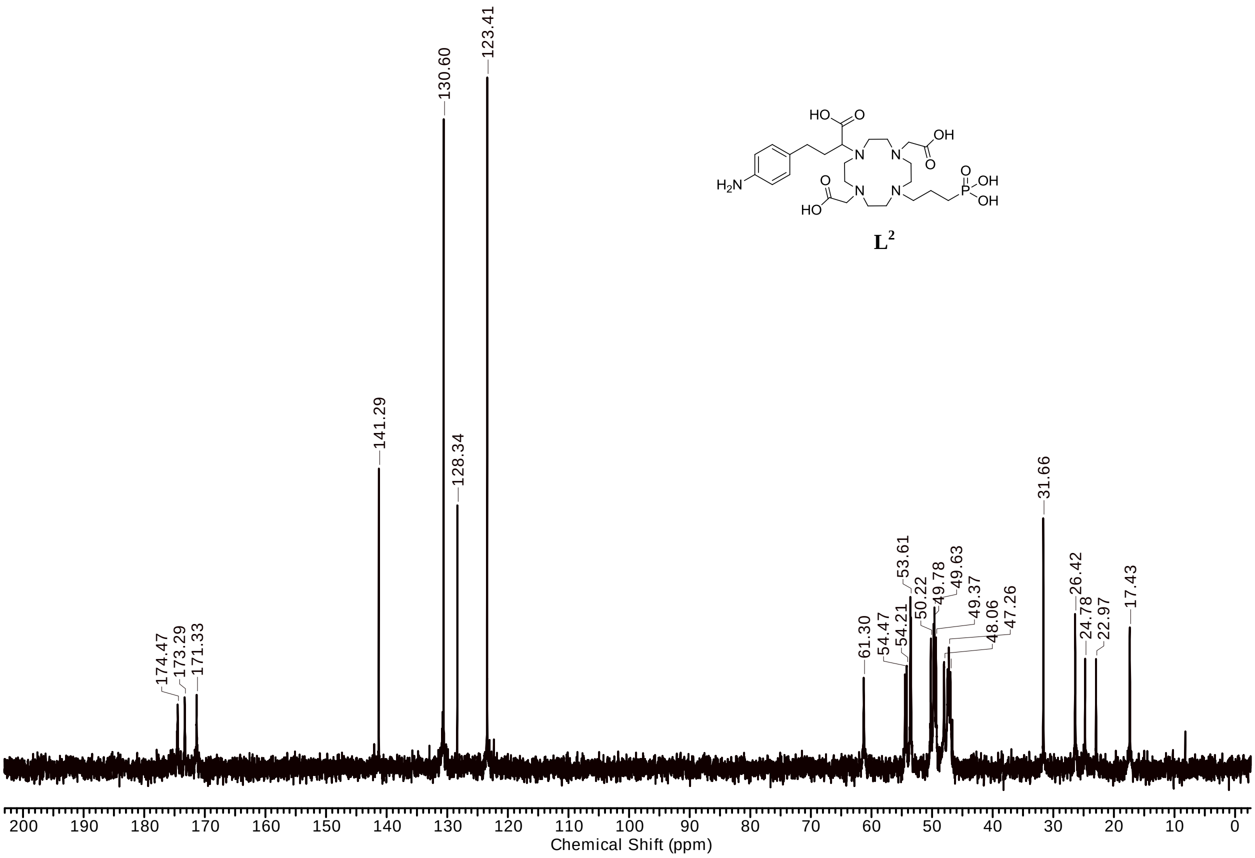

$\mathbf{L^2}$

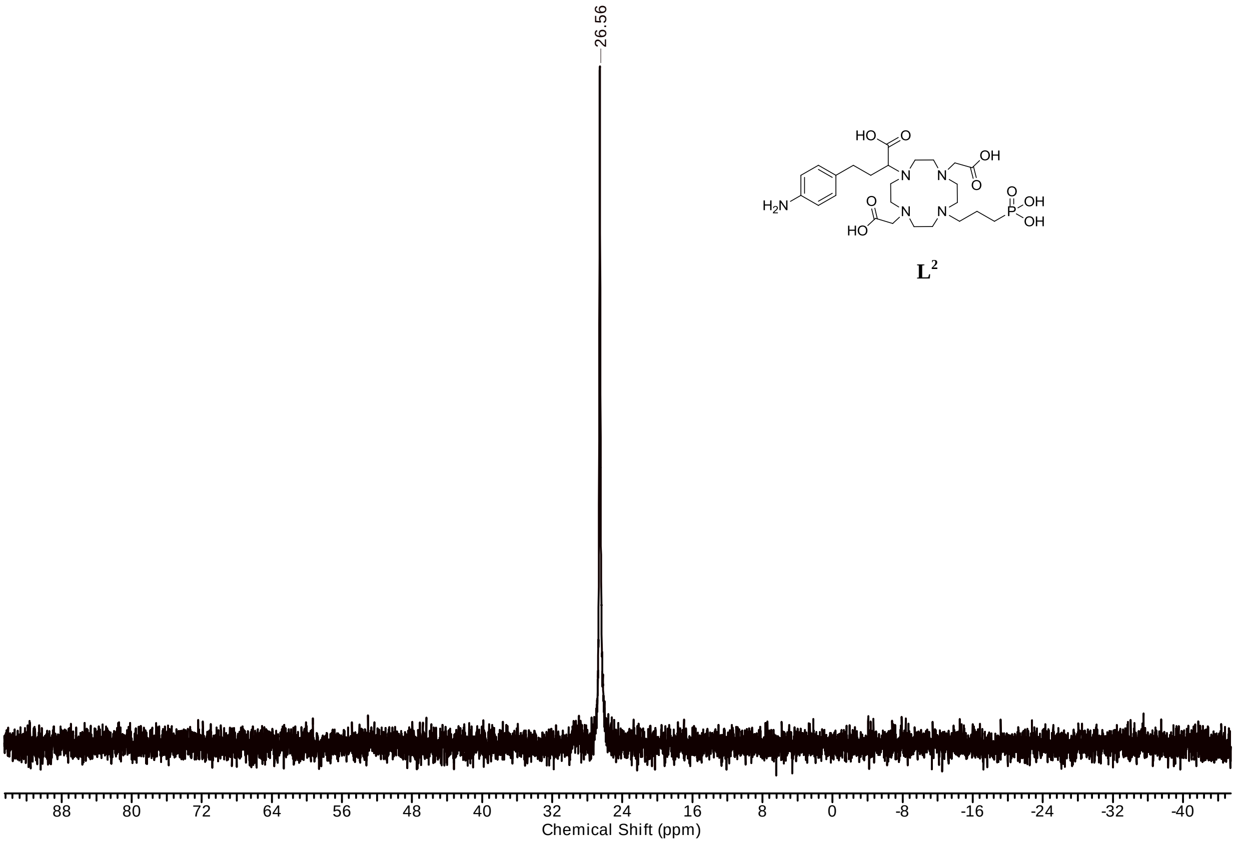

$\mathbf{L^2}$

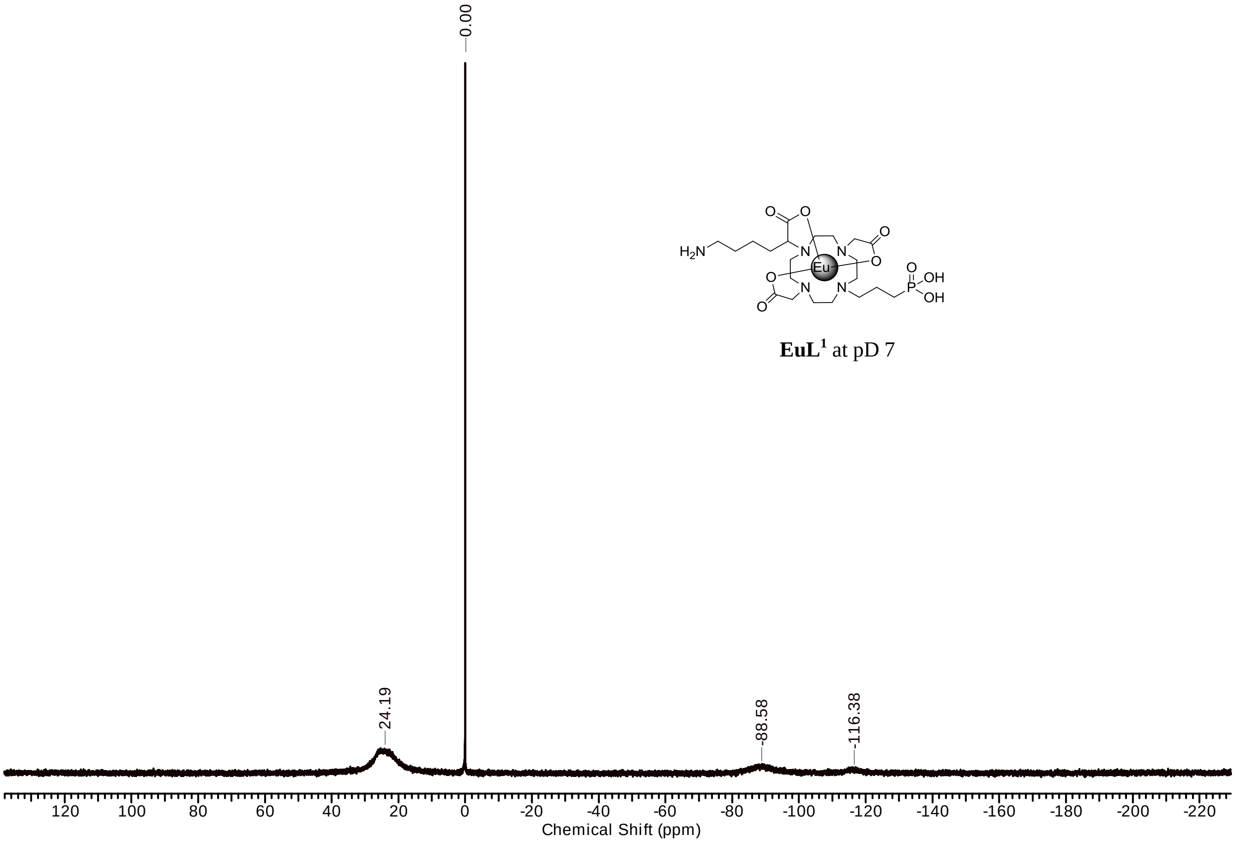

EuL^1 at pD 7

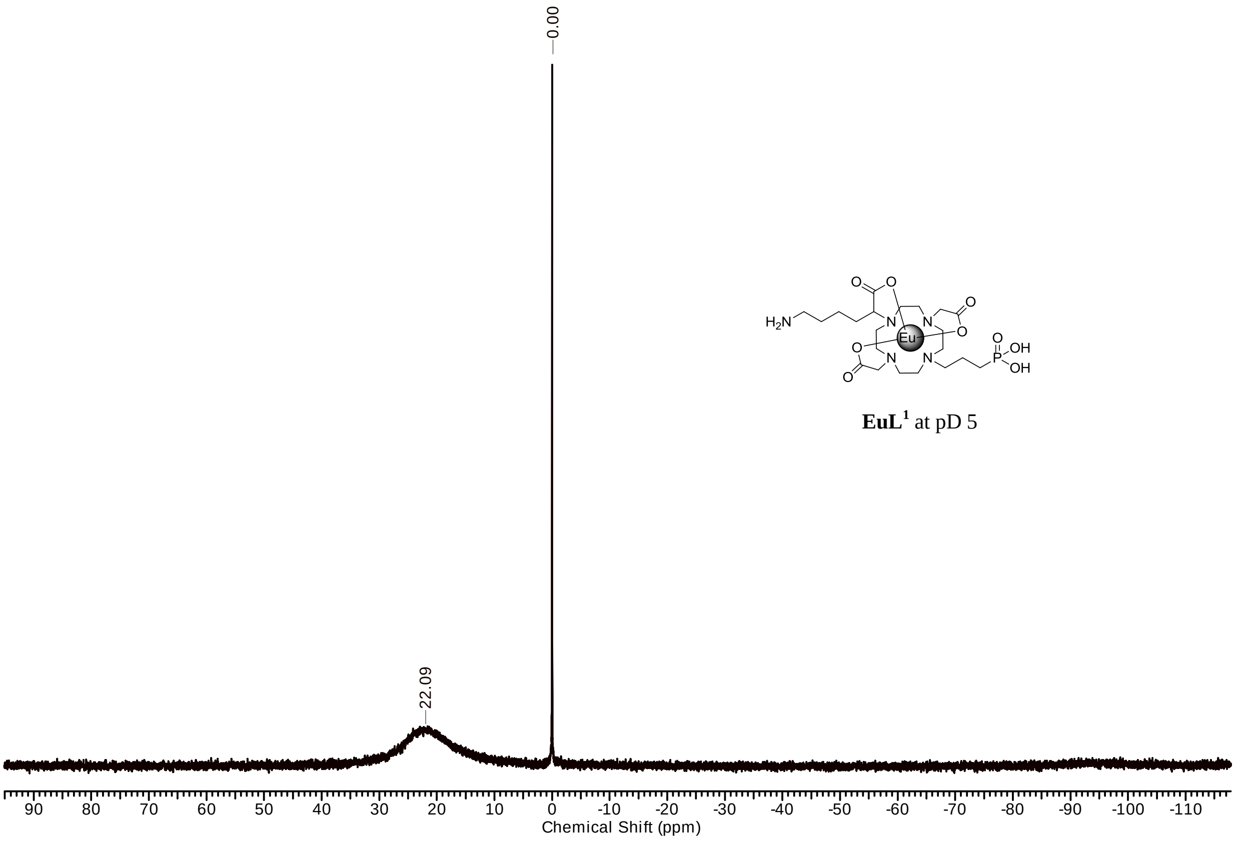

EuL^1 at pD 5

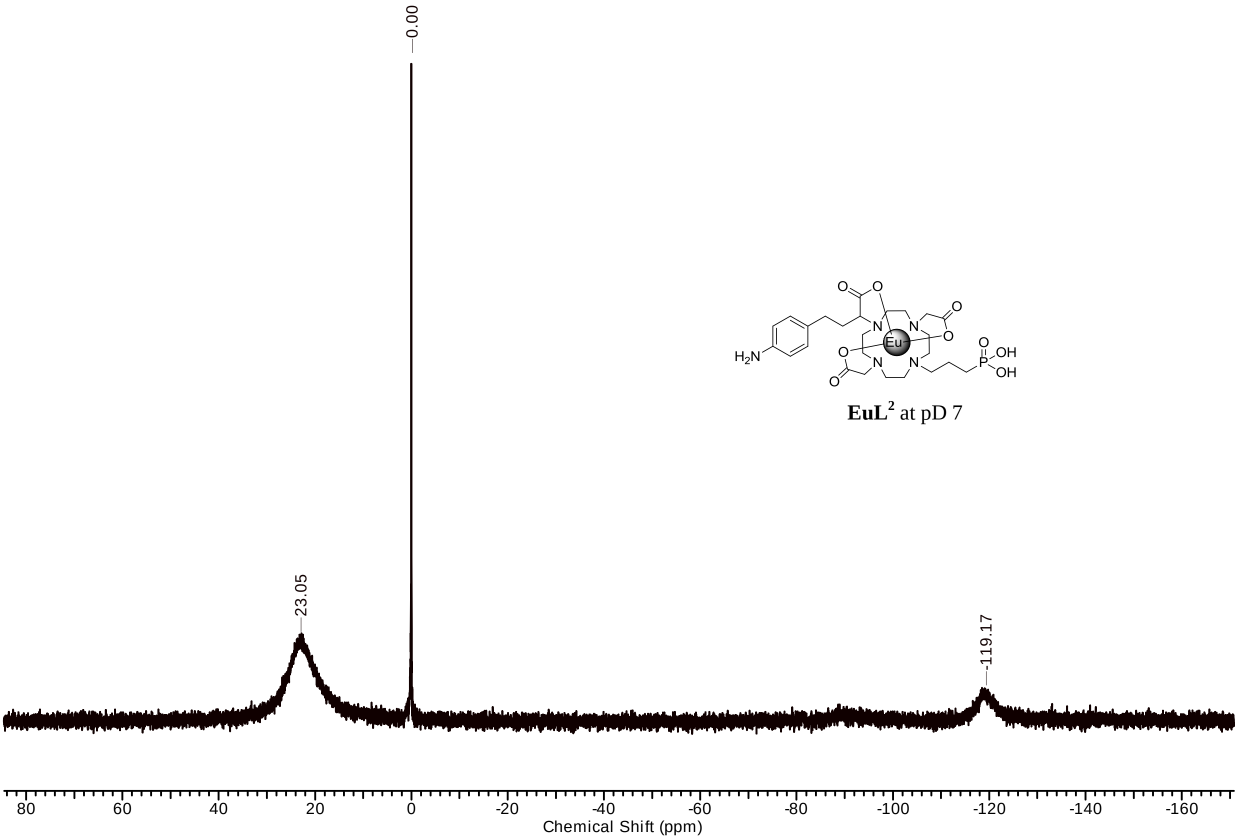

EuL^2 at pD 7

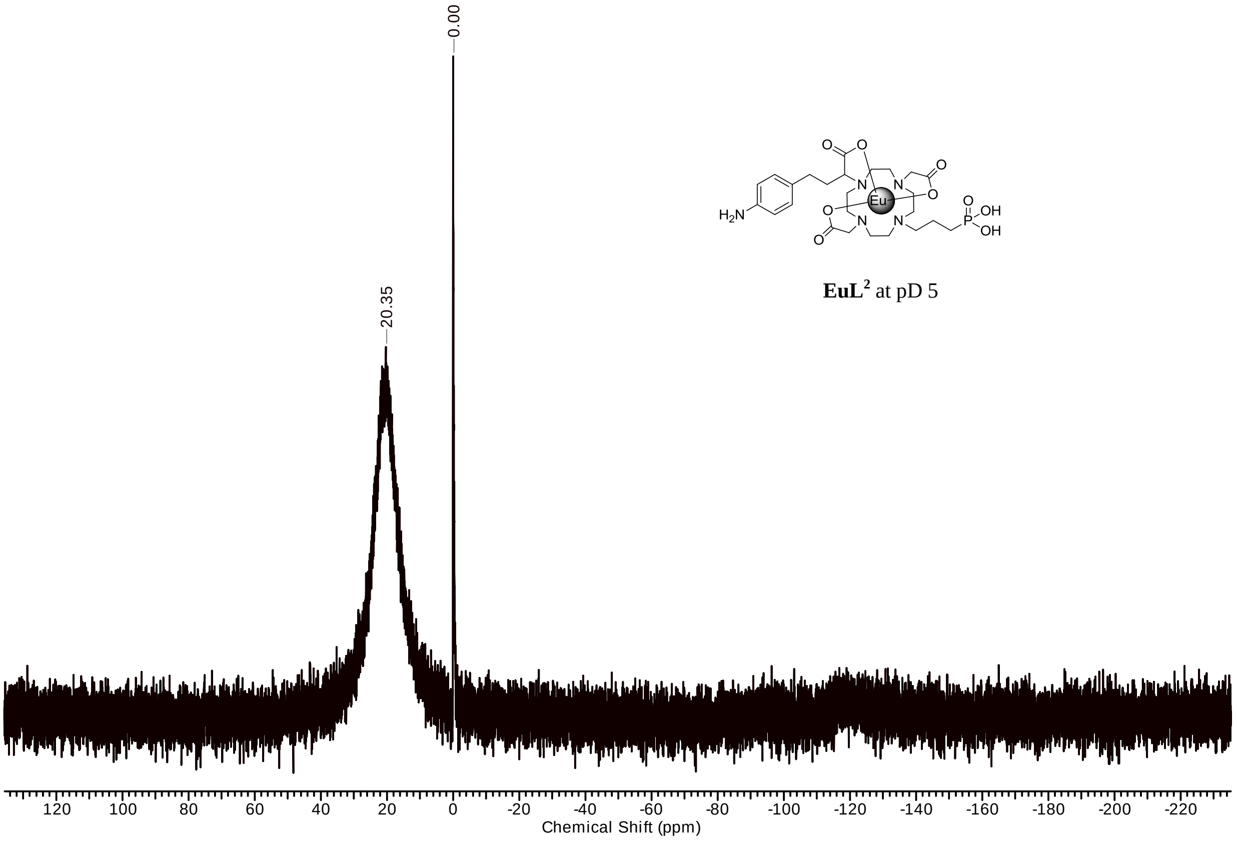

EuL^2 at pD 5

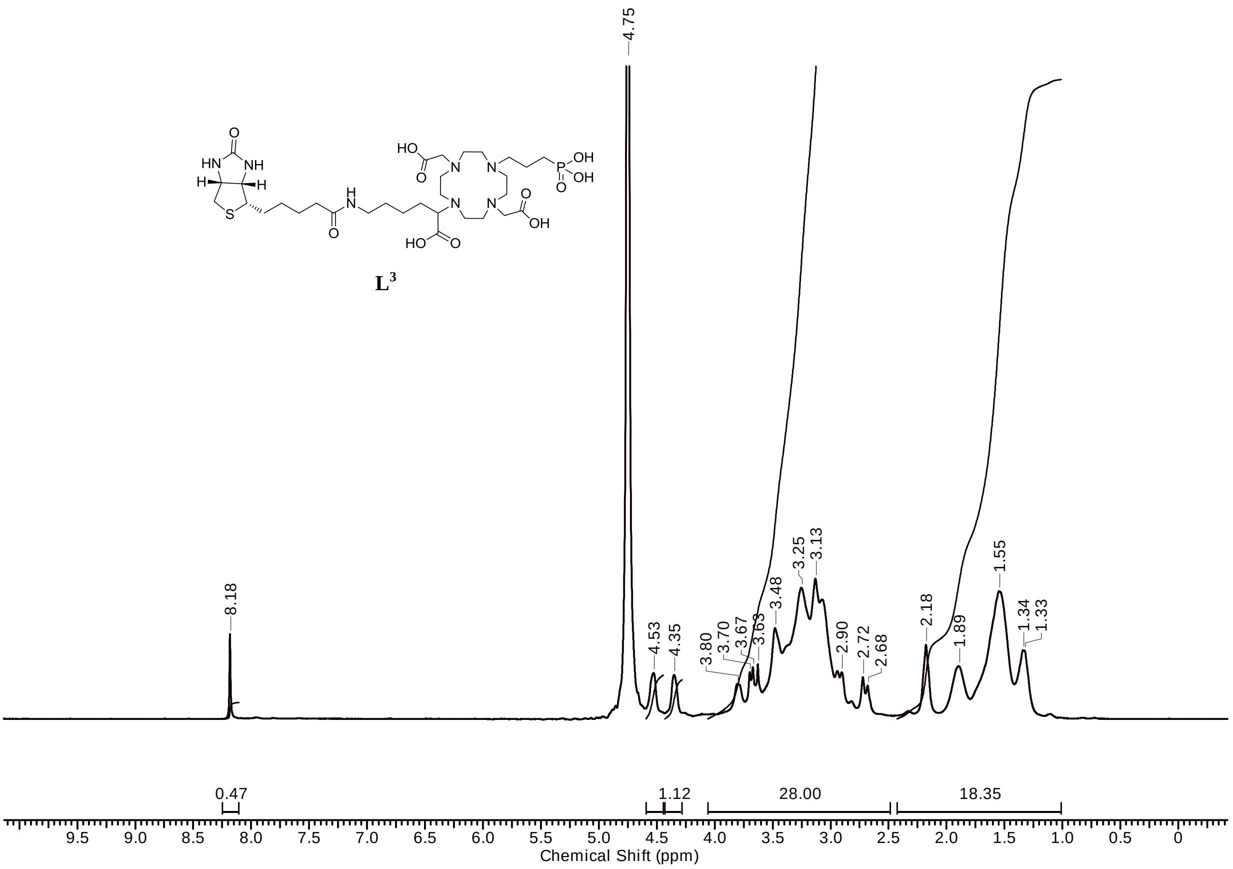
L^3
HN
NH
O
H
S
HO
N
P
OH
8.18
4.75
4.53
4.35
3.80
3.70
3.67
3.63
3.48
3.25
3.13
2.90
2.72
2.68
2.18
1.89
1.55
1.34
1.33
0.47
1.12
28.00
18.35
9.5
9.0
8.5
8.0
7.5
7.0
6.5
6.0
5.5
5.0
4.5
4.0
3.5
3.0
2.5
2.0
1.5
1.0
0.5
0
Chemical Shift (ppm)

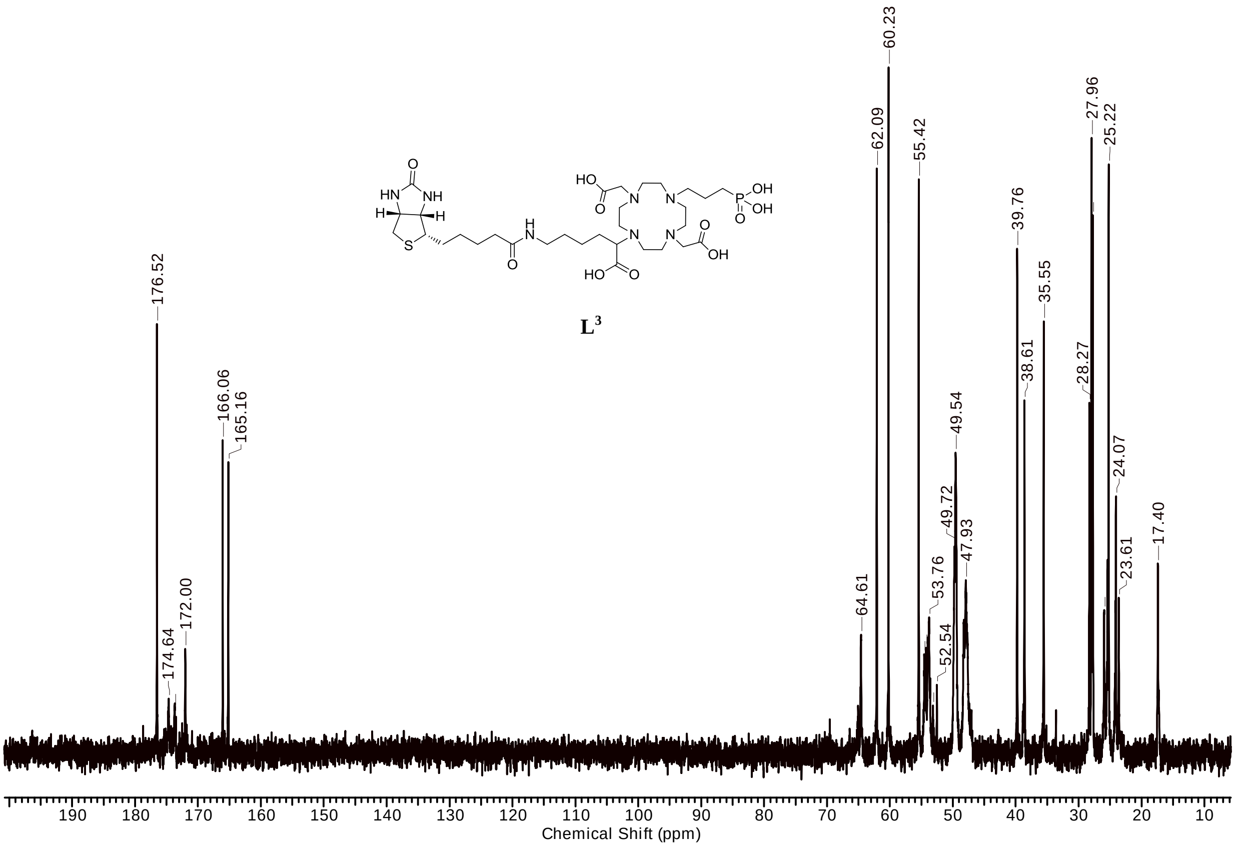
L^3
HN
NH
O
H
S
HO
N
P
OH
176.52
174.64
172.00
166.06
165.16
64.61
62.09
60.23
55.42
53.76
52.54
49.72
49.54
47.93
39.76
38.61
35.55
28.27
27.96
25.22
24.07
23.61
17.40
190
180
170
160
150
140
130
120
110
100
90
80
70
60
50
40
30
20
10
Chemical Shift (ppm)

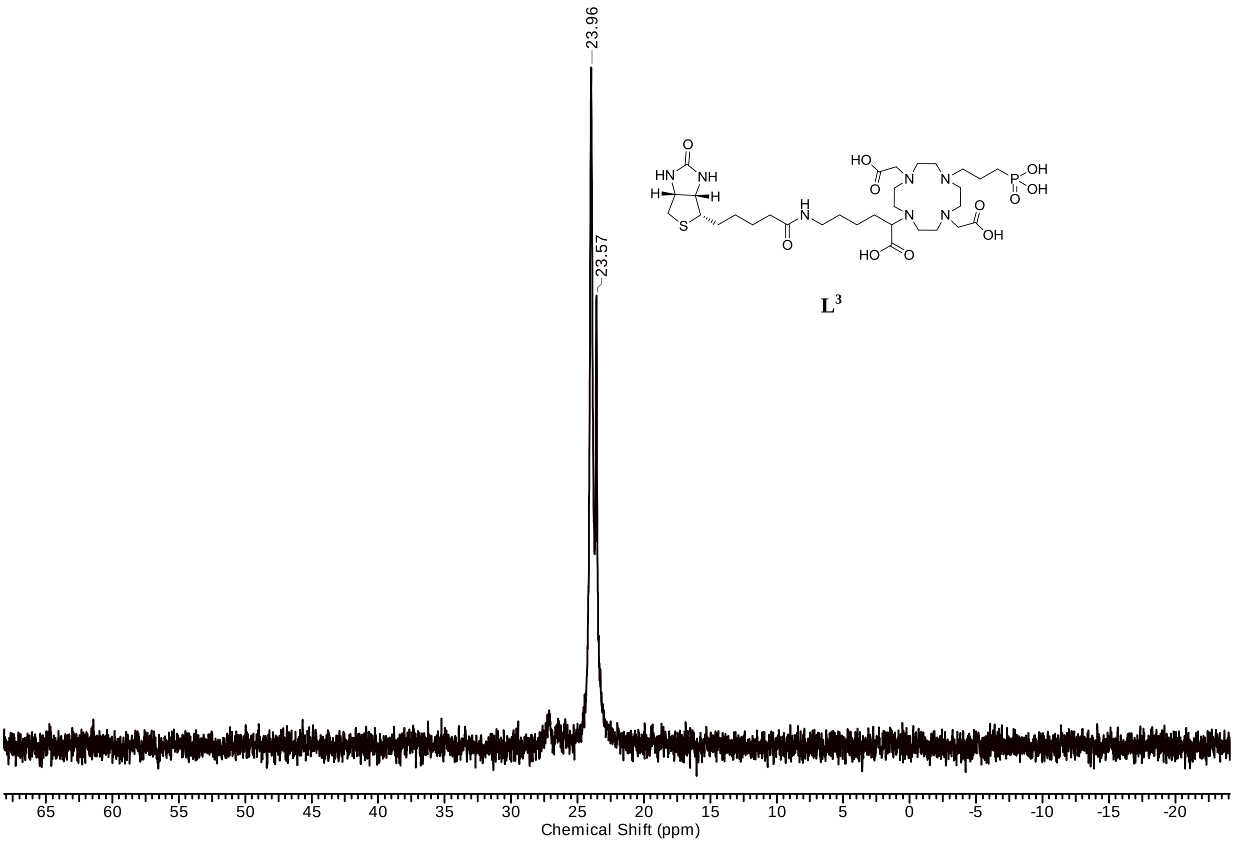
23.96
23.57
HN
NH
O
H
S
HO
N
OH
P
65
60
55
50
45
40
35
30
25
20
15
10
5
0
-5
-10
-15
-20
Chemical Shift (ppm)

L^3

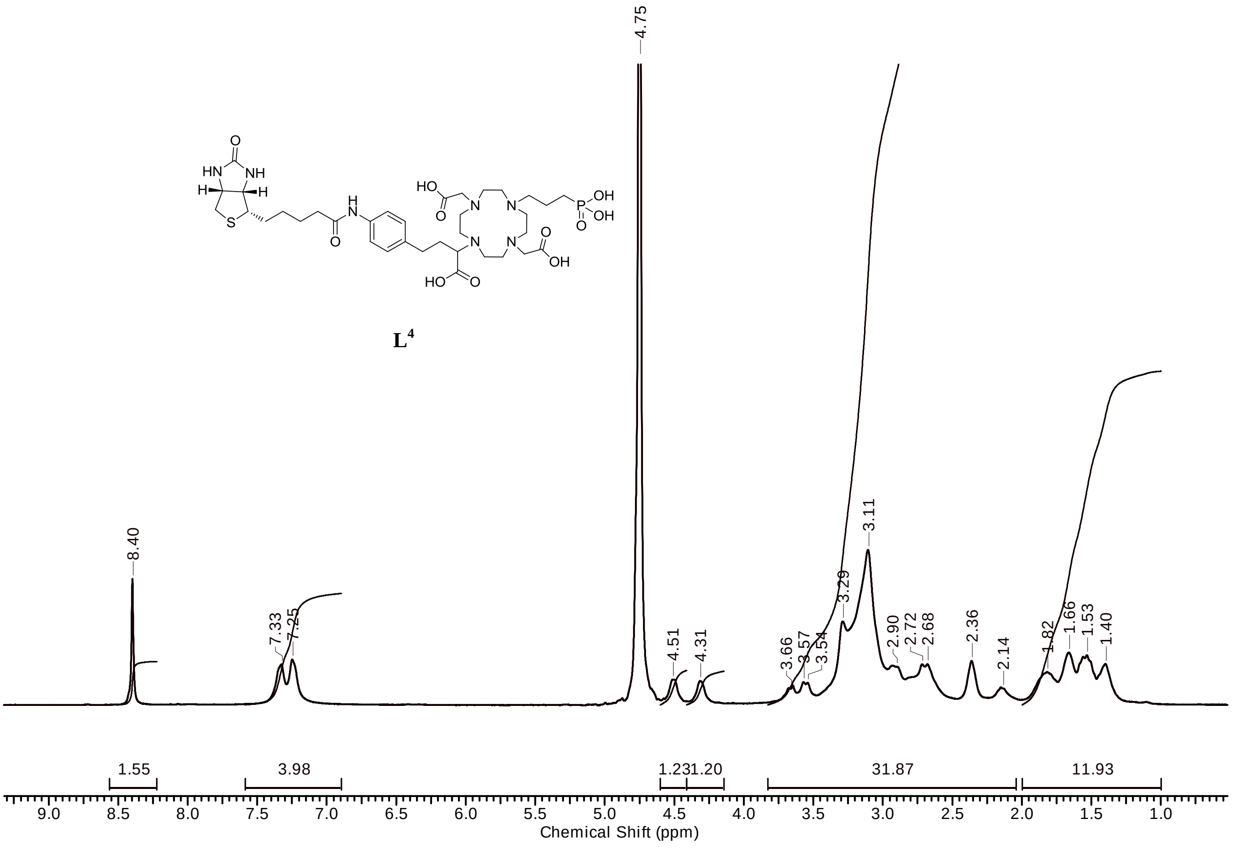
4.75
8.40
7.33
7.25
4.51
4.31
3.66
3.57
3.54
3.29
3.11
2.90
2.72
2.68
2.36
2.14
1.82
1.66
1.53
1.40
1.55
3.98
1.23
1.20
31.87
11.93
HN
NH
O
H
S
HO
N
OH
P
9.0
8.5
8.0
7.5
7.0
6.5
6.0
5.5
5.0
4.5
4.0
3.5
3.0
2.5
2.0
1.5
1.0
Chemical Shift (ppm)

L^4

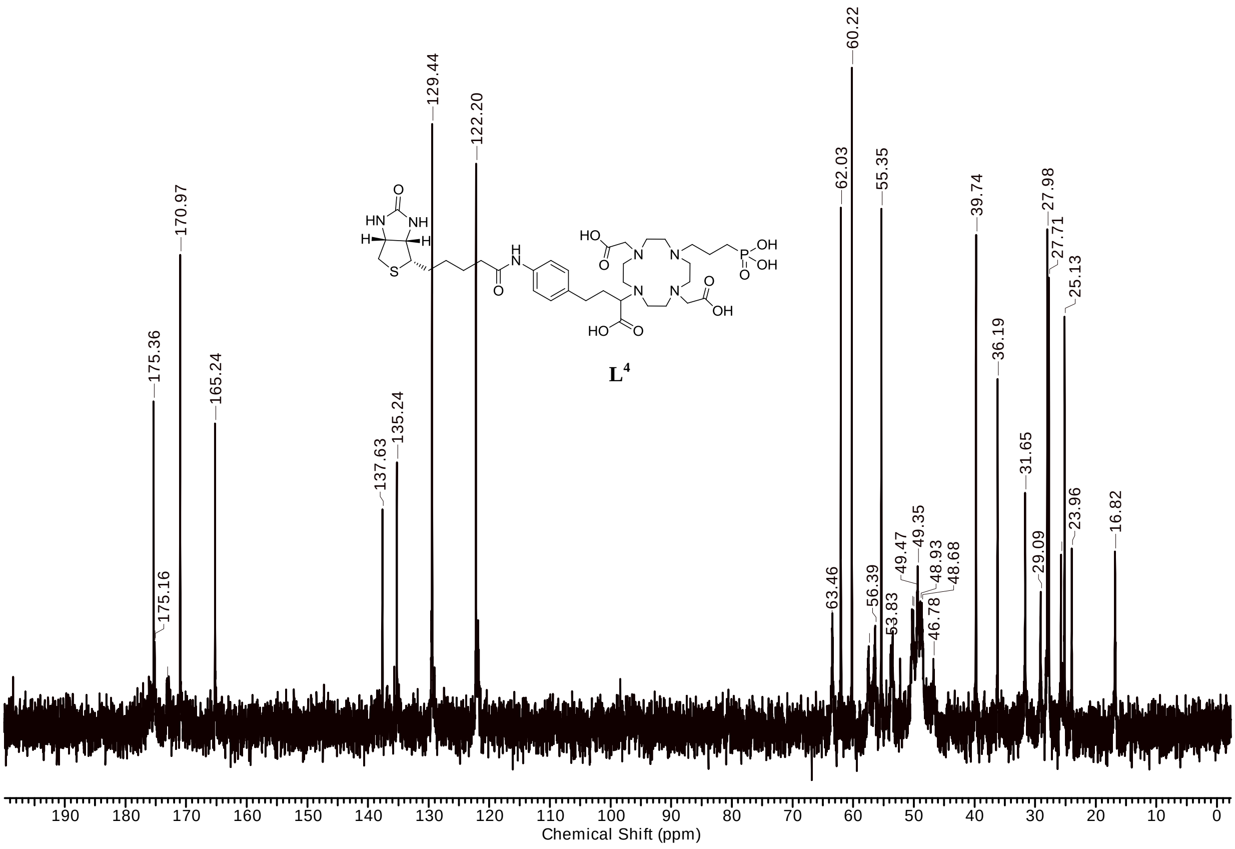
175.36
175.16
170.97
165.24
137.63
135.24
129.44
122.20
63.46
62.03
60.22
56.39
55.35
53.83
49.47
49.35
48.93
48.68
46.78
39.74
36.19
31.65
29.09
27.98
27.71
25.13
23.96
16.82
HN
NH
O
H
H
S
N
H
O
HO
O
N
N
N
N
P
OH
OH
O
O
OH
HO
O
190
180
170
160
150
140
130
120
110
100
90
80
70
60
50
40
30
20
10
0
Chemical Shift (ppm)

L^4

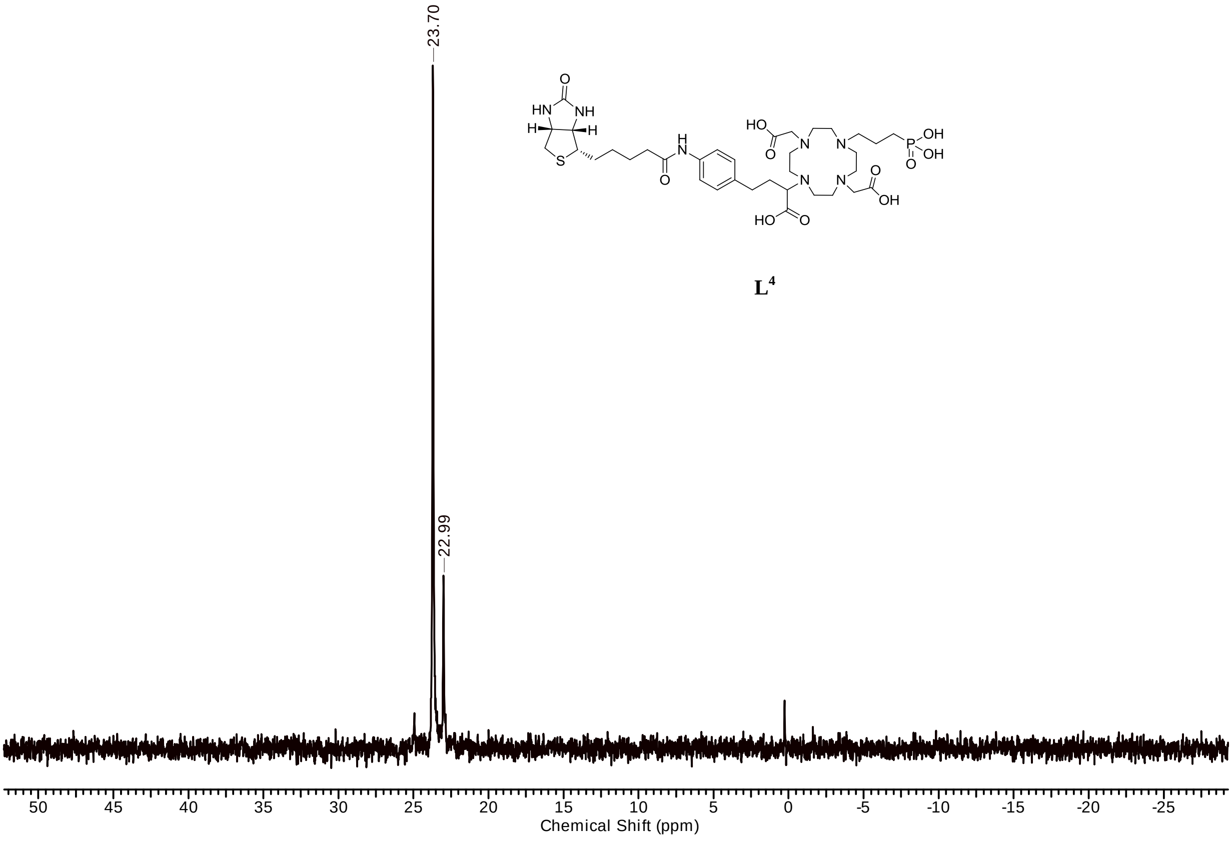
23.70
22.99
HN
NH
O
H
H
S
N
H
O
HO
O
N
N
N
N
P
OH
OH
O
O
OH
HO
O
50
45
40
35
30
25
20
15
10
5
0
-5
-10
-15
-20
-25
Chemical Shift (ppm)

L^4

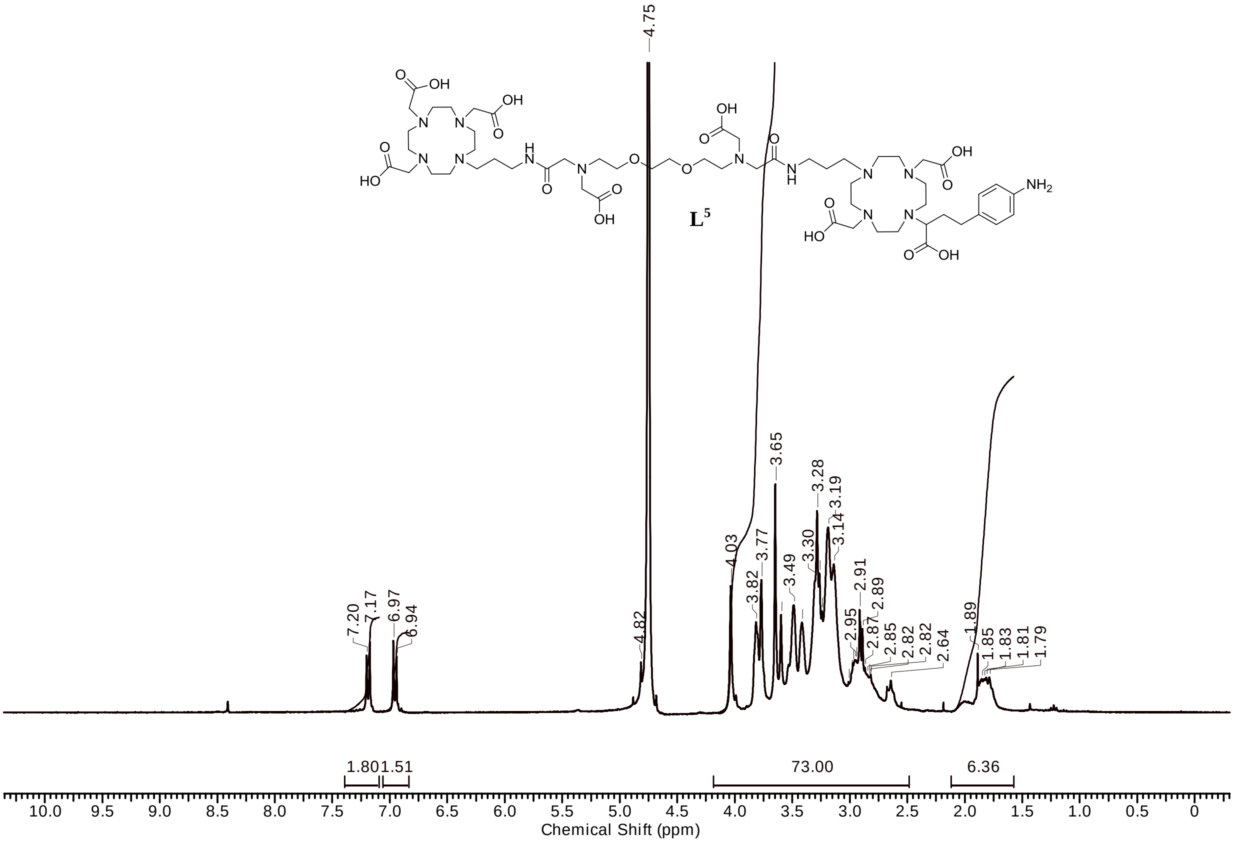
4.75
L5
NH2
7.20
7.17
6.97
6.94
4.82
4.03
3.82
3.77
3.65
3.49
3.30
3.28
3.19
3.14
2.95
2.91
2.89
2.87
2.85
2.82
2.82
2.64
1.89
1.85
1.83
1.81
1.79
1.80
1.51
73.00
6.36
10.0 9.5 9.0 8.5 8.0 7.5 7.0 6.5 6.0 5.5 5.0 4.5 4.0 3.5 3.0 2.5 2.0 1.5 1.0 0.5 0
Chemical Shift (ppm)

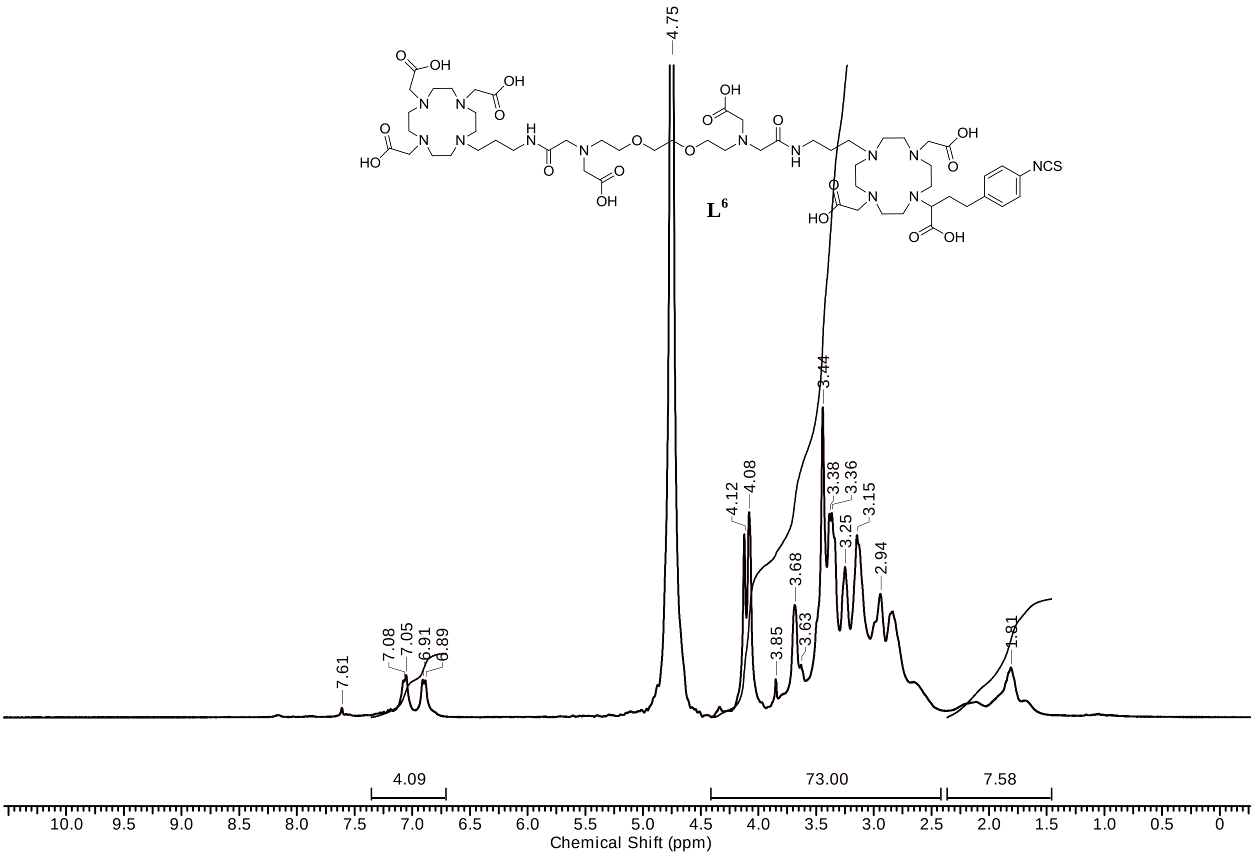
4.75
L6
NCS
7.61
7.08
7.05
6.91
6.89
4.12
4.08
3.85
3.68
3.63
3.44
3.38
3.36
3.25
3.15
2.94
1.81
4.09
73.00
7.58
10.0 9.5 9.0 8.5 8.0 7.5 7.0 6.5 6.0 5.5 5.0 4.5 4.0 3.5 3.0 2.5 2.0 1.5 1.0 0.5 0
Chemical Shift (ppm)

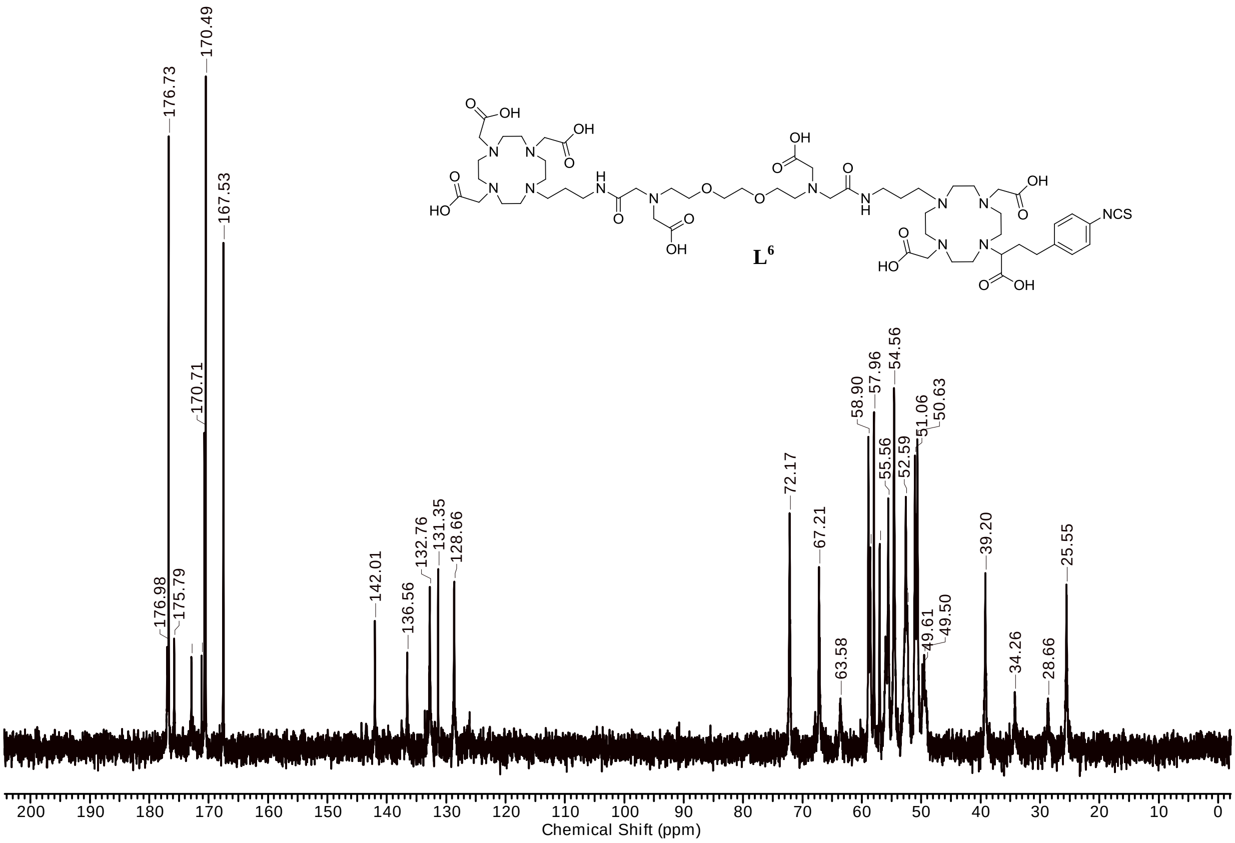
L6
NCS
176.98
176.73
175.79
170.71
170.49
167.53
142.01
136.56
132.76
131.35
128.66
72.17
67.21
63.58
58.90
57.96
55.56
54.56
52.59
51.06
50.63
49.61
49.50
39.20
34.26
28.66
25.55
Chemical Shift (ppm)

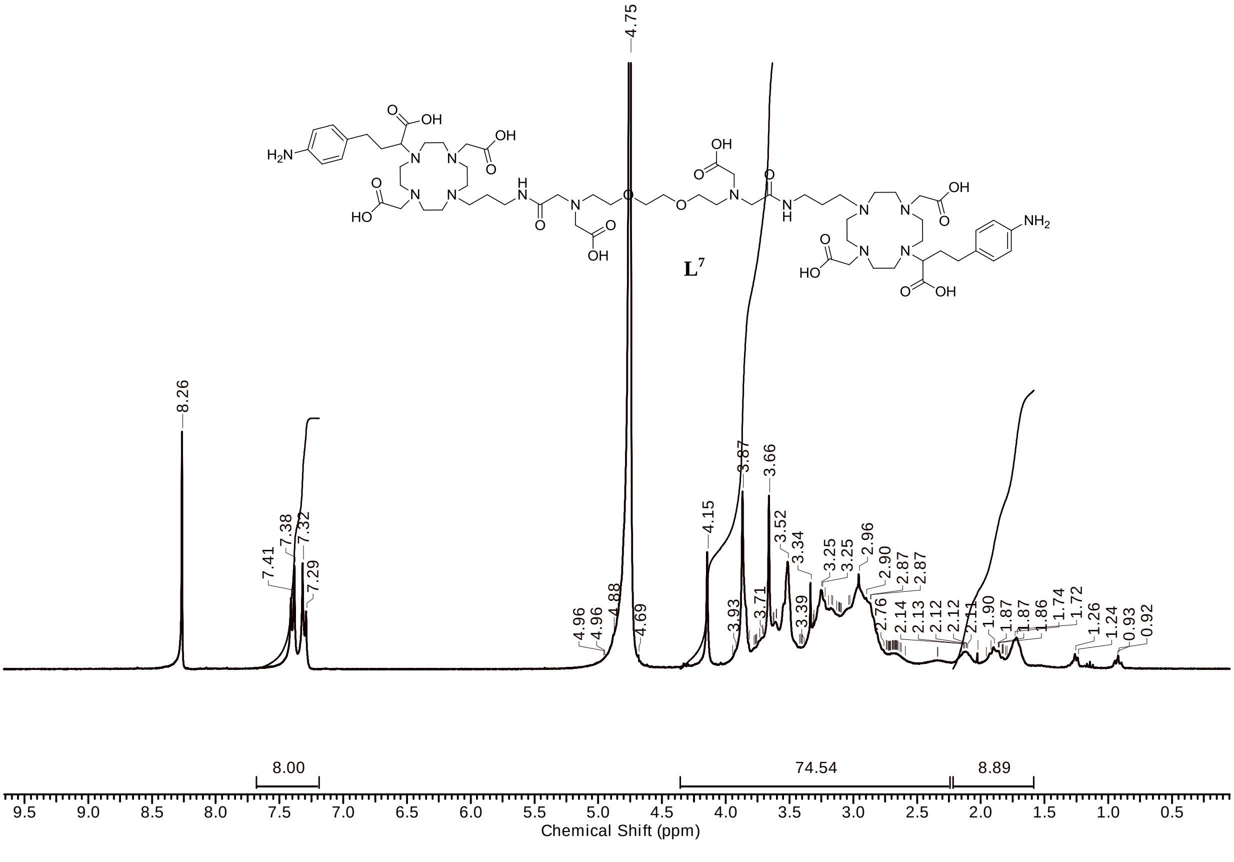
L7
NH_2
H_2N
8.26
7.41
7.38
7.32
7.29
4.96
4.96
4.88
4.75
4.69
4.15
3.93
3.87
3.71
3.66
3.52
3.39
3.34
3.25
3.25
2.96
2.90
2.87
2.87
2.76
2.14
2.13
2.12
2.12
2.11
1.90
1.87
1.87
1.86
1.74
1.72
1.26
1.24
0.93
0.92
8.00
74.54
8.89
Chemical Shift (ppm)

Annexure II

References

1. James, M. L.; Gambhir, S. S., A molecular imaging primer: modalities, imaging agents, and applications. *Physiological Reviews* **2012,** *92*, 897-965.

2. Merbach, A. E.; Toth, E., *The chemistry of contrast agents in medical magnetic resonance imaging*. Wiley: Chichester, 2001; p xii, 471 p.

3. Bloch, F.; Hansen, W. W.; Packard, M., The nuclear induction experiment. *Physical Review* **1946,** *70*, 474-485.

4. Dutton, P. L.; Leigh, J. S.; Scarpa, A., *Frontiers of biological energetics : electrons to tissues*. Academic Press: New York, 1978; p P. 752.

5. Ananta, J. S.; Godin, B.; Sethi, R.; Moriggi, L.; Liu, X. W.; Serda, R. E.; Krishnamurthy, R.; Muthupillai, R.; Bolskar, R. D.; Helm, L.; Ferrari, M.; Wilson, L. J.; Decuzzi, P., Geometrical confinement of gadolinium-based contrast agents in nanoporous particles enhances T(1) contrast. *Nat. Nanotechnol.* **2010,** *5*, 815-821.

6. Johansson, L.; Bjornerud, A., The utility of superparamagnetic contrast agents in MRI: theoretical consideration and applications in the cardiovascular system. *Nmr in Biomedicine* **2004,** *17*, 465-477.

7. Wang, Y. X. J.; Hussain, S. M.; Krestin, G. P., Superparamagnetic iron oxide contrast agents: physicochemical characteristics and applications in MR imaging. *European Radiology* **2001,** *11*, 2319-2331.

8. Weissleder, R.; Bogdanov, A.; Neuwelt, E. A.; Papisov, M., Long-circulating iron-oxides for MR imaging. *Advanced Drug Delivery Reviews* **1995,** *16*, 321-334.

9. Weissleder, R.; Moore, A.; Mahmood, U.; Bhorade, R.; Benveniste, H.; Chiocca, E. A.; Basilion, J. P., In vivo magnetic resonance imaging of transgene expression. *Nature Medicine* **2000,** *6*, 351-354.

10. Bulte, J. W. M.; Kraitchman, D. L., Iron oxide MR contrast agents for molecular and cellular imaging. *Nmr in Biomedicine* **2004,** *17*, 484-499.

11. Dobson, J.; Pankhurst, Q. A.; Connolly, J.; Jones, S. K., Applications of magnetic nanoparticles in biomedicine. *Journal of Physics D-Applied Physics* **2003,** *36*, R167-R181.

12. Toth, E.; Kubicek, V., Design and function of metal complexes as contrast agents in MRI. In *Advances in Inorganic Chemistry, Vol 61: Metal Ion Controlled Reactivity*, VanEldik, R.; Hubbard, C. D., Eds.2009; Vol. 61, pp 63-129.

13. Cotton, S., *Lanthanide and actinide chemistry*. Wiley: Chichester, 2006; p xiv, 263 p.

14. Port, M.; Idee, J.-M.; Medina, C.; Robic, C.; Sabatou, M.; Corot, C., Efficiency, thermodynamic and kinetic stability of marketed gadolinium chelates and their possible clinical consequences: a critical review. *Biometals* **2008,** *21*, 469-490.

15. Thomsen, H. S., Nephrogenic systemic fibrosis: a serious late adverse reaction to gadodiamide. *European Radiology* **2006,** *16*, 2619-2621.

16. Aime, S.; Botta, M.; Fasano, M.; Terreno, E., Lanthanide(III) chelates for NMR biomedical applications. *Chemical Society Reviews* **1998,** *27*, 19-29.

17. Lauffer, R. B., Paramagnetic metal-complexes as water proton relaxation agents for NMR imaging-Theory and design. *Chem. Rev.* **1987,** *87*, 901-927.

18. Solomon, I., Relaxation processes in a system of 2 spins. *Physical Review* **1955,** *99*, 559-565.

19. Solomon, I.; Bloembergen, N., Nuclear magnetic interactions in the HF molecule. *Journal of Chemical Physics* **1956,** *25*, 261-266.

20. Bloembergen, N.; Morgan, L. O., Proton relaxation times in paramagnetic solutions effects of electron spin relaxation. *Journal of Chemical Physics* **1961,** *34*, 842-&.

21. Raymond, K. N.; Werner, E. J.; Datta, A.; Jocher, C. J., High-Relaxivity MRI Contrast Agents: Where Coordination Chemistry Meets Medical Imaging. *Angewandte Chemie-International Edition* **2008,** *47*, 8568-8580.

22. Aime, S.; Calabi, L.; Cavallotti, C.; Gianolio, E.; Giovenzana, G. B.; Losi, P.; Maiocchi, A.; Palmisano, G.; Sisti, M., Gd-AAZTA (-): A new structural entry for an improved generation of MRI contrast agents. *Inorganic Chemistry* **2004,** *43*, 7588-7590.
23. Angelovski, G.; Mamedov, I., Cation-Responsive MRI Contrast Agents Based on Gadolinium(III). *Current Inorganic Chemistry* **2011,** *1*, 76-90.
24. Bruce, J. I.; Dickins, R. S.; Govenlock, L. J.; Gunnlaugsson, T.; Lopinski, S.; Lowe, M. P.; Parker, D.; Peacock, R. D.; Perry, J. J. B.; Aime, S.; Botta, M., The selectivity of reversible oxy-anion binding in aqueous solution at a chiral europium and terbium center: Signaling of carbonate chelation by changes in the form and circular polarization of luminescence emission. *Journal of the American Chemical Society* **2000,** *122,* 9674-9684.
25. Alpoim, M. C.; Urbano, A. M.; Geraldes, C.; Peters, J. A., Determinatio of the number of inner-sphere water-molecules in lanthanide(III)polyaminocarboxylate complexes *J. Chem. Soc.-Dalton Trans.* **1992**, 463-467.
26. Horrocks, W. D.; Sudnick, D. R., Lanthanide ion probes of stucture in biology- Laser induced luminescence decay contants provide a direct measure of the number of metal-coordinated watr-molecules. *Journal of the American Chemical Society* **1979,** *101*, 334-340.
27. Horrocks, W. D.; Schmidt, G. F.; Sudnick, D. R.; Kittrell, C.; Bernheim, R. A., Laser-induced lanthanide ion luminescence lifetime measurement by direct excitation of metal-ion levels-New class of structural probe for calcium-binding proteins and nucleic-acids. *Journal of the American Chemical Society* **1977,** *99,* 2378-2380.
28. Parker, D.; Williams, J. A. G., Getting excited about lanthanide complexation chemistry. *J. Chem. Soc.-Dalton Trans.* **1996**, 3613-3628.
29. Beeby, A.; Clarkson, I. M.; Dickins, R. S.; Faulkner, S.; Parker, D.; Royle, L.; de Sousa, A. S.; Williams, J. A. G.; Woods, M., Non-radiative deactivation of the excited states of europium, terbium and ytterbium complexes by proximate energy-matched OH, NH and CH oscillators: an improved luminescence method for establishing solution hydration states. *Journal of the Chemical Society-Perkin Transactions 2* **1999**, 493-503.
30. Caravan, P.; Raitsimring, A. M.; Astashkin, A. V.; Baute, D.; Goldfarb, D.; Poluektov, O. G.; Lowe, M. P.; Zech, S. G., Determination of the hydration number of gadolinium(III) complexes by high-field pulsed O-17 ENDOR spectroscopy. *Chemphyschem* **2006,** *7*, 1590-1597.
31. Lukes, I.; Hermann, P.; Kotek, J.; Kubicek, V., Gadolinium(III) complexes as MRI contrast agents: ligand design and properties of the complexes. *Dalton Transactions* **2008**, 3027-3047.
32. Lukes, I.; Rudovsky, J.; Botta, M.; Hermann, P.; Hardcastle, K. I.; Aime, S., PAMAM dendrimeric conjugates with a Gd-DOTA phosphinate derivative and their adducts with polyaminoacids: The interplay of global motion, internal rotation, and fast water exchange. *Bioconjugate Chemistry* **2006,** *17*, 975-987.
33. Revel, D.; Casali, C.; Janier, M.; Canet, E.; Obadia, J. F.; Benderbous, S.; Corot, C., Evaluation of Gd-DOTA-labeled dextran polymer as an intravascular MR contrast agent for myocardial perfusion. *Academic Radiology* **1998,** *5*, S214-S218.
34. Caravan, P.; Cloutier, N. J.; Greenfield, M. T.; McDermid, S. A.; Dunham, S. U.; Bulte, J. W. M.; Amedio, J. C.; Looby, R. J.; Supkowski, R. M.; Horrocks, W. D.; McMurry, T. J.; Lauffer, R. B., The interaction of MS-325 with human serum albumin and its effect on proton relaxation rates. *Journal of the American Chemical Society* **2002,** *124*, 3152-3162.
35. Merbach, A. E.; Livramento, J. B.; Weidensteiner, C.; Prata, M. I. M.; Allegrini, P. R.; Geraldes, C. F. G. C.; Helm, L.; Kneuer, R.; Santos, A. C.; Schmidt, P.; Toth, E., First in vivo MRI assessment of a self-assembled metallostar compound endowed with a remarkable high field relaxivity. *Contrast Media & Molecular Imaging* **2006,** *1*, 30-39.

36. Aime, S.; Barge, A.; Botta, M.; Parker, D.; DeSousa, A. S., Prototropic vs whole water exchange contributions to the solvent relaxation enhancement in the aqueous solution of a cationic Gd3+ macrocyclic complex. *Journal of the American Chemical Society* **1997,** *119*, 4767-4768.

37. Aime, S.; Botta, M.; Fasano, M.; Paoletti, S.; Terreno, E., Relaxometric determination of the exchange rate of the coordinated water protons in a neutral Gd-III chelate. *Chemistry-a European Journal* **1997,** *3*, 1499-1504.

38. Caravan, P.; Ellison, J. J.; McMurry, T. J.; Lauffer, R. B., Gadolinium(III) chelates as MRI contrast agents: Structure, dynamics, and applications. *Chem. Rev.* **1999,** *99*, 2293-2352.

39. Raymond, K. N.; Thompson, M. K.; Botta, M.; Nicolle, G.; Helm, L.; Aime, S.; Merbach, A. E., A highly stable gadolinium complex with a fast, associative mechanism of water exchange. *Journal of the American Chemical Society* **2003,** *125*, 14274-14275.

40. Botta, M.; Hardcastle, K. I.; Fasano, M.; Digilio, G., Experimental evidence for a second coordination sphere water molecule in the hydration structure of YbDTPA - Insights for a re-assessment of the relaxivity data of GdDTPA. *European Journal of Inorganic Chemistry* **2000**, 971-977.

41. Mamedov, I.; Mishra, A.; Angelovski, G.; Mayer, H. A.; Palsson, L. O.; Parker, D.; Logothetis, N. K., Synthesis and characterization of lanthanide complexes of DO3A-alkylphosphonates. *Dalton Trans* **2007**, 5260-7.

42. Mordon, S.; Devoisselle, J. M.; Maunoury, V., In-vivo pH measurement and imaging of tumor-tissue using a pH-sensitive fluorescent-probe (5,6-carboxyfluorescein)-Instrumental and experimental studies. *Photochemistry and Photobiology* **1994,** *60*, 274-279.

43. Perez-Mayoral, E.; Negri, V.; Soler-Padros, J.; Cerdan, S.; Ballesteros, P., Chemistry of paramagnetic and diamagnetic contrast agents for Magnetic Resonance Imaging and Spectroscopy pH responsive contrast agents. *European Journal of Radiology* **2008,** *67*, 453-458.

44. Sherry, A. D.; De Leon-Rodriguez, L. M.; Lubag, A. J. M.; Malloy, C. R.; Martinez, G. V.; Gillies, R. J., Responsive MRI Agents for Sensing Metabolism in Vivo. *Accounts of Chemical Research* **2009,** *42*, 948-957.

45. Sherry, A. D.; Zhang, S. R.; Wu, K. C., A novel pH-sensitive MRI contrast agent. *Angewandte Chemie-International Edition* **1999,** *38*, 3192-3194.

46. Yoo, B.; Pagel, M. D., An overview of responsive MRI contrast agents for molecular imaging. *Front. Biosci.* **2008,** *13*, 1733-1752.

47. Chang, C. J.; Que, E. L., Responsive magnetic resonance imaging contrast agents as chemical sensors for metals in biology and medicine. *Chemical Society Reviews* **2010,** *39*, 51-60.

48. Yang, C.-T.; Chuang, K.-H., Gd(III) chelates for MRI contrast agents: from high relaxivity to "smart", from blood pool to blood-brain barrier permeable. *Medchemcomm* **2012,** *3*, 552-565.

49. Li, W. H.; Meade, T. J.; Fraser, S. E., A calcium-sensitive magnetic resonance imaging contrast agent. *Journal of the American Chemical Society* **1999,** *121*, 1413-1414.

50. Angelovski, G.; Fouskova, P.; Mamedov, I.; Canals, S.; Toth, E.; Logothetis, N. K., Smart magnetic resonance imaging agents that sense extracellular calcium fluctuations. *Chembiochem* **2008,** *9*, 1729-34.

51. Dhingra, K.; Fouskova, P.; Angelovski, G.; Maier, M. E.; Logothetis, N. K.; Toth, E., Towards extracellular Ca2+ sensing by MRI: synthesis and calcium-dependent H-1 and O-17 relaxation studies of two novel bismacrocyclic Gd3+ complexes. *Journal of Biological Inorganic Chemistry* **2008,** *13*, 35-46.

52. Dhingra, K.; Maier, M. E.; Beyerlein, M.; Angelovski, G.; Logothetis, N. K., Synthesis and characterization of a smart contrast agent sensitive to calcium. *Chemical Communications* **2008**, 3444-3446.

53. Mishra, A.; Fouskova, P.; Angelovski, G.; Balogh, E.; Mishra, A. K.; Logothetis, N. K.; Toth, E., Facile synthesis and relaxation properties of novel bispolyazamacrocyclic Gd3+ complexes: An attempt towards calcium-sensitive MRI contrast agents (vol 47, pg 1375, 2008). *Inorganic Chemistry* **2008,** *47*, 3460-3460.

54. Mamedov, I.; Henig, J.; Fouskova, P.; Toth, E.; Logothetis, N. K.; Angelovski, G.; Mayer, H. A., Influence of Calcium-Induced Aggregation on the Sensitivity of Aminobis(methylenephosphonate)-Containing Potential MRI Contrast Agents. *Inorganic Chemistry* **2011,** *50*, 6472-6481.

55. Mamedov, I.; Logothetis, N. K.; Angelovski, G., Structure-related variable responses of calcium sensitive MRI probes. *Organic & Biomolecular Chemistry* **2011,** *9*, 5816-5824.

56. Mamedov, I.; Canals, S.; Henig, J.; Beyerlein, M.; Murayama, Y.; Mayer, H. A.; Logothetis, N. K.; Angelovski, G., In Vivo Characterization of a Smart MRI Agent That Displays an Inverse Response to Calcium Concentration. *Acs Chemical Neuroscience* **2010,** *1*, 819-828.

57. Chang, C. J.; Que, E. L., A smart magnetic resonance contrast agent for selective copper sensing. *Journal of the American Chemical Society* **2006,** *128*, 15942-15943.

58. Que, E. L.; Gianolio, E.; Baker, S. L.; Wong, A. P.; Aime, S.; Chang, C. J., Copper-Responsive Magnetic Resonance Imaging Contrast Agents. *Journal of the American Chemical Society* **2009,** *131*, 8527-8536.

59. Hanaoka, K.; Kikuchi, K.; Urano, Y.; Nagano, T., Selective sensing of zinc ions with a novel magnetic resonance imaging contrast agent. *Journal of the Chemical Society-Perkin Transactions 2* **2001**, 1840-1843.

60. Major, J. L.; Parigi, G.; Luchinat, C.; Meade, T. J., The synthesis and in vitro testing of a zinc-activated MRI contrast agent. *Proceedings of the National Academy of Sciences of the United States of America* **2007,** *104*, 13881-13886.

61. Youn, J. H.; McDonough, A. A., Recent Advances in Understanding Integrative Control of Potassium Homeostasis. In *Annual Review of Physiology*,2009; Vol. 71, pp 381-401.

62. Hifumi, H.; Tanimoto, A.; Citterio, D.; Komatsu, H.; Suzuki, K., Novel 15-crown-5 ether or beta-diketone incorporated gadolinium complexes for the detection of potassium ions or magnesium and calcium ions. *Analyst* **2007,** *132*, 1153-1160.

63. Livramento, J. B.; Toth, E.; Sour, A.; Borel, A.; Merbach, A. E.; Ruloff, R., High relaxivity confined to a small molecular space: A metallostar-based, potential MRI contrast agent. *Angewandte Chemie-International Edition* **2005,** *44*, 1480-1484.

64. Paris, J.; Gameiro, C.; Humblet, V.; Mohapatra, P. K.; Jacques, V.; Desreux, J. F., Auto-assembling of ditopic macrocyclic lanthanide chelates with transition-metal ions. Rigid multimetallic high relaxivity contrast agents for magnetic resonance Imaging. *Inorganic Chemistry* **2006,** *45*, 5092-5102.

65. Ruloff, R.; van Koten, G.; Merbach, A. E., Novel heteroditopic chelate for self-assembled gadolinium(III) complex with high relaxivity. *Chemical Communications* **2004**, 842-843.

66. Aime, S.; Botta, M.; Fasano, M.; Terreno, E., Paramagnetic Gd-III-Fe-III heterobimetallic complexes of DTPA-bis-salicylamide. *Spectrochimica Acta Part a-Molecular and Biomolecular Spectroscopy* **1993,** *49*, 1315-1322.

67. Moats, R. A.; Fraser, S. E.; Meade, T. J., A "smart" magnetic resonance imaging agent that reports on specific enzymatic activity. *Angewandte Chemie-International Edition in English* **1997,** *36*, 726-728.

68. Louie, A. Y.; Huber, M. M.; Ahrens, E. T.; Rothbacher, U.; Moats, R.; Jacobs, R. E.; Fraser, S. E.; Meade, T. J., In vivo visualization of gene expression using magnetic resonance imaging. *Nature Biotechnology* **2000,** *18*, 321-325.

69. Duimstra, J. A.; Femia, F. J.; Meade, T. J., A gadolinium chelate for detection of beta-glucuronidase: A self-immolative approach. *Journal of the American Chemical Society* **2005,** *127*, 12847-12855.

70. Giardiello, M.; Lowe, M. P.; Botta, M., An esterase-activated magnetic resonance contrast agent. *Chemical Communications* **2007**, 4044-4046.

71. Nivorozhkin, A. L.; Kolodziej, A. F.; Caravan, P.; Greenfield, M. T.; Lauffer, R. B.; McMurry, T. J., Enzyme-activated Gd3+ magnetic resonance imaging contrast agents with a prominent receptor-induced magnetization enhancement. *Angewandte Chemie-International Edition* **2001,** *40*, 2903-2906.

72. Arena, F.; Singh, J. B.; Gianolio, E.; Stefania, R.; Aime, S., beta-Gal Gene Expression MRI Reporter in Melanoma Tumor Cells. Design, Synthesis, and in Vitro and in Vivo Testing of a Gd(III) Containing Probe Forming a High Relaxivity, Melanin-Like Structure upon beta-Gal Enzymatic Activation. *Bioconjugate Chemistry* **2011,** *22*, 2625-2635.

73. Griffiths, J. R., Are cancer cells acidic. *British Journal of Cancer* **1991,** *64*, 425-427.

74. Vaupel, P.; Kallinowski, F.; Okunieff, P., Blood-flow, oxygen and nutrient supply, and metabolic microenvironment of human-tumors-A review. *Cancer Research* **1989,** *49*, 6449-6465.

75. Wikehooley, J. L.; Haveman, J.; Reinhold, H. S., The relevance of tumor pH to the treatment of malignant disease. *Radiotherapy and Oncology* **1984,** *2*, 343-366.

76. Tannock, I. F.; Rotin, D., Acid pH in tumors and its potential for therapeutic exploitation. *Cancer Research* **1989,** *49*, 4373-4384.

77. Van Den Berg, A. P.; Wike-Hooley, J. L.; Van Den Berg-Blok, A. E.; Vna Der Zee, J.; Reinhold, H. S., Tumar pH in human mammary carcinoma. *European Journal of Cancer and Clinical Oncology* **1982,** *18*, 457-462.

78. Calderwood, S. K.; Dickson, J. A., pH and tumar response to hyperthermia. *Advances in Radiation Biology* **1983,** *10*, 135-190.

79. Martin, G. R.; Jain, R. K., Noninvasive measurement of interstitial pH profiles in normal and neoplastic tissue using flurescence ratio imaging microscopy. *Cancer Research* **1994,** *54*, 5670-5674.

80. Stubbs, M.; Bhujwalla, Z. M.; Tozer, G. M.; Rodrigues, L. M.; Maxwell, R. J.; Morgan, R.; Howe, F. A.; Griffiths, J. R., An assessment of P-31 MRS as a method of measuring pH in rat-tumors. *Nmr in Biomedicine* **1992,** *5*, 351-359.

81. Lyng, H.; Olsen, D. R.; Southon, T. E.; Rofstad, E. K., P-31 nuclear magnetic resonance spectroscopy in-vivo of 6-human-melanoma xenograft lines-Tumor bioenergetic status and blood-supply. *British Journal of Cancer* **1993,** *68*, 1061-1070.

82. Mordon, S.; Devoisselle, J. M.; Soulie, S., Fluorescence spectroscopy of pH in-vivo using a dual-emission fluorophore (C-SNAFL-1). *Journal of Photochemistry and Photobiology B-Biology* **1995,** *28*, 19-23.

83. Frullano, L.; Catana, C.; Benner, T.; Sherry, A. D.; Caravan, P., Bimodal MR-PET Agent for Quantitative pH Imaging. *Angewandte Chemie-International Edition* **2010,** *49*, 2382-2384.

84. Lowe, M. P.; Parker, D.; Reany, O.; Aime, S.; Botta, M.; Castellano, G.; Gianolio, E.; Pagliarin, R., pH-dependent modulation of relaxivity and luminescence in macrocyclic gadolinium and europium complexes based on reversible intramolecular sulfonamide ligation. *Journal of the American Chemical Society* **2001,** *123*, 7601-7609.

85. Caravan, P., Strategies for increasing the sensitivity of gadolinium based MRI contrast agents. *Chemical Society Reviews* **2006,** *35*, 512-523.

86. Aime, S.; Caravan, P., Biodistribution of Gadolinium-Based Contrast Agents, Including Gadolinium Deposition. *Journal of Magnetic Resonance Imaging* **2009,** *30*, 1259-1267.

87. Sherry, A. D.; Ali, M. M.; Woods, M.; Caravan, P.; Opina, A. C. L.; Spiller, M.; Fettinger, J. C., Synthesis and relaxometric studies of a dendrimer-based pH-responsive MRI contrast agent. *Chemistry-a European Journal* **2008,** *14*, 7250-7258.

88. Aime, S.; Gianolio, E.; Napolitano, R.; Fedeli, F.; Arena, F., Poly-beta-cyclodextrin based platform for pH mapping via a ratiometric (19)F/(1)H MRI method. *Chemical Communications* **2009**, 6044-6046.

89. Green, N. M., Avidin and Streptavidin. *Methods in Enzymology* **1990,** *184,* 51-67.

90. Guenin, E.; Monteil, M.; Bouchemal, N.; Prange, T.; Lecouvey, M., Syntheses of phosphonic esters of alendronate, pamidronate and neridronate. *European Journal of Organic Chemistry* **2007**, 3380-3391.

91. Lowe, M. P.; Giardiello, M.; Botta, M., An esterase-activated magnetic resonance contrast agent. *Chemical Communications* **2007**, 4044-4046.

92. Kovacs, Z.; Sherry, A. D., pH-controlled selective protection of polyaza macrocycles. *Synthesis* **1997**, 759-763.

93. Eisenwiener, K. P.; Powell, P.; Macke, H. R., A convenient synthesis of novel bifunctional prochelators for coupling to bioactive peptides for radiometal labelling. *Bioorganic & Medicinal Chemistry Letters* **2000,** *10*, 2133-2135.

94. Wardle, N. J.; Herlihy, A. H.; So, P.-W.; Bell, J. D.; Bligh, S. W. A., Synthesis of a novel 'smart' bifunctional chelating agent 1-(2- beta,D-galactopyranosyloxylethyl)-7-(1-carboxy-3- 4-aminophenyllpr opyl)-4,10-bis(carboxymethyl)-1,4,7,10-tetraazacyclododecane (Gal-PA-DO3A-NH2) and its Gd(III) complex. *Bioorganic & Medicinal Chemistry* **2007,** *15*, 4714-4721.

95. Corsi, D. M.; Platas-Iglesias, C.; van Bekkum, H.; Peters, J. A., Determination of paramagnetic lanthanide(III) concentrations from bulk magnetic susceptibility shifts in NMR spectra. *Magnetic Resonance in Chemistry* **2001,** *39*, 723-726.

96. Horrocks, W. D.; Bolender, J. P.; Smith, W. D.; Supkowski, R. M., Photosensitized near infrared luminescence of ytterbium(III) in proteins and complexes occurs via an internal redox process. *Journal of the American Chemical Society* **1997,** *119*, 5972-5973.

97. Wilchek, M.; Bayer, E. A., Introduction to avidin-biotin technology. *Methods in Enzymology* **1990,** *184*, 5-13.

98. Lehtolainen, P.; Wirth, T.; Taskinen, A. K.; Lehenkari, P.; Leppanen, O.; Lappalainen, M.; Pulkkanen, K.; Marttila, A.; Marjomaki, V.; Airenne, K. J.; Horton, M.; Kulomaa, M. S.; Yla-Herttuala, S., Targeting of biotinylated compounds to its target tissue using a low-density lipoprotein receptor-avidin fusion protein. *Gene Therapy* **2003,** *10*, 2090-2097.

99. Breitz, H. B.; Weiden, P. L.; Press, O.; Appelbaum, J. W.; Bryan, J. K.; Gaffigan, S.; Stone, D.; Axworthy, D.; Fisher, D.; Reno, J., Pretargeted radioimmunotherapy (PRIT (TM)) for treatment of non-Hodgkin's lymphoma (NHL): Initial phase I/II study results. *Cancer Biother. Radiopharm.* **2000,** *15*, 15-29.

100. Su, J.; Chen, F.; Cryns, V. L.; Messersmith, P. B., Catechol Polymers for pH-Responsive, Targeted Drug Delivery to Cancer Cells. *Journal of the American Chemical Society* **2011,** *133*, 11850-11853.

101. Horowitz, P.; Mock, D. M.; Langford, G.; Dubois, D.; Criscimagna, N., A fluorometric assay for the biotin avidininteraction based on displacement of the fluorescent-probe 2-anilinonaphthalene-6-sulfonic acid. *Anal. Biochem.* **1985,** *151*, 178-181.

102. Dwek, R. A., *Nuclear magnetic resonance (N.M.R.) in biochemistry: applications to enzyme systems*. Clarendon Press: Oxford, 1973; p xviii, 395 p.

103. Livramento, J. B.; Weidensteiner, C.; Prata, M. I. M.; Allegrini, P. R.; Geraldes, C.; Helm, L.; Kneuer, R.; Merbach, A. E.; Santos, A. C.; Schmidt, P.; Toth, E., First in vivo MRI assessment of a self-assembled metallostar compound endowed with a remarkable high field relaxivity. *Contrast Media & Molecular Imaging* **2006,** *1*, 30-39.
104. Meldolesi, J., Calcium signalling - Oscillation, activation, expression. *Nature* **1998,** *392*, 863-+.
105. Burgoyne, R. D., Neuronal calcium sensor proteins: generating diversity in neuronal Ca^{2+} signalling. *Nature Reviews Neuroscience* **2007,** *8*, 182-193.
106. Silver, I. A.; Erecinska, M., Intracellular and extracellular changes of Ca^{2+} in hypoxia and ischema in rat-brain in vivo. *Journal of General Physiology* **1990,** *95*, 837-866.
107. Pawley, J. B., *Handbook of biological confocal microscopy*. 3rd ed.; Springer: New York, NY, 2006; p xxviii, 985 p.
108. Somjen, G. G., *Ions in the brain : normal function, seizures, and strokes*. Oxford University Press: New York; Oxford, 2004; p xxix, 470 p.
109. Popov, K.; Ronkkomaki, H.; Lajunen, L. H. J., Critical evaluation of stability constants of phosphonic acids (IUPAC technical report). *Pure Appl. Chem.* **2001,** *73*, 1641-1677.
110. Matczak-Jon, E.; Kurzak, B.; Kamecka, A.; Sawka-Dobrowolska, W.; Kafarski, P., Interactions of zinc(II), magnesium(II) and calcium(II) with iminodimethylenediphosphonic acids in aqueous solutions. *Journal of the Chemical Society-Dalton Transactions* **1999**, 3627-3637.
111. Dhingra, K.; Fouskova, P.; Angelovski, G.; Maier, M. E.; Logothetis, N. K.; Toth, E., Towards extracellular Ca^{2+} sensing by MRI: synthesis and calcium-dependent ^{1}H and ^{17}O relaxation studies of two novel bismacrocyclic Gd^{3+} complexes. *Journal of Biological Inorganic Chemistry* **2008,** *13*, 35-46.
112. Merrifield, R. B., Solid phase peptide synthesis. I. Synthesis of a tetrapeptide. *Journal of the American Chemical Society* **1963,** *85*, 2149-&.
113. Lam, K. S., Application of combinatorial library methods in cancer research and drug discovery. *Anti-Cancer Drug Design* **1997,** *12*, 145-167.
114. Lam, K. S.; Lebl, M.; Krchnak, V., The "one-bead-one-compound" combinatorial library method. *Chem. Rev.* **1997,** *97*, 411-448.
115. Chillemi, F.; Merrifie.Rb, Use of min-dinitrophenylhistidine in solid-phase synthesis of tricosapeptides 124-146 of human hemoglobin beta chain. *Biochemistry* **1969,** *8*, 4344-&.
116. Merrifie.Rb, Automated synthesis of peptides. *Science* **1965,** *150*, 178-&.
117. Huo, C.; Chan, T. H., A novel liquid-phase strategy for organic synthesis using organic ions as soluble supports. *Chemical Society Reviews* **2010,** *39*, 2977-3006.
118. Lu, J.; Toy, P. H., Organic Polymer Supports for Synthesis and for Reagent and Catalyst Immobilization. *Chem. Rev.* **2009,** *109*, 815-838.
119. Boas, U.; Brask, J.; Jensen, K. J., Backbone Amide Linker in Solid-Phase Synthesis. *Chem. Rev.* **2009,** *109*, 2092-2118.
120. Dioos, B. M. L.; Vankelecom, I. F. J.; Jacobs, P. A., Aspects of immobilisation of catalysts on polymeric supports. *Advanced Synthesis & Catalysis* **2006,** *348*, 1413-1446.
121. Guillier, F.; Orain, D.; Bradley, M., Linkers and cleavage strategies in solid-phase organic synthesis and combinatorial chemistry. *Chem. Rev.* **2000,** *100*, 2091-2157.
122. James, I. W., Linkers for solid phase organic synthesis. *Tetrahedron* **1999,** *55*, 4855-4946.
123. Pedersen, S. L.; Tofteng, A. P.; Malik, L.; Jensen, K. J., Microwave heating in solid-phase peptide synthesis. *Chemical Society Reviews* **2012,** *41*, 1826-1844.
124. Sammelson, R. E.; Kurth, M. J., Carbon-carbon bond-forming solid-phase reactions. Part II. *Chem. Rev.* **2001,** *101*, 137-202.

125. Isidro-Llobet, A.; Alvarez, M.; Albericio, F., Amino Acid-Protecting Groups. *Chem. Rev.* **2009,** *109*, 2455-2504.
126. Pattabiraman, V. R.; Bode, J. W., Rethinking amide bond synthesis. *Nature* **2011,** *480*, 471-479.
127. Eifler-Lima, V. L.; Graebin, C. S.; Uchoa, F. D. T.; Duarte, P. D.; Correa, A. G., Highlights in the Solid-Phase Organic Synthesis of Natural Products and Analogues. *Journal of the Brazilian Chemical Society* **2010,** *21*, 1401-1423.
128. Lorsbach, B. A.; Kurth, M. J., Carbon-carbon bond forming solid-phase reactions. *Chem. Rev.* **1999,** *99*, 1549-1581.
129. Bhorade, R.; Weissleder, R.; Nakakoshi, T.; Moore, A.; Tung, C. H., Macrocyclic chelators with paramagnetic cations are internalized into mammalian cells via a HIV-tat derived membrane translocation peptide. *Bioconjugate Chem.* **2000,** *11*, 301-305.
130. Heppeler, A.; Froidevaux, S.; Eberle, A. N.; Maecke, H. R., Receptor targeting for tumor localisation and therapy with radiopeptides. *Curr. Med. Chem.* **2000,** *7*, 971-994.
131. Hsieh, H. P.; Wu, Y. T.; Chen, S. T.; Wang, K. T., Direct solid-phase synthesis of octreotide conjugates: Precursors for use as tumor-targeted radiopharmaceuticals. *Bioorg. Med. Chem.* **1999,** *7*, 1797-1803.
132. Peterson, J. J.; Pak, R. H.; Meares, C. F., Total solid-phase synthesis of 1,4,7,10-tetraazacyclododecane-N,N ',N '',N '''-tetraacetic acid-functionalized peptides for radioimmunotherapy. *Bioconjugate Chem.* **1999,** *10*, 316-320.
133. De Leon-Rodriguez, L. M.; Kovacs, Z.; Dieckmann, G. R.; Sherry, A. D., Solid-phase synthesis of DOTA-peptides. *Chemistry-a European Journal* **2004,** *10*, 1149-1155.
134. Kiviniemi, A.; Makela, J.; Makila, J.; Saanijoki, T.; Liljenback, H.; Poijarvi-Virta, P.; Lonnberg, H.; Laitala-Leinonen, T.; Roivainen, A.; Virta, P., Solid-Supported NOTA and DOTA Chelators Useful for the Synthesis of 3 '-Radiometalated Oligonucleotides. *Bioconjugate Chem.* **2012,** *23*, 1981-1988.
135. Masuda, R.; Oishi, S.; Ohno, H.; Kimura, H.; Saji, H.; Fujii, N., Concise site-specific synthesis of DTPA-peptide conjugates: Application to imaging probes for the chemokine receptor CXCR4. *Bioorg. Med. Chem.* **2011,** *19*, 3216-3220.
136. Yoo, B.; Sheth, V. R.; Pagel, M. D., An amine-derivatized, DOTA-loaded polymeric support for Fmoc solid phase peptide synthesis. *Tetrahedron Letters* **2009,** *50*, 4459-4462.
137. De Leon-Rodriguez, L. M.; Kovacs, Z., The synthesis and chelation chemistry of DOTA-peptide conjugates. *Bioconjugate Chem.* **2008,** *19*, 391-402.
138. Kovacs, Z.; De Leon-Rodriguez, L. M., Conjugation of 1,4,7,10-tetraazacyclododecane-1,4,7,10-tetracetic acid (DOTA) and its derivatives to peptides: Synthesis, applications and future prospects. *Mini-Reviews in Organic Chemistry* **2007,** *4*, 281-291.
139. Langereis, S.; Dirksen, A.; De Waal, B. F. M.; Van Genderen, M. H. P.; De Lussanet, Q. G.; Hackeng, T. M.; Meijer, E. W., Solid-phase synthesis of a cyclic NGR-functionalized Gd(III)DTPA complex. *Eur. J. Org. Chem.* **2005**, 2534-2538.
140. Jensen, K. J.; Alsina, J.; Songster, M. F.; Vagner, J.; Albericio, F.; Barany, G., Backbone Amide Linker (BAL) strategy for solid-phase synthesis of C-terminal-modified and cyclic peptides. *Journal of the American Chemical Society* **1998,** *120*, 5441-5452.
141. Bui, C. T.; Rasoul, F. A.; Ercole, F.; Pham, Y.; Maeji, N. J., Efficiencies of reductive amination reactions on different solid supports. *Tetrahedron Letters* **1998,** *39*, 9279-9282.
142. Sherry, A. D.; Kovacs, Z., pH-controlled selective protection of polyaza macrocycles. *Synthesis* **1997**, 759-763.
143. Valeur, B., *Molecular fluorescence : principles and applications*. Wiley-VCH: Weinheim ; Chichester, 2002; p xiv, 387 p.

144. Mock, D. M.; Lankford, G.; Horowitz, P., A study of the interaction of avidin with 2-anilinonaphthalene-6-sulfonic acid as a probe of the biotin binding-site. *Biochimica Et Biophysica Acta* **1988,** *956*, 23-29.

145. Parac-Vogt, T. N.; Kimpe, K.; Laurent, S.; Vander Elst, L.; Burtea, C.; Chen, F.; Muller, R. N.; Ni, Y. C.; Verbruggen, A.; Binnemans, K., Synthesis, characterization, and pharmacokinetic evaluation of a potential MRI contrast agent containing two paramagnetic centers with albumin binding affinity. *Chemistry-a European Journal* **2005,** *11*, 3077-3086.

Sandip M. Vibhute

Date of Birth: 15th November, 1981.

Nationality: Indian

Family status: Married

E-mail: sandip.vibhute@tuebingen.mpg.de

Education

- **PhD, pursuing since June 2009**
    - **Max Planck Institute for Biological Cybernetics, Tübingen and Dept. of Organic Chemistry, University of Tübingen, Germany**.
    - **Thesis Title:** Synthetic Modifications of Responsive MRI Contrast Agents- Development of Multifunctional Conjugates for Novel Class of fMRI.
    - Supervisors: Priv.–Doz. Dr. Goran Angelovski, Prof. Nikos K. Logothetis and Prof. Martin E. Maier.

- **Master of Science, Organic Chemistry, 2003 – 2005.**
    - **University of Pune, India.**
    - First class with distinction (76.65%).

- **Bachelor of Science, Chemistry, 2000 – 2003.**
    - **Shivaji University Kolhapur, India.**
    - First class with distinction (80%).

- **Secondary school Certificate, 1998.**
    - **Board of Secondary and Higher Secondary School, Pune, India.**
    - First class with distinction (77.73%).

Employment

- **Research Scientist I** at Dept. of Medicinal Chemistry, **Albany Molecular Research Inc**., Singapore Research Centre, Singapore. **Mar 2008 to Apr 2009**.

- **Research Chemist** at Dept. of Medicinal Chemistry, New Drug Discovery Research, **Ranbaxy Research Laboratories Ltd.,** Gurgaon, India. **Aug 2007 to Feb 2008**.

- **Research Associate** at Dept. of Synthetic Organic Chemistry, **Jubilant Chemsys Ltd.**, Noida, India. **Jan 2006 to Jul 2007**.

Publication/Conference Paper

- **S. M. Vibhute**, J. Engelmann, T. Verbić, M. E. Maier, N. K. Logothetis, G. Angelovski. “Synthesis and Characterization of pH-sensitive, Biotinylated MRI Contrast Agents and Their Conjugates with Avidin” ***Org. Biomol. Chem*. 2013, 11(8), 1294-1305**. Highlighted as cover picture.

- **S. M. Vibhute**, J. Engelmann, T. Verbić, M. E. Maier, N. K. Logothetis, G. Angelovski. “Synthetic modifications of pH-sensitive contrast agents for attachment to functional molecules and its utilization in biotin-avidin system” **Frontiers in Medicinal Chemistry**, Munich, Germany (Mar 2013).

Talk

- **S. M. Vibhute**, J. Engelmann, T. Verbić, M. E. Maier, N. K. Logothetis, G. Angelovski. “Synthetic modifications of pH-sensitive contrast agents for attachment to functional molecules and its utilization in biotin-avidin system” **COST Action TD1004 annual Meeting, Theranostics Imaging and Therapy**, Kings College London, UK (Oct 2012).